MURILLO PETERLINI TAVARES

DESVENDANDO O SECRETOMA DO FUNGO FITOPATOGÊNICO *Chrysoporthe cubensis* LPF-1 CULTIVADO EM BIOMASSA LIGNOCELULÓSICA COMO POTENCIAL FONTE DE ENZIMAS PARA PRODUÇÃO DE BIOETANOL

Tese apresentada à Universidade Federal de Viçosa, como parte das exigências do Programa de Pós-Graduação em Bioquímica Aplicada, para obtenção do título de *Doctor Scientiae*.

VIÇOSA
MINAS GERAIS – BRASIL
2019

Ficha catalográfica preparada pela Biblioteca Central da Universidade Federal de Viçosa - Câmpus Viçosa

T
T231d
2019

Tavares, Murillo Peterlini, 1990-
Desvendando o secretoma do fungo fitopatogênico *Chrysoporthe cubensis* LPF-1 cultivado em biomassa lignocelulósica como potencial fonte de enzimas para produção de bioetanol / Murillo Peterlini Tavares. – Viçosa, MG, 2019.
xiii, 174f. : il. (algumas color.) ; 29 cm.

Inclui apêndices.
Orientador: Valéria Monteze Guimarães.
Tese (doutorado) - Universidade Federal de Viçosa.
Inclui bibliografia.

1. *Chrysoporthe cubensis*. 2. Proteômica. 3. Enzimas. 4. Secreções. 5. Biomassa. 6. Lignocelulose. 7. Etanol. I. Universidade Federal de Viçosa. Departamento de Bioquímica e Biologia Molecular. Programa de Pós-graduação em Bioquímica Aplicada. II. Título.

CDD 22 ed. 579.567

MURILLO PETERLINI TAVARES

DESVENDANDO O SECRETOMA DO FUNGO FITOPATOGÊNICO *Chrysoporthe cubensis* LPF-1 CULTIVADO EM BIOMASSA LIGNOCELULÓSICA COMO POTENCIAL FONTE DE ENZIMAS PARA PRODUÇÃO DE BIOETANOL

Tese apresentada à Universidade Federal de Viçosa, como parte das exigências do Programa de Pós-Graduação em Bioquímica Aplicada, para obtenção do título de *Doctor Scientiae*.

APROVADA: 08 de julho de 2019.

Gabriela Piccolo Maitan-Alfenas

Rafaela Inês de Souza Ladeira Ázar

William de Castro Borges

Tiago Antônio de Oliveira Mendes
(Coorientador)

Valéria Monteze Guimarães
(Orientadora)

DEDICATÓRIA

Aos meus pais, meu irmão e minha irmã

Dedico.

AGRADECIMENTOS

À minha mãe, Adriana, por me ensinar a ser sempre educado, ser compreensivo, amoroso, dedicado, a ter fé e valorizar a educação acima de tudo. Por abrir mão do conforto e de bens materiais para me dar uma educação de qualidade. Por ser dedicada, atenciosa e ser a melhor mãe que existe.

Ao meu pai, Wilson (*in memoriam*), que partiu de forma digna e corajosa para uma nova jornada, mas que no seu curto tempo de vida me ensinou a ser honesto, justo, ser firme quando as circunstâncias exigem firmeza, sempre ser solidário e ser corajoso para enfrentar as adversidades da vida.

Aos meus irmãos, Gabriella e Guilherme, pelo companheirismo, pela união, pela amizade fraternal.

À Universidade Federal de Viçosa, por proporcionar muitos amigos e um ambiente bonito e agradável para um aprendizado de qualidade e ampliação do meu conhecimento.

Ao Programa de Pós-Graduação em Bioquímica Aplicada, pela oportunidade de realização do curso e por oferecer todas as condições possíveis para uma formação acadêmica de qualidade.

Ao Instituto de Biotecnologia Aplicada à Agropecuária (BIOAGRO) e seus funcionários, por fornecer a estrutura e as condições para a realização deste trabalho.

À Coordenação de Aperfeiçoamento de Pessoal de Nível Superior (CAPES), pela bolsa de estudos concedida, pois sem este auxílio seria impossível cursar o doutorado e executar esta pesquisa. Desejo que estes tempos obscuros de desvalorização da educação e da pesquisa sejam passageiros e que outros estudantes tenham a oportunidade de receber essas bolsas que mantêm viva a ciência no Brasil.

Ao Conselho Nacional de Desenvolvimento Científico e Tecnológico (CNPq) por financiar este projeto de pesquisa e possibilitar as condições materiais para a realização deste trabalho.

À Professora Valéria Monteze Guimarães, por me orientar com dedicação e atenção, por sempre confiar no meu potencial e me tratar com muito carinho e respeito, por direcionar minha caminhada durante o doutorado e o desenvolvimento desta pesquisa, pelo respeito as minhas limitações e incentivo

a ampliação do meu conhecimento e contribuição para meu amadurecimento como pesquisador, por ser um exemplo de professora que defende e luta pela defesa de uma educação pública de qualidade e acessível a todos, por sua ética e dignidade, mas principalmente por seu olhar humano para com todos. Agradeço o apoio e compreensão nos momentos difíceis e as risadas nos momentos alegres no decorrer dos quase 10 anos que tive o privilégio de tê-la como professora e orientadora.

Ao Professor Sebastião Tavares de Rezende por ter me concedido a minha primeira bolsa de iniciação científica, a disponibilizar seu laboratório para o desenvolvimento da minha pesquisa e por sempre me tratar com muito carinho e atenção.

Ao Professor Tiago, pela coorientação, pela paciência, dedicação e amizade, e por aceitar participar da banca examinadora.

À Professora Gabriela, a doutora Rafaela e ao professor William, por aceitarem participar da banca examinadora e por toda contribuição neste trabalho e em minha formação.

À minha querida estagiária Riziane, sempre muito competente, prestativa, inteligente, eficiente e divertida. O trabalho ficou menos árduo e mais agradável com sua companhia e ajuda.

Ao meu amigo e colega de trabalho Túlio, sem sua ajuda este trabalho não seria realizado. Agradeço a ajuda nos experimentos, a troca de conhecimentos e discussão de ideias durante esses anos de laboratório, ao aprendizado teórico e prático compartilhado sempre com muita paciência e atenção, e a companhia nestes anos de doutorado.

A minha amiga Roberta, pela amizade de muito tempo e que só aumentou durante os anos, pelo apoio incondicional, pela ajuda nos experimentos, pela companhia dentro e fora do laboratório, pelos ótimos conselhos, pelas risadas e pelos cafés, e por dividir a carga e o peso do doutorado que cai sobre nós.

Aos meus amigos do Laboratório de Análises Bioquímicas, os que já passaram e os que ainda estão por lá, mas que fizeram parte em algum momento do meu aprendizado. Agradeço aos meus amigos Tiago, Ednilson, Marcele, Amanda, Bella, Mari, Polly, Camila, Elisa, Rafa Ladeira, Yan, Luiz, Marina e Lílian. Trabalhar neste laboratório sempre foi prazeroso, tornando meu trabalho mais produtivo e leve.

Aos amigos do laboratório de Biologia Molecular e Filogeografia, em especial a Rafa Ventorim, sempre muito prestativa.

À minha amiga Lari, pela companhia e amizade sincera de mais de 10 anos.

A todos os meus amigos da graduação em Bioquímica e da pós-graduação, pela companhia descontraída, pela diversão e amizade.

Aos amigos que fiz durante todos esses anos na UFV.

Aos meus amigos do alojamento, em especial aos amigos do 2011. Pelo companheirismo, convivência sempre em harmonia, pelo ambiente agradável de moradia, pelas risadas, diversão e aprendizado.

Ao RU, que me alimentou todos esses anos, não era tão bom quanto a comida feita pela minha mãe, mas me alimentou com qualidade e de forma digna.

A todos os professores que ajudaram na minha formação acadêmica.

A Deus, por cuidar de mim e da minha família.

A todos que contribuíram, direta e indiretamente, para a realização deste trabalho.

Muito obrigado!

BIOGRAFIA

Murillo Peterlini Tavares, filho de Wilson Tavares e Adriana de Cássia Peterlini Tavares, nasceu na cidade de São Paulo, estado de São Paulo, em 29 de maio de 1990.

Em fevereiro de 2009 iniciou seus estudos no curso de bacharelado em Bioquímica, pela Universidade Federal de Viçosa (UFV), Minas Gerais.

De setembro de 2012 a agosto de 2013 participou do programa sanduíche Ciências Sem Fronteiras em que cursou um ano de sua graduação no curso de licenciatura em Bioquímica da Universidade Nova de Lisboa (FCT- UNL), em Portugal.

Em janeiro de 2015, graduou-se no curso de bacharelado em Bioquímica, pela UFV.

Em fevereiro de 2015 ingressou no Programa de Pós-Graduação, em nível de Doutorado em Bioquímica Aplicada na UFV, sob a orientação da Profa. Valéria Monteze Guimarães.

Em julho de 2019 concluiu os requisitos necessários para obter o título de *Doctor Scientiae*, no dia 08 de julho, com defesa de tese intitulada: "Desvendando o secretoma do fungo fitopatogênico *Chrysoporthe cubensis* LPF-1 cultivado em biomassa lignocelulósica como potencial fonte de enzimas para produção de bioetanol".

RESUMO

TAVARES, Murillo Peterlini, D.Sc., Universidade Federal de Viçosa, julho de 2019. **Desvendando o secretoma do fungo fitopatogênico *Chrysoporthe cubensis* LPF-1 cultivado em biomassa lignocelulósica como potencial fonte de enzimas para produção de bioetanol**. Orientador: Valéria Monteze Guimarães. Coorientadores: Tiago Antônio de Oliveira Mendes e Marina Quádrio Raposo Branco Rodrigues.

A crescente preocupação com a escassez de combustíveis fósseis e o aumento da emissão de gases do efeito estufa, tem resultado no aumento do interesse em nível global por fontes de energia alternativas que sejam sustentáveis. Esforços têm sido feitos para atingir esses objetivos, como o desenvolvimento de tecnologias que utilizam a biomassa de resíduos agroindustriais para a produção de biocombustíveis. Nesse contexto, o Brasil se destaca como o maior produtor de cana-de-açúcar do mundo. A utilização da biomassa lignocelulósica proveniente do bagaço de cana-de-açúcar para a produção de etanol de segunda geração torna-se uma alternativa promissora para a redução dos impactos ambientais provenientes do uso de combustíveis fósseis. Considerando o processo de conversão bioquímica de biomassa em etanol, a hidrólise enzimática é normalmente referida como a etapa limitante, devido ao custo elevado de enzimas comerciais. Dessa forma, o desenvolvimento de bioprocessos para produção das enzimas *on-site* e estratégias para aumentar o rendimento final da hidrólise enzimática são necessários para assegurar que a conversão de biomassa se torne financeiramente viável em etapas de produção em larga escala. Uma vez que o extrato enzimático do fungo fitopatogênico *Chrysoporthe cubensis* LPF-1 apresentou elevada eficiência para sacarificação da biomassa lignocelulósica em diferentes abordagens, tornou-se essencial conhecer detalhadamente as enzimas e proteínas secretadas por este fungo, especialmente aquelas envolvidas na hidrólise de biomassa. Para tanto, o objetivo deste trabalho foi caracterizar pela primeira vez os perfis proteicos produzidos e secretados por *C. cubensis* crescido em estado semi-sólido tendo o farelo de trigo ou bagaço de cana-de açúcar como fontes de carbono, e realizar a integração de predições *in silico* obtidas por ferramentas computacionais com os dados de proteômica obtidos por espectrometria de massas. A integração dos resultados computacionais com os dados proteômicos possibilitou o aumento da identificação das proteínas secretadas e a previsão de todo o potencial de secreção do fungo que pode ser induzido por outras fontes de carbono ou condições de cultivo, evidenciando seu real potencial como microrganismo produtor de lignocelulases.

O presente trabalho demonstrou que *C. cubensis* foi capaz de secretar um maior número e variedade de enzimas ativas em carboidratos do que microrganismos reconhecidamente consideradas excelentes fontes de enzimas industriais, como os fungos do gênero *Aspergillus* e *Penicillium*. Também foi observado que *C. cubensis* apresentou composição do secretoma com características exclusivas de acordo com a fonte de carbono ao qual foi cultivado, revelando uma grande plasticidade no perfil de secreção enzimática do fungo. *C. cubensis* é capaz de produzir diferentes coquetéis enzimáticos eficientes que podem ser aplicados em uma variedade de biomassas lignocelulósica com características distintas, o que normalmente não é encontrado em produtos comerciais que possuem composição definida e aplicação restrita às biomassas comumente utilizadas. Além disso, *C. cubensis* foi capaz de secretar famílias de enzimas que têm sido extensivamente estudadas como alvos de grande interesse biotecnológico, como as oxidases de multi-cobre (MCOs). *C. cubensis* foi capaz de secretar duas MCOs quando cultivado em uma mistura de farelo de trigo e casca de laranja na proporção 3:1. A fração purificada contendo as duas MCOs catalisou a oxidação dos compostos fenólicos produzidos pelo pré-tratamento alcalino do bagaço de cana-de-açúcar, o que resultou em melhores rendimentos de sacarificação deste material, demonstrando serem enzimas promissoras para aplicações em hidrólise de biomassa e de grande potencial biotecnológico. Dessa forma, *C. cubensis* emerge como alternativa promissora para a produção de enzimas lignocelulolíticas clássicas e como fonte de novos alvos enzimáticos para a indústria de bioetanol.

ABSTRACT

TAVARES, Murillo Peterlini, D.Sc., Universidade Federal de Viçosa, July, 2019. **Unraveling the secretome of phytopathogenic fungus *Chrysoporthe cubensis* LPF-1 grown on lignocellulosic biomass as a potential source of enzymes for bioethanol production**. Adviser: Valéria Monteze Guimarães. Co-advisers: Tiago Antônio de Oliveira Mendes and Marina Quádrio Raposo Branco Rodrigues.

The growing worldwide concern over the shortage of fossil fuels and the increase in emissions of greenhouse gases have resulted in an increased global interest for sustainable and alternative energy sources. Efforts have been made to achieve these goals, such as the development of technologies that use biomass from agricultural residues for the production of biofuels. In this context, Brazil stands out as the largest producer of sugarcane in the world. The use of lignocellulosic biomass from the sugarcane bagasse for second-generation ethanol becomes a promising alternative for the reduction of environmental impacts from the use of fossil fuels. Concerning the biochemical process of converting biomass to ethanol, the enzymatic hydrolysis is usually referred to be the limiting step because of the high cost of commercial enzymes. Thus, the development of bioprocesses for the production of *on-site* enzymes and strategies to increase the final yield of enzymatic hydrolysis are necessary to ensure that biomass conversion becomes financially feasible in large-scale production steps. Since the enzymatic extract of the phytopathogenic fungus *Chrysoporthe cubensis* LPF-1 showed high efficiency for saccharification of the lignocellulosic biomass in different approaches, it became essential to know in detail the enzymes and proteins secreted by this fungus, especially those involved in the hydrolysis of biomass. The aim of this work was to characterize for the first time the protein profiles produced and secreted by *C. cubensis* after growth in semi-solid media having the wheat bran or sugarcane bagasse as carbon sources and to perform the integration of *in silico* predictions obtained by computational tools with proteomic data obtained by mass spectrometry. The integration of the computational results with the proteomic data allowed the increase of the identification of the secreted proteins and the prediction of a complete secretion potential of the fungus that can be induced by other carbon sources or cultivation conditions, evidencing its real potential as a microorganism that produces lignocellulolytic enzymes. The present work demonstrated that *C. cubensis* is able to secrete a greater number and variety of carbohydrate-active enzymes than microorganisms recognized excellent sources of industrial enzymes, as fungi of the genus *Aspergillus* and *Penicillium*. It was also observed that *C. cubensis* presented a secretome composition with exclusive characteristics according to the carbon source to which it was

cultivated, revealing the great plasticity in the profile of enzymatic secretion by the fungus. *C. cubensis* is capable to produce different enzymatic cocktails that can be applied in a variety of lignocellulosic biomasses with distinct characteristics, which cannot be found in commercial products that have a defined composition and a restricted application to the commonly used biomasses. In addition, this fungus was able to secrete families of enzymes that have been extensively studied as targets of great biotechnological interest, such as multi-copper oxidases (MCOs). *C. cubensis* was able to secrete two MCOs when grown in a mixture of wheat bran and orange peel in the ratio of 3:1. The purified fraction containing two MCOs catalyzed the oxidation of the phenolic compounds produced by the alkaline pretreatment of sugarcane bagasse, which resulted in improved saccharification yields of this material, demonstrating that they are promising enzymes for hydrolysis applications of biomass and of great biotechnological potential. In this way, *C. cubensis* emerges as a promising alternative for the production of classical lignocellulolytic enzymes and as a source of new enzymatic targets for the bioethanol industry.

SUMÁRIO

INTRODUÇÃO GERAL

A crescente preocupação com a escassez de combustíveis fósseis, o aumento da emissão de gases do efeito estufa e a poluição do ar pela combustão incompleta, tem resultado no aumento do interesse por fontes de energia alternativas que sejam sustentáveis e limpas. Na Conferência entre as Partes sobre o Clima (COP 21) realizada em Paris (2015), 195 países adotaram o primeiro acordo universal para a luta contra as alterações climáticas e o aquecimento global, além de estabelecer que devam ser feitos esforços para que haja redução das emissões de gases do efeito estufa, de maneira que não ameace a produção de alimentos (BRASIL, 2015). Cabe ressaltar que o Brasil é signatário do acordo e firmou um compromisso internacional de reduzir em 37% as emissões até 2025, e reduzir em 43% as emissões até 2030, com base nos dados de 2005 (BRASIL, 2015).

Frente ao problema observado, esforços têm sido feitos para atingir esses objetivos, como o desenvolvimento de tecnologias que utilizam a biomassa de resíduos agroindustriais como matéria-prima para a produção de biocombustíveis. Dentro desse cenário, o Brasil se destaca como o maior produtor de cana-de-açúcar do mundo. Na safra 2017/2018 produziu 641.066 mil toneladas, sendo 596.330 mil toneladas somente na região centro-sul (UNICA, 2018). Sabe-se também que as usinas de açúcar e etanol geram de 195 a 315 Kg de bagaço por tonelada de cana-de-açúcar (NETO et al., 2011). Logo, seguindo a tendência mundial, a indústria sucroalcooleira brasileira tem manifestado interesse em tecnologias sustentáveis que possam ser agregadas à sua cadeia produtiva. Benefícios econômicos, sociais e ambientais são esperados como consequência. Nesse contexto, a utilização da biomassa lignocelulósica proveniente do bagaço de cana-de-açúcar para a produção de etanol de segunda geração torna-se uma alternativa promissora para a redução dos impactos ambientais provenientes do uso de combustíveis fósseis.

A biomassa lignocelulósica é a mais abundante e também a maior fonte de carbono renovável do nosso planeta e, assim, sua conversão apresenta vantagens significativas sobre outras estratégias de energia alternativa (DASHTBAN; SCHRAFT; QIN, 2009). Considerando o processo completo de conversão bioquímica de biomassa lignocelulósica em etanol, a hidrólise enzimática é normalmente referida como a etapa limitante, devido ao custo elevado de enzimas comerciais. A degradação enzimática da lignocelulose requer a ação combinada de celulases, hemicelulases e ligninases que atuam em sinergismo promovendo a liberação de hexoses e pentoses para a subsequente fermentação. Coquetéis enzimáticos comerciais utilizados para a sacarificação de

materiais lignocelulósicos apresentam uma eficiência abaixo do ideal para uma produção comercial em larga-escala. Diante deste quadro, é necessária uma prospecção contínua por microrganismos celulolíticos que sejam capazes de produzir glicosil hidrolases e componentes acessórios em grande quantidade, em proporções balanceadas e que promovam a degradação de biomassa lignocelulósica eficientemente.

Fungos fitopatogênicos têm sido utilizados para a produção de enzimas celulolíticas, entretanto, poucos estudos têm abordado uma análise mais abrangente quanto à identidade e função deste conjunto de enzimas extracelulares, o secretoma. Avanços nas técnicas de análises proteômicas e de bioinformática tem possibilitado o aumento do número de investigações do secretoma de muitos fungos filamentosos, sendo essas análises indispensáveis para o conhecimento da identidade, função e interação do arsenal de enzimas extracelulares que participam da degradação de biomassa lignocelulósica.

Nessa conjuntura, trabalhos recentes mostraram que o fungo fitopatogênico *Chrysoporthe cubensis*, quando cultivado sob fermentação em estado sólido usando farelo de trigo como fonte de carbono, apresenta grande capacidade para produção de enzimas com alta eficiência para hidrólise da biomassa lignocelulósica, comparado aos coquetéis enzimáticos comerciais. O extrato de *C. cubensis* apresentou atividades enzimáticas específicas elevadas principalmente em relação a endoglucanase (331,84 U/mg de proteína), β-glicosidase (29,48 U/mg de proteína), β-xilosidase (2,95 U/mg de proteína), pectinase (127,46 U/mg de proteína) e lacase (2,49 U/mg de proteína). O estudo comparativo de sacarificação do bagaço de cana pré-tratado com 1% (m/v) de H_2SO_4 ou 1% (m/v) de NaOH, usando carga de 8% (m/v) de sólidos e 10 U FPase/g de bagaço e o extrato enzimático de *C. cubensis,* e três misturas enzimáticas comerciais mostrou que o extrato de *C. cubensis* promoveu maior liberação de glicose e xilose (FALKOSKI et al., 2013; MAITAN-ALFENAS et al., 2015).

Estudos adicionais demonstraram que o *blend* enzimático produzido a partir dos fungos *Chrysoporthe cubensis* e *Penicillium pinophilum* 50:50 (v/v) apresentou sinergismo, especialmente para as atividades de FPase e endoglucanase, que foram 76% e 48% maiores do que o teórico, respectivamente. Esta mistura de enzimas aplicada ao bagaço de cana previamente submetido ao pré-tratamento alcalino promoveu eficiência de hidrólise de glucana de 60% e conversão de xilana superior a 90%. O aumento da temperatura de hidrólise de 45 ºC para 50 °C também resultou num aumento de 16 - 20% na conversão de glucana e xilana. A mistura dos extratos enzimáticos exibiu grande potencial de aplicação no processo de hidrólise da lignocelulose (VISSER et al., 2013).

Posteriormente, estudos de reciclagem das enzimas presentes no *blend* enzimático de *C. cubensis* e *P. pinophilum* indicaram potencial para aplicação na sacarificação do bagaço de cana-de-açúcar. Verificou-se que a mistura das enzimas de *C. cubensis* e *P. pinophilum* foi eficiente para a hidrólise enzimática desta biomassa, e que uma parte significativa da atividade das enzimas pode ser recuperada por reciclagem da fração insolúvel. Valores de produtividade de enzimas (g de glicose/mg proteína enzimática) em todos os períodos de reciclagem foram de 2,4 e 3,7 para a aplicação de 15 e 30 de FPU/g de glucana, representando um aumento de mais de dez vezes ao obtido em um processo em batelada com a mesma mistura de enzimas e um aumento ainda maior em comparação com as celulases comerciais. A utilização de toda a fração de sólidos insolúveis foi suficiente para permitir a reciclagem das enzimas aderidas à biomassa, o que é um indicativo do método ser eficaz para aumentar a produtividade das enzimas (VISSER et al., 2015).

Uma vez que o extrato enzimático de *C. cubensis* apresentou elevada eficiência para sacarificação da biomassa lignocelulósica em diferentes abordagens, torna-se essencial conhecer detalhadamente as enzimas e proteínas secretadas por este fungo, especialmente aquelas envolvidas na hidrólise da biomassa vegetal. O estudo do secretoma permite não só a identificação do arsenal de enzimas e proteínas produzidas pelo *C. cubensis* quando cultivado nas condições definidas, mas também fornece informações qualitativas e quantitativas das proteínas de interesse e possibilita a compreensão dos mecanismos hidrolíticos e oxidativos para a sacarificação eficiente do bagaço de cana-de-açúcar.

Dessa forma, o presente estudo abordou aspectos relacionados a estratégias para a redução do custo das enzimas celulolíticas desde a etapa de produção "*on-site*"; predição das proteínas potencialmente secretadas utilizando técnicas computacionais; caracterização do coquetel enzimático secretado pelo fungo *Chrysoporthe cubensis* cultivado em diferentes fontes de carbono; aplicação na sacarificação da biomassa vegetal; e estudo detalhado de uma família de enzimas promissoras, as oxidases de multi-cobre, com interesse biotecnológico na detoxificação de compostos fenólicos oriundos do pré-tratamento alcalino de biomassa lignocelulósicas.

A integração dos resultados computacionais com os dados proteômicos proporciona economia de tempo e auxilia na identificação de enzimas e proteínas auxiliares secretadas pelo fungo, com potencial interesse para sacarificação de biomassa lignocelulósica, contribuindo para melhor compreensão das bases moleculares do sistema hidrolítico de *C. cubensis*. Os conhecimentos adquiridos com o estudo do secretoma de

C. cubensis permitem aprimorar as propriedades do coquetel enzimático deste fungo, tornando-o mais vantajoso e eficiente para aplicação industrial.

Assim, o objetivo geral deste trabalho consiste em desvendar as potencialidades do arsenal enzimático do *Chrysoporthe cubensis* LPF-1, mostrando-o como alternativa para a produção de coquetéis de baixo custo ou como fonte de novas enzimas para suplementação de produtos comerciais já estabelecidos e, dessa forma, contribuir para a pesquisa relacionada à produção de etanol de segunda geração. A tecnologia gerada com esta pesquisa está inserida no contexto internacional de sustentabilidade e de demandas pelo aprimoramento de tecnologias que possibilitem ultrapassar os desafios no processo de conversão do material lignocelulósico em açúcares fermentescíveis para a produção de etanol de segunda geração.

A tese de doutorado aqui apresentada foi dividida em quatro capítulos. No capítulo 1 é apresentada uma revisão bibliográfica atualizada sobre os principais conceitos abordados e informações importantes que serão necessários para a compreensão dos próximos capítulos da tese. Os demais capítulos foram escritos no formato de artigo científico na língua inglesa de acordo com as regras das revistas aos quais serão posteriormente submetidos. O capítulo 2 traz os resultados de um estudo comparativo entre o secretoma predito de *Chrysoporthe cubensis*, utilizando ferramentas computacionais, com o secretoma experimental de *C. cubensis* cultivado em meio semi-sólido, tendo o farelo de trigo como fonte de carbono. Este estudo possibilitou a comparação de todo o potencial predito de secreção do fungo em relação às enzimas ativas em carboidrato e as enzimas secretadas de fato em uma fonte de indução padrão. Estes resultados foram submetidos na forma de artigo científico para a revista Bioresource Technology, cumprindo as exigências do Programa de Pós-graduação em Bioquímica Aplicada.

O capítulo 3 refere-se a um estudo do secretoma experimental do fungo *C. cubensis* quando cultivado em duas fontes de carbono distintas, farelo de trigo e bagaço de cana-de-açúcar. Neste estudo foi possível a realização de análises quantitativas das proteínas presentes em cada extrato enzimático, analisar as diferenças em termos de composição e de diversidade, além de possibilitar a compreensão das principais diferenças e do potencial que cada extrato bruto apresenta para a sacarificação de diferentes biomassas lignocelulósicas.

No capítulo 4, foi realizado estudos aprofundados de todos os membros de uma família de enzimas auxiliares de grande interesse biotecnológico. A família de enzimas de atividades auxiliares 1 (AA1) de *C. cubensis*, constituída por enzimas de multi-cobre

(MCOs). Posteriormente, essas enzimas foram induzidas, produzidas, parcialmente purificadas e aplicadas na oxidação de compostos fenólicos formados durante o pré-tratamento do bagaço-de-cana.

No final da tese são apresentadas as conclusões gerais do trabalho desenvolvido no presente doutorado.

REFERÊNCIAS

BRASIL. Política Nacional sobre Mudança do Clima – PNMC, 2015. Disponível em: <http://www.planalto.gov.br/ccivil_03/_ato2007-2010/2009/lei/l12187.htm>. Acesso em: 15 de maio de 2019.

DASHTBAN, M.; SCHRAFT, H.; QIN, W. Fungal bioconversion of lignocellulosic residues; Opportunities & perspectives. **International Journal of Biological Sciences**, v. 5, n. 6, p. 578–595, 2009.

FALKOSKI, D. L. et al. *Chrysoporthe cubensis*: A new source of cellulases and hemicellulases to application in biomass saccharification processes. **Bioresource Technology**, v. 130, p. 296–305, 2013.

MAITAN-ALFENAS, G. P. et al. The influence of pretreatment methods on saccharification of sugarcane bagasse by an enzyme extract from *Chrysoporthe cubensis* and commercial cocktails: A comparative study. **Bioresource technology**, v. 192, p. 670–6, set. 2015.

NETO, H. F. D. S. et al. Produção e produtividade de bagaço da cana-de-açúcar ao longo da safra, visando a cogeração de energia. **Enciclopédia Biosfera**, v. 7, n. 12, p. 8, 2011.

UNICA. Relatório final da safra 2017/2018. Região Centro-Sul, 2018. Disponível em: <http://www.unicadata.com.br/listagem.php?idMn=88>. Acesso em: 15 de maio de 2019.

VISSER, E. M. et al. Production and application of an enzyme blend from *Chrysoporthe cubensis* and *Penicillium pinophilum* with potential for hydrolysis of sugarcane bagasse. **Bioresource Technology**, v. 144, p. 587–594, 2013.

VISSER, E. M. et al. Increased enzymatic hydrolysis of sugarcane bagasse from enzyme recycling. **Biotechnology for Biofuels**, v. 8, n. 1, p. 1–9, 2015.

CAPÍTULO 1

1. REVISÃO BIBLIOGRÁFICA

1.1. Biomassa lignocelulósica

A biomassa lignocelulósica é o material mais abundante presente na Terra e é composto principalmente por celulose, hemicelulose, lignina e pectina. Em combinação com enzimas associadas à parede celular vegetal, proteínas estruturais e proteoglicanos, estes componentes formam uma rede intrincada capaz de fornecer resistência para a parede celular vegetal (POPPER et al., 2011).

Alguns exemplos de biomassa, como os resíduos agrícolas e florestais, são compostos por cerca de 70% de carboidratos (celulose, hemicelulose e pectina), os quais podem ser hidrolisados em monômeros de açúcar que servem como matéria-prima para a produção de compostos bioquímicos e combustíveis com elevado interesse industrial, como etanol, metanol, ácido lático e outros (RAVINDRAN; ADAV; SZE, 2012). O Brasil é o segundo maior produtor de etanol no mundo, que é produzido da fermentação do suco extraído da cana-de-açúcar. Tendo em vista a grande produção de bagaço de cana, a agregação de valor a esse resíduo através da sacarificação enzimática para a produção de bioetanol de segunda geração (**Fig. 1**), tem surgido como uma alternativa para o aumento da produtividade e, consequentemente, da receita da indústria sucroalcooleira (DE SOUZA et al., 2013). A biomassa lignocelulósica pode produzir até 50% mais etanol em comparação com as refinarias de primeira geração (HARRIS et al., 2014; LOSORDO et al., 2016).

Figura 1: Da biomassa ao etanol celulósico. Em destaque, algumas etapas fundamentais da produção em grande escala de etanol celulósico (2G) (US DOE, 2007).

Entretanto, o uso dessa biomassa apresenta um grande desafio devido à estrutura complexa da parede celular vegetal, sendo necessário diversos tipos de enzimas para sua hidrólise. Essas enzimas representam a maior parte dos custos associados a produção de bioetanol 2G. A redução dos custos do processo de sacarificação pode ser atingida através da compreensão de mecanismos hidrolíticos e de secreção de enzimas de microrganismos que hidrolisam polissacarídeos (BORIN et al., 2015). Para manter os custos de produção de etanol dentro de uma faixa favorável, a contribuição de custo das enzimas na produção de etanol de segunda geração deve ser menor que 0,4 dólares/galão de etanol (0,1 dólar/litro de etanol) (VALDIVIA et al., 2016). Os custos de produção de açúcar celulósico (aproximadamente 100 dolares/tonelada) seriam ideais caso atingissem um preço mínimo de venda de etanol menor do que 2 dolares/galão (0,53 dólares/litro) (CHANDEL et al., 2019).

1.2. Enzimas lignocelulolíticas

Uma grande variedade de enzimas com diferentes especificidades é requerida para a completa despolimerização dos componentes da lignocelulose. A hidrólise enzimática de carboidratos de plantas emerge como a tecnologia mais proeminente para a conversão da biomassa em monômeros de açúcar e posterior fermentação para a produção de bioetanol. Estas enzimas atuam de maneira cooperativa e sinérgica, ou seja, a atividade das enzimas atuando juntas é maior do que a adição de suas atividades individuais.

Para a hidrólise completa da celulose é requerida a ação sinérgica de quatro tipos de celulases: endoglucanases (EC 3.2.1.4), celobiohidrolases (EC 3.2.1.176), exoglicohidrolases (EC 3.2.1.74) e β-glicosidases (EC 3.2.1.21) (**Fig. 2**). As endoglucanases atuam randomicamente catalisando a hidrólise de ligações glicosídicas β-1,4 internas nas cadeias de celulose, produzindo cadeias com extremidades livres para as celobiohidrolases e exoglicohidrolases, que liberam celobiose e glicose, respectivamente. As β-glicosidases hidrolisam celobiose em glicose (LYND et al., 2002). Outro grupo distinto são as polissacarídeos monooxigenases cobre-dependentes (LPMOs), anteriormente conhecida como proteínas GH61, que catalisam a clivagem oxidativa de ligações glicosídicas na superfície da celulose sem a necessidade de separação das cadeias de glucano, aumentando a acessibilidade do substrato para as enzimas hidrolíticas (BEESON et al., 2012).

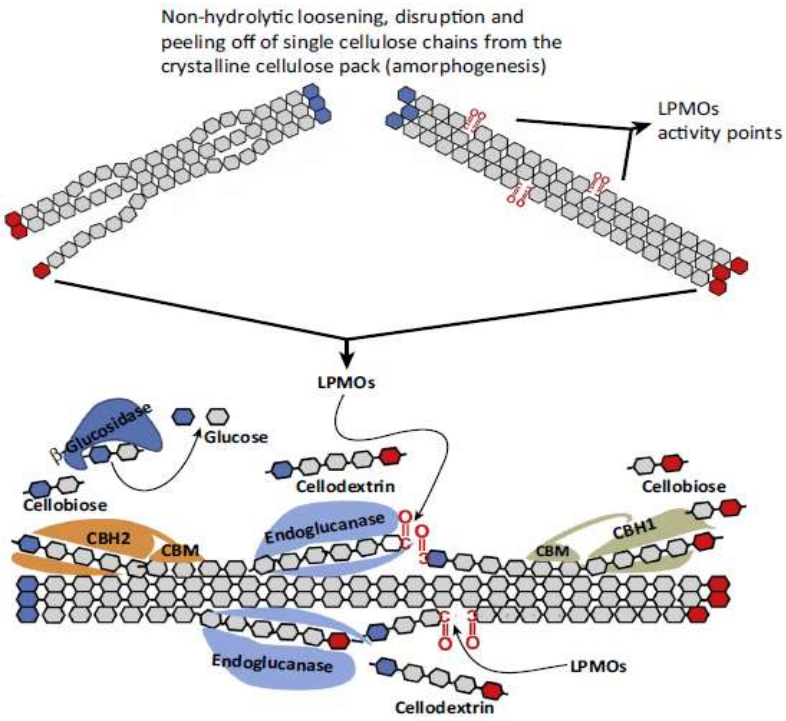

Figura 2: Clivagem oxidativa e hidrolítica da celulose cristalina a açúcares monoméricos por celulases clássicas e pelas mono-oxigenases líticas de polissacarídeos (LPMOs) (GUPTA et al., 2016).

Hemicelulose tem uma composição mais variada se comparada a celulose e, consequentemente, requer um elevado número de tipos de enzimas para ser hidrolisada eficientemente. Essas enzimas podem ser divididas em enzimas de despolimerização, que são responsáveis por agir na cadeia principal, e enzimas que atuam removendo os

substituintes. As principais enzimas que atuam na degradação da xilana são: endoxilanases, que clivam as ligações da xilana em oligossacarídeos curtos, e β-xilosidases, que clivam pequenos xilo-oligossacarídeos em xilose (**Fig. 3**). De maneira similar, as principais enzimas que atuam na degradação de mananas são as endomananases e as β-manosidases. Entretanto, tanto xilanas quanto mananas geralmente possuem diferentes substituintes ligados à cadeia principal, como arabinose, acetil, galactose e glicose, sendo necessária a atuação de enzimas desramificadoras que removam esses substituintes e permitam o acesso das enzimas que atuam nas cadeias principais. Algumas dessas enzimas auxiliares são: α-L-arabinofuranosidase, α-glucuronidase, ácido ferúlico esterase, α-galactosidase, feruroloil esterase, acetilxilana esterase e acetilmanana esterase (MEYER; ROSGAARD; SORENSEN, 2009) (**Fig. 3**).

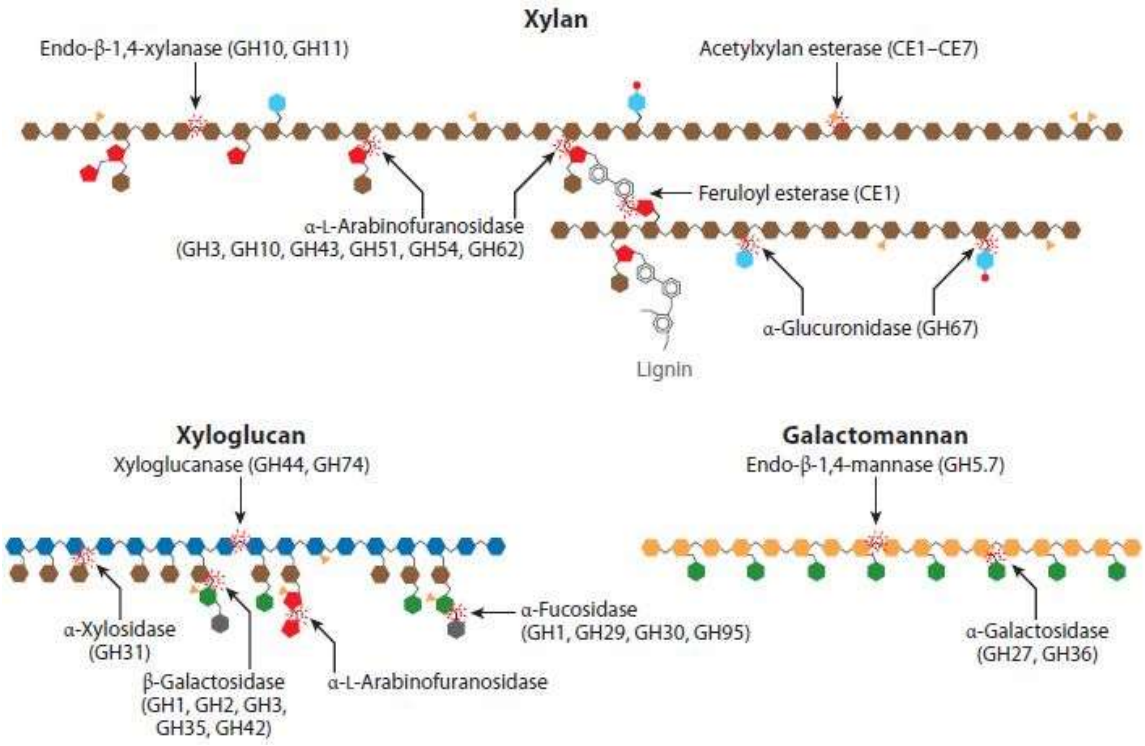

Figura 3: Enzimas envolvidas na clivagem dos principais polissacarídeos constituintes da hemicelulose (xilana, xiloglucana, galactomanana) (GLASS et al., 2013).

Entre todos os polissacarídeos da parede celular vegetal, a pectina tem a maior complexidade estrutural, sendo composta por 4 classes de polissacarídeos principais: homogalacturonanos (HG), ramnogalacturonanos I (RG-I), xilogalacturonanos (XG) e ramnogalacturonanos II (RG- II) (XIAO; ANDERSON, 2013). As enzimas que atuam sobre esses polissacarídeos são referidas como enzimas acessórias, sendo que um vasto grupo de enzimas atua em conjunto para a degradação eficiente da pectina. As principais

enzimas necessárias para a hidrólise de pectina são as glicosil hidrolases poligalacturonases, ramnogalacturonases; e as polissacarídeos-liases de pectina, pectato-liases, ramnogalacturonan liases; além das carboidrato esterases como metilesterases de pectina, acetilesterases de pectina e acetilesterases de ramnogalacturonano (GLASS et al., 2013). Entre as enzimas fundamentais para a despolimerização da cadeia lateral de RG-I estão as arabinanases, arabinosidases/α-arabinofuranosidases, α- e β-galactosidases, β-glucuronidases e feruloil esterases (GLASS et al., 2013) (**Fig. 4**).

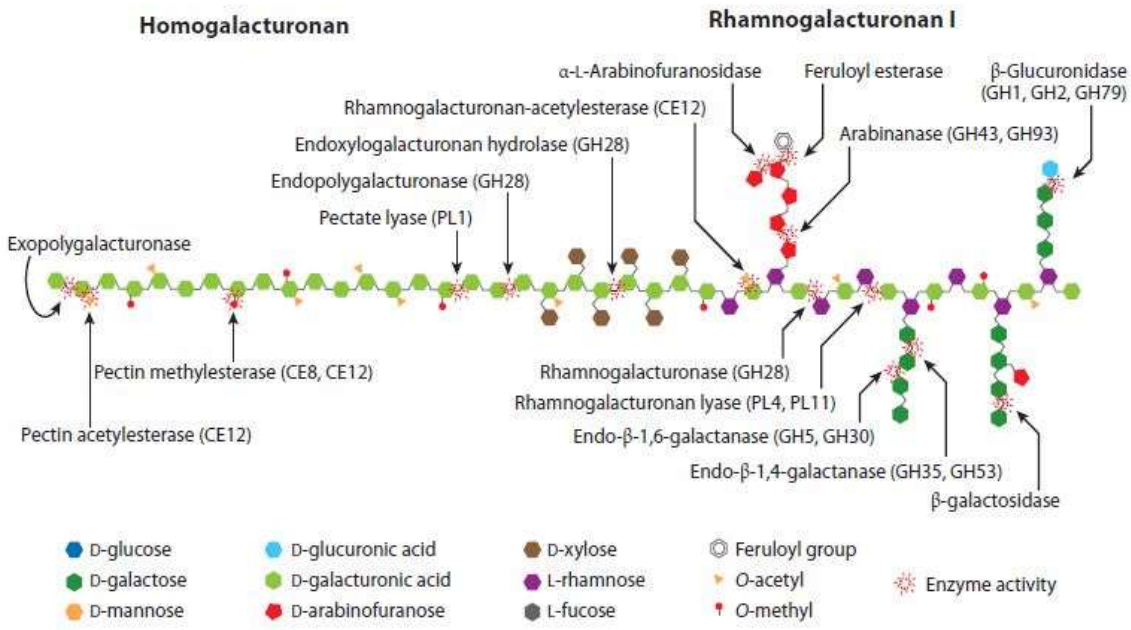

Figura 4: Enzimas envolvidas na clivagem dos principais polissacarídeos constituintes da pectina (homogalacturonanos e rhamnogalacturonanos I) (GLASS et al., 2013).

A despolimerização da lignina envolve uma ampla variedade de oxidases e peroxidases que são responsáveis pela geração de radicais livres altamente reativos e não-específicos (radicais arila e fenóxi) capazes de promover reações degradativas. As ligninas peroxidases (Lip), manganês peroxidases (MnP), peroxidases versáteis (VP), lacases e peroxidases de descoloração de corantes (DyP) são consideradas as enzimas oxidativas mais comuns e representativas do sistema lignolítico (ABDEL-HAMID; SOLBIATI; CANN, 2013) (**Fig. 5**).

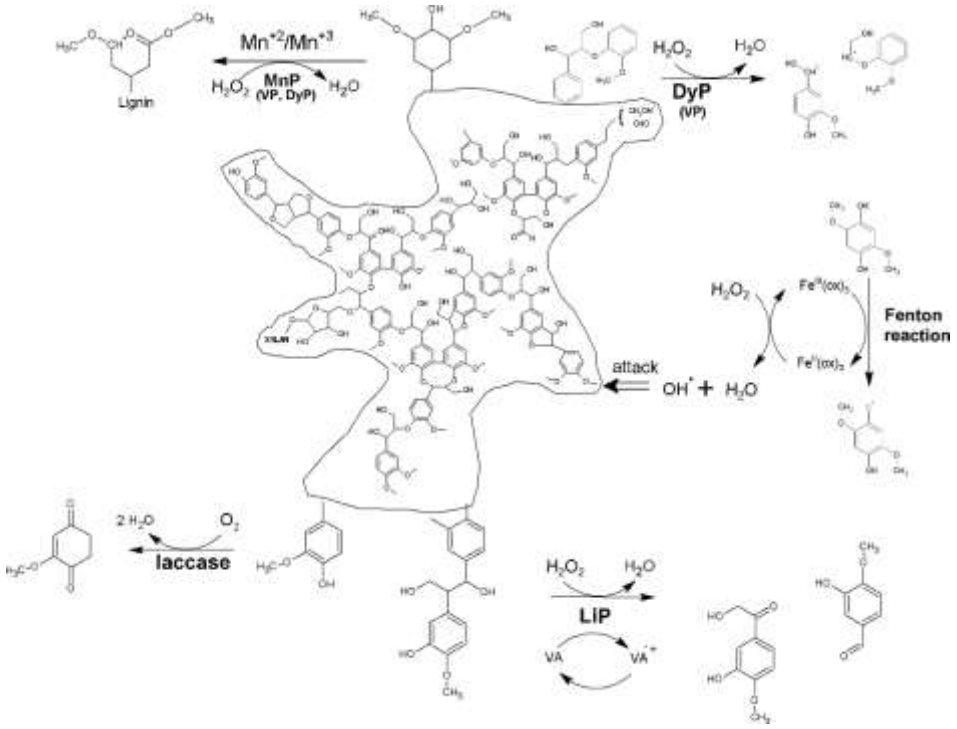

Figura 5: Comparação da degradação de lignina por peroxidases e lacase. MnP - peroxidase de manganês, VP - peroxidase versátil, LiP - peroxidase de lignina, DyP - peroxidase descolorante, ox oxalato, VA - álcool veratrílico. Entre parênteses, outras enzimas capazes de catalisar reações similares são apresentadas (JANUSZJ et al., 2017).

Recentemente, foram identificadas proteínas não hidrolíticas pertencentes a organismos celulolíticos. Estas proteínas podem ser utilizadas como fatores de aumento da atividade de celulases devido à capacidade de promoverem a desaglomeração da celulose através da separação das microfibrilas (ARANTES; SADDLER, 2010). Proteínas com função catalítica não caracterizada incluem as expansinas, swoleninas e loseninas, as quais aumentam a acessibilidade da celulose através do rompimento da rede de ligações de hidrogênio inter e intra-cadeia.

1.3. Fermentação em estado sólido

O processo de fermentação em estado sólido (SSF) pode ser definido como o cultivo de microrganismos em contato direto com um substrato insolúvel constituinte de uma matriz sólida úmida, sendo este substrato uma fonte de carbono e energia (HÖLKER; HÖFER; LENZ, 2004). Grande parte dos fungos ascomicetos e basidiomicetos isolados da natureza foram encontrados crescendo em substratos sólidos, com apenas poucas espécies isoladas de ambientes aquático. Dessa forma, a fermentação em estado sólido

tenta se aproximar das condições fisiológicas naturais do microrganismo e seu ambiente de crescimento (HÖLKER; HÖFER; LENZ, 2004).

Embora a maioria dos processos industriais de produção em larga escala de celulases por microrganismos utilize a tradicional fermentação submersa (SmF), nas últimas duas décadas a SSF vem conquistando o interesse devido a seus benefícios técnicos e econômicos em relação a SmF que incluem menor custo, produtividade volumétrica de enzimas superior, concentração de produtos relativamente alta, menor geração de efluentes, menor demanda de aeração, não requer agitação, equipamentos para a fermentação mais simples, menor risco de contaminação e minimização da repressão catabólica (CAMASSOLA; DILLON, 2007; SINGHANIA et al., 2010).

Os fungos são capazes de se adaptarem a diferentes condições de crescimento e ajustar seu metabolismo de acordo com as fontes de carbono e nitrogênio as quais foram submetidos (GIRARD et al., 2013). O conjunto de proteínas secretadas é modulado de maneira dinâmica de acordo com as condições de crescimento e as fontes nutritivas, possibilitando a degradação de substratos complexos fora da célula e posterior captação de moléculas menores (BIANCO; PERROTTA, 2015). A utilização de um meio sintético simples só permite a caracterização parcial das proteínas secretadas, entretanto, um meio complexo contribui para a secreção de um arsenal enzimático mais diversificado capaz de digerir quase na sua totalidade a parede celular vegetal (GIRARD et al., 2013).

Recentes estudos de caracterização do secretoma de fungos lignocelulolíticos têm utilizado com êxito o farelo ou a palha de trigo como substratos para obtenção de uma elevada e diversificada produção de celulases (ADAV; RAVINDRAN; SZE, 2011; SALVACHÚA et al., 2013). A alta capacidade do farelo de trigo em induzir eficientemente a produção de celulases pode estar relacionada com a sua composição contendo elevadas concentrações de proteínas (13-19%) e hemicelulose (mais de 30%), aliada a baixas concentrações de lignina (3-6%) (SUN et al., 2008). O baixo conteúdo de lignina permite maior digestibilidade do farelo de trigo se comparado a outras fontes ricas em celulose cristalina e lignina. O alto nível de hemicelulose fornece uma rica fonte de açúcares (hexoses, arabinose e xilose), os quais podem ser rapidamente metabolizados e favorecer o crescimento rápido de microrganismos. Além disso, acredita-se que a fragmentação inicial da hemicelulose do farelo de trigo libera oligossacarídeos capazes de induzir a síntese de enzimas hidrolíticas. O alto conteúdo de proteínas permite uma proporção de carbono e nitrogênio (C/N) balanceada, sendo uma característica determinante para o crescimento eficiente de microrganismos e obtenção de bioprodutos

específicos advindos da SSF (BRIJWANI; OBEROI; VADLANI, 2010; SUN et al., 2008).

1.4. *Chrysoporthe cubensis*

Muitos fungos fitopatogênicos produzem um arsenal de enzimas lignocelulolíticas extracelulares para romper a barreira da parede celular vegetal e obter nutrientes para sua sobrevivência, enquanto criam mecanismos para subverter as respostas de defesa da planta hospedeira (GIBSON et al., 2011). Isto sugere que estes microrganismos podem produzir quantidades significativas de enzimas com elevada eficiência catalítica de maneira estritamente regulada e coordenada, sendo considerados potenciais fontes de enzimas para a produção de biocombustíveis (GIBSON et al., 2011).

Chrysoporthe cubensis é um patógeno bem descrito de várias espécies de árvores localizadas em áreas tropicais e subtropicais (GRYZENHOUT et al., 2006). Este fitopatógeno pode causar sérios danos em plantações comerciais de espécies sensíveis e clones. Pode ser considerado o principal causador da doença de cancro em espécies de Eucalyptus, que resulta na formação de lesões profundas e bem definidas na região do caule, e ocasiona perdas de produtividade, qualidade e volume da madeira (GUIMARÃES et al., 2010). Em fungos fitopatogênicos existe uma estreita relação entre a capacidade de secretar elevados níveis de hidrolases e a virulência destes microrganismos (KIKOT; HOURS; ALCONADA, 2009). *C. cubensis* não é uma exceção a esta relação e é capaz de produzir elevadas concentrações de celulases e hemicelulases, principalmente β-glicosidades, xilanases e algumas enzimas acessórias de interesse (FALKOSKI et al., 2013; VISSER et al., 2013).

1.5. Proteômica de fungos filamentosos

O termo protêomica foi utilizado pela primeira vez em 1995 (WASINGER et al., 1995), e refere-se ao estudo do conjunto de proteínas expressas por uma célula, tecido ou organismo em uma condição específica (BHADAURIA et al., 2007). A proteômica possibilita a identificação e quantificação do número de proteínas em um contexto celular específico, além de tornar possível a análise do estado celular, alterações que ocorrem durante diferentes estágios de crescimento e desenvolvimento, ou interações e sinergismo de proteínas frente a uma resposta decorrente de fatores ambientais. Dessa forma, os avanços da proteômica mostram-se úteis no estudo de sistemas biológicos altamente complexos e dinâmicos (CHEN; HARMON, 2006).

Informações proteicas obtidas por técnicas de proteômica são particularmente relevantes em sistemas eucarióticos, como fungos degradadores de lignocelulose, pois fornecem uma nova compreensão sobre análises de localização-específica (subproteoma), além de trazer novos dados de modificações pós-traducionais importantes para a localização e atividade proteica, como por exemplo, fosforilação, glicosilação e presença de peptídeo-sinal (BIANCO; PERROTTA, 2015).

As metodologias empregadas em uma análise proteômica podem ser classificadas nos tipos *botton-up* (*shotgun*) e *top-down* (**Fig. 6**). A metodologia *botton-up* pode seguir duas estratégias distintas: a solução proteica complexa é seguida de uma etapa de pré-fracionamento *in-gel* e então realiza-se a etapa de digestão tríptica, ou a digestão ocorre diretamente na amostra proteica complexa, e os peptídeos proteolíticos são separados. As amostras tripsinizadas obtidas nas duas estratégias serão submetidas à cromatografia líquida (LC), seguida de análise por um sistema em que dois espectrômetros de massa são utilizados em sequência, separados por uma câmara de colisão (MS/MS) (ALFARO et al., 2014).

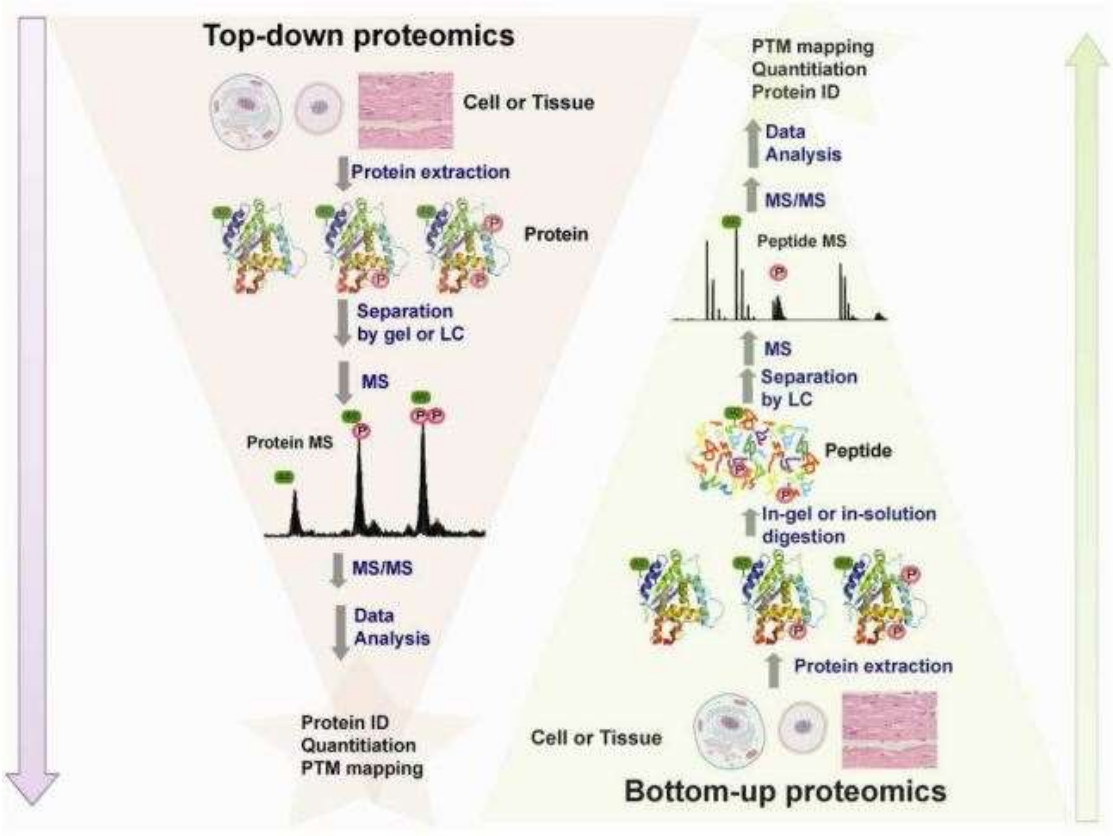

Figura 6: Ilustração esquemática das diferenças entre análises proteômicas dos tipos *botton-up* (*shotgun*), nas quais as proteínas não são submetidas a etapa de formação de peptídeos trípticos e permanecem intactas, e *top-down* (GREGORICH; CHANG; GE, 2014), nas quais a proteínas são fragmentadas em peptídeos na etapa de digestão *in-gel* ou em solução.

A proteômica tipo *top-down*, ao contrário, é um processo aplicado com sucesso na caracterização de proteínas intactas, que serão submetidas à análise por espectrometria de massas (MS). As abordagens *shotgun* possuem muitas vantagens, como sua execução simples, sensibilidade e reprodutibilidade, mesmo para proteomas complexos. No entanto, as respostas obtidas são fragmentos de um todo e, embora seja possível a identificação de uma proteína com base em poucos peptídeos, as modificações pós-traducionais não são reconhecidas, o que pode ser considerado uma limitação da técnica. Além disso, um peptídeo pode ser perdido durante a cromatografia ou não gerar espectros de massas adequados (ARMIROTTI; DAMONTE, 2010). Contudo, a metodologia *shotgun* ainda é reconhecida pela sua eficiência em identificar peptídeos com precisão por (MS) e sequenciá-los por (MS/MS), sendo a metodologia geralmente mais aplicada (ALFARO et al., 2014).

Em estudos de proteômica, a extração de proteínas e preparo da amostra representam etapas cruciais para o êxito das análises de espectrometria de massas. Fungos filamentosos podem conter cerca de 31% de proteínas em relação ao peso seco total, e são considerados um material biológico recalcitrante, o que torna a extração de proteínas um grande desafio. Em relação às proteínas secretadas por fungos filamentosos, as mesmas encontram-se em baixas concentrações no meio de cultura, geralmente 5-50 µg/mL (FRAGNER et al., 2009), além de estarem na presença de quantidades variáveis de metabólitos e compostos interferentes, como polissacarídeos, ácidos-graxos, materiais mucilaginosos, fenóis e outros compostos aromáticos, os quais interferem nas medições espectrofotométricas e promovem a superestimação da quantidade total de proteínas (KAO et al., 2008). Assim, diferentes procedimentos de extração, precipitação e solubilização são necessários para maximizar o rendimento de proteínas e suas posteriores identificações.

Muitas estratégias têm sido adotadas para aumentar a cobertura e detecção de proteínas secretadas por fungos, como trabalhos com protocolos de preparação de amostras de secretomas que consistem em deglicosilações por vias enzimáticas ou químicas (GÓMEZ-MENDOZA et al., 2014). Diferentes métodos de precipitação de amostras proteicas têm sido empregados para promover a concentração e purificação parcial dos extratos, como precipitação por fenol/metanol, ácido tricloroacético/acetona, clorofórmio/metanol ou etanol, e protocolos otimizados de precipitação por ácido tricloroacético/tampão de acetona a frio (FRAGNER et al., 2009). Alguns trabalhos de secretoma de fungos filamentosos têm reportado o uso de filtração (0,22 µm) das amostras, seguida de precipitação com TCA 10% à 4ºC, e

sucessivas lavagens com acetona a frio para clarificar o extrato do secretoma (ADAV et al., 2010). Outros autores optam por filtração dos extratos, seguidos de liofilização (ADAV et al., 2011; LIAO et al., 2014) ou diálise em sistemas de ultrafiltração tangencial (SALVACHÚA et al., 2013), com o objetivo de purificar as amostras de secretoma fúngico.

Em abordagens proteômicas *botton-up*, após as etapas de preparo e concentração das amostras, realiza-se as etapas de separação baseadas em gel ou livres de gel, com o objetivo de reduzir a complexidade da amostra biológica e os riscos de identificações equivocadas. Técnicas de separação baseadas em gel de eletroforese unidimensional (1D SDS-PAGE) ou bidimensional (2D) são métodos muito populares por serem robustos e simples (BIANCO et al., 2015) (**Fig. 7**).

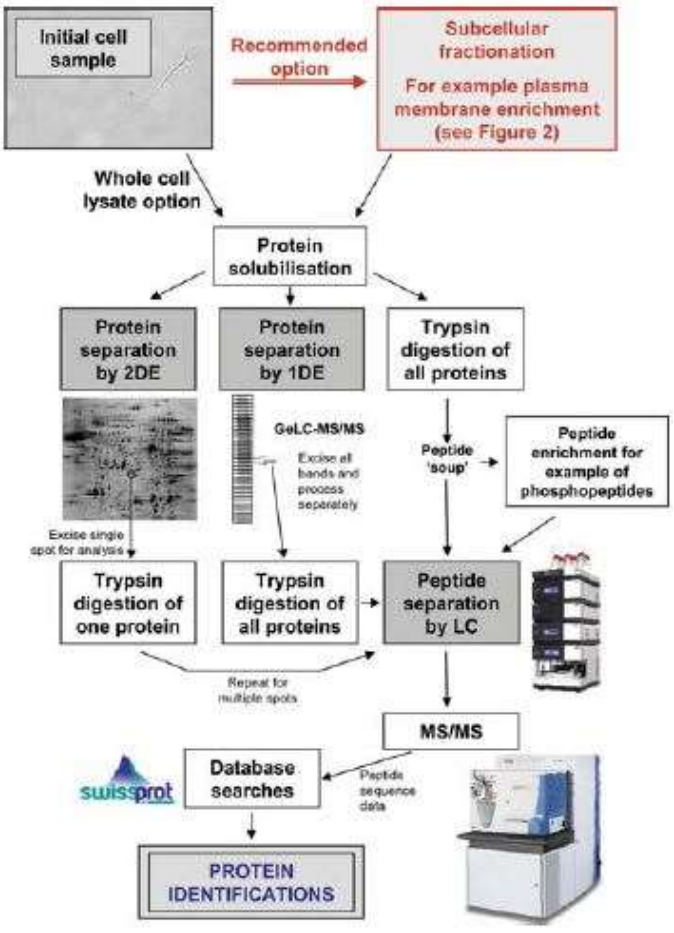

Figura 7: Estratégias de identificação do perfil global de amostras proteicas (BREWIS et al., 2010)**.**

A digestão de proteínas separadas por técnicas baseadas em gel é historicamente um procedimento chave para a facilitação da identificação de proteínas por espectrometria de massas. As vantagens de uma etapa de pré-fracionamento dos extratos proteicos utilizando o gel unidimensional (SDS-PAGE) incluem: completa solubilização da proteína pelo SDS, alta tolerância para sais, tampões e detergentes, além de uma digestão consistente por tripsina. Adicionalmente, o SDS-PAGE permite um nível intermediário de controle de qualidade (padrão de coloração por *Comassie)* antes da digestão in-gel (PIERSMA et al., 2013).

O gel bidimensional (2D) é a plataforma dominante em proteômica de fungos. A separação consiste em duas etapas eletroforéticas consecutivas. Na primeira dimensão, as proteínas são resolvidas de acordo com seus pontos isoelétricos (pIs), normalmente utilizando a técnica de focalização isoelétrica (IEF). Na segunda dimensão, as proteínas são submetidas a uma eletroforese com direção perpendicular à IEF em um gel desnaturante (SDS-PAGE), e então separadas de acordo com os pesos moleculares correspondentes (RABILLOUD et al., 2009). As principais vantagens do gel 2D são: elevada capacidade de separação e a possibilidade de realização de experimentos de perfis proteicos em larga escala. Entretanto, existem alguns aspectos desfavoráveis da técnica, como a baixa reprodutibilidade e pouca resolução de proteínas com baixa abundância e propriedades físico-químicas extremas, incluindo domínios transmembrana, ponto isoelétrico e tamanho (ISSAQ; VEENSTRA, 2008). A limitação das técnicas baseadas em gel tem conduzido ao recente desenvolvimento de abordagens baseadas na combinação da separação de proteínas por 1D SDS-PAGE seguido de digestão *in-gel* e separação das frações peptídicas por cromatografia líquida acoplada a espectrometria de massas (LC-MS/MS), técnica referida como GeLC-MS/MS (DZIECIATKOWSKA; HILL; HANSEN, 2014).

Diferentes campos de pesquisa têm adotado o uso da abordagem GeLC-MS/MS devido à capacidade em fornecer um elevado número de identificação de proteínas se comparado às técnicas usuais de trabalho em proteômica, além de promover uma eficiente identificação de proteínas hidrofóbicas e de baixo peso molecular, permitindo uma alta cobertura do proteoma (GAO; STUART; FEENER, 2008).

Embora caracterizados por massa molecular (e ponto isoelétrico no caso de gel 2D) e purificados ou fracionados por cromatografia líquida, os analitos necessitam de identificação por espectrometria de massas (CHEN, 2008). A técnica consiste na ionização de um composto e na avaliação da razão massa/carga (*m/z*) dos íons gerados.

O equipamento é composto por uma fonte de ionização, um ou mais analisadores de massas e um detector. O primeiro componente gera íons peptídicos ou proteicos transferindo prótons (H^+) para as moléculas sem alterar sua estrutura química. Os íons são acelerados por campo elétrico e separados por *m/z* no analisador de massas, ou então são selecionados de acordo com uma *m/z* previamente determinada e fragmentados em um processo denominado em tandem (MS/MS). Finalmente, os íons passam pelo detector, que é conectado a um computador com softwares para interpretação dos dados.

A espectrometria de massas tem emergido como uma ferramenta central na análise de proteínas em larga escala. Nos últimos anos, a análise de peptídeos tem impulsionado avanços tecnológicos na espectrometria de massas, principalmente quanto ao desenvolvimento de múltiplos instrumentos híbridos, com diferentes analisadores de massas, detectores e fontes de ionização. Essas combinações têm aumentado a acurácia para detecção de peptídeos precursores e para a detecção de íons gerados por fragmentação (ZHANG et al., 2010).

1.6. Secretoma de fungos filamentosos

Em 2000, Tjalsma *et al.* criaram o termo "secretoma" em seu estudo com a eubactéria *Bacillus subtilis*. Foi definido que o secretoma consistia em todas as proteínas secretadas e a maquinaria de secreção da bactéria (TJALSMA et al., 2000). Em 2010, Agrawal *et al.* sugeriram uma definição mais ampla, na qual o secretoma refere- se a um grupo global de proteínas secretadas para o espaço extracelular por uma célula, tecido, órgão, ou organismo em determinado momento e condição, por intermédio de mecanismos secretores conhecidos ou desconhecidos, envolvendo organelas secretoras constitutivas e reguladas (AGRAWAL et al., 2010).

Os secretomas de muitas espécies de fungos foram investigados recentemente. Revindran *et al*. (2012) isolaram e caracterizaram um novo fungo filamentoso identificado como *Coniochaeta sp*. capaz de degradar materiais lignocelulósicos de áreas de manguezal. O secretoma deste fungo crescido em palha de milho foi analisado por LC-MS/MS e obteve-se a identificação de 107 enzimas potencialmente lignocelulolíticas, revelando um único sistema de enzimas extracelulares constituído por complexos multienzimáticos de celulases (29%), hemicelulases (17%), outras glicosil hidrolases (10%), proteases (24%), enzimas degradadoras de proteínas (7%) e proteínas hipotéticas (13%) (RAVINDRAN; ADAV; SZE, 2012). A análise do secretoma de *Coniochaeta sp*. revelou um grande potencial para a degradação de

biomassa lignocelulósica deste novo isolado (RAVINDRAN; ADAV; SZE, 2012).

Manavalan *et al*. (2012) reportaram pela primeira vez a análise do secretoma do fungo *Ganoderma lucidum* cultivado em bagaço de cana. As enzimas lignocelulolíticas secretadas foram identificadas por LC-MS/MS, incluindo celulases (exoglucanases e endoglucanases, celobiase), hemicelulases (endoxilanases, α-galactosidases), celobiose desidrogenase, glicosil hidrolases, transaldolase, acil-CoA desidrogenase, MnP, lacases, glutationa reductases, fosfatases e proteases. Consequentemente, *G. lucidum* é um candidato em potencial para a produção de enzimas lignocelulolíticas e capaz de converter substratos complexos em açúcares simples eficientemente para a produção de biocombustíveis (MANAVALAN et al., 2012).

Silva *et al*. (2012), realizaram estudos de complexos multienzimáticos presentes no secretoma de *Trichoderma harzianum* crescido em bagaço de cana, por meio de análise de Blue native-PAGE. Os resultados obtidos revelaram a presença de 3 complexos distintos representados como I, II e III, o que é pouco descrito para fungos filamentosos, já que estes normalmente secretam enzimas hidrolíticas de forma individual que agem de maneira sinérgica na degradação de polissacarídeos. Na análise do secretoma, foram identificadas celobiohidrolases I e II, alfa-L-arabinofuranosidase, xilana-β-1,4- xilosidase, acetilxilana esterases, cutinases, endo-β-1,4-xilanase, swolenina e proteínas putativas, que podem agir degradando os componentes da parede celular de plantas (DA SILVA et al., 2012).

Com o objetivo de investigar o sistema enzimático envolvido na degradação da lignocelulose, Salvachúa *et al.* (2013) analisaram, por 2D-PAGE e nano LC-MS/MS, o secretoma do fungo da podridão branca *Irpex lacteus* e compararam com o secretoma dos fungos *Phanerochaete chrysosporium* e *Pleurotus ostreatus* crescidos em palha de trigo. Na fermentação em estado sólido, *I. lacteus* secreta proteases, manganês peroxidases e enzimas produtoras de H_2O_2, além de um conjunto de celulases e xilanases, com exceção das enzimas que degradam celulose e hemicelulose nos seus monossacarídeos. Em contraste, foi observado um significativo aumento de β-glicosidases quando *I. lacteus* cresceu em cultura líquida. *P. chrysosporium* secretou mais enzimas relacionadas à hidrolise total dos polissacarídeos e *P. ostreatus* produziu, em proporção, mais oxidoredutases. Os padrões de proteínas secretadas durante o crescimento de *I. lacteus* crescido em palha de trigo mais as diferenças observadas entre os diferentes secretomas justificam a aptidão deste fungo para processos de biotratamento na produção de etanol 2G e sugerem novas misturas de enzimas interessantes para uma hidrólise eficiente (SALVACHÚA et al., 2013).

O secretoma de fungos termofílicos têm sido caracterizados devido à elevada capacidade de produção de enzimas industrias por estes microorganismos. Winger *et al*. (2014) investigaram o secretoma de *Thermomyces lanuginosus* SSBP cultivado em espigas de milho e encontraram importantes enzimas envolvidas na sacarificação da hemicelulose e outras enzimas de interesse industrial. O perfil de proteínas revelou nove glicosil hidrolases incluindo xilanase (GH11), β-xilosidase (GH43), β-glicosidase (GH3), α-galactosidase (GH36) e trealose hidrolase (GH65). Duas enzimas de *Thermomyces* produzidas comercialmente (lipase e amilase), foram identificadas. Outras enzimas de potencial comercial ainda não exploradas em *Thermomyces* foram identificadas, incluindo glutaminase, frutose-bifosfato aldolase e cianato hidratase, o que indica que este fungo tem habilidade de utilizar material lignocelulósico para produzir enzimas importantes para vários processos industriais (WINGER et al., 2014).

Mahajan *et al.* (2016) reportaram a importância do fungo termofílico *Malbranchea cinnamomea* como uma fonte alternativa de enzimas lignocelulolíticas para suplementar coquetéis comerciais. A análise do secretoma usando LC-MS/MS orbitrap mostrou que o fungo crescido em talos de cenoura produz um espectro de glicosil hidrolases (celulases e hemicelulases), polissacarídeo liases, carboidrato esterases, além de celobioses desidrogenases. O fracionamento das proteínas do secretoma por cromatografia líquida permitiu a identificação de proteínas hidrolases dependentes de metal que aparentemente não possuem atividade hidrolítica, entretanto, proporcionaram o aumento da sacarificação em 5,7 vezes na presença de Mn^{2+}. A adição de diferentes frações do secretoma em celulases comerciais (Novozymes: Cellic CTec2) resultou no aumento da hidrólise de 1,57 a 3,43 vezes, mostrando que essas novas proteínas podem aumentar o potencial hidrolítico de enzimas lignocelulolíticas (MAHAJAN et al., 2016).

O secretoma de fungos fitopatogênicos também têm sido recentemente explorados. Tiwari *et al*. (2014) determinaram o perfil de proteínas extracelulares do fungo *Phoma exigua* crescido em α-celulose como fonte única de carbono, utilizando cromatografia líquida acoplada com espectrometria de massas (LC-MS/MS). Foram identificadas 33 proteínas presentes no secretoma, entre elas 52% pertencem às famílias das glicosil hidrolases. O sistema hidrolítico consiste em celulases, hemicelulases, e outras proteínas hipotéticas incluindo GH3, GH5, GH6, GH7, GH11, GH20, GH32 e GH54. A ação sinérgica desse novo coquetel de enzimas permite a sacarificação eficiente de palha de trigo que foi submetida ao tratamento alcalino, revelando um grande potencial deste secretoma para a hidrólise de biomassa lignocelulósica

(TIWARI et al., 2014).

1.7. Predição de genes de *Chrysoporthe cubensis*

A predição de genes em organismos eucarióticos é um grande desafio, devido ao enorme tamanho do genoma, à ocorrência de regiões repetitivas, à baixa densidade gênica, além da presença de genes interrompidos (genes com regiões intrônicas) (SARASWATHY; RAMALINGAM, 2011). As ferramentas computacionais de predição de genes geralmente se enquadram em duas categorias: detecção de homologia de sequências ou predição de genes *ab initio*. Ambas apresentam vantagens e desvantagens, entretanto, quando as duas abordagens são combinadas, fornecem um método poderoso, confiável e robusto de predição (HAAS et al., 2011).

Na predição de genes por homologia ou empírica, a identificação de genes é baseada em pesquisa de homologia em bancos de dados conhecidos (DNA genômico, cDNA, dbEST ou proteína), utilizando métodos de alinhamento local. A comparação de duas ou mais sequências genômicas homólogas (inter ou intraspécies) facilita a identificação de éxons conservados (SLEATOR, 2010). Quando combinada com sensores de sinal, esta informação permite refinar os limites da região e modelar com mais precisão a estrutura e a organização dos genes (SLEATOR, 2010).

A predição de genes *ab initio* ou *de novo* é pautada em modelos probabilísticos, como o Modelo Oculto de Markov (HMM), que são treinados para encontrar padrões característicos nos genes, como éxons, sítios de splicing, códons de início e de término, íntrons, e regiões inter-gênicas do DNA, baseado no genoma de um organismo específico conhecido e bem caracterizado (SARASWATHY; RAMALINGAM, 2011). O arquivo de entrada para esse software é simplesmente a sequência de letras que define uma sequência do genoma, e a saída são as coordenadas das estruturas de genes previstas para essa sequência, juntamente com a sequência proteica correspondente (HAAS et al., 2011). Existe uma grande variedade desses programas disponíveis hoje, incluindo o programa Augustus (STANKE; MORGENSTERN, 2005).

As análises *in silico* de fungos filamentosos permite a identificação de alvos promissores para a expressão heteróloga e que tenham todas as características relevantes para a aplicação biotecnológica em processos de sacarificação enzimática de biomassas lignocelulósicas. Os conhecimentos dos aspectos estruturais das enzimas de interesse possibilitam o aprimoramento das características essenciais para os processos biotecnológicos por meio de técnicas de engenharia enzimática, como por exemplo, mutagênese sítio-dirigida. A superexpressão bem-sucedida dos alvos permite a

abrangência na aplicação dessas enzimas, como a imobilização e desenvolvimento de biossensores ou até mesmo a suplementação de coquetéis comercias já estabelecidos, tornando-os mais eficientes (**Fig. 8**).

Figura 8: Fluxo de trabalho de ferramentas computacionais para a predição e anotação funcional de proteínas de interesse biotecnológico e os diferentes ramos da bioquímica que podem ser seguidos após a etapa de seleção.

1.8. Predição de proteínas secretadas (bioinfosecretoma)

O bioinfosecretoma consiste na predição do secretoma por meio de ferramentas de bioinformática que se baseiam na identificação de sinais de secreção em proteínas putativas correspondentes aos modelos de genes que são anotados automaticamente numa sequência do genoma (ALFARO et al., 2014). Essas análises são possíveis devido à conservação de características específicas entre as proteínas secretadas que podem ser usadas para predizer a localização celular das proteínas via métodos *in silico*. Nos organismos eucariotos, proteínas secretadas podem ser identificadas pela presença de uma sequência de peptídeo-sinal (SP) clivável presente na extremidade N-terminal, que é tipicamente composta por 15 a 30 aminoácidos. Essas sequências de peptídeo-sinal não apresentam alta homologia, mas mostram praticamente a mesma composição estrutural que consiste em uma sequência central hidrofóbica flanqueada por regiões N- e C-terminais hidrofílicas, com aminoácidos conservados nas posições relativas aos sítios de clivagem -3 e -1 (VON HEIJNE, 1985).

O primeiro trabalho de predição do secretoma de um fungo basidiomiceto por ferramentas de bioinformática foi realizado para *Phanerochaete chrysosporium* (WYMELENBERG et al., 2005). Foram preditas 268 proteínas secretadas baseadas na primeira versão do genoma deste fungo, embora este número tenha sido considerado subestimado devido o modelo de gene anotado ser incompleto (MARTINEZ et al., 2004). Entretanto, análises baseadas na segunda versão do genoma possibilitaram a identificação de 768 proteínas do secretoma (WYMELENBERG et al., 2006). Outro exemplo de caracterização do secretoma via métodos *in silico* foram as análises realizadas para o fitopatógeno de milho *Ustilago maydis*. Utilizando as ferramentas SignalP e TargetP, foram identificadas 776 possíveis proteínas secretadas. Após a utilização de ferramentas de refinamento (TMHMM), que levam em consideração proteínas que podem ser transmembranas, foi possível a redução da predição para 168 proteínas secretadas e 336 proteínas com outras funções (MUELLER et al., 2008).

1.9. Banco de dados de enzimas ativas em carboidratos (CAZy)

As enzimas com atividades sobre carboidratos (CAZymes) promovem a polimerização, despolimerização, e modificação de glicanos e glicoconjugados em um vasto conjunto de vias biológicas, por meio de seus domínios proteicos funcionais (módulos catalíticos e de ligação a carboidratos) (LOMBARD et al., 2014). O sistema de classificação das enzimas ativas em carboidratos baseado na similaridade de sequências de aminoácidos, no dobramento proteico e no mecanismo de catálise enzimática, é continuamente integrado e minunciosamente atualizado no banco de dados CAZy (http://www.cazy.org) desde 1998 (LEVASSEUR et al., 2013). O CAZy contava em 2016 com 359 famílias modulares subdivididas nas seguintes classes de acordo com a ação das enzimas em glicanos ou glicocojugados: glicosil hidrolases (GHs); glicosil transferases (GTs); polissacarídeo liases (PLs); carboidrato-esterases (CEs), módulos de ligação a carboidrato (CBMs); e mais recentemente as enzimas de atividade auxiliares (AA) (TERRAPON et al., 2017). Em 2019, até o presente momento, o CAZY conta com 165 famílias de GHs, 108 famílias de GTs, 37 famílias de PLs, 16 famílias de CEs, 16 famílias de AAs e 85 CBMs, totalizando 427 famílias modulares, e em constante expansão do número de novas famílias (http://www.cazy.org).

As famílias de enzimas pertencentes a cada classe são criadas baseadas em proteínas experimentalmente caracterizadas e descritas na literatura, sendo continuamente povoadas com sequências proteicas com similaridade significativa depositadas em bancos de dados públicos de proteínas (CANTAREL et al., 2009). As

enzimas ativas em carboidratos exibem uma estrutura modular que pode ser definida como uma unidade funcional e estrutural. Todos os integrantes de uma mesma família possuem um segmento em comum (modulo catalítico ou de ligação), que caracteriza a família em questão, e que é definido por uma abordagem semi-automática baseada em análises da estrutura tridimensional da proteína, estudos de deleção e comparação de sequência (CANTAREL et al., 2009). A presença de enzimas que atuam em diferentes substratos pertencentes a uma mesma família impede uma anotação funcional direta e geral, sendo necessário subdivisões dentro das famílias para agrupar adequadamente as enzimas de acordo com a similaridade de sequência e especificidade (TERRAPON et al., 2017). Análises filogenéticas podem contribuir para a definição de subfamílias formadas por grupos de proteínas que são mais homogêneos em suas propriedades funcionais (ASPEBORG et al., 2012; MAJZLOVÁ; PUKAJOVÁ; JANEČEK, 2013; STAM et al., 2006).

O grande sucesso do CAZy está relacionado com seu rigoroso processo de classificação baseado em métodos semiautomáticos, sua equipe de curadores manuais que capturam dados estruturais e funcionais da literatura e mantém o banco de dados atualizado, o fato de usar a variabilidade da arquitetura modular das CAZymes no seu sistema de classificação e sua integração com o Genbank (BENSON et al., 2013), UniProt (CONSORTIUM, 2017) e o Protein Data Bank (PDB; http://www.rcsb.org/ (BERMAN et al., 2000)). Recentemente, programas de anotação baseados na classificação por famílias do CAZy, como por exemplo, o dbCAN (Base de dados para anotação de enzimas ativas em carboidratos) (YIN et al., 2012), têm sido utilizados para auxiliar a anotação funcional de enzimas secretadas por fungos (SCHNEIDER et al., 2016) .

1.10. A nova classe do CAZy: Enzimas de Atividade Auxiliar (AAs)

A desconstrução da parede celular de plantas requer a identificação de um repertório completo de enzimas que atuam em carboidratos juntamente com enzimas que degradam a lignina. Enzimas lignolíticas não atuam em carboidratos, mas como a lignina está invariavelmente e intimamente relacionada à celulose e à hemicelulose na parede celular vegetal, as enzimas lignolíticas atuam de forma cooperativa com as celulases e hemicelulases clássicas (LEVASSEUR et al., 2013). Com a necessidade de classificar as enzimas que atuam diretamente na lignina ou que atuam na celulose cristalina por mecanismos não clássicos, criou-se uma nova classe, as “Enzimas de Atividade Auxiliar” (AAs), que integram enzimas com potencial habilidade em facilitar o acesso de outras

CAZymes aos carboidratos incrustados na parede celular vegetal, seja atuando por meio de mecanismos oxidativos nas miofibrilas de celulose cristalina e criando novos pontos de acesso para outras enzimas, como é o caso das LPMOs, ou por meio de enzimas que atuam na desconstrução da lignina por mecanismos redox (LEVASSEUR et al., 2013). Até a presente data existem 16 famílias de AAs, sendo 7 famílias de LPMOs depositadas no Banco de dados de enzimas ativas em carboidratos, sendo formadas pelas famílias AA9, AA10, AA11, AA13, AA14, AA15 e mais recentemente a família AA16 (FILIATRAULT-CHASTEL et al., 2019).

O fungo fitopatogênico *Chrysoporthe cubensis*, além de secretar glicosil hidrolases (GH) e enzimas acessórias, produz enzimas de atividades auxiliares (AAs), como as lacases da família AA1 (FALKOSKI et al., 2013). A presença de um amplo espectro de tipos de enzimas pode explicar a eficiência do extrato enzimático deste fungo se comparado com coquetéis comerciais, sendo a presença de lacases neste coquetel um fator preponderante para a maior eficiência deste extrato enzimático, já que a lacase pode promover a degradação da lignina, que é um obstáculo para o processo de hidrólise (MAITAN-ALFENAS et al., 2015).

As enzimas da família AA1 são oxidases de multi-cobre (MCOs) que usam difenóis e compostos aromáticos como doadores de elétrons para reduzir o oxigênio molecular a água. A família AA1 é habitualmente dividida em subfamílias, incluindo as lacases, ferroxidases, ascorbato oxidases, enzimas de pigmento e enzimas com dupla atividade de lacase/ferroxidase (COURTY et al., 2009; HOEGGER et al., 2006).

As ascorbato oxidases promovem a oxidação do L-ascorbato em dehidroascorbato. Em plantas, sugere-se que a enzima participe no sistema redox envolvendo o ácido ascórbico e pode estar envolvida na reorganização da parede celular vegetal e em várias vias de sinalização celular (PIGNOCCHI et al., 2003). Em abóboras, a expressão da enzima aumenta durante o crescimento do calo, desenvolvimento de frutos, alongamento e muda (KISU et al., 1997). Está presente em tecidos jovens e em crescimento de tabaco, sendo induzida por auxina, o que sugere o envolvimento no crescimento celular (PIGNOCCHI et al., 2003). Em fungos, a função das ascorbato oxidases não é clara, mas pode estar relacionada a atividades antioxidantes, crescimento de hifas e resistência a cianeto (WANG et al., 2009).

Em fungos, as ferroxidases são em grande maioria enzimas de membrana envolvidas em mecanismos de captação de ferro. O ferro é um elemento indispensável para quase todos os organismos, e está envolvido em reações redox de células vivas, além de atuar como cofator de enzimas essenciais para a manutenção do metabolismo (HAAS,

2003; KOSMAN, 2003). Entretanto, os níveis intracelulares inadequados de ferro podem ser perigosos devido sua participação na produção de radicais hidroxil por reações de Fenton/Haber Weiss (HALLIWELL; GUTTERIDGE, 1992). Assim, a homeostase de ferro deve ser finamente controlada através da regulação dos sistemas de captação, transporte e estocagem de ferro para o ambiente intracelular (ALBAROUKI; DEISING, 2013). As ferroxidases participam do sistema de Assimilação do Ferro Reduzido (RIA), caracterizado por duas etapas redox antagônicas que ocorrem na membrana plasmática. Primeiro ocorre a redução do íon Fe^{3+} insolúvel do ambiente externo em Fe^{2+} solúvel por uma ferroredutase (Fr1) presente na membrana da célula e, posteriormente, o Fe^{2+} é direcionado para um complexo de membrana formado pela ferroxidase (Fet3), que irá oxidar o Fe^{2+} a Fe^{3+}, e uma permease (Ftr1) que irá possibilitar a internalização do íon Fe^{3+} (KOSMAN, 2010).

Outra função fisiológica importante exercida pelas oxidases de multi-cobre está relacionada à participação das enzimas de pigmento na via DOPA de síntese de melanina em fungos (LANGFELDER et al., 2003). A melanização é essencial para a sobrevivência, pois promove a estabilidade da parede celular fúngica, proteção contra radiação ultra-violeta (UV), proteção contra variações de temperatura e metais, além de estar intimamente relacionado com a virulência de fungos patogênicos por aumentar a resistência contra os sistemas de defesa do hospedeiro e promover maior aderência do fungo no tecido hospedeiro (JEON et al., 2012; NOSANCHUK; CASADEVALL, 2003; PIHET et al., 2009). O papel dessas enzimas na melanogênese envolve a indução de acoplamentos oxidativos de compostos fenólicos produzidos endógena ou exogenamente, promovendo assim a formação de pigmentos poliméricos (JEON et al., 2012).

As lacases são o maior subgrupo dentro das MCOs, e devido ao seu amplo espectro de atuação em diferentes substratos, tem recebido mais atenção para aplicações biotecnológicas (VISWANATH et al., 2014). Existem lacases/ferroxidases descritas que podem atuar tanto na oxidação de compostos fenólicos quanto na oxidação de Fe^{2+}, apresentando uma dupla função e dois sítios catalíticos diferentes, um sítio hidrofóbico no qual os compostos fenólicos serão oxidados, e outro bolsão catalítico no qual ocorrerá a oxidação do Fe^{2+} (KUES; RUHL, 2011). As enzimas PfaL de *Phanerochaete flavido-alba* e Mco1 de *Phanerochaete chrysosoporium* apresentam atividades de lacase e ferroxidase, entretanto, exercem ambas as atividades em diferentes níveis de catálise. Em Mco1, a atividade de ferroxidase é mais forte do que a atividade de lacase, ao contrário da enzima PfaL (LARRONDO et al., 2003; RODRÍGUEZ-RINCÓN et al., 2010).

1.11. Lacases: características estruturais e mecanismo de ação

As lacases (EC 1.10.3.2) são oxidases de multi-cobre que catalisam a oxidação de um amplo espectro de substratos orgânicos, como compostos difenólicos, polifenólicos, diaminas, fenóis substituídos e aminas aromáticas, por mecanismos de transferência de elétrons (KIISKINEN; VIIKARI; KRUUS, 2002). As lacases são amplamente distribuídas em fungos basidiomicetos e ascomicetos, mas também podem ser encontradas em plantas, bactérias e alguns insetos (GIARDINA et al., 2010). Usualmente, são glicoproteínas extracelulares e monoméricas com massa molecular de 55-85 KDa, sendo que o conteúdo de carboidratos presentes nas lacases secretadas é em torno de 25% da massa molecular total, com 3 a 10 sítios de N-glicosilação potencialmente preditos (MOROZOVA et al., 2007).

As lacases fúngicas, assim como as outras oxidases de multi-cobre, possuem três domínios de ligação ao cobre (denominados D1, D2 e D3) sendo que cada domínio apresenta o padrão de dobramento do tipo Barril-β formado por motivos do tipo Chave-grega; além de possuir quatro íons cobre (Cu^{2+}) localizados em quatro tipos distintos de sítios de ligação a metal (denominados T1, T2 e T3, e T3') distribuídos nos três domínios da enzima (GIARDINA et al., 2010). O sítio T1 é mononuclear, está localizado no domínio D3, e é caracterizado pela forte absorvância próximo ao comprimento de onda de 600nm, que resulta na coloração azul intensa apresentada pela enzima neste comprimento de onda. Já os outros três sítios de ligação ao cobre formam um cluster trinuclear composto pelo sítio T2 mononuclear, que não pode ser detectado a 600 nm mas é detectado por espectroscopia de ressonância paramagnética eletrônica (EPR), e o sítio binuclear T3-T3', que absorve a 330 nm mas não apresenta sinal na EPR (PALMIERI et al., 1997). O sítio trinuclear (T2-T3-T3') fica localizado na interface entre os dos domínios D1 e D3. A distância entre o sítio mononuclear T1 e sítio trinuclear T2-T3-T3' é de aproximadamente 13Å (HAKULINEN; ROUVINEN, 2015) (**Fig. 9**).

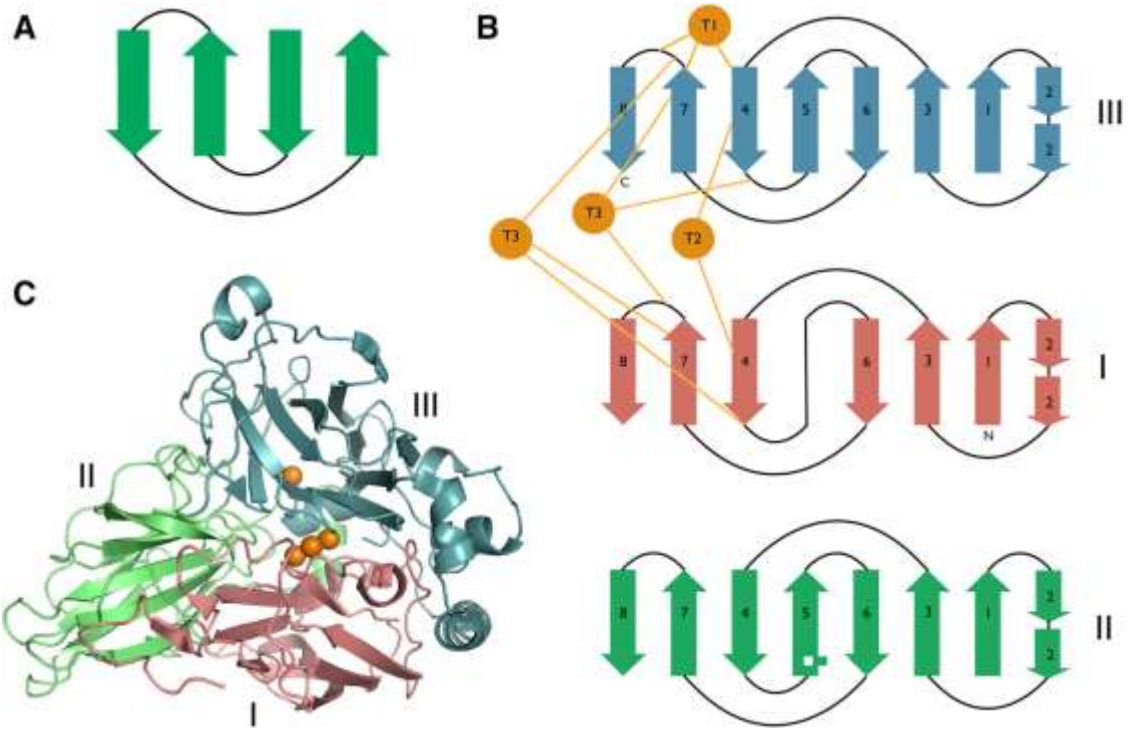

Figura 9: A) Motivo chave-grega clássico. B) Diagrama esquemático de topologia dos domínios cupredoxina em lacase de *M. albomyces*. O primeiro domínio é mostrado em vermelho. O segundo domínio em verde e o terceiro domínio em azul. Os cobres são representados como esfera laranjas e suas coordenações são mostradas. C) O diagrama em fita mostra o dobramento Barril-β de cada domínio da lacase de *M. albomyces*. (HAKULINEN; ROUVINEN, 2015).

A geometria dos sítios de ligação ao cobre é similar entre as oxidases de multi-cobre. Os três íons de cobre do sítio trinuclear apresentam uma geometria triangular e estão coordenados a oito resíduos de histidina (His) no total; o íon cobre T3 está coordenado a três His (átomos NE2 do anel imidazólico); o íon cobre T3' está coordenado a três His (dois átomos NE2 e um ND1 do anel imidazólico); e o íon cobre T2 está coordenado a duas His (átomos NE2) e uma molécula de H_2O. No sítio mononuclear, o íon cobre T1 é coordenado a dois resíduos de His (átomos ND1) e um resíduo de Cys (átomo SG) (HAKULINEN; ROUVINEN, 2015; SOLOMON; AUGUSTINE; YOON, 2008) (**Fig. 10**).

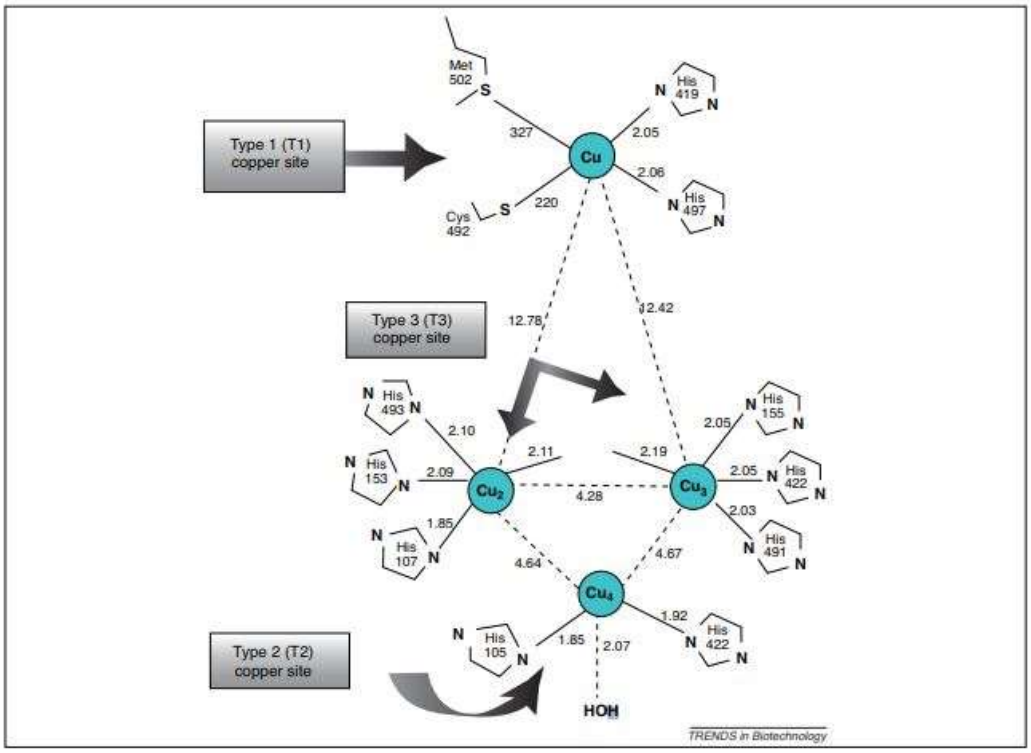

Figura 10: Ilustração representando a orientação em relação aos átomos de cobre e as distâncias de ligação em ångström (Å). A estrutura tridimensional usada para a representação da lacase CotA de *Bacillus subtilis* (SANTHANAM et al., 2011).

O mecanismo de ação das lacases envolve três etapas. Primeiro, o Cu T1 é reduzido pela ação do substrato fenólico, que será oxidado. Então o elétron é internamente transferido do CuT1 até o centro trinuclear (formado pelos átomos de cobre T2, T3, e T3'), por uma distância próxima de 13Å, pela via de transferência His-Cys (RIVERA-HOYOS et al., 2013). O oxigênio molecular se liga ao centro trinuclear por uma ativação assimétrica através de um local de ligação ao substrato localizado perto da His ligada ao centro CuT1. O oxigênio molecular entra por um canal próximo ao CuT1 e é direcionado ao centro trinuclear, onde será o aceptor de elétrons, originando uma molécula de H_2O, sendo esta liberada para o ambiente externo da enzima por um canal próximo ao centro trinuclear (DESAI; NITYANAND, 2011; GIANFREDA; XU; BOLLAG, 1999). O canal de entrada de oxigênio molecular parece ser restrito ao acesso de outros agentes oxidantes que não sejam O_2. Durante o estado estacionário do processo, H_2O_2 não é detectado fora da enzima, indicando que a redução de quatro elétrons do O_2 para H_2O ocorre (GIANFREDA; XU; BOLLAG, 1999). Portanto, a oxidação de quatro moléculas de substrato é necessária para produzir uma redução completa do O_2 em H_2O (DESAI; NITYANAND, 2011; SOLOMON; AUGUSTINE; YOON, 2008).

1.12. Impacto social, econômico e tecnológico da produção de etanol lignocelulósico (2G)

A escassez de combustíveis fósseis tem conduzido à busca por fontes renováveis de energia. No Brasil, a produção de etanol de segunda geração a partir do bagaço de cana-de-açúcar é uma estratégia bastante promissora, visto que o Brasil é o maior produtor de cana-de-açúcar do mundo. Mesmo que parte do bagaço de cana-de-açúcar produzido hoje nas indústrias seja usado para queima e cogeração de energia, ainda há grande excedente desse subproduto, que quando utilizado para a produção de etanol de segunda geração pode proporcionar um aumento na produtividade em etanol de até 50% em relação ao nível atual (MILANEZ et al., 2015).

Em 2011, foi iniciada a implementação das três primeiras plantas de usinas de etanol lignocelulósico (2G) no Brasil, das quais duas em escala comercial e outra demonstrativa, o que significou um passo importante, já que essa tecnologia se limitava a iniciativas em escalas laboratorial e piloto. Contudo, a capacidade dessas plantas, em conjunto, chega a pouco mais de 140 milhões de litros por safra, volume ainda pequeno quando comparado aos níveis de importação de gasolina. O ápice da importação de gasolina ocorreu em 2012, quando o país importou 3,8 bilhões de litros. Em 2014, foram importados 2,2 bilhões de litros de gasolina (MILANEZ et al., 2015). Diante desse quadro, o governo brasileiro declarou uma nova política nacional para biocombustíveis (RenovaBio), em dezembro de 2017, com o objetivo de promover a produção de etanol e biodiesel a partir de várias fontes disponíveis no Brasil (BRASIL, 2018).

A produção de etanol a partir do bagaço de cana-de-açúcar poderá se tornar uma estratégia ainda mais atrativa se este processo for economicamente viável e vantajoso. A etapa de sacarificação enzimática para liberação dos açúcares fermentescíveis é considerada um dos principais obstáculos à produção extensiva de etanol a partir do bagaço de cana, principalmente devido aos altos custos de produção das enzimas lignocelulolíticas. Este processo requer misturas ou coquetéis de enzimas mais diversificados do que aqueles disponíveis para os processos de produção de biocombustíveis de primeira geração.

Atualmente, o mercado de enzimas é dominado por multinacionais, como a empresa de biotecnologia de origem dinamarquesa Novozymes e a companhia americana Genencor (incorporada a uma joint venture denominada DuPont Danisco Cellulosic Ethanol LLC), que fornecem coquetéis celulolíticos em larga escala às usinas de de fabricação de etanol de segunda geração. Outras multinacionais, como a americana Dupont, a holandesa DSM e espanhola Abengoa, também desenvolveram coquetéis de

celulases para a hidrólise em grande escala, mas essas enzimas não estão prontamente disponíveis no mercado. A companhia de biotecnologia finlandesa Metgen desenvolveu um coquetel de celulases, o "MetZyme® SUNO ™" formulado para melhorar a hidrólise de biomassa lignocelulósica e produção de bioquímicos e biocombustíveis de forma eficiente (CHANDEL et al., 2019). Existem outros produtores de celulases comerciai, mas suas produções ainda estão em estágios iniciais de desenvolvimento (CHANDEL et al., 2019).

Para a produção de etanol celulósico (2G), várias empresas em todo o mundo montaram plantas pilotos e instalações de produção usando diferentes biomassas como matéria-prima, como o bagaço de cana-de-açúcar, a palha de cana-de-açúcar e a palha de milho. A **Tabela 1** apresenta alguns exemplos importantes de empresas que estão liderando este setor energético.

A escassez de enzimas produzidas no Brasil é uma realidade preocupante, pois torna o país dependente de tecnologia estrangeira neste mercado tão promissor e estratégico. As enzimas que compõem os coquetéis enzimáticos disponíveis atualmente para a sacarificação da biomassa lignocelulósica são produzidas principalmente pelos fungos *Aspergillus spp*. e *Trichoderma spp* (MAKELA; DONOFRIO; DE VRIES, 2014).

Tabela 1: Produtores mundiais de etanol celulósico em escala comercial e suas capacidades de produção. Tabela adaptada de (CHANDEL et al., 2019).

Name of company	Feedstock	Procedural configuration	Ethanol production capacity
Raizen Energia, Costa Pinto São Paulo, Brazil	Sugarcane bagasse	Steam explosion- (logen process), yeast fermentation	40 million liters year^{-1}
Gran Bio and Beta Renewables Alagoas, Brazil	Sugarcane straw/ bagasse	ProesaTM process, hydrolysis, fermentation	64 510 (21.6 MM gal. year^{-1})
Poet-DSM Advanced Biofuels Emmetsburg, IA, USA	Corn stover	Pretreatment, hydrolysis and yeast fermentation	59 734 (20 MM gal. year^{-1})
Abengoa, Hugoton, KS, USA	Corn stover	Pretreatment, hydrolysis and yeast fermentation	74 667 (25 MM gal. year^{-1})
DuPont Industrial BioSciences Nevada, IA, USA	Corn stover	Pretreatment, hydrolysis, bacterial fermentation	89 600 (30 MM gal. year^{-1})
Praj Industries	Mixed feedstock	Pretreatment, hydrolysis and GMO yeast fermentation	1 million liters per year
Centro de Tecnologia Canaviera (CTC)-Piracicaba, Brazil	Sugarcane bagasse	Continuous steam explosion, hydrolysis and yeast fermentation	3 million liters per year

Apesar dos avanços nessa área da pesquisa, as misturas enzimáticas atuais ainda têm um custo elevado e não contém todas as enzimas necessárias e nas proporções adequadas para degradar total e eficientemente a celulose e a hemicelulose presentes nas biomassas, nas condições dos processos existentes. Novas misturas enzimáticas são requeridas para tornar a produção de biocombustíveis de segunda geração econômica e

tecnicamente mais viável. Para isso, é importante a seleção de fungos que sejam produtores de novas enzimas mais robustas, com alto poder de conversão da biomassa em açúcares fermentescíveis. Além disso, para desonerar o processo global de produção de etanol, é importante que seja realizada a otimização da produção das enzimas pelos fungos, utilizando meios de cultivo mais simples e adequados à indução do complexo enzimático, como por exemplo, o farelo de trigo.

Com o desenvolvimento desse trabalho, espera-se identificar novas enzimas e promover o conhecimento da composição do coquetel enzimático de *C. cubensis* para otimizar sua produção, bem como aprimorá-lo para aplicação industrial, e consequentemente, torná-lo mais eficiente e de menor custo para hidrólise da celulose e hemicelulose do bagaço de cana-de-açúcar, contribuindo para a diminuição da importação das enzimas e garantindo, no futuro, o domínio dessa tecnologia inovadora para contribuir com as políticas de sustentabilidade ambiental.

2. REFERÊNCIAS

1. ABDEL-HAMID, A. M.; SOLBIATI, J. O.; CANN, I. K. O. Insights into lignin degradation and its potential industrial applications. **Advances in applied microbiology**, v. 82, p. 1–28, 2013.
2. ADAV, S. S. et al. Quantitative iTRAQ secretome analysis of *Aspergillus niger* reveals novel hydrolytic enzymes. **Journal of Proteome Research**, v. 9, n. 8, p. 3932–3940, 2010.
3. ADAV, S. S.; RAVINDRAN, A.; SZE, S. K. Quantitative proteomic analysis of lignocellulolytic enzymes by *Phanerochaete chrysosporium* on different lignocellulosic biomass. **Journal of Proteomics**, v. 75, n. 5, p. 1493–1504, 2011.
4. AGRAWAL, G. K. et al. Plant secretome: Unlocking secrets of the secreted proteins. **Proteomics**, v. 10, p. 799–827, 2010.
5. ALBAROUKI, E.; DEISING, H. B. Infection structure-specific reductive iron assimilation is required for cell wall integrity and full virulence of the maize pathogen *Colletotrichum graminicola*. **Molecular plant-microbe interactions : MPMI**, v. 26, n. 6, p. 695–708, 2013.
6. ALFARO, M. et al. Comparative analysis of secretomes in basidiomycete fungi. **Journal of Proteomics**, v. 102, p. 28–43, 2014.
7. ARANTES, V.; SADDLER, J. N. Access to cellulose limits the efficiency of enzymatic hydrolysis: the role of amorphogenesis. **Biotechnology for biofuels**, v. 3, p. 4, 2010.
8. ARMIROTTI, A.; DAMONTE, G. Achievements and perspectives of top-down proteomics. **Proteomics**, v. 10, n. 20, p. 3566–76, 2010.
9. ASPEBORG, H. et al. Evolution, substrate specificity and subfamily classification of glycoside hydrolase family 5 (GH5). **BMC Evol Biol**, v. 12, 2012.
10. BEESON, W. T. et al. Oxidative cleavage of cellulose by fungal copper-dependent polysaccharide monooxygenases. **Journal of the American Chemical Society**, v. 134, n. 2, p. 890–892, 2012.
11. BENSON, D. A. et al. GenBank. **Nucleic Acids Research**, v. 41, n. D1, p. 36–42, 2013.
12. BERMAN, H. M. et al. The protein data bank. **Nucleic acids research**, v. 28, n. 1, p. 235–242, 2000.
13. BHADAURIA, V. et al. Advances in fungal proteomics. **Microbiological Research**, v. 162, n. 3, p. 193–200, 2007.
14. BIANCO, L.; PERROTTA, G. Methodologies and Perspectives of Proteomics Applied to Filamentous Fungi : From Sample Preparation to Secretome Analysis. **International Journal of Molecular Sciences**, v. 16, n. 3, p. 5803–5829, 2015.
15. BORIN, G. P. et al. Comparative Secretome Analysis of *Trichoderma reesei* and *Aspergillus niger* during Growth on Sugarcane Biomass. **PloS one**, v. 10, n. 6, p. 1–20, 2015.
16. BRASIL. Ministério de Minas e Energia, 2018. Disponível em:

<http://www.mme.gov.br/documents/ 10584/55980549/RenovaBio.pdf/>. Acesso em: 10 de junho de 2019.

17. BREWIS, I. A.; GADELLA, B. M. Sperm surface proteomics: from protein lists to biological function. **Molecular human reproduction**, v. 16, n. 2, p. 68–79, fev. 2010.

18. BRIJWANI, K.; OBEROI, H. S.; VADLANI, P. V. Production of a cellulolytic enzyme system in mixed-culture solid-state fermentation of soybean hulls supplemented with wheat bran. **Process Biochemistry**, v. 45, n. 1, p. 120–128, 2010.

19. CAMASSOLA, M.; DILLON, A. J. P. Production of cellulases and hemicellulases by *Penicillium echinulatum* grown on pretreated sugar cane bagasse and wheat bran in solid-state fermentation. **Journal of Applied Microbiology**, v. 103, n. 6, p. 2196–2204, 2007.

20. CANTAREL, B. L. et al. The Carbohydrate-Active EnZymes database (CAZy): an expert resource for Glycogenomics. **Nucleic Acids Res**, v. 37, 2009.

21. CHANDEL, A. K. et al. Comparative analysis of key technologies for cellulosic ethanol production from Brazilian sugarcane bagasse at a commercial scale. **Biofuels, Bioproducts and Biorefining**, v. 0, n. 0, 2019.

22. CHEN, C.-H. (WINSTON). Review of a current role of mass spectrometry for proteome research. **Analytica Chimica Acta**, v. 624, n. 1, p. 16–36, 2008.

23. CHEN, S.; HARMON, A. C. Advances in plant proteomics. **Proteomics**, v. 6, n. 20, p. 5504–5516, 2006.

24. CONSORTIUM, T. U. UniProt: the Universal Protein knowledgebase. **Nucleic Acids Research**, v. 45, p. 158–169, 2017.

25. COURTY, P. E. et al. Phylogenetic analysis, genomic organization, and expression analysis of multi-copper oxidases in the ectomycorrhizal basidiomycete *Laccaria bicolor*. **New Phytologist**, v. 182, n. 3, p. 736–750, 2009.

26. DA SILVA, A. J. et al. Blue native-PAGE analysis of *Trichoderma harzianum* secretome reveals cellulases and hemicellulases working as multienzymatic complexes. Proteomics, v. 12, n. 17, p. 2729–2738, 2012

27. DE SOUZA, A. P. et al. Sugarcane as a Bioenergy Source: History, Performance, and Perspectives for Second-Generation Bioethanol. **Bioenergy Research**, v. 7, n. 1, p. 24–35, 2013.

28. DESAI, S. .; NITYANAND, C. Microbial laccases and their applications: A Review. **Asian Journal of Biotechnology**, v. 3, n. 2, p. 98–124, 2011.

29. DZIECIATKOWSKA, M.; HILL, R.; HANSEN, K. C. GeLC-MS/MS Analysis of Complex Protein Mixtures. **Shotgun Proteomics**. v. 1156, p. 1–13, 2014.

30. FALKOSKI, D. L. et al. *Chrysoporthe cubensis*: A new source of cellulases and hemicellulases to application in biomass saccharification processes. **Bioresource Technology**, v. 130, p. 296–305, 2013.

31. FILIATRAULT-CHASTEL, C. et al. AA16, a new lytic polysaccharide monooxygenase family identified in fungal secretomes. **Biotechnology for Biofuels**, v. 12, n. 1, p. 55, 2019.

32. FRAGNER, D. et al. Optimized protocol for the 2-DE of extracellular proteins from higher basidiomycetes inhabiting lignocellulose. **Electrophoresis**, v. 30, n. 14, p. 2431–41, 2009.

33. GAO, B.-B.; STUART, L.; FEENER, E. P. Label-free quantitative analysis of one-dimensional PAGE LC/MS/MS proteome: application on angiotensin II-stimulated smooth muscle cells secretome. **Molecular & cellular proteomics : MCP**, v. 7, n. 12, p. 2399–2409, 2008.

34. GIANFREDA, L.; XU, F.; BOLLAG, J.-M. Laccases: A Useful Group of Oxidoreductive Enzymes. **Bioremediation Journal**, v. 3, n. 1, p. 1–26, 1999.

35. GIARDINA, P. et al. Laccases: A never-ending story. **Cellular and Molecular Life Sciences**, v. 67, n. 3, p. 369–385, 2010.

36. GIBSON, D. M. et al. Plant pathogens as a source of diverse enzymes for lignocellulose digestion. **Current Opinion in Microbiology**, v. 14, n. 3, p. 264–270, 2011.

37. GIRARD, V. et al. Secretomes: The fungal strike force. **Proteomics**, v. 13, n. 3–4, p. 597–608, 2013.

38. GÓMEZ-MENDOZA, D. et al. Secretomic Survey of *Trichoderma harzianum* Grown on Plant Biomass Substrates. **Journal of Proteome**, v. 13, n. 4, p. 1810–1822, 2014.

39. GUPTA, V. K. et al. Fungal Enzymes for Bio-Products from Sustainable and Waste Biomass. **Trends in Biochemical Science**s, v. 41, n. 7, p. 633–645, 2016.

40. GLASS, N. L. et al. Plant Cell Wall Deconstruction by Ascomycete Fungi. **Annual Review of Microbiology**, v. 67, n. 1, p. 477–498, 2013.

41. GREGORICH, Z. R.; CHANG, Y.-H.; GE, Y. Proteomics in heart failure: top-down or bottom-up? **Pflugers Archiv : European journal of physiology**, v. 466, n. 6, p. 1199–1209, 2014.

42. GRYZENHOUT, M. et al. Novel hosts of the Eucalyptus canker pathogen *Chrysoporthe cubensis* and a new *Chrysoporthe* species from Colombia. **Mycological research**, v. 110, n. 7, p. 833–45, 2006.

43. GUIMARÃES, L. M. D. S. et al. Genetic control of *Eucalyptus urophylla* and *E. grandis* resistance to canker caused by *Chrysoporthe cubensis*. **Genetics and Molecular Biology**, v. 33, n. 3, p. 525–531, 2010.

44. HAAS, B. J. et al. Approaches to Fungal Genome Annotation. **Mycology**, v. 2, n. 3, p. 118–141, 2011.

45. HAAS, H. Molecular genetics of fungal siderophore biosynthesis and uptake: The role of siderophores in iron uptake and storage. **Applied Microbiology and Biotechnology**, v. 62, n. 4, p. 316–330, 2003.

46. HAKULINEN, N.; ROUVINEN, J. Three-dimensional structures of laccases. **Cellular and Molecular Life Sciences**, v. 72, n. 5, p. 857–868, 2015.

47. HALLIWELL, B.; GUTTERIDGE, J. M. C. Biologically relevant metal ion-dependent hydroxyl radical generation An update. **FEBS Letters**, v. 307, n. 1, p. 108–112, 1992.

48. HARRIS, P. V. et al. New enzyme insights drive advances in commercial ethanol

production. **Current Opinion in Chemical Biology**, v. 19, n. 1, p. 162–170, 2014.

49. HOEGGER, P. J. et al. Phylogenetic comparison and classification of laccase and related multicopper oxidase protein sequences. **FEBS Journal**, v. 273, n. 10, p. 2308–2326, 2006.

50. HÖLKER, U.; HÖFER, M.; LENZ, J. Biotechnological advantages of laboratory-scale solid-state fermentation with fungi. **Applied Microbiology and Biotechnology**, v. 64, n. 2, p. 175–186, 2004.

51. ISSAQ, H. J.; VEENSTRA, T. D. Two-dimensional polyacrylamide gel electrophoresis (2D-PAGE): Advances and perspectives. **BioTechniques**, v. 44, n. 5, p. 697–700, 2008.

52. JANUSZ, G. et al. Lignin degradation: microorganisms, enzymes involved, genomes analysis and evolution. **FEMS Microbiology Reviews**, v. 41, n. 6, p. 941–962, 27 out. 2017.

53. JEON, J. R. et al. Laccase-catalysed oxidations of naturally occurring phenols: From in vivo biosynthetic pathways to green synthetic applications. **Microbial Biotechnology**, 2012.

54. KAO, S. H. et al. Evaluating the compatibility of three colorimetric protein assays for two-dimensional electrophoresis experiments. **Proteomics**, v. 8, n. 11, p. 2178–2184, 2008.

55. KIISKINEN, L. L.; VIIKARI, L.; KRUUS, K. Purification and characterisation of a novel laccase from the ascomycete *Melanocarpus albomyces*. **Applied Microbiology and Biotechnology**, v. 59, n. 2–3, p. 198–204, 2002.

56. KIKOT, G. E.; HOURS, R. A.; ALCONADA, T. M. Contribution of cell wall degrading enzymes to pathogenesis of *Fusarium graminearum*: a review. **Journal of Basic Microbiology**, v. 49, n. 3, p. 231–241, 2009.

57. KISU, Y. et al. Cloning of the Pumpkin Ascorbate Oxidase Gene and Analysis of a Cis- Acting Region Involved in Induction by Auxin. **Plant Cell Physiology**, v. 38, n. 5, p. 631–637, 1997.

58. KOSMAN, D. J. Molecular mechanisms of iron uptake in fungi. **Molecular Microbiology**, v. 47, n. 5, p. 1185-1197, 2003.

59. KOSMAN, D. J. Redox cycling in iron uptake, efflux, and trafficking. **Journal of Biological Chemistry**, v. 285, n. 35, p. 26729–26735, 2010.

60. KUES, U.; RUHL, M. Multiple Multi-Copper Oxidase Gene Families in Basidiomycetes – What for? **Current Genomics**, v. 12, n. 2, p. 72–94, 2011.

61. LANGFELDER, K. et al. Biosynthesis of fungal melanins and their importance for human pathogenic fungi. **Fungal Genetics and Biology**, v. 38, n. 2, p. 143–158, 2003.

62. LARRONDO, L. F. et al. A Novel Extracellular Multicopper Oxidase from *Phanerochaete chrysosporium* with Ferroxidase Activity. **Applied and Environmental Microbiology**, v. 69, n. 10, p. 6257–6263, 2003.

63. LOSORDO, Z. et al. Cost competitive second-generation ethanol production from hemicellulose in a Brazilian sugarcane biorefinery. **Biofuels, Bioproducts and Biorefining**, v. 10, n. 5, p. 589–602, 1 set. 2016.

64. LEVASSEUR, A. et al. Expansion of the enzymatic repertoire of the CAZy database to integrate auxiliary redox enzymes. **Biotechnology for Biofuels**, v. 6, n. 1, p. 41, 2013.

65. LOMBARD, V. et al. The carbohydrate-active enzymes database (CAZy) in 2013. **Nucleic Acids Research**, v. 42, n. D1, p. 490–495, 2014.

66. LYND, L. R. et al. Microbial cellulose utilization: fundamentals and biotechnology. **Microbiology and Molecular Biology Reviews**, v. 66, n. 3, p. 506–577, 2002.

67. MAHAJAN, C. et al. *Malbranchea cinnamomea*: A thermophilic fungal source of catalytically efficient lignocellulolytic glycosyl hydrolases and metal dependent enzymes. **Bioresource Technology**, v. 200, p. 55–63, 2016.

68. MAITAN-ALFENAS, G. P. et al. The influence of pretreatment methods on saccharification of sugarcane bagasse by an enzyme extract from *Chrysoporthe cubensis* and commercial cocktails: A comparative study. **Bioresource technology**, v. 192, p. 670–6, set. 2015.

69. MAJZLOVÁ, K.; PUKAJOVÁ, Z.; JANEČEK, Š. Tracing the evolution of the α-amylase subfamily GH13-36 covering the amylolytic enzymes intermediate between oligo-1,6-glucosidases and neopullulanases. **Carbohydrate Research**, v. 367, p. 48–57, 2013.

70. MAKELA, M. R.; DONOFRIO, N.; DE VRIES, R. P. Plant biomass degradation by fungi. **Fungal genetics and biology** : FG & B, v. 72, p. 2–9, 2014.

71. MANAVALAN, T. et al. Secretome analysis of *Ganoderma lucidum* cultivated in sugarcane bagasse. **Journal of Proteomics**, v. 77, p. 298–309, 2012.

72. MARTINEZ, D. et al. Genome sequence of the lignocellulose degrading fungus *Phanerochaete chrysosporium* strain RP78. **Nature biotechnology**, v. 22, n. 6, p. 695–700, 2004.

73. MEYER, A. S.; ROSGAARD, L.; SORENSEN, H. R. The minimal enzyme cocktail concept for biomass processing. **Journal of Cereal Science**, v. 50, n. 3, p. 337–344, 2009.

74. MILANEZ, A. Y. et al. De promessa a realidade : como o etanol celulósico pode revolucionar a indústria da cana-de-açúcar - uma avaliação do potencial competitivo e sugestões de política públicaBiocombustíveis BNDES setorial. [s.l: s.n.]. Disponível em: <https://web.bndes.gov.br/bib/jspui/bitstream/1408/4283/1/BS41-De promessa a realidade_como o etanol celulósico pode revolucionar a indústria da cana-de-açúcar.pdf>.

75. MOROZOVA, O. V. et al. “Blue” laccases. **Biochemistry (Moscow)**, v. 72, n. 10, p. 1136–1150, 2007.

76. MUELLER, O. et al. The secretome of the maize pathogen *Ustilago maydis*. **Fungal Genetics and Biology**, v. 45, n. SUPPL. 1, p. S63–S70, 2008.

77. NOSANCHUK, J. D.; CASADEVALL, A. The contribution of melanin to microbial pathogenesis. **Cellular Microbiology**, v. 5, n. 4, p. 203–223, 2003.

78. PALMIERI, G. et al. A Novel White Laccase from *Pleurotus ostreatus* A Novel White Laccase from *Pleurotus ostreatus.* **the Journal of Biological Chemistry**,

v. 272, n. 50, p. 31301–31307, 1997.

79. PIERSMA, S. R. et al. Whole gel processing procedure for GeLC-MS/MS based proteomics. **Proteome Science**, v. 11, n. 1, p. 17, 2013.

80. PIGNOCCHI, C. et al. The Function of Ascorbate Oxidase in Tobacco 1. **Plant Physiology**, v. 132, p. 1631–1641, 2003.

81. PIHET, M. et al. Melanin is an essential component for the integrity of the cell wall of *Aspergillus fumigatus* conidia. **BMC Microbiology**, v. 9, n. 1, p. 177, 2009.

82. POPPER, Z. A. et al. Evolution and Diversity of Plant Cell Walls: From Algae to Flowering Plants. **Annual Review of Plant Biology, Vol 62**, v. 62, p. 567–588, 2011.

83. RABILLOUD, T. et al. Power and limitations of electrophoretic separations in proteomics strategies. **Mass spectrometry reviews**, v. 28, p. 816–843, 2009.

84. RAVINDRAN, A.; ADAV, S. S.; SZE, S. K. Characterization of extracellular lignocellulolytic enzymes of *Coniochaeta sp*. during corn stover bioconversion. **Process Biochemistry**, v. 47, n. 12, p. 2440–2448, 2012.

85. RIVERA-HOYOS, C. M. et al. Fungal laccases. **Fungal Biology Reviews**, v. 27, n. 3–4, p. 67–82, 2013.

86. RODRÍGUEZ-RINCÓN, F. et al. Molecular and structural modeling of the *Phanerochaete flavido-alba* extracellular laccase reveals its ferroxidase structure. **Archives of Microbiology**, v. 192, n. 11, p. 883–892, 2010.

87. SALVACHÚA, D. et al. Differential proteomic analysis of the secretome of *Irpex lacteus* and other white-rot fungi during wheat straw pretreatment. **Biotechnology for Biofuels**, v. 6, n. 1, p. 115–129, 2013.

88. SANTHANAM, N. et al. Expression of industrially relevant laccases : prokaryotic style. **Trends in Biotechnology**, v. 29, n. 10, p. 480–489, 2011.

89. SARASWATHY, N.; RAMALINGAM, P. Genome sequence assembly and annotation. **Concepts and Techniques in Genomics and Proteomics**, p. 109–121, 2011.

90. SCHNEIDER, W. D. H. et al. *Penicillium echinulatum* secretome analysis reveals the fungi potential for degradation of lignocellulosic biomass. **Biotechnology for biofuels**, v. 9, n. 1, p. 66, 2016.

91. SINGHANIA, R. R. et al. Advancement and comparative profiles in the production technologies using solid-state and submerged fermentation for microbial cellulases. **Enzyme and Microbial Technology**, v. 46, n. 7, p. 541–549, 2010.

92. SLEATOR, R. D. An overview of the current status of eukaryote gene prediction strategies. **Gene**, v. 461, n. 1–2, p. 1–4, 2010.

93. SOLOMON, E. I.; AUGUSTINE, A. J.; YOON, J. O2 Reduction to H_2O by the multicopper oxidases. **Dalton Transactions**, v. 9226, n. 30, p. 3921, 2008.

94. STAM, M. R. et al. Dividing the large glycoside hydrolase family 13 into subfamilies: towards improved functional annotations of alpha-amylase-related proteins. **Protein Eng Des Sel**, v. 19, 2006.

95. STANKE, M.; MORGENSTERN, B. AUGUSTUS: A web server for gene prediction in eukaryotes that allows user-defined constraints. **Nucleic Acids Research**, v. 33, n. SUPPL. 2, p. 465–467, 2005.

96. SUN, X. et al. The effects of wheat bran composition on the production of biomass-hydrolyzing enzymes by *Penicillium decumbens*. **Applied Biochemistry and Biotechnology**, v. 146, n. 1–3, p. 119–128, 2008.

97. TERRAPON, N. et al. The CAZy Database/the Carbohydrate-Active Enzyme (CAZy) Database: Principles and Usage Guideline. In: KIYOKO, F.; KINOSHITA, A. (Eds.). **A Practical Guide to Using Glycomics Databases**. 1. ed. Japan: Springer Japan, 2017. p. IX, 370.

98. TIWARI, R. et al. Unwrapping the hydrolytic system of the phytopathogenic fungus *Phoma exigua* by secretome analysis. **Process Biochemistry**, v. 49, n. 10, p. 1630–1636, 2014.

99. TJALSMA, H. et al. Signal Peptide-Dependent Protein Transport in Bacillus subtilis: a Genome-Based Survey of the Secretome. **Microbiology and Molecular Biology Reviews**, v. 64, n. 3, p. 515–547, 2000.

100. US DOE. Bringing Biological Solutions to Energy Challenges, 2007. Disponível em: <https://public.ornl.gov/site/gallery/detail.cfm?id=252&topic=53&citation=&general=&restsection=&webid=blank>. Acesso em: 10 de junho de 2019.

101. VALDIVIA, M. et al. Biofuels 2020: Biorefineries based on lignocellulosic materials. **Microbial biotechnology**, v. 9, n. 5, p. 585–594, set. 2016.

102. VISWANATH, B. et al. Fungal laccases and their applications in bioremediation. **Enzyme Research**, v. 2014, 2014.

103. VON HEIJNE, G. Signal sequences. The limits of variation. **Journal of Molecular Biology**, v. 184, n. 1, p. 99–105, 1985.

104. WANG, L. et al. Ascorbic acid conversion to erythroascorbic acid, mediated by ubiquitin. **Biochemical and Biophysical Research Communications**, v. 384, n. 2, p. 210–214, 2009.

105. WASINGER, V. C. et al. Progress with gene-product mapping of the Mollicutes:Mycoplasma genitalium. **Electrophoresis**, v. 16, n. 1, p. 1090–1094, 1995.

106. WINGER, A M. et al. Secretome analysis of the thermophilic xylanase hyper-producer *Thermomyces lanuginosus* SSBP cultivated on corn cobs. **Journal of industrial microbiology & biotechnology**, v. 41, p. 1687–1696, 2014.

107. WYMELENBERG, A. VANDEN et al. The *Phanerochaete chrysosporium* secretome: Database predictions and initial mass spectrometry peptide identifications in cellulose-grown medium. **Journal of Biotechnology**, v. 118, n. 1, p. 17–34, 2005.

108. WYMELENBERG, A. VANDEN et al. Computational analysis of the *Phanerochaete chrysosporium* v2.0 genome database and mass spectrometry identification of peptides in ligninolytic cultures reveal complex mixtures of secreted proteins. **Fungal Genetics and Biology**, v. 43, n. 5, p. 343–356, 2006.

109. XIAO, C.; ANDERSON, C. T. Roles of pectin in biomass yield and processing

for biofuels. **Frontiers in Plant Science**, v. 4, n. March, p. 1–7, 2013.

110. YIN, Y. et al. DbCAN: A web resource for automated carbohydrate-active enzyme annotation. **Nucleic Acids Research**, v. 40, n. W1, p. 445–451, 2012.

111. ZHANG, G. et al. Protein quantitation using mass spectrometry. In: **Computational Biology**. [s.l.] Humana Press, Totowa, NJ, v. 673, p. 211–222, 2010.

CAPÍTULO 2

Secretomics insights into the biomass hydrolysis potentials of the phytopathogenic fungus *Chrysoporthe cubensis*

Secretomics insights into the biomass hydrolysis potentials of the phytopathogenic fungus *Chrysoporthe cubensis*

Murillo Peterlini Tavares[1], Túlio Morgan[1], Riziane Ferreira Gomes[1], Marina Quádrio Raposo Branco Rodrigues[1], Bruno Mattei[2], William de Castro Borges[2], Sebastião Tavares de Rezende[1], Tiago Antônio de Oliveira Mendes[1], Valéria Monteze Guimarães[1,*]

[1]Department of Biochemistry and Molecular Biology, Universidade Federal de Viçosa, Av. PH Rolfs, s/n, 36570-900, Viçosa, MG, Brazil.
[2]Department of Biological Science, Universidade Federal de Ouro Preto, Campus universitário Morro do Cruzeiro, 35400-000, Ouro Preto, MG, Brasil.

*** Corresponding Author**
Email: vmonteze@ufv.br
Telephone: (+55 31) 3612 2462

Abstract

The phytopathogenic fungus *Chrysoporthe cubensis* LPF-1 has a great capacity for the production of highly efficient enzymes for lignocellulosic biomass hydrolysis. Herein, the bioinfosecretome of *C. cubensis* was identified by computational predictions of secreted proteins combined with the integration of the proteomic analysis using 1D-LC-MS/MS. I*n silico* secretome predicted 565 putative genes capable of encoding secreted proteins, including 274 CAZymes. Proteomics analysis confirmed 313 proteins, being 137 CAZymes classified as Glycosyl Hydrolases (GH), Polysaccharide Lyases (PL), Carbohydrate Esterases (CE) and Auxiliary Activities enzymes (AA), which indicates the presence of classical and oxidative cellulolytic mechanisms. The diversity of enzymes from the extract shows the versatility of this fungus to act in complex biomasses. This study provides an insight concerning the lignocellulose-degradation mechanisms by *C. cubensis* LPF-1 and allows for the identification of a number of enzymes that are potentially useful for further improvement of the industrial lignocellulose bioconversion process

Keywords

Chrysoporthe cubensis, bioinfosecretome, secretome, CAZymes, lignocellulosic biomass.

1. Introduction

Lignocellulosic biomass is the most abundant material on Earth and it consists mainly of cellulose, hemicellulose, pectin and lignin. The combination with surface enzymes, structural proteins, lipids, proteoglycan, and others minor component forms an intricate network capable of providing resistance to the plant cell wall (Popper et al., 2011). Biomass from agricultural and forestry residues are composed of about 70% of carbohydrates including cellulose, hemicellulose and pectin. These polysaccharides can be enzymatically hydrolyzed to sugar monomers, which serve as feedstock for the production of biochemical and fuels, such as lactic acid, ethanol, methanol and others (Ravindran et al., 2012).

Due to the complex structure of the plant cell wall and recalcitrance of its components, the complete enzymatic degradation of lignocellulose requires the combined action of cellulases, hemicellulases, ligninases, and non- hydrolytic accessory proteins (Harris et al., 2014). The synergistic action of these enzymes promotes the release of hexoses and pentoses, which may be subsequently fermented to products of interest (Hu et al., 2015). However, this step of enzymatic saccharification constitutes the main bottleneck for the technical and economic viability of several biotechnological processes that involve hydrolysis of plant cell wall polysaccharides, such as the production of second generation ethanol (Correa et al., 2016). The enzymes and auxiliary proteins used for this purpose are usually from fungi origin, therefore the efficiency and the costs of saccharification can be reduced by understanding the hydrolytic or oxidative mechanisms and secretion of these enzymes from microorganisms (Borin et al., 2015).

Many phytopathogenic fungi produce an arsenal of extracellular lignocellulolytic enzymes to breakdown the barrier of the plant cell wall and to obtain nutrients for their survival while creating mechanisms to subvert host plant defense responses (Gibson et al., 2011). Among them, the ascomycete fungus *Chrysoporthe cubensis* is a well-documented pathogen of several tree species in tropical and subtropical areas of the world (Gryzenhout et al., 2006). This fungus can cause serious damage to commercial plantations of susceptible species and clones, being considered the main cause of cancer disease in Eucalyptus species (Guimarães et al., 2010). In phytopathogenic fungi, there is a close relationship between virulence and the ability to secrete high levels of hydrolases (Kikot et al., 2009). *C. cubensis* is not an exception to this and it is capable of producing high concentrations of cellulases and hemicellulases, mainly β-glucosidases, xylanases and some accessory enzymes (Falkoski et al., 2013).

A recent work has shown that *C. cubensis* LPF-1 cultivated under solid state fermentation using wheat bran as a carbon source was able to increase the ability to produce highly efficient enzymes to hydrolyze sugarcane bagasse compared to the commercial enzymatic cocktails Multifect® CL, Multifect® XL and Accellerase® 1500 (Maitan-Alfenas et al., 2015). Therefore, it is essential to know in detail the enzymes and proteins secreted by *C. cubensis* LPF-1, especially those involved in the hydrolysis of the plant biomass. In this work, we present the first characterization of a complete protein profile secreted by *C. cubensis* LPF-1 grown in a semi-solid state with wheat bran as a carbon source. This study was performed by integration of *in silico* predictions of secretome based on genome sequence with proteomic data was obtained by mass spectrometry.

2. Materials and methods

2.1. Materials

All chemicals were produced from Sigma Chemical Co. (St. Louis, MO, USA), Merck (Darmstadt, Germany), Himedia Laboratories Co. (Mumbai, Maharashtra, India), Vetec Fine Chemical (Duque de Caxias, RJ, Brazil), Bio-Rad Laboratories (Hercules, CA, USA), unless otherwise stated and were used without further purification. Wheat bran was obtained on the local market. All organic solvents and solid chemicals were of analytical grade.

2.2. Gene prediction

The draft genome of *Chrysoporthe cubensis* isolates number CMW 10028 (Wingfield et al., 2015) were retrieved from the NCBI database (www.ncbi.nlm.nih.gov) under the accession number LJCY00000000. The 954 Scaffold sequences of the genome were submitted as an input file in the *ab initio* gene prediction program AUGUSTUS (http://bioinf.uni-greifswald.de/augustus/) (Stanke and Morgenstern, 2005) using default parameters and trained on genes models for *Neurospora crassa*. The BUSCO v2 (https://busco.ezlab.org/v2/) (Simão et al., 2015) dataset for fungi, comprising 1438 single-copy orthologue genes from 85 fungal strain, was used to evaluate the quality and the confidence of the genome assembly and predicted gene sets.

2.3. Bioinfosecretome prediction and functional annotation

The following computational tools were employed to predict protein-based features in the secretome prediction pipeline. As a first strategy, the prediction of the *C. cubensis* secreted proteins was performed using the web analysis tool SECRETOOL (http://genomics.cicbiogune.es/SECRETOOL/Secretool.php) (Cortázar et al., 2014), according to the pipeline tools for classical secretion, following default parameters, with the exception for SignalP cut-off probability set to 0.5. Simultaneously, the predicted proteome was subjected to a second identification strategy to increase the coverage of identified CAZymes. Proteins were screened using the dbCAN2 meta server (http://cys.bios.niu.edu/dbCAN2/index.php) (Yohe et al., 2018), integrating three tools/databases for automated CAZymes annotation: HMMER; DIAMOND and Hotpep. Hits were considered positive when identified by at least one method. The dbCAN2 was used to generate a list of all CAZymes present in the complete proteome, and posteriorly, the DeepLoc-1.0 (http://www.cbs.dtu.dk/services/DeepLoc/) (Almagro Armenteros et al., 2017) was used for the prediction of subcellular localization. Proteins targeted to the nonclassical secretion pathway were identified using SecretomeP 2.0 Server (http://www.cbs.dtu.dk/services/SecretomeP/) (Bendtsen et al., 2005). Only the sequences labeled as extracellular CAZymes were retained and assembled in a common list with the proteins identified by SECRETOOL.

Function assignment and annotation by InterPro terms (InterProScan, EBI) and enzyme classification codes (E.C) were determined using the Blast2GO software suite.57 (https://www.blast2go.com/) (Talon et al., 2008). The protein sequences were functionally annotated based on searches using BLASTp version 2.2.21 (Altschul et al., 1990). For each query sequence, the software first detects up to 20 homolog sequences in the non-redundant (nr) NCBI database restricted to the fungi taxonomy filter, with a minimum expected value of 1.0E-3 and a high scoring segment pair cutoff of 33. CAZymes were functionally annotated by the dbCAN2 and classified according to CAZy catalytic group as glycosyl hydrolases (GHs), polysaccharide lyases (PLs), carbohydrate esterases (CEs), carbohydrate binding modules (CBMs). Proteins containing glycosyltransferases (GTs) modules were identified but not included in further analysis. For each predicted protein, theoretical mass weight (Mw) and isoelectric point (pI) were calculated by Compute pI/Mw tool (https://web.expasy.org/compute_pi/).

2.4. Microorganism and molecular identification

The fungus *C. cubensis* LPF-1 was obtained from the mycological collection of the Laboratory of Forest Pathology, Universidade Federal de Viçosa, MG, Brazil. This isolate was identified based on morphological, microscopic and molecular analyses. For molecular identification, the mycelium of a 7 days culture grown on a potato dextrose agar (PDA) plate was collected and ground in a mortar with liquid nitrogen, and the total DNA was extracted using DNeasy Plant Mini Kit (Qiagen), according to the recommended instructions. Amplification of the ITS regions of the nuclear rRNA gene was achieved using primers ITS1 (5′-TCCGTAGGTGAACCTTGCGG-3′) and ITS4 (5′-TCCTCCGCTTATTGATATGC-3′) with the genomic DNA as a template. The PCR-amplified product was sequenced in Applied Biosystems 3730XL Sequencer (Macrogen Inc., Seoul, Korea). The ITS sequence was compared with the NCBI database for species confirmation using BLASTn version 2.2.21 (Altschul et al., 1990).

2.5. Inoculum preparation and culture conditions

Initially, 10 agar plugs cut out of a 7 day-old colony of *C. cubensis* grown on PDA plates were transferred to 250 ml Erlenmeyer flasks containing 100 ml of previously sterilized medium with the following composition, in g/L; glucose, 10.0; NH_4NO_3, 1.0; KH_2PO_4, 1.0; $MgSO_4$, 0.5 and yeast extract, 2.0. The flasks were placed under shaking at 150 rpm, 28 °C, for 5 days. The culture obtained was aseptically homogenized and used to prepare the culture in the semi-solid state. The enzymatic production, via semi-solid fermentation (SSF), was carried out in 250 mL Erlenmeyer flasks containing 12.5 g of wheat bran and 18.75 mL of the culture media (final moisture of 60%) with the following composition, in g/L: NH_4NO_3, 1.0; KH_2PO_4, 1.5; $MgSO_4$, 0.5; $CuSO_4$, 0.25 and yeast extract, 2.0. Furthermore, $MnCl_2$ (0.1 mg/L), H_3BO_3 (0.075 mg/L), Na_2MoO_4 (0.02 mg/L), $FeCl_3$ (1.0 mg/L) and $ZnSO_4$ (3.5 mg/L) were also added to the medium as trace elements. The flasks were autoclaved at 120 ºC for 20 min and then inoculated with 10 mL (approximately 1.5 x 10^6 spores/mL). The flasks remained at 28 ºC in a controlled temperature chamber and the extraction of secreted enzymes was performed after 7 days of fermentation. Experiments were carried out in triplicate. The proteins secreted during SSF were extracted with sodium acetate buffer, 50 mM, pH 5, at a ratio of 10:1 (buffer/dry substrate), under the agitation of 150 rpm for 60 min at room temperature. The crude extract was collected by filtration through nylon cloth followed by centrifugation at 15000

g for 10 min at 4 ºC to remove cell debris. Clarified supernatants from the three biological replicates were pooled and stored at 20 ºC for further analysis.

2.6. Enzyme assays and protein concentration

To verify the viability of the enzymatic extract obtained after the SSF, enzymatic assays were performed in 100 mM sodium acetate buffer, pH 5, at 50 ºC. The enzymatic assays were carried out in triplicate. Relative standard deviations of the measurements were below 10%.

Cellulase activity (FPase) was assayed as described by (Ghose, 1987). The reaction mixture containing 100 µl of diluted enzyme and 1.4 ml of sodium acetate buffer (50 mM, pH 5.0) was incubated with one filter paper strip (Whatman No. 1; 1 x 6 cm) at 50 ºC for 60 min. The amount of total reducing sugars released was estimated by the dinitrosalicylic acid (DNS) method (Miller, 1959). The activities of endoglucanase (CMCase), xylanase, mannanase, polygalacturonase and amylase were determined using the substrates carboxymethylcellulose (CMC) (1% w/v), xylan birchwood (1% w/v), locust bean gum (0.4% w/v), polygalacturonic acid (0.2% w/v), and starch (1% w/v), respectively. The assays were performed using 100 µL of crude secretome and 400 µL of specific substrates prepared in sodium acetate buffer, 100 mM, pH 5. After incubation at 50 º C for 30 min, the DNS reagent was added to determine the concentration of reducing sugars released (Miller, 1959). One enzyme activity unit (U) was defined as the amount of enzyme which released a µmol of the product (equivalent glucose, xylose, mannose, galacturonic acid) per minute under assay conditions used for all activities.

The activities of β-glucosidase, β-xylosidase, β-mannosidase, α-galactosidase, β-galactosidase, α-arabinofuranosidase, and cellobiohydrolase were measured by monitoring the release of ρ-nitrophenol from ρ-nitrophenyl-β-D-glucopyranoside (ρNPβGlc), ρ-nitrophenyl-β-D-xilopiranosídeo (ρNPβXil), ρ-nitrophenyl-β-D-manopiranosídeo (ρNPβMan), ρ-nitrophenyl-α-D-galactopyranoside (ρNPαGal), ρ-nitrophenyl-β-D-galactopyranoside (ρNPβGal), ρ-nitrophenyl-α-D-arabinopyranosyl (ρNPαAra) and p-nitrophenyl-β-D-cellobioside (ρNPβCel) as synthetic substrates, respectively. The reaction mixture contained 100 µL of appropriately diluted enzyme solution, 125 µL of synthetic substrate solution (1 mM final concentration) and 275 µl of 100 mM sodium acetate buffer, pH 5. The enzymatic reaction was incubated at 50 ºC for 30 min and stopped by addition of 0.5 mL sodium carbonate solution (0.5 M). Absorbance was measured at 410 nm and the amount of ρ-nitrophenol released was estimated by a

standard curve. One enzyme activity unit (U) was defined as the amount of enzyme which ρ-nitrophenol per minute under the assay conditions used.

The pectin lyase activity was determined by the addition of 1.5 mL of enzyme extract in 1 mL of pectin (2.5% w/v) (Delgado et al., 1993). The assay was carried out at 50 °C for 30 min. Aliquots of 500 µL were removed and added to 4.5 mL of HCl 0.01 mol/L, to stop the reaction. The absorbance of the samples was measured at 235 nm. The pectin lyase activity was calculated using the molar extinction coefficient of the product formed Δ-4,5 -galacturonide, 5.55 x 10^4 $M^{-1}cm^{-1}$.

The laccase activity was determined by monitoring the oxidation of the 2,2'-Azino-bis(3-ethylbenzothiazoline-6-sulfonic acid) substrate (ABTS). The reaction mixtures contained 100 µL of the appropriately diluted enzyme solution, 350 µL of the buffer and 50 µL of ABTS 10 mM. This mixture was incubated at 50 ºC for 10 min and the absorbance was immediately measured at 420 nm. Laccase activity was calculated by the Lambert-Beer principle using a molar extinction coefficient of 3.6 × 10^4 M^{-1} cm^{-1} (Visser et al., 2015). A unit of enzyme activity was defined as the amount of enzyme required to produce 1 µmol of the corresponding product per minute in the condition used in the assay. Protein concentration was determined by (Bradford, 1976), using bovine serum albumin (BSA) as standard.

2.7. Secreted protein precipitation and quantification

The crude extract was filtered using syringe filters with a 0.22 µm polyvinylidene difluoride (PVDF) membrane (Millipore, Germany). Pre-chilled ethanol (100%) was added to the chilled crude enzyme extracts in a 10:1 ratio and the mixture was kept at −20 ºC overnight. The samples were centrifuged at 8000 g for 20 min at 4 ºC. The pellets were allowed to dry at room temperature to remove residual solvents. The pellets were reconstituted in an appropriate volume of lysis buffer (8 M urea; 2 M thiourea; 4% CHAPS), and the protein content was determined using the Bradford method (Bradford, 1976).

2.8. SDS-PAGE and in-gel trypsin digestion

The protein sample (30 µg) was subjected to a boiling denaturation step in the presence of the buffer (0.0625 M final concentration of Tris-HCl pH 6.8, 2% SDS, 10% glycerol, 5% mercaptoethanol) for 5 minute and subsequently applied in sodium dodecyl sulfate-polyacrylamide gel electrophoresis (SDS-PAGE) on a 4% polyacrylamide

stacking gel and a 10% polyacrylamide-resolving gel. Samples were run in an electrophoretic Mini-Protean II system (Bio-Rad) using 20 mA constant current (variable voltage) and a running time of approximately 20 minutes. The gel was stained with Coomassie Brilliant Blue G-250 and the protein band (approximately 0.5cm x 1cm) was excised. The gel slices were fragmented into smaller pieces (approximately 1 mm^2), and then washed with 50% acetonitrile (ACN) containing 20 mM ammonium bicarbonate (NH_4HCO_3) buffer, and subjected to destaining. Gel pieces were reduced and alkylated with dithiothreitol (DTT) (50 mM) and iodoacetamide (100 mM), respectively. After 3 washes with 50% ACN containing 20mM NH_4HCO_3 buffer, the samples were dried and then subjected to overnight digestion with sequencing grade modified trypsin solution (20 ng/µL Trypsin Gold from Promega in 20 mM NH_4HCO_3) for 18 h at 37 °C. Tryptic peptides were extracted with 0.1% (v/v) trifluoroacetic acid (TFA) in 50% (v/v) ACN twice, and the pooled was dried in a Speed Vacuum system. Peptides were reconstituted in 20 µl of 2% (v/v) ACN and 0.1% (v/v) TFA.

2.9. Identification of proteins by LC-MS/MS analysis

The digested peptides were analyzed on the Q-Exactive ™ mass spectrometer (Thermo Scientific), connecting to a nanoUHPLC UltiMate® 3000 (Dionex®) system via a nanospray ion source. The samples were injected into the chromatograph by a trapping system using an Acclaim PepMap100 C18 column (75 µm i.d × 2 cm, 3 µm, 100 Å, Thermo Scientific), and then directed to an Acclaim PepMap100 C18 capillary column (75 µm i.d × 15 cm, 2 µm, 100 Å, Thermo Scientific). A linear gradient was started from 3.8 to 50% of buffer B (80% acetonitrile and 0.1% formic acid) in buffer A (0.1% formic acid) at 300 $nl.min^{-1}$, over 120 min, followed by a sharp ramp to 99% B. LC-MS/MS operated a data-dependent acquisition method, in positive ion mode, with a MS1 resolution of 70.000 in the 300 – 2000 m/z range and a maximum injection time of 120 ms. The MS2 spectra were obtained with a resolution of 35000, with a maximum injection time of 120 ms. Up to 12 more intense precursor ions with charge between 2 to 4 were isolated with a 2 m/z window and fragmented by high-energy collisional dissociation with a normalized collision energy of 28 – 30 V.

Raw MS/MS spectra were submitted to database search and de novo sequencing using PEAKS software, version 8.5. The search was performed against in house database of *C. cubensis* containing 12418 protein sequences, with the following settings: (i) trypsin was used to digest the proteins, allowing two missed cleavages; (ii) error tolerances of up to 10 ppm for precursors and 0.1 Da for product ions; (iii) cysteine carbamidomethylation

(+57.02 Da) as a fixed modification; (iv) methionine oxidation (+15.99 Da) as variable modifications; (v) peptide mass error tolerance was set at 10 ppm for precursor ion and 0.1 Da for fragment ions. For protein identification, the desired False Discovery Rate (FDR) estimation was set as 1%. Protein identifications were accepted if they contained at least two identified peptides and one unique peptide. The relative abundance of proteins was estimated by the label-free quantification (LFQ) method using the ion intensity approach. The quantification of a target protein was estimated by the area under curve (AUC) of the ion current from the three most intense of its identified peptides and normalized by the total ion current of the LC-MS run (Ruas et al., 2019).

3. Results and discussion

3.1. Overview of *Chrysoporthe cubensis* secreted proteins

In this study, 562 putative genes capable of encoding secretable proteins were identified, corresponding to 4.6% of the total proteins potentially produced by *C. cubensis*. These values are similar to the computational prediction of fungi-secreted proteins known as good producers of lignocellulolytic enzymes, such as *Pleurotus ostreatus*, whose bioinfosecretome showed 554 putatively secreted proteins, representing 4.5% of the total proteins (Alfaro et al., 2016). The proteomic analysis of the crude extract of *C. cubensis* LPF-1, grown in wheat bran, allowed the detection of 313 proteins. The electrophoretic profile of the proteins from *C. cubensis* LPF-1 crude extract is shown in **Fig. 1A**.

Analysis of the *C. cubensis in silico* secretome predicted 273 Carbohydrate-active enzymes (CAZymes). This value corresponds to 48.8% of the bioinfosecretome and 2.2% of the predicted proteome. CAZymes are the group with the highest number of representatives in the bioinfosecretome (**Fig. 2A**). Most of the predicted CAZymes showed molecular weight from 20 to 120 kDa and their predicted isoelectric points occupy an acidic range of 3.5 to 5.5, typical of enzymes secreted by fungi (**Fig. 1B**).

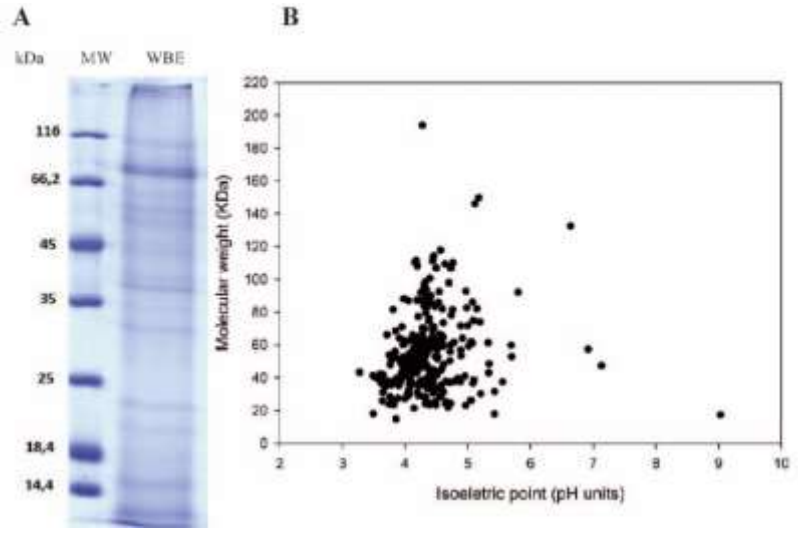

Figure 1: (A) SDS-PAGE analysis of crude enzymatic extract produced by *Chrysoporthe cubensis* LPF-1grown in semi-solid medium containing wheat bran as carbon source. MW - molecular weight markers; WBE - crude enzymatic extract from *C. cubensis*. (B) Distribution of CAZymes from the predicted bioinfosecretome as a function of molecular weight and isoelectric point.

The proteomic analysis of experimental secretome revealed that between the 313 detected proteins, 137 were CAZymes, corresponding to 43.8% of the secreted proteins (**Fig. 2D**). This result confirms that in the experimental secretome, CAZymes are the major protein group. Proteases and peptidases account for 4.1% of bioinfosecretome and 11.2% of the experimental secretome (**Fig. 2A, 2D**). In phytopathogenic fungi, the secretion of proteases is essential, since these enzymes may play a key role during the penetration, lysis, and colonization of host cells, acting on proteins that are part of the cell wall (Ramada et al., 2016). Proteolysis is involved in different physiological functions, such as germination, sporulation, aerial mycelium formation, nutrition and adaptation to different environmental conditions, being fundamental for fungus survival (Chandrasekaran et al., 2016). In addition on generating nutrients by fungal cells, lipases enable the penetration of specialized fungal structures and potentially degrade components of the host cell cuticle (Gonzalez et al., 2016). Lipases corresponded to 5.3% of bioinfosecretome and were observed in *C. cubensis* extract, making up 7.7% of the detected proteins (**Fig. 2A, D**).

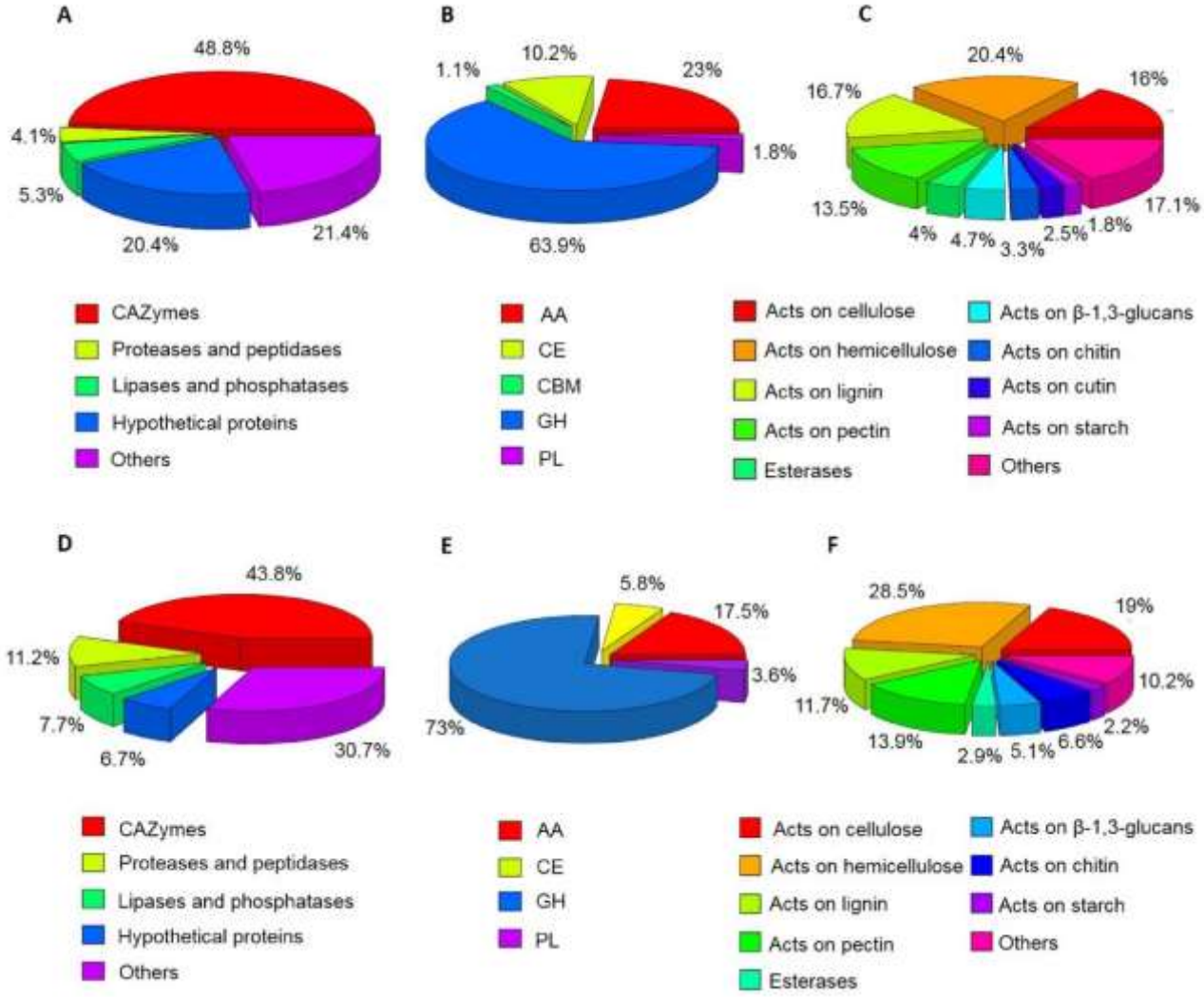

Figure 2: Pie charts of the functional classification of proteins predicted in the bioinfosecretome and identified in the experimental secretome. Classification based on the main enzymatic activities, for bioinfosecretome (A), and secretome (D). Classification based on CAZy classes, for bioinfosecretome (B), and secretome (E). Classification based on the preferred substrates of CAZymes, for bioinfosecretome (C), and secretome (E).

Hypothetical proteins, for which no function could be predicted based on genome annotations and a BLAST analysis against sequenced *C. cubensis* genome comprised 117 proteins, which represents 20.7% of the fungal bioinfosecretome. On the other hand, in the *C. cubensis* LPF-1 experimental secretome, 21 hypothetical proteins of unknown function were detected, contributing with 6.7% of the secretome. The hypothetical proteins are potential candidates for future functional annotations since these proteins could represent new targets not previously described and possibly could have a

biotechnological interest.

In both, predicted and experimental secretome, the distribution of the carbohydrate-acting proteins in the CAZy classes shows a similar profile (**Fig. 2B, 2E**). There was a predominance of glycosyl hydrolases and auxiliary activity enzymes, which represent more than 80% of CAZymes. These enzymes have a broad spectrum of substrate specificities and the combined activities allow the depolymerization of lignocellulose. For cellulose degradation, three major types of enzymes act synergistically: endoglucanases (EC 3.2.1.4), cellobiohydrolases (EC 3.2.1.176) and β-glucosidases (EC 3.2.1.21) (Horn et al., 2012). For the hydrolysis of hemicellulose, a more complex set of enzymes is necessary. In the case of hydrolysis of xylan, the action of endo-β-1,4-xylanase (EC 3.2.1.8), β-xylosidase (EC 3.2.1.37) and some accessory enzymes are required. Auxiliary activities enzymes, such as laccases, peroxidases, cellobiose dehydrogenases (CDH) and lytic polysaccharide monooxygenases (LPMO), have also emerged as promising targets for application in the saccharification of biomass and production of 2G ethanol. The *C. cubensis* bioinfosecretome and secretome exhibited similar profile especially concerning to enzymes that act on cellulose, hemicellulose, lignin, and pectin (**Fig. 2C, 2E**).

Usually, the enzymes of commercial cocktails intended for the hydrolysis of plant biomass, are derived from fungi of the genus *Aspergillus* and *Trichoderma*, which exhibit high efficiency in the production of a broad range of cellulases and hemicellulases (Florencio et al., 2016). For the *Aspergillus niger* secretome cultivated in sugarcane biomass, it was detected 65 enzymes directly related to biomass degradation (22% of the 292 CAZymes encoded by its genome), whereas *Trichoderma reesei* cultivated in the same condition, secreted 24 enzymes (10% of the 228 CAZymes) (Borin et al., 2015). *C. cubensis* LPF-1 cultivated in wheat bran shows superior performance in comparison with these main industrial sources of enzymes, producing 109 enzymes that act on lignocellulosic biomass (39% of the 278 CAZymes).

3.2. Distribution and functional annotation of CAZy families

The predicted and potentially secreted CAZymes from *C. cubensis* are distributed in four CAZy classes, occupying 74 distinct families (**Fig. 3A - D**).

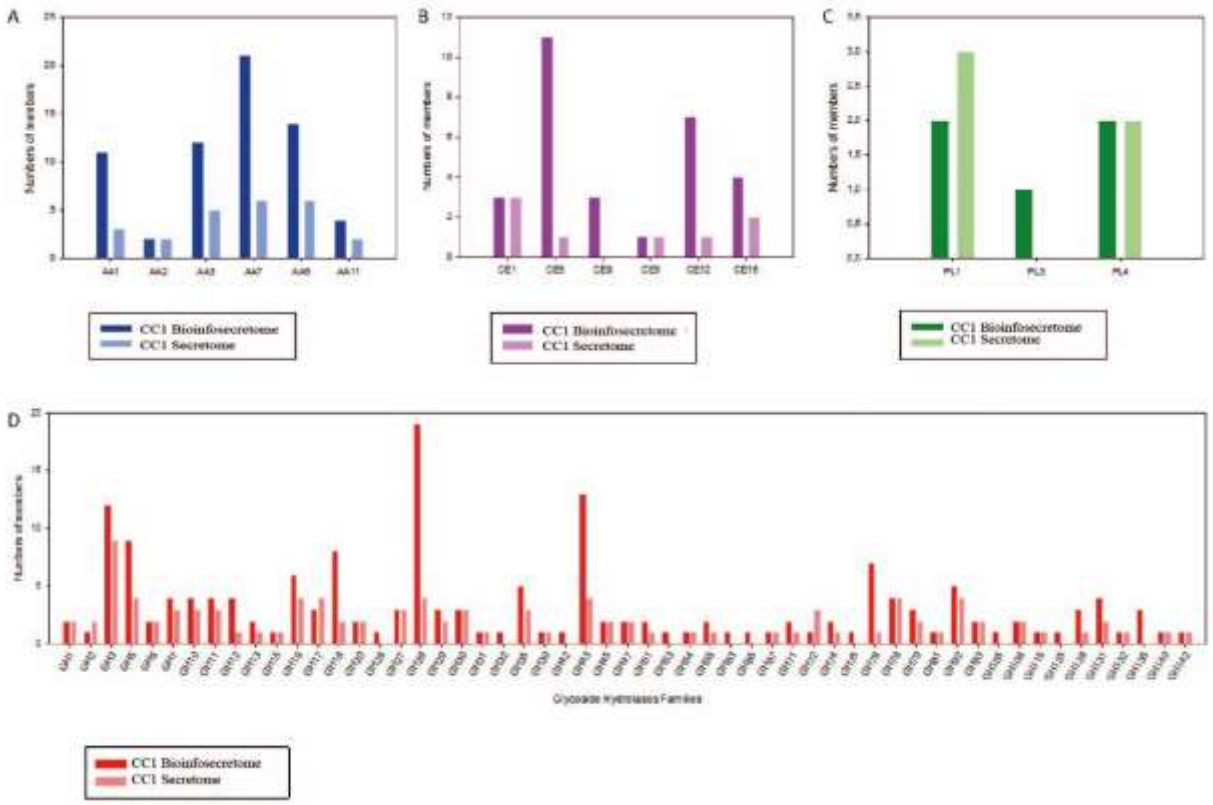

Figure 3: Number of protein members predicted by bioinfosecretome and identified in the proteomic-based secretome. Bar charts represent in (A), auxiliary activity enzymes; (B), carbohydrate esterases; (C) polysaccharides lyases; (D), glycosyl hydrolases.

3.2.1. Auxiliary activity enzymes

The predicted and secreted auxiliary activity proteins from *C. cubensis* LPF-1 belong to 6 distinct families. Of 63 predicted auxiliary activity proteins, 24 proteins were detected in the *C. cubensis* LPF-1 secretome (**Fig. 3A**). These auxiliary activities enzymes from *C. cubensis* LPF-1 secretome belong to the following families: AA1 (3 multi-copper oxidases); AA3 (4 glucose-methanol-choline oxidoreductase - GMCs); AA7 (6 glucooligosaccharide oxidases) and AA9 (6 LPMOs). Besides, the *C. cubensis* LPF-1 secretome contained enzymes belong to AA11 (2 enzymes with activity in the oxidation of chitin) and AA2 (2 peroxidases).

The high variety of detected enzymes belonging to AA families follows the characteristic of these enzymes to act in collaboration with each other to increase the lignin deconstruction and oxidative degradation of cellulose and chitin. Peroxidases class

II of the AA2 family act in the conversion of hydrogen peroxide, which is formed during the oxidative reactions in oxygen and water, catalyzed by enzymes of AA3 and AA7 families. Thus, peroxidase activity leads to a protective effect against the toxicity of reactive oxygen species (ROS) generated from hydrogen peroxide during Fenton reactions (Nekiunaite et al., 2016). There was synergy between laccases AA1 and oxireductases AA3 in the production of hydroxyl radicals. Synergy also occurs between cellobiose dehydrogenase (CDH) of the AA3_1 subfamily, which can donate electrons to the monooxygenases of the AA9 family (LPMO), for the oxidative cleavage of cellulose polymers (Miyauchi et al., 2017). Although most of the enzymes belong to auxiliary activity families (AA1 to AA8) do not act directly on carbohydrates, these enzymes catalyze the deconstruction of lignin by oxidative mechanisms. However, the enzymes of families AA9 and AA10, catalyze oxidative reactions that promote the disruption of cellulose in crystalline regions, providing new access points for traditional GHs (Tandrup et al., 2018). Some AAs act on the cleavage of other polymers by oxidative mechanisms, such as chitin (AA11, AA15), starch (AA13) and xylan (AA14) (Tandrup et al., 2018).

Commercial cocktails containing LPMOs or that are supplemented with these enzymes showed superior saccharification performance (Cannella et al., 2012). *C. cubensis* presents a high number of predicted and potentially secreted LPMOs, with 13 members of the AA9 family. The presence of a large number and diversity of representatives of AA families could explain the efficiency of its enzymatic cocktail.

3.2.2. Carbohydrate Esterases

Of the 28 Carbohydrate Esterase enzymes potentially secreted by *C. cubensis,* eight members were detected in the experimental secretome (**Fig. 3B**), which belong to families CE1 (3), CE5 (1), CE9 (1), CE12 (1) and CE16 (2). The substrate specificity of these carbohydrate esterases is diverse, such as the members of the CE1 family, that share common activities of carboxylesterase and endo-1,4-β-xylanase. The CE8 enzymes act on pectin with pectinesterase activity, while CE5 enzymes may act on cutin and catalyze the breakdown of cutin ester bonds, releasing cutin monomers, and play a key role in the process of fungal infection of aerial plant organs (Nakamura et al., 2017).

3.2.3. Polysaccharide lyases

The *in silico* secretome revealed five Polysaccharide lyases (PL), which belong to the families PL1 (2), PL3 (1) and PL4 (4), being detected in the secretome only

representatives of families PL1 and PL4 (**Fig. 3C**). Three PL1 enzymes were found in the experimental secretome. Pectin, a highly branched structural heteropolysaccharide, is present on the primary cell wall of plants and it is usually associated with cellulose fibers (Berlin et al., 2007). An extensive set of CAZymes is required for the complete depolymerization of pectin components, including polysaccharide lyases. These enzymes cleave polysaccharide chains containing uronic acid employing a β-elimination mechanism to generate unsaturated hexenuronic acid residues and a novel reducing end (Berlin et al., 2007).

3.2.4 Glycosyl Hydrolases

C. cubensis bioinfosecretome analysis showed that the most profusely predicted enzymes belong to GH classes, with 175 distinct members occupying 54 families (**Fig 3D**). In experimental secretome, the presence of 100 unique glycosyl hydrolases, which occupy 45 distinct families, represent 57.5% of the potentially secreted GHs, indicating that a large number of predicted enzymes are functional. Members of the 9 GH families were not secreted by *C. cubensis* under these conditions, but these enzymes could be potentially active when induced under different culture media and growth conditions. The GH class comprises the most active enzymes for the degradation of lignocellulose, in particular, the cellulases of the families GH1, GH3, GH5, GH45 and GH74, and the xylanases of the GH3, GH10, GH11, and GH39 families. At least 29 GH families are involved in the plant biomass degradation (Zhao et al., 2013), and GH2, GH3, GH5, GH27, GH31, GH35, GH43, GH74, GH78 enzymes tend to be more abundant in the fungal secretome (Zhao et al., 2013).

In the *C. cubensis* bioinfosecretome, the families with the highest number of predicted members were GH3, GH5, GH16, GH18, GH28, GH43, and GH76, containing 12, 9, 7, 8, 19, 13 and 7 members, respectively; while in the experimental secretome, these families contained 9, 4, 4, 2, 4, 4, and 1 expressed members, respectively. Of the 12 enzymes predicted belonging to the GH3 family, 11 were β-glucosidases. In the experimental secretome, 9 different types of β-glucosidases were detected. Organisms known to be efficient in the enzymatic hydrolysis of biomass, such as *Penicillium* and *Aspergillus* species, secrete a wide variety and amount of β-glucosidases (Falkoski et al., 2013). The activity of β-glucosidase in enzyme cocktails reduces the inhibition of cellulases by cellobiose and has a synergistic effect with cellobiohydrolases or endoglucanases (Gruno et al., 2004). The bioinfosecretome analysis showed that of the 9

enzymes belonging to the GH5 family, 6 were endo-1,4-beta-D-glucanases, while in the *C. cubensis* LPF-1 extract, 4 distinct enzymes were detected, but with activities on cellulose, hemicellulose, and pectin. Four members of the GH16 family acting on hemicellulose, such as endo-1,3 (4)-beta-glucanases were predicted and 3 were detected in the *C. cubensis* extract. The GH18 and GH20 families form the chitinolytic machinery predicted for *C. cubensis* bioinfosecretome, with 5 and 2 members respectively.

The GH18 endochitinases, together with the GH20 exochitinases, act synergistically in the depolymerization of chitin and cell wall degradation (Do Vale et al., 2012). The experimental secretome presented 4 enzymes of the chitinolytic machinery, 2 GH18 and 2 GH20. The GH28 family is the most populous of the bioinfosecretome, possessing 19 enzymes that act on the pectin, including 14 polygalacturonases, 3 rhamnogalacturonase, and 2 galacturonan 1,4-alpha-galacturonidase. Interestingly, the 4 enzymes of the GH28 family detected in the *C. cubensis* extract are polygalacturonases. The pectinolytic potential of this enzymatic extract is confirmed by the high value of polygalacturonase activity (**Table 1**).

It should be noted that 12 of the identified predicted glycosyl hydrolases have carbohydrate binding modules (CBMs) belonging to seven different families. Among these, 11 enzymes were present in the crude extract, 4 GHs with CBM1 (GH5, GH7, GH30, and GH45), two of which acting in cellulose (GH7 and GH45). The CBM1 is a type A CBM, which acts on crystalline cellulose and provides increased cellulase concentration on the surface of the insoluble substrate. In addition, this CBM promotes the recognition of specific sites on the local substrate and induces cellulose rupture, which facilitates the catalytic activity of cellulases and hemicellulases (Harris et al., 2014). The presence of CBM1 enzymes in *C. cubensis* extract would allow more efficient degradation of the substrate, providing the action of other enzymes in the regions of high recalcitrance of lignocellulosic biomass.

Table 1: Activities of enzymes in the crude extract from *Chrysoporthe cubensis* LPF-1 grown in semi-solid medium containing wheat bran and their relative abundances estimated by the label-free quantification (LFQ) method using the ion intensity approach. The enzymatic activities values are the average of three repetitions and standard deviations did not exceed 10% of the mean.

Enzyme	Enzymatic activity (U/mL)	Nº of distinct members	CAZy families	Relative abundance (%)
Endoglucanase	4.75 ± 0.34	9	GH5, GH6, GH7, GH12, GH45	15.18
β-Cellobiohydrolase	1.11 ± 0.03	5	GH6, GH7	13.21
β-Glucosidase	1.71 ± 0.02	11	GH1, GH132	5.33
α-Amylase	0.95 ± 0.02	1	GH15	3.23
Xylanase	42.61 ± 6.58	6	GH10, GH11	3.02
β-Xylosidase	0.12 ± 0.001	2	GH3, GH39	0.38
α-Arabinofuranosidase	0.21 ± 0.01	2	GH51, GH54	0.55
α-Galactosidase	0.02 ± 0.0001	3	GH27	0.33
β-Galactosidase	0.01 ± 0.0002	3	GH2, GH35	0.29
Laccase	0.03 ± 0.0002	2	AA1	0.27
β-Mannosidase	0.14 ± 0,004	1	GH2	0.10
β-Mannanase	4.66 ± 0.02	1	GH5	0.12
Polygalacturonase	2.19 ± 0.14	3	GH28	0.21
Pectin lyase	20.05 ± 0.31	2	PL1_4	0.07

3.3. The carbon source and the *C. cubensis* secretome composition

Fungi can adapt to different growth conditions and adjust their metabolism according to the carbon and nitrogen sources in which they were submitted (Girard et al., 2013). The secreted protein pool is dynamically modulated according to growth conditions and nutrient sources, allowing the degradation of complex substrates outside the cell and subsequent uptake of smaller molecules (Bianco and Perrotta, 2015). *C. cubensis* LPF-1 was able to secrete a diverse repertoire of lignocellulolytic enzymes when cultured in semi-solid medium containing wheat bran as a carbon source (**Fig. 4**). This fungus was able to secrete approximately 39% of the CAZymes predicted by the bioinfosecretome, demonstrating the great induction power of wheat bran, and proving the advantage of using this carbon source as a standard inductor.

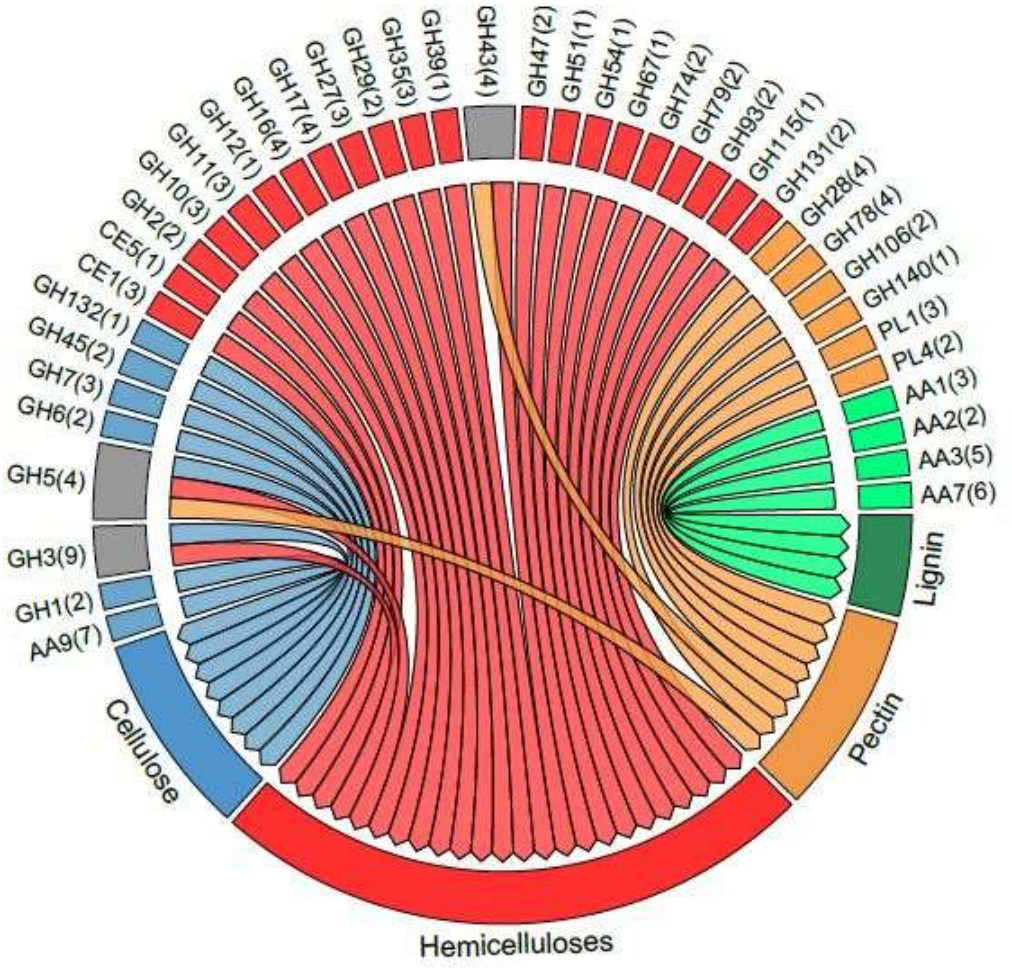

Figure 4: CAZymes of the extract of *C. cubensis* according to the substrate of action. Circus plot showing members of the CAZy families detected in the secretome of *C. cubensis* grown in wheat bran and the main components of the lignocellulosic biomass. The arrows represent the enzymes with activity against the following substrates: cellulose (blue); hemicellulose (red); pectin (orange); lignin (green); and different substrates (gray).

The high capacity of wheat bran to efficiently induce cellulases production may be related to its composition, which is elevated in proteins (13 – 19%) and hemicellulose (more than 30%), together with low concentrations of lignin (3 – 6%) (Sun et al., 2008). The low lignin content enables higher digestibility of wheat bran compared to other sources rich in crystalline cellulose and lignin. Additionally, the high level of hemicellulose provides a rich source of sugars (hexoses, arabinose, and xylose), which can be rapidly metabolized and, the high protein content allows a balanced carbon and nitrogen (C/N) ratio. These characteristics allow the efficient growth of microorganisms and result in specific bioproducts from SSF (Sun et al., 2008).

The *C cubensis* crude extract showed high enzymatic activities mainly in relation to xylanase (42.61 U/mL), mannanase (4.66 U/mL), endoglucanase (4.75 U/mL), β-

glycosidase (1.71 U/mL), β-cellobiohydrolase (1.11 U/mL) and pectin lyase (20,50 U/mL) (**Table 1**). In addition to *C cubensis* extract showing high endoglucanase activity, these enzymes are significantly present in the experimental secretome and contribute with 15.18% of the relative abundance. The enzymatic extract has a large number of distinct members that act on non-reducing (GH6) and reducing (GH7) ends of cellulose. Although there is a great diversity of these cellulases, one endoglucanase (g2236.t1) corresponding to 12.94% of the relative abundance of the extract, indicating that this enzyme plays a fundamental role in the processes of cellulose deconstruction.

The β-cellobiohydrolases are also present in high amounts in *C. cubensis* extract, with 13.21% relative abundance and high diversity of members. However, they have a lower enzymatic activity (1.11 U/mL). In contrast, xylanases, which are present in smaller quantities in the experimental secretome (3.02%), have much higher enzymatic activity (42.61 U/ml) (**Table 1**). There is no direct relationship between relative abundance and enzymatic activity, as intrinsic characteristics of each enzyme and extrinsic factors related to the cooperative action may influence the catalytic capacity of each member, reflecting the enzymatic activity values.

The high relative abundance of endoglucanases, β-cellobiohydrolase, β-glucosidase and xylanase, associated with the great diversity and considerable enzymatic activities are indicative of the potential of this fungus to deconstruct cellulose and hemicellulose. Other hemicellulases, pectinases and accessory enzymes, although less abundant, have considerable enzyme activity values (**Table 1**). The presence of a broad spectrum of enzyme types may explain the efficiency of this enzymatic extract in the saccharification of alkali-pretreated sugarcane bagasse when compared to commercial cocktails (Maitan-Alfenas et al., 2015).

The *C. cubensis* secretome analysis showed that CAZymes from 40 different families act on cellulose, hemicellulose, lignin and pectin (**Fig. 4**), which is equivalent to 73% of the total members of the CAZy families. The secretome composition comprises members of the three main types of GHs that act on cellulose, such as cellobiohydrolases (GH6, GH7, and GH45); endoglucanases (GH5, GH6, GH7, GH12, GH45); and β-glucosidases (GH1, GH3, GH132), in addition to AA9. Thus, this fungus has the potential to produce a complete enzyme arsenal for the deconstruction of cellulose fibers.

An important characteristic of this *C. cubensis* secretome is the high number of detected enzyme families that act on hemicellulose (**Fig. 4**). Arabinoxylan is the main structural component of the cereal cell wall, corresponding to 10.9 – 26% of wheat bran based on a dry matter (Gebruers et al., 2008). The presence of a large quantity of this

hemicellulose component probably favored the secretion of enzymes, such as xylanases (GH10, GH11), which promote hydrolysis of the arabinoxylan main chain, β-xylosidases (GH3, GH39), which hydrolyze β-1,4-D-xylans and xylobiose by removing successive D-xyloses residues from non-reducing ends. In addition, other families of accessory enzymes that degrade arabinoxylan, such as α-arabinofuranosidase (GH51, GH54), α-glucuronidase (GH67), feruloyl esterases (CE1) and acetylxylan esterases (CE1, CE5) were produced by *C. cubensis* LPF-1. This fungus also secreted enzymes that act on xyloglucans, such as xyloglucanases (GH12, GH74), β-galactosidases (GH2, GH35), α-fucosidases (GH29), and mannan degrading enzymes, such as β-mannanases (GH5), β-mannosidases (GH2), α-mannosidases (GH47) and α-galactosidases (GH27).

Complex culture media contribute to the secretion of a more diversified enzymatic arsenal capable of digesting almost the entire plant cell wall (Girard et al., 2013). Under these growth conditions in wheat bran, *C. cubensis* was also able to secrete a pectinolytic arsenal necessary for the efficient degradation of pectin. Among them, there are polygalacturonases and α-galacturonidases (GH28), α-rhamnosidases (GH78), polysaccharide lyases, including the pectinases, pectate lyases of the PL1 family and the rhamnogalacturonases of the PL4 family and enzyme, which act on the substitutional side chains of rhamnogalacturonase I, such as arabinases (GH43) and galactanases (GH5). This high diversity of pectinases makes this fungus potentially interesting for biotechnological applications related to the deconstruction of the pectin. The efficient performance of the *C. cubensis* LPF-1 enzymatic extract during saccharification (Falkoski et al., 2013) can be explained, in part, by the higher activities of hemicellulases and pectinases. Although these enzymes do not directly act on the cellulose hydrolysis, their activity promotes the removal of the non-cellulosic polysaccharides that cover the cellulose fibers, providing the access of the cellulases to the substrate (Berlin et al., 2007).

Wheat bran was able to induce the expression of 6 LPMOs concerning a total of 14 predicted from *C. cubensis* bioinfosecretome. This diversity of LPMOs constitute a high number of exclusive members if compared to many filamentous fungi extensively known as good producers of biomass degradation enzymes. *T. reezei* cultivated in sugarcane bagasse, and *A. fumigatus* cultivated in cellulose secrete, respectively, 3 and 2 different LPMOs (Gupta et al., 2016). Many works show the importance of supplementing enzymatic cocktails with LPMOs. Recent studies showed that the supplementation of a mixture of Celluclast and Novozymes 188 with TaAA9A from *Thermoascus aurantiacu*s improved glucose yields by up to 32% for steam-exploded birchwood (Müller et al., 2015). Presently, a new generation of cocktail commercially

available for biomass degradation incorporates LPMOs in their composition, such as Cellic® Ctec2 and Cellic® Ctec3 from Novozymes (Harris et al., 2014). LPMOs help to increase the cellulose conversion yield and to reduce the enzymatic loading of other enzymes which necessary for biomass saccharification (Cannella et al., 2012). The presence of a great diversity of LPMOs in *C. cubensis* crude extract may explain in part, the efficient performance of this enzymatic cocktail in the saccharification of lignocellulosic biomasses.

Besides, the presence of laccase (0.03 U/mL) (**Table 1**), which only traces of this activity where measured in commercial mixtures (Maitan-Alfenas et al., 2015), could also be an important factor associated with the proven efficiency of this cocktail for the biomass saccharification. Laccases have been used as a delignifying pretreatment tool and for decreasing the toxicity of lignin-derived compounds, which could hamper enzymatic saccharification and subsequent fermentation steps (Rodríguez-Zúñiga et al., 2015). The presence of laccase activity in *C. cubensis* extract mitigated deactivation due to phenols on xylanase and other hemicellulases, thus helping these xylan hydrolyzing enzymes to display tolerance to phenolic inhibitors/deactivating compounds (Ladeira Ázar et al., 2018). The laccases in *C. cubensis* extract may potentiate the performance of LPMOs because Laccase-Mediated System (LMS) can depolymerize lignin from pre-treated lignocellulosic biomass, and the released phenolic molecules can donate electrons to LPMOs, increasing the overall enzymatic hydrolysis of cellulose (Brenelli et al., 2018). The synergism between LPMOs and laccases may be a differential of this extract concerning commercial cocktails and may contribute to the high potential of performance in different biomasses.

Another relevant feature is the presence of starch-degrading enzymes, such as α-glucan branching enzymes (GH13), glucoamylases (GH15) and α-glucosidases (GH31), and enzymes that act on β-1,3-glucans, including (GH17, GH64, GH81, GH128), glucan endo-1,3-alpha-glucosides (GH71) and β-1,3-glucanosyl-transglycosylases (GH72). The high induction of these enzymes may be a consequence of the large amount of starch present in the wheat bran composition (14 – 25 %), and may also be considered a source rich in β-glucans (2.1 - 2.5 %) (Prückler et al., 2014). The presence of amylases, together with phytases in the extract of *C. cubensis* LPF-1 indicate a possible commercial relevance since glucoamylases are one of the main enzymes for 1st generation biofuels. Companies such as Verenium and Novozymes develop more stable variants of alpha-amylases, while Dupont in its Spezyme RSL product provides a mixture of alpha-amylase and phytase applied to ethanol (Harris et al., 2014).

3.4. Quality of bioinfosecretome coverage for CAZymes prediction

In silico predictions provide a comprehensive view of the complete set of possible secreted proteins, which allows a preliminary analysis of the potential, diversity, and exclusivity of the secretome protein pool, regardless of the conditions under which the fungus is submitted. The bioinfosecretome was able to predict 108 CAZymes detected in the crude extract of *C. cubensis* (**Fig. 5**), corresponding to a coverage of 78.83% about the total CAZymes identified in the secretome.

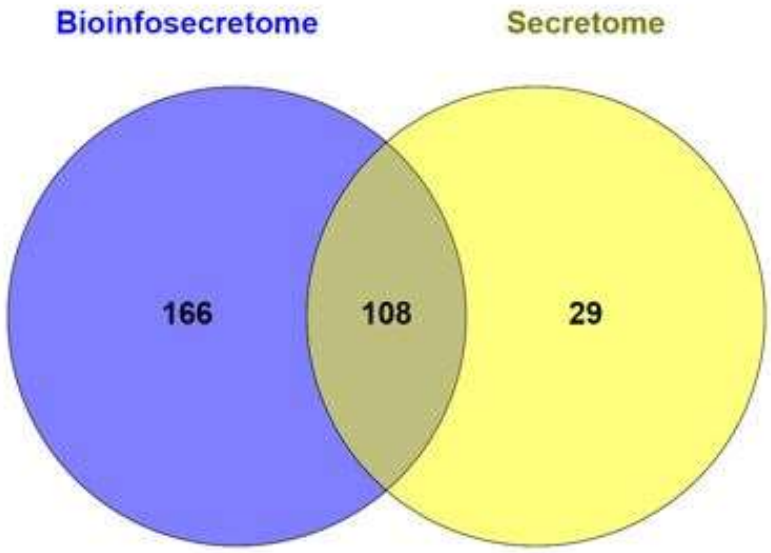

Figure 5: Comparison of the CAZymes present in the bioinfosecretome and secretome. Venn diagram representing unique and common C. cubensis CAZymes predicted by bioinfosecretome (blue circle) and identified in the experimental secretome (yellow circle). The Venn diagram was prepared using Venny 2.1.0 online tools.

The 29 proteins found exclusively in the crude extract (**Fig. 5**), have other annotated subcellular locations and, therefore, were not predicted as secreted by classical pathways. According to the predictions of subcellular localization, there are a predominance of plasma membrane proteins (16), cytoplasm (7) and peroxisomes (3). When using the *ab initio* tool for predicting protein secretion by non-classical pathways to analyze the secretome exclusive proteins, 34.5% (10) were considered as secreted by non-conventional mechanisms, with a predominance of enzymes that had been predicted as located in the membrane (5) and the cytoplasm (4).

The possible causes of these proteins from other cellular localizations to be present in the *C. cubensis* extract would be ruptures generated by the mechanical extraction

process of the enzymes from fungi culture; probable genomic assembly errors that prevent the presence of peptide signals or even other secretion pathways with unknown patterns. The presence of proteins from other compartments in the extracellular environment was observed in 11 different species of fungi (Zamith-miranda et al., 2018). A suggested mechanism is the secretion of proteins by fungal extracellular vesicles (EV), which can transport proteins related to metabolic processes (Rodrigues et al., 2014). The secretion of CAZymes by EVs correlates with the need for constant remodeling of the fungal cell wall, either by physiological aspects such as, nutritional need, pathogenicity, cell growth and development of hyphae, or even in response to environmental changes, such as temperature changes and pH (Nimrichter et al., 2016).

The presence of CAZymes possibly secreted by non-classical pathways was limiting the complete prediction of *in silico* analyses. However, the bioinfosecretome presented high coverage, refined and high-quality approach for the prediction of CAZymes secreted by fungi. The computational workflow employed in this work can be extended to the prediction of other fungi, providing a comprehensive character of the applied approach and easy to apply as an initial step in prospecting processes of organisms that produce enzymes of biotechnological interest.

3.5. Discovering new target enzymes that are potentially suitable for lignocellulose degradation

C. cubensis has been shown to be an excellent producer of canonical lignocellulolytic enzymes traditionally used in biomass saccharification, sush as β-glycosidases and β-cellobiohydrolases. Furthermore, the enzymatic extract of this fungus grown in wheat bran emerges as an excellent source of enzymes that have been studied as new targets for cocktail supplementation (Binod et al., 2019), such as polygalacturonases (g5388.t1; g2515.t1; g4428.t1), pectin liases (g2458.t1; g6932.t1), feruloyl esterases (g7688.t1; g9922.t1; g7342.t1), the accessory enzymes α-arabinofuranosidases (g6428.t1; g11408) and β-galactosidases (g120.t1; g6058.t1; g1186), laccases (g594.t1; g6312.t1) and LPMOs (g1304.t1; g1799.t1; g2964.t1; g5754.t1; g6620.t1; g9830.t1), which imply the high lignocellulolytic capacity demonstrated by this fungus and may be selected as promising targets for future studies.

It was noteworthy the presence of 6 hypothetical proteins (g4231.t1; g7768.t1; g11041.t1; g5160.t1; g5798.t1; g2373.t1) with high relative abundance in the C. cubensis extract. The detection of these hypothetical extracellular proteins at high relative abundance in the experimental secretome suggests that unknown proteins with relevant

roles in biomass degradation remain to be properly studied and developed, to understand its role in the saccharification of lignocellulosic biomass.

4. Conclusions

This study reports the first comprehensive insight into the repertoire of proteins present in the high-performance secretome of *C. cubensis* LPF-1. The integration of in silico predictions of *C. cubensis* secretome, based on genome sequence, with the proteomic data, obtained by mass spectrometry from enzymatic extract produced by *C. cubensis* LPF-1 grown in a semi-solid state with wheat bran, allowed to characterize the complete protein profile secreted by this fungus. The diversity of enzymes shows the versatility of this fungus in adapting the secretion of proteins to act in complex biomasses and reflects the efficiency of the enzymatic cocktail for degradation of the lignocellulosic biomass. These findings clearly indicate that *C. cubensis* enzymes cocktail has great potential for second-generation technologies using lignocellulosic agricultural waste as an inexpensive and sustainable alternative for the production of value-added chemicals and biofuels.

Authors' contributions

MPT performed cultures, bioinfosecretome and secretome studies, enzymatic assays, data interpretation and discussion, and drafted the manuscript. TM and RFG participated in secretome and bioinfosecretome studies, enzymatic assays, data interpretation and discussion. MQRBR and STR participated in data interpretation and discussion. VMG and TAOM conceived the study, participated in data interpretation and discussion and prepared final version of the manuscript. All authors read and approved the final manuscript.

Acknowledgments

We acknowledge the Fundação de Amparo à Pesquisa do Estado de Minas Gerais (FAPEMIG), Coordenação de Aperfeiçoamento de Pessoal de Nível Superior (CAPES) for the scholarship granted to the first author and Conselho Nacional de Desenvolvimento Científico e Tecnológico (CNPq) for the resources provided to complete this experiment. We also thank the Laboratory of Enzymology and Proteomics of the Federal University of Ouro Preto by the support in the mass spectrometric analysis.

References

1. Alfaro, M., Castanera, R., Lavín, J.L., Grigoriev, I. V., Oguiza, J.A., Ramírez, L., Pisabarro, A.G., 2016. Comparative and transcriptional analysis of the predicted secretome in the lignocellulose-degrading basidiomycete fungus *Pleurotus ostreatus*. Environ. Microbiol. 18, 4710–4726. https://doi.org/10.1111/1462-2920.13360

2. Almagro Armenteros, J.J., Sønderby, C.K., Sønderby, S.K., Nielsen, H., Winther, O., 2017. DeepLoc: prediction of protein subcellular localization using deep learning. Bioinformatics 33, 3387–3395. https://doi.org/10.1093/bioinformatics/btx431

3. Altschul, S.F., Gish, W., Miller, W., Myers, E.W., Lipman, D.J., 1990. Basic local alignment search tool. J. Mol. Biol. 215, 403–410. https://doi.org/10.1016/S0022-2836(05)80360-2

4. Bendtsen, J.D., Kiemer, L., Fausbøll, A., Brunak, S., 2005. Non-classical protein secretion in bacteria. BMC Microbiol. 5, 1–13. https://doi.org/10.1186/1471-2180-5-58

5. Berlin, A., Maximenko, V., Gilkes, N., Saddler, J., 2007. Optimization of Enzyme Complexes for Lignocellulose Hydrolysis. Biotechnol. Bioenginnering 97, 287–296. https://doi.org/10.1002/bit

6. Bianco, L., Perrotta, G., 2015. Methodologies and Perspectives of Proteomics Applied to Filamentous Fungi : From Sample Preparation to Secretome Analysis. Int. J. Mol. Sci. 16, 5803–5829. https://doi.org/10.3390/ijms16035803

7. Binod, P., Gnansounou, E., Sindhu, R., Pandey, A., 2019. Enzymes for second generation biofuels: Recent developments and future perspectives. Bioresour. Technol. Reports 5, 317–325. https://doi.org/10.1016/J.BITEB.2018.06.005

8. Borin, G.P., Sanchez, C.C., Souza, A.P. De, Santana, S. De, Souza, A.T. De, Franco, A., Leme, P., Squina, M., Buckeridge, M., Goldman, G.H., De, J.V., 2015. Comparative Secretome Analysis of *Trichoderma reesei* and *Aspergillus niger* during Growth on Sugarcane Biomass. PLoS One 10, 1–20. https://doi.org/10.1371/journal.pone.0129275

9. Bradford, M.M., 1976. A rapid and sensitive method for the quantitation of microgram quantities of protein utilizing the principle of protein-dye binding. Anal. Biochem. 72, 248–254. https://doi.org/10.1016/0003-2697(76)90527-3

10. Brenelli, L., Squina, F.M., Felby, C., Cannella, D., 2018. Laccase-derived lignin compounds boost cellulose oxidative enzymes AA9. Biotechnol. Biofuels 11, 10. https://doi.org/10.1186/s13068-017-0985-8

11. Cannella, D., Hsieh, C.C., Felby, C., Jørgensen, H., 2012. Production and effect of aldonic acids during enzymatic hydrolysis of lignocellulose at high dry matter content. Biotechnol. Biofuels 5, 26. https://doi.org/10.1186/1754-6834-5-26

12. Chandrasekaran, M., Thangavelu, B., Chun, S.C., Sathiyabama, M., 2016. Proteases

from phytopathogenic fungi and their importance in phytopathogenicity. J. Gen. Plant Pathol. https://doi.org/10.1007/s10327-016-0672-9

13. Correa, L.J., Badino, A.C., Cruz, A.J.G., 2016. Mixing design for enzymatic hydrolysis of sugarcane bagasse: methodology for selection of impeller configuration. Bioprocess Biosyst. Eng. 39, 285–294. https://doi.org/10.1007/s00449-015-1512-6

14. Cortázar, A.R., Aransay, A.M., Alfaro, M., Oguiza, J.A., Lavín, J.L., 2014. SECRETOOL: Integrated secretome analysis tool for fungi. Amino Acids 46, 471–473. https://doi.org/10.1007/s00726-013-1649-z

15. Delgado, L., Trejo, B.A., Huitrón, C., Aguilar, G., 1993. Pectin lyase from Aspergillus sp. CH-Y-1043. Appl Microbiol Biotechnol 39, 515–519.

16. Do Vale, L.H.F., Gómez-Mendoza, D.P., Kim, M.S., Pandey, A., Ricart, C.A.O., Edivaldo, X.F.F., Sousa, M. V., 2012. Secretome analysis of the fungus *Trichoderma harzianum* grown on cellulose. Proteomics 12, 2716–2728. https://doi.org/10.1002/pmic.201200063

17. Falkoski, D.L., Guimarães, V.M., de Almeida, M.N., Alfenas, A.C., Colodette, J.L., de Rezende, S.T., 2013. *Chrysoporthe cubensis*: A new source of cellulases and hemicellulases to application in biomass saccharification processes. Bioresour. Technol. 130, 296–305. https://doi.org/10.1016/j.biortech.2012.11.140

18. Florencio, C., Cunha, F.M., Badino, A.C., Farinas, C.S., Ximenes, E., Ladisch, M.R., 2016. Secretome analysis of *Trichoderma reesei* and *Aspergillus niger* cultivated by submerged and sequential fermentation processes: Enzyme production for sugarcane bagasse hydrolysis. Enzyme Microb. Technol. 90, 53–60. https://doi.org/10.1016/j.enzmictec.2016.04.011

19. Gebruers, K., Dornez, E., Boros, D., Fraś, A., Dynkowska, W., Bedo, Z., Rakszegi, M., Delcour, J.A., Courtin, C.M., 2008. Variation in the content of dietary fiber and components thereof in wheats in the healthgrain diversity screen. J. Agric. Food Chem. 56, 9740–9749. https://doi.org/10.1021/jf800975w

20. Ghose, T.., 1987. Measurement of cellulase activities. Pure Appl. Chem. 59, 257–268. https://doi.org/10.1351/pac198759020257

21. Gibson, D.M., King, B.C., Hayes, M.L., Bergstrom, G.C., 2011. Plant pathogens as a source of diverse enzymes for lignocellulose digestion. Curr. Opin. Microbiol. 14, 264–270. https://doi.org/10.1016/j.mib.2011.04.002

22. Girard, V., Dieryckx, C., Job, C., Job, D., 2013. Secretomes: The fungal strike force. Proteomics 13, 597–608. https://doi.org/10.1002/pmic.201200282

23. Gruno, M., Valjamae, P., Pettersson, G., Johansson, G., 2004. Inhibition of the *Trichoderma reesei* cellulases by cellobiose is strongly dependent on the nature of the substrate. Biotechnol. Bioeng. 86, 503–511. https://doi.org/10.1002/bit.10838

24. Gryzenhout, M., Rodas, C.A., Mena, J., Clegg, P., Wingfield, B.D., Wingfield, M.J., Breuil, C., 2006. Novel hosts of the Eucalyptus canker pathogen *Chrysoporthe*

cubensis and a new Chrysoporthe species from Colombia. Mycol. Res. 110, 833–845. https://doi.org/10.1016/j.mycres.2006.02.010

25. Guimarães, L.M.D.S., de Resende, M.D.V., Lau, D., Rosse, L.N., Alves, A.A., Alfenas, A.C., 2010. Genetic control of *Eucalyptus urophylla* and *E. grandis* resistance to canker caused by *Chrysoporthe cubensis*. Genet. Mol. Biol. 33, 525–531. https://doi.org/10.1590/S1415-47572010005000069

26. Gupta, V.K., Steindorff, A.S., de Paula, R.G., Silva-Rocha, R., Mach-Aigner, A.R., Mach, R.L., Silva, R.N., 2016. The Post-genomic Era of *Trichoderma reesei*: What's Next? Trends Biotechnol. https://doi.org/10.1016/j.tibtech.2016.06.003

27. Harris, P. V, Xu, F., Kreel, N.E., Kang, C., Fukuyama, S., 2014. New enzyme insights drive advances in commercial ethanol production. Curr. Opin. Chem. Biol. https://doi.org/10.1016/j.cbpa.2014.02.015

28. Horn, S.J., Vaaje-Kolstad, G., Westereng, B., Eijsink, V.G., 2012. Novel enzymes for the degradation of cellulose. Biotechnol Biofuels 5. https://doi.org/10.1186/1754-6834-5-45

29. Hu, J., Chandra, R., Arantes, V., Gourlay, K., Susan van Dyk, J., Saddler, J.N., 2015. The addition of accessory enzymes enhances the hydrolytic performance of cellulase enzymes at high solid loadings. Bioresour. Technol. 186, 149–53. https://doi.org/10.1016/j.biortech.2015.03.055

30. Kikot, G.E., Hours, R.A., Alconada, T.M., 2009. Contribution of cell wall degrading enzymes to pathogenesis of *Fusarium graminearum* : a review. J. Basic Microbiol. 49, 231–241. https://doi.org/10.1002/jobm.200800231

31. Ladeira Ázar, R.I.S., Morgan, T., dos Santos, A.C.F., de Aquino Ximenes, E., Ladisch, M.R., Guimarães, V.M., 2018. Deactivation and activation of lignocellulose degrading enzymes in the presence of laccase. Enzyme Microb. Technol. 109, 25–30. https://doi.org/10.1016/J.ENZMICTEC.2017.09.007

32. Maitan-Alfenas, G.P., Visser, E.M., Alfenas, R.F., Nogueira, B.R.G., de Campos, G.G., Milagres, A.F., de Vries, R.P., Guimarães, V.M., 2015. The influence of pretreatment methods on saccharification of sugarcane bagasse by an enzyme extract from *Chrysoporthe cubensis* and commercial cocktails: A comparative study. Bioresour. Technol. 192, 670–6. https://doi.org/10.1016/j.biortech.2015.05.109

33. Miller, G.L., 1959. Use of Dinitrosalicylic Acid Reagent for Determination of Reducing Sugar. Anal. Chem. 31, 426–428. https://doi.org/10.1021/ac60147a030

34. Miyauchi, S., Navarro, D., Grisel, S., Chevret, D., Berrin, J.G., Rosso, M.N., 2017. The integrative omics of white-rot fungus *Pycnoporus coccineus* reveals co-regulated CAZymes for orchestrated lignocellulose breakdown. PLoS One 12, 1–17. https://doi.org/10.1371/journal.pone.0175528

35. Müller, G., Várnai, A., Johansen, K.S., Eijsink, V.G.H., Horn, S.J., 2015. Harnessing the potential of LPMO-containing cellulase cocktails poses new demands on processing conditions. Biotechnol. Biofuels 8, 1–9. https://doi.org/10.1186/s13068-

015-0376-y

36. Nakamura, A.M., Nascimento, A.S., Polikarpov, I., 2017. Structural diversity of carbohydrate esterases. Biotechnol. Res. Innov. 1, 35–51.

37. Nekiunaite, L., Arntzen, M., Svensson, B., Vaaje-Kolstad, G., Hachem, M.A., 2016. Lytic polysaccharide monooxygenases and other oxidative enzymes are abundantly secreted by *Aspergillus nidulans* grown on different starches. Biotechnol. Biofuels 9, 1–16. https://doi.org/10.1186/s13068-016-0604-0

38. Nimrichter, L., Souza, M.M. De, Poeta, M. Del, Nosanchuk, J.D., Joffe, L., Tavares, P.D.M., Rodrigues, M.L., Lev, S., 2016. Extracellular Vesicle-Associated Transitory Cell Wall Components and Their Impact on the Interaction of Fungi with Host Cells. Front. Microbiol. 7, 1–11. https://doi.org/10.3389/fmicb.2016.01034

39. Popper, Z.A., Michel, G., Herve, C., Domozych, D.S., Willats, W.G.T., Tuohy, M.G., Kloareg, B., Stengel, D.B., 2011. Evolution and Diversity of Plant Cell Walls: From Algae to Flowering Plants. Annu. Rev. Plant Biol. Vol 62 62, 567–588. https://doi.org/10.1146/annurev-arplant-042110-103809

40. Prückler, M., Siebenhandl-ehn, S., Apprich, S., Höltinger, S., Haas, C., Schmid, E., Kneifel, W., 2014. LWT - Food Science and Technology Wheat bran-based biorefinery 1 : Composition of wheat bran and strategies of functionalization. LWT - Food Sci. Technol. 56, 211–221. https://doi.org/10.1016/j.lwt.2013.12.004

41. Ramada, M.H.S., Steindorff, A.S., Bloch, C., Ulhoa, C.J., 2016. Secretome analysis of the mycoparasitic fungus *Trichoderma harzianum* ALL 42 cultivated in different media supplemented with *Fusarium solani* cell wall or glucose. Proteomics 16, 477–490. https://doi.org/10.1002/pmic.201400546

42. Ravindran, A., Adav, S.S., Sze, S.K., 2012. Characterization of extracellular lignocellulolytic enzymes of *Coniochaeta sp*. during corn stover bioconversion. Process Biochem. 47, 2440–2448. https://doi.org/10.1016/j.procbio.2012.10.003

43. Rodrigues, M.L., Nakayasu, E.S., Almeida, I.C., Nimrichter, L., 2014. The impact of proteomics on the understanding of functions and biogenesis of fungal extracellular vesicles. J. Proteomics. https://doi.org/10.1016/j.jprot.2013.04.001

44. Rodríguez-Zúñiga, U.F., Cannella, D., Giordano, R. de C., Giordano, R. de L.C., Jørgensen, H., Felby, C., 2015. Lignocellulose pretreatment technologies affect the level of enzymatic cellulose oxidation by LPMO. Green Chem. 17, 2896–2903. https://doi.org/10.1039/C4GC02179G

45. Ruas, F.A.D., Barboza, N.R., Castro-Borges, W., Guerra-Sa, R., 2019. Manganese alters expression of proteins involved in the oxidative stress of *Meyerozyma guilliermondii*. J. Proteomics 196, 173–188. https://doi.org/10.1016/j.jprot.2018.11.001

46. Simão, F.A., Waterhouse, R.M., Ioannidis, P., Kriventseva, E. V, Zdobnov, E.M., 2015. BUSCO: Assessing genome assembly and annotation completeness with single-copy orthologs. Bioinformatics 31, 3210–3212.

https://doi.org/10.1093/bioinformatics/btv351

47. Stanke, M., Morgenstern, B., 2005. AUGUSTUS: A web server for gene prediction in eukaryotes that allows user-defined constraints. Nucleic Acids Res. 33, 465–467. https://doi.org/10.1093/nar/gki458

48. Sun, X., Liu, Z., Qu, Y., Li, X., 2008. The effects of wheat bran composition on the production of biomass-hydrolyzing enzymes by *Penicillium decumbens*. Appl. Biochem. Biotechnol. 146, 119–128. https://doi.org/10.1007/s12010-007-8049-3

49. Talon, M., Robles, M., Garcia-Gomez, J.M., Conesa, A., Nueda, M.J., Nagaraj, S.H., Gotz, S., Terol, J., Dopazo, J., Williams, T.D., 2008. High-throughput functional annotation and data mining with the Blast2GO suite. Nucleic Acids Res. 36, 3420–3435. https://doi.org/10.1093/nar/gkn176

50. Tandrup, T., Frandsen, K.E.H., Johansen, K.S., Berrin, J.-G., Lo Leggio, L., 2018. Recent insights into lytic polysaccharide monooxygenases (LPMOs). Biochem. Soc. Trans. BST20170549. https://doi.org/10.1042/BST20170549

51. Visser, E.M., Leal, T.F., de Almeida, M.N., Guimarães, V.M., 2015. Increased enzymatic hydrolysis of sugarcane bagasse from enzyme recycling. Biotechnol. Biofuels 8, 1–9. https://doi.org/10.1186/s13068-014-0185-8

52. Wingfield, B.D., Barnes, I., de Beer, Z.W., De Vos, L., Duong, T.A., Kanzi, A.M., Naidoo, K., Nguyen, H.D.T., Santana, Q.C., Sayari, M., Seifert, K.A., Steenkamp, E.T., Trollip, C., van der Merwe, N.A., van der Nest, M.A., Wilken, P.M., Wingfield, M.J., 2015. IMA Genome-F 5: Draft genome sequences of *Ceratocystis eucalypticola*, *Chrysoporthe cubensis*, *C. deuterocubensis*, *Davidsoniella virescens*, *Fusarium temperatum*, *Graphilbum fragrans*, *Penicillium nordicum*. IMA Fungus 6, 493–506. https://doi.org/10.5598/imafungus.2015.06.02.13

53. Yohe, T., Xu, Y., Huang, L., Yin, Y., Yang, Z., Wu, P., Entwistle, S., Busk, P.K., Zhang, H., 2018. dbCAN2: a meta server for automated carbohydrate-active enzyme annotation. Nucleic Acids Res. 46, W95–W101. https://doi.org/10.1093/nar/gky418

54. Zamith-miranda, D., Nimrichter, L., Rodrigues, M.L., Nosanchuk, J.D., 2018. Fungal extracellular vesicles : modulating host e pathogen interactions by both the fungus and the host. Microbes Infect. 1–4.

55. Zhao, Z., Liu, H., Wang, C., Xu, J.-R., 2013. Comparative analysis of fungal genomes reveals different plant cell wall degrading capacity in fungi. BMC Genomics 14. https://doi.org/10.1186/1471-2164-14-274

CAPÍTULO 3

Secretome diversity and quantitative analysis of the phytopathogenic fungus *Chrysoporthe cubensis* LPF-1 in the presence of different carbon sources

Secretome diversity and quantitative analysis of phytopathogenic fungus *Chrysoporthe cubensis* LPF-1 in the presence of different carbon sources

Murillo Peterlini Tavares[1], Túlio Morgan[1,2], Riziane Ferreira Gomes[1], Marina Quádrio Raposo Branco Rodrigues[1], Bruno Mattei[3], William de Castro Borges[3], Sebastião Tavares de Rezende[1], Tiago Antônio de Oliveira Mendes[1], Valéria Monteze Guimarães[1,*]

[1]Department of Biochemistry and Molecular Biology, Universidade Federal de Viçosa, Av. PH Rolfs, s/n, 36570-900, Viçosa, MG, Brazil

[2]Department of Bioinformatic, Universidade Federal de Minas Gerais, Av. Pres. Antônio Carlos, 6627, 31270-901 - Pampulha, Belo Horizonte, MG, Brazil

[3]Department of Biological Science, Universidade Federal de Ouro Preto, Campus universitário Morro do Cruzeiro, 35400-000, Ouro Preto, MG, Brasil

*** Corresponding Author**

Email: vmonteze@ufv.br

Telephone: (+55 31) 3612 2462

Abstract

The phytopathogenic fungus *Chrysoporthe cubensis* LPF-1 is an important source of lignocellulolytic enzymes. This work aims to explore the profile of secreted proteins involved in lignocellulose degradation and comparing the secretomes of *C. cubensis* afther growth on wheat bran and sugarcane bagasse. The secreted proteins were quantitatively analyzed by liquid chromatography-tandem mass spectrometry. Label-free proteomic analysis showed that the fungus produced a spectrum of Carbohydrate-Active Enzymes (CAZymes) with exclusive characteristics for each extract. Saccharification of alkaline pretreated sugarcane bagasse by SBE promotes the higher release of glucose (8.11 g/L), comparable to the performance of commercial cocktails, while WBE promotes the higher release of xylose (5,71 g/L), with superior performance than commercial cocktails. Our data provide an in-depth analysis of the complex set of enzymes implicated in the high lignocellulolytic capacity shown by this fungus which facilitates the selection of promising targets for the development of the future biorefineries.

Keywords

Chrysoporthe cubensis, wheat bran, sugarcane bagasse, secretome, biomass saccharification.

1. Introduction

Worldwilde concern about fossil fuel shortages increased greenhouse gas emissions, and air pollution from incomplete combustion has resulted in increased interest in alternative, sustainable and clean energy sources (Li et al., 2013). Therefore, efforts have been made to achieve these objectives, such as the development of technologies that use lignocellulosic biomass as a feedstock for the production of biofuels (Li et al., 2013). Lignocellulosic materials are the most abundant natural renewable resource in the world (Jung et al., 2015). Lignocellulosic biomass is composed mostly of three primary components: cellulose, hemicellulose and lignin. A significant amount of these materials is often produced as a waste by-product from agricultural practices, mainly from several agro-based industries (Anwar et al., 2014).

Considering the large production of sugarcane bagasse in Brazil, the value added to this residue through the enzymatic saccharification for the production of second-generation (2G) bioethanol, is an alternative for the increase of productivity, and consequently, the revenue of the sugar and alcohol industry (de Souza et al., 2013). In this context, the use of lignocellulosic biomass from sugarcane bagasse for the production of second-generation ethanol becomes a promising alternative for the reduction of environmental impacts from the use of fossil fuels. The application of enzymes to catalyze the degradation of cellulose to glucose and hemicellulose to free sugars has been considered the most viable strategy to provide second-generation ethanol with a good cost-benefit ratio (Himmel et al., 2007). However, the use of this biomass presents a great challenge due to the complex structure of the plant cell wall, being necessary many types of hydrolytic enzymes, including cellulases, hemicellulases, ligninases, pectinases, auxiliary enzymes (LPMOs, laccases, catalases, peroxidases) (Rai et al., 2016), and others non-hydrolytic proteins, such as expansins and swolenins.

These enzymes account for most of the costs associated with the production of bioethanol. The reduction of the costs of the saccharification process can be achieved through the understanding of hydrolytic mechanisms and the secretion of enzymes from microorganisms that hydrolyze polysaccharides (Borin et al., 2015). In addition to the search for new enzymes, enhancement of enzyme mixtures for specific lignocellulosic substrates is of interest, with increasing recognition of the fact that a "one size fits all" approach may not be optimal in the most efficient in the design of more efficient biomass processing (Chylenski et al., 2017). Thus, it is necessary to know new sources of enzymes and especially new fungal extracts (enzymatic consortium) that have high performance in

the degradation of a broad spectrum of lignocellulosic biomass with different characteristics.

The prospecting of new microorganisms, as well as the use of microorganisms recognized as good producers of lignocellulolytic enzymes are important in the design of new enzymatic products. Moreover, the exploitation of lignocellulosic residues to grow microorganisms in solid-state fermentation (SSF) provides an inexpensive source of enzymes. This approach facilitates the reuse and the addition of value to waste, which reduces environmental pollution (Lopes et al., 2018).

The composition of the secreted enzymes by any fungus varies according to its biological characteristics and changes continuously in response to the environmental conditions (Papagianni, 2004) to which the fungus is subjected. Therefore, the same fungus cultivated in different lignocellulosic biomasses produces different protein profiles, being these characteristics exploited to understand the hydrolytic mechanisms of each fungus. The comprehensive identification and quantification of the secretome of cellulolytic strains in different carbon sources may be a useful approach to the understanding of their unique and special enzymatic systems, as well as to determine the industrial application of these strains to bioenergy production.

Recent works have shown that the phytopathogenic fungus *Chrysoporthe cubensis* cultivated under solid-state fermentation using wheat bran as a carbon source presents great capacity for the production of enzymes with high efficiency for hydrolysis of the lignocellulosic biomass, compared to the commercial enzymatic cocktails (Maitan-Alfenas et al., 2015). *C. cubensis* is a versatile fungus, being able to grow on different complex substrates. Recently, *C. cubensis* has also demonstrated high potential for the production of cellulases and hemicellulases when grown under solid-state fermentation (SSF) with sugarcane bagasse (SCB) *in natura*, as a carbon source (Dutra et al., 2017). Knowing the high potential of this fungus for the production of lignocellulases, a comparative study of the secretome obtained under different conditions provides qualitative and quantitative information of the proteins of interest and enable the understanding of hydrolytic mechanisms for the efficient saccharification of agro-industrial waste.

In order to discover new enzymes and to provide a comparison with commercial enzymatic cocktails regarding the performance in saccharification of biomasses, secreted extracellular protein detected in extracts of *C. cubensis* grown in sugarcane bagasse and wheat bran were identified, quantified and compared using a high-throughput, quantitative, label-free based, LC-MS/MS proteomic approach.

2. Materials and methods

2.1. Materials

All chemicals were produced from Sigma Chemical Co. (St. Louis, MO, USA), Merck (Darmstadt, Germany), Himedia Laboratories Co. (Mumbai, Maharashtra, India), Vetec Fine Chemical (Duque de Caxias, RJ, Brazil), Bio-Rad Laboratories (Hercules, CA, USA). Wheat bran was obtained on the local market. Sugarcane bagasse (SBC) was kindly donated by Jatiboca Sugar and Ethanol Plant, Urucânia, MG, Brazil. All reagents used were of analytical grade.

2.2. Microorganism and culture conditions

The fungus *C. cubensis* LPF-1 used in this study was obtained from the mycological collection of the Forest Pathology Laboratory of the Federal University of Viçosa, MG, Brazil. Spores were stored in a glycerol solution (10%) at -80ºC. Glycerol stocks were grown on potato dextrose agar (PDA) plates at 28ºC and periodically subcultured. The inoculum was prepared by culturing the fungus under submerged fermentation in 250 mL Erlenmeyer flasks as described by (Falkoski et al., 2013). The culture was immediately inoculated in the semi-solid culture media.

C. cubensis LPF-1 was cultured under semi-solid state fermentation (SSF) using wheat bran as carbon source, as previously described (de Sousa Gomes et al., 2016), or *in natura* sugarcane bagasse, as described by (Dutra et al., 2017). The secreted proteins produced during SSF was extracted using 50 mM sodium acetate buffer, pH 5, at a ratio of 10:1 (buffer/dry substrate) under the agitation of 180 rpm for 60 min at 25 °C. The solid portion was separated by filtration through nylon cloth followed by centrifugation at 15,000g for 10 min. Clarified supernatants from 3 biological replicates were grouped and the crude extract, referred to as the secretome, was stored at −20 °C.

2.3. Enzyme activity measurements and protein determination

In order to comprehensively evaluate the capacity of lignocellulose hydrolysis, lignocellulolytic enzyme activities were measured. All enzymatic assays were carried out in 100 mM sodium acetate buffer, pH 5, at 50 ºC, in technical triplicate. Standard deviations of activity measurements were less than 10%. Endoglucanase and FPase (global cellulase activity) activities were determined using carboxymethyl cellulose (CMC) and Whatman No. 1 filter paper (1 x 6 cm) as substrates, respectively, according

to previously described standard conditions (Ghose, 1987). The total reducing sugars liberated during the enzymatic assays were quantified by the dinitrosalicylic acid (DNS) method (Miller, 1959), using glucose as a standard.

The activities of xylanase, polygalacturonase, mannanase, and amylase were determined using as substrates xylan birchwood (1% w/v), polygalacturonic acid (0.2% w/v), locust bean gum (0.4% w/v) and starch (1% w/v), respectively. Crude extract or previously diluted commercial cocktails (100μL) were mixed with 400 μL of substrates prepared in buffer and incubated for 30 min. Total reducing sugars released were determined by the DNS method.

The activities of α-glucosidase, β-glucosidase, β-xylosidase, β-mannosidase, α-galactosidase, β-galactosidase, α-arabinofuranosidase and cellobiohydrolase were measured by monitoring the release of ρ-nitrophenol from ρ-nitrophenyl-α-D-glucopyranoside (ρNPαGlc), ρ-nitrophenyl-β-D-glucopyranoside (ρNPβGlc), ρ-nitrophenyl-β-D-xilopiranosídeo (ρNPβXil), ρ-nitrophenyl-β-D-manopiranosídeo (ρNPβMan), ρ-nitrophenyl-α-D-galactopyranoside (ρNPαGal), ρ-nitrophenyl-β-D-galactopyranoside (ρNPβGal), ρ-nitrophenyl-α-D-arabinopyranosyl (ρNPαAra) and p-nitrophenyl-β-D-cellobioside (ρNPβCel) as synthetic substrates, respectively. The reaction mixture contained 100 μL of diluted enzyme solution, 125 μL of synthetic substrate solution (1 mM final concentration) and 275 μl of 100 mM sodium acetate buffer, pH 5. The reaction was incubated for 30 min and stopped by addition of 0.5 mL sodium carbonate solution (0.5 M). Absorbance was immediately measured at 410 nm and the amount of ρ-nitrophenol released was estimated by a standard curve.

Laccase activity was determined by monitoring the oxidation of the 2,2'-azino-bis (3-ethylbenzothiazoline-6-sulfonic acid) (ABTS) substrate. The mixture contained 100 μL of enzyme solution, 350 μL buffer and 50 μL of 10mM ABTS. It was incubated for 10 min and, after the incubation, absorbance was immediately measured at 420 nm. Laccase activity was calculated using a molar extinction coefficient of 3.6×10^4 $M^{-1}cm^{-1}$ (Maitan-Alfenas et al., 2015).

Pectin lyase activity was determined by monitoring the increase in absorbance at 235 nm according to (Delgado et al., 1993), with modifications. The reaction mixture containing 1.0 ml of pectin (2.5% w/v) and 1.5 ml culture filtrate was incubated at 50° C for 30 min. A 0.5 ml aliquot was taken from the reaction mixture and added to a test tube containing 4.5 ml of HC1 (0.01 M) to stop the reaction. One unit of pectin lyase activity was defined as the amount of enzyme that produced an increase in absorbance of 0.1 at 235 nm in the reaction mixture under the assay conditions.

The enzymatic activity was expressed in international units (U) for all enzymes activity assays. A unit of enzyme activity was defined as the amount of enzyme required to produce 1 μmol of the corresponding product per minute in the assay condition. The Bradford method (Bradford, 1976) was utilized to determine protein concentration using bovine serum albumin as standard.

2.4. Proteomic analysis

2.4.1. Secretome preparation and short run in 1D gel electrophoresis

The crude extract was filtered using syringe filters with a 0.22 μm polyvinylidene difluoride membrane (PVDF) (Millipore, Germany). Chilled ethanol (100%) was added in the crude enzyme extracts (10:1 ratio). The mixture was kept at −20 ºC overnight, followed by centrifugation at 8000 × g for 20 min at 4 ºC. Pellets were allowed to dry at room temperature to remove residual solvents and were reconstituted in an appropriate volume of lysis buffer (8 M urea; 2 M thiourea; 4% CHAPS). Total protein concentration was determined using Bradford assay (Bradford, 1976). The protein samples (30 μg) were subjected to a boiling denaturation step in the presence of sample buffer (0.0625M final concentration of Tris-HCl pH 6.8, 2% SDS, 10% glycerol, 5% mercaptoethanol) for 5 minutes and subsequently applied in sodium dodecyl sulfate-polyacrylamide gel electrophoresis (10% SDS-PAGE). A short run was performed for 20 min until the proteins entered the gel forming a single band. This procedure aimed to concentrate the proteins and to eliminate possible interference from secondary metabolites and pigments in samples (Queiroz et al., 2018).

2.4.2. Protein digestion and LC-MS/MS analyses

The gel band containing each sample was excised, fragmented into smaller pieces (approximately 1 mm^2), and then washed with 50% acetonitrile (ACN) containing 20mM ammonium bicarbonate (NH_4HCO_3) buffer. After, gel pieces were reduced and alkylated with dithiothreitol (DTT) (50mM) and iodoacetamide (100mM), respectively. After 3 washes with 50% ACN containing 20mM NH_4HCO_3 buffer, the samples were dried. Finally, a trypsin (Promega®) solution (20 ng/μL) was added to each tube and trypsinolysis was proceeded overnight at 37 °C. Digested peptides were extracted from gel pieces with 0.1% (v/v) trifluoroacetic acid (TFA) in 50% (v/v) ACN twice, and the

pooled was dried. Peptides were reconstituted in 20 µl of 2% (v/v) ACN and 0.1% (v/v) TFA.

Tryptic peptides were analyzed on the Q-Exactive ™ mass spectrometer (Thermo Scientific), connecting to a nanoUHPLC UltiMate® 3000 (Dionex®) system with nanospray ion source. Samples were injected into the chromatograph by a trapping system using an Acclaim PepMap100 C18 column (75 µm i.d × 2 cm, 3 µm, 100 Å, Thermo Scientific), and directed to an Acclaim PepMap100 C18 capillary column (75 µm i.d × 15 cm, 2 µm, 100 Å, Thermo Scientific). A linear gradient was started from 3.8 to 50% of buffer B (80% acetonitrile and 0.1% formic acid) in buffer A (0.1% formic acid) at 300 $nl.min^{-1}$, over 120 min, followed by a sharp ramp to 99% B. LC-MS/MS operated a data-dependent acquisition method, in positive ion mode, with a MS1 resolution of 70.000 (300–2000 m/z range) and a maximum injection time of 120 ms. MS2 spectra were obtained with a resolution of 35000, with a maximum injection time of 120 ms. Up to 12 more intense precursor ions with charge between 2 and 4 were isolated with a 2 m/z window and fragmented by high-energy collisional dissociation with a normalized collision energy of 28–30 V.

2.4.3. Data analysis

The obtained spectra were submitted to database search, de novo sequencing, and quantification using PEAKS Studio 8 software (Bioinformatics Solutions Inc.). The search was performed against in house database of *C. cubensis* containing 12418 protein sequences. Parameters considered: (i) Enzymatic specificity of trypsin (K/R not before P), allowing up to two missed cleavage sites; (ii) Error tolerances of up to 10 ppm for precursors and 0.1 Da for product ions; (iii) Cysteine carbamidomethylation (+57.02 Da) and methionine oxidation (+15.99 Da) were set respectively as fixed and variable modifications; (iv) peptide mass error tolerance was set at 10 ppm for precursor ion and 0.1 Da for fragment ions and retention time shift of 3 min were allowed in this process. The decoy-fusion feature was activated and peptide-spectrum matches kept at 1% of False Discovery Ratio (FDR). Extracted ion chromatograms (XIC) from up to 2 most intense unique peptides were averaged to infer protein abundance. Relative protein quantification was performed and statistically tested using the PEAKS Q module (ANOVA method). Only proteins exhibiting p-value ≤ 0.5 and protein fold change ≥ 1.5 were considered differentially abundant between samples of *C. cubensis* enzymatic extract grown in sugarcane bagasse (WBE) and *C. cubensis* enzymatic extract grown in wheat bran (SBE).

The relative protein abundance in each condition concerning the abundance in reference condition was represented as a heat map of the representative proteins of each protein group.

2.5. Bioinformatics analysis and protein annotation

Function assignment, annotation by InterPro terms, enzyme classification codes (EC) and categorization based on the molecular function, biological process, and cellular component, were determined using the Blast2GO software suite.5.7 (https://www.blast2go.com/) (Talon et al., 2008). All of the protein sequences were functionally annotated based on searches using BLASTp version 2.2.21 (Altschul et al., 1990). For each query sequence, the software first detects up to 20 homolog sequences in the non-redundant (nr) NCBI database restricted to the fungi taxonomy filter, with a minimum expected value of 1.0E-3 and a high scoring segment pair cutoff of 33.

Proteins identified in mass spectrometry experiments were also screened using the dbCAN2 meta server (http://cys.bios.niu.edu/dbCAN2/index.php) (Yohe et al., 2018) and classified according to CAZy catalytic group as auxiliary activities enzymes (AAs), glicosil hidrolases (GHs), polysaccharide lyases (PLs), carbohydrate esterases (CEs) and carbohydrate binding modules (CBMs). Posteriorly, the DeepLoc-1.0 (http://www.cbs.dtu.dk/services/DeepLoc/) (Almagro Armenteros et al., 2017) was used for the prediction of subcellular locations. Proteins targeted to the nonclassical secretion pathway were identified using SecretomeP 2.0 Server (http://www.cbs.dtu.dk/services/SecretomeP/) (Bendtsen et al., 2005). For each protein, theoretical mass weight (Mw) and isoelectric point (pI) were calculated by Compute pI/Mw tool (https://web.expasy.org/compute_pi/) (Bjellqvist et al., 1993).

2.6. Biomass pretreatment and composition analysis

Sugarcane bagasse was washed and dried in an oven at 70 ºC until reaching a constant mass, after which it was further milled (particle size less than 1 mm) and submitted to alkaline pretreatment. NaOH 1.5% (w/v) were used to pretreat the milled sugarcane bagasse samples at a solid loading of 10% (w/v). The pretreatments were performed in an autoclave at 121 °C for 60 min. The pretreated materials were filtered using a Buchner funnel fitted with filter paper. The solid fraction was washed with distilled water, sealed in a hermetic vessel and stored at -20 ºC. The chemical composition

of the alkali-treated sugarcane bagasse was determined according to described by (Maitan-Alfenas et al., 2015).

2.7. Sugarcane bagasse saccharification assays

The crude enzymatic extracts produced by *C. cubensis* cultivated in wheat bran (WBE) or sugarcane bagasse (SBE), and commercial cocktails (Multifect® CL and Celluclast® 1.5L) were applied in a biomass saccharification experiment. The *C. cubensis* enzymatic extracts were concentrated 6-fold before the experiment using an Amicon Ultrafiltration system (Millipore Co. - Billerica, MA, USA) and a YM-10 (Cut-off Mr 10,000 Da) membrane filter. Enzymatic saccharification of alkali-treated sugarcane bagasse was performed in 25 mL Erlenmeyer flasks with 12 mL working volume, at an initial solid concentration of 8% dry matter (w/v) in 100 mM sodium acetate buffer at pH 5.0. The enzyme loading was 10 FPase units per gram of biomass. Tetracycline (40 mg/L) and sodium azide (10 mM) were also added to the reaction mixture to inhibit microbial contamination. Biological triplicates, as well as positive and negative controls, were performed for the saccharification of each enzymatic extract. The reactions were carried out in an orbital shaker at 250 rpm and 50 °C. After 72h, samples (1.0 mL) were taken from the reaction mixture and immediately heated to 100 °C to denature the enzymes, cooled, centrifuged for 5 min at 15,000 g, and stored at -20 ºC.

Glucose and xylose were quantified using high-performance liquid chromatography (HPLC) with a Shimadzu series 10A chromatograph (Shimadzu, Kyoto, Japan). The HPLC was equipped with an Aminex HPX-87P column (300 x 7.8 mm) and a refractive index detector. The column was eluted with water at a flow rate of 0.6 mL/min and it operated at 80 ºC. Statistical analysis of data was performed using R software through analysis of variance (ANOVA) followed by Tukey's test at a significance level of 5%. The standard deviation was also calculated for all assays.

3. Results and discussion

3.1. Comparison of proteins identified in extracts of *C. cubensis*

WBE and SBE showed similar global protein profile in relation to the main enzymatic activities (**Fig. 1A**), with a predominance of CAZymes. However, WBE presents a greater number of representatives with other functions, indicating a greater diversity.

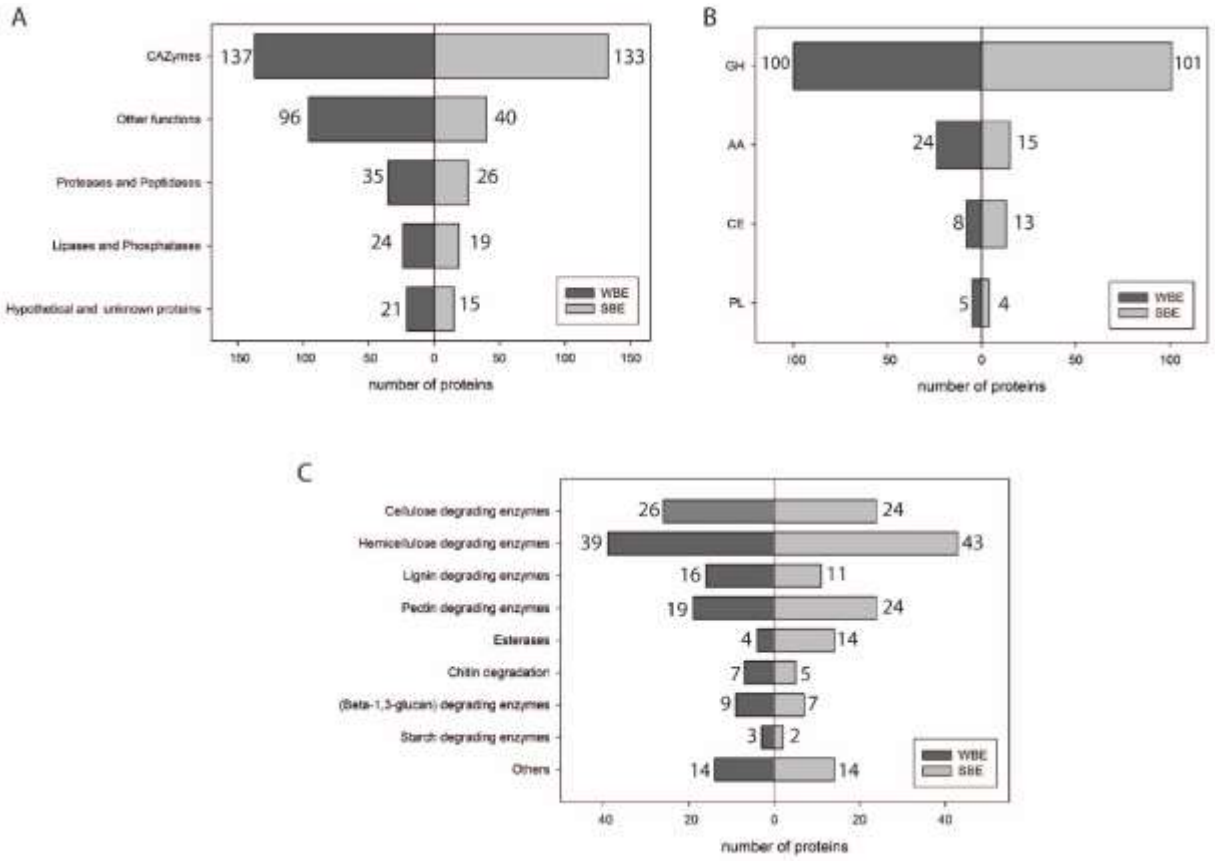

Figure 1: Bar charts of the functional classification of proteins identified in the *C. cubensis* secretomes (WBE and SBE) identified by proteomics. The dark gray bars positioned on the left refer to WBE and the light gray bars positioned on the right refer to SBE. (A) Classification based on the main enzymatic activities. (B) Classification based on CAZy classes. (C) Classification based on the preferred substrates of CAZymes.

About CAZymes (**Fig. 1B**), in general, no significant differences were observed regarding the number of representatives for each CAZy class. In WBE a relatively higher number of AAs was observed compared to SBE. There were also no significant differences in WBE and SBE about the number of representatives acting on CAZymes preferred substrates (**Fig. 1C**). Thus, more detailed relative quantification analyzes are necessary for a complete understanding of the composition of each extract.

3.2. Analysis of relative and cumulative abundance of proteins

To evaluate the complexity of the *C. cubensis* extract, relationships between the area under the curve values (AUC) of the precursor ion peaks and the number of identified proteins were represented. The graphs (**Fig. 2A-B**) show similarity to the distorted and abruptly decreasing distribution in the abundance of WBE and SBE proteins, which shows the presence of a small number of very abundant proteins and a large number of proteins present in trace amounts.

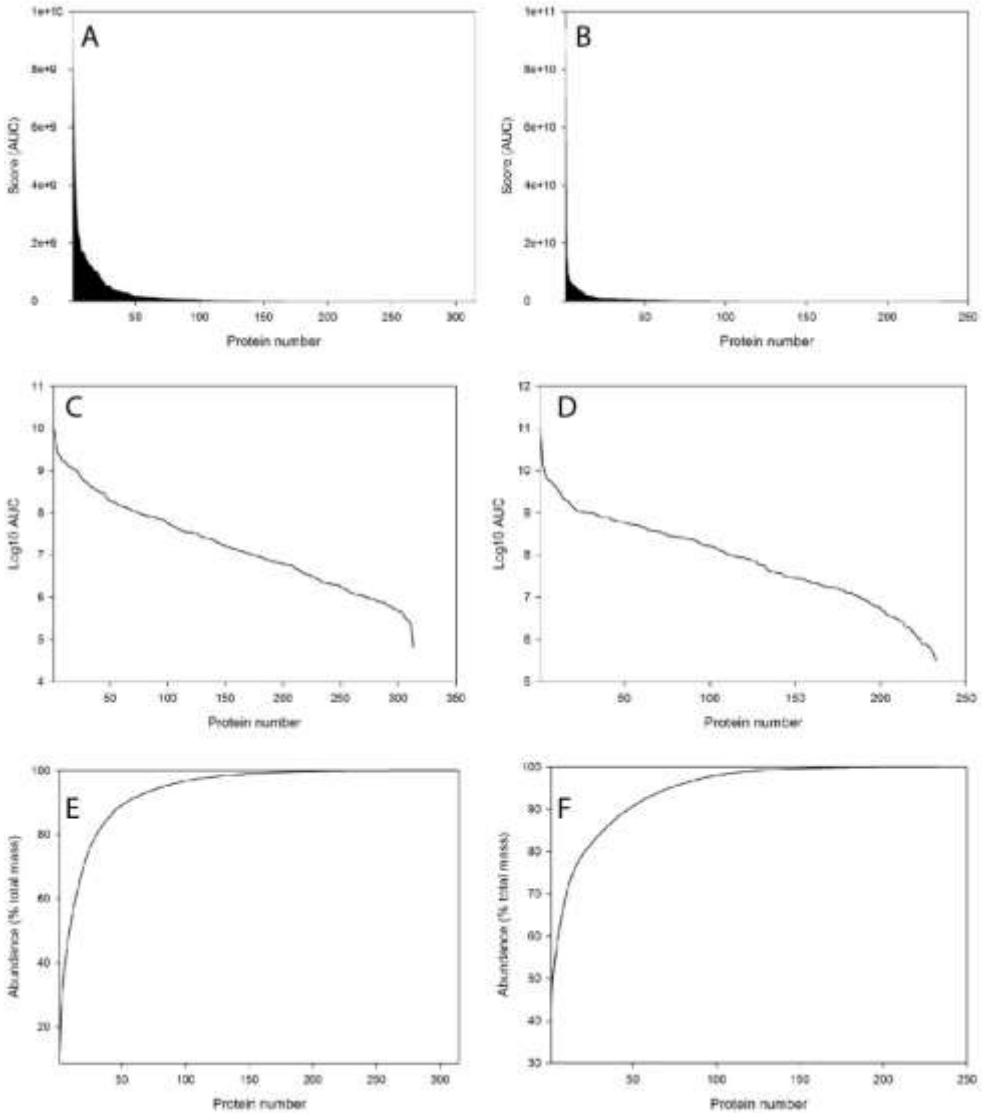

Figure 2: Protein distribution identified via shotgun analysis. Protein abundance determined using the absolute Area Under Curve (AUC) values recorded for each protein identified in WBE (A) and SBE (B). The abundance of proteins concerning the number of identified (log10AUC) in WBE (C) and SBE (D). Cumulative abundance of proteins identified in WBE (E) and SBE (F).

The dynamic range of the AUC value (AUC/10^6) of the 313 proteins identified in WBE varied from 9230 to 0.0653, and for the 233 SBE proteins ranged from 93900 to 0.315, representing a difference of five orders of magnitude. This shows the high capacity of this method for the detection and identification of proteins present at different levels of expression and the identification of proteins present at very low levels. To make the interpretation of graphs (**Fig. 2A-B**) visually more accessible, we have a logarithmic representation of the AUC axis, providing the identification of three distinct regions in the graph (**Fig. 2C-D**). The first portion, distributed in ascending way, corresponds to a small number of proteins identified with greater abundance. In the intermediate region of the graph, a high number of proteins that occupy the same quantitative range can be observed and correspond to the vast majority of proteins identified in the extracts. In the last descending portion, a small number of proteins identified with significantly low abundance values are found.

In the graphs (**Fig. 2E-F**), the WBE and SBE proteins were arranged in descending order of abundance according to their respective AUCs to record the total accumulated area, and the percentage contribution of each was determined. Subsequently, cumulative abundances were determined. In both cases, a small number of proteins contribute significantly to the total abundance in the samples. Considering the WBE composition, 53 proteins contribute about 90% of the cumulative abundance, including 9 proteins that contribute 50% of the total mass of the 313 identified proteins (**Table 1**).

Table 1: Number of distinct enzymes grouped as to the substrate of action. Only proteins that account for 90% of the cumulative abundance in extracts of *C. cubensis* grown in wheat bran (WBE) and sugarcane bagasse (SBE) were considered.

Proteins	WBE	SBE
Most abundant proteins (90% C.A)	53	47
CAZymes	31	39
Lignocellulases	24	32
Act on cellulose	7	11
Act on hemicellulose	7	13
Act on lignin	2	0
Act on pectin	3	5
Act on β-1,3 glucans	5	3
Others	8	2

Considering the 53 most abundant proteins, there are 32 CAZymes, and together they present 63.3% of cumulative abundance, which demonstrates the great contribution in terms of CAZymes abundance in WBE composition. Of the 32 most abundant CAZymes, 24 are involved in the decomposition of lignocellulosic material, including enzymes that act on cellulose (7), hemicellulose (7), lignin (2), pectin (3) and β-1, 3 glucans (5) (**Table 1**). The other 8 CAZymes act on non-lignocellulosic substrates, with emphasis on enzymes that act on starch (2) and chitin (1). The presence of enzymes that act on different substrates among the most abundant reveals a diversified CAZymes composition of this extract. Considering 90% of cumulative abundance for WBE proteins, 26.7% corresponds to the abundance of proteins that do not fit the CAZymes classification, highlighting 6 hypothetical non-defined function proteins, which together correspond to 13.32%. It is noteworthy for this group of proteins because this effect in the enzymatic cocktail of WBE does not know it. Another very representative group among the most abundant are proteases (5.68%), which can act on the constituent proteins of the plant cell wall.

Regarding the SBE composition, 47 proteins contribute with about 90% of the cumulative abundance and only 3 proteins that act in the deconstruction of cellulose, contribute with 53% of the total mass of the 233 identified proteins (**Table 1**). It should be noted that the most abundant protein is a cellulase of the GH7 family (cellulose-1,4-β-cellobiosidase) that cleave cellobiose molecules the reducing end of a cellulose chain (Glass et al., 2013) and contributes with 41.43% of the total abundance, presenting a relative abundance 3 times higher in SBE than WBE. The other two proteins most abundant in SBE are a 1, 4-β-cellobiosidase of the GH6 family that acts on the non-reducing ends of cellulose and a lytic polysaccharide monooxygenase of the AA9 family, which aid in the depolymerization both amorphous and crystalline cellulose by non-oxidative mechanisms (Harris et al., 2014). Considering the 47 most abundant proteins, 39 are CAZymes that correspond to 83.9% of cumulative abundance. Of these, 32 act on the decomposition of lignocellulosic material, including enzymes that act on cellulose (11), hemicellulose (13), pectin (5) and β-1,3-glucans (3) (**Table 1**). Thus, there is a low presence of non-lignocellulolytic CAZymes.

Considering a cumulative abundance of 90%, WBE has a greater diversity of proteins among the most abundant (53) compared to SBE (47). However, it has a smaller number of CAZymes that act on lignocellulosic biomass (24) in relation to SBE (32). Besides, considering this same cumulative abundance, only 14 proteins are present in the

two extracts, mostly CAZymes (11) that possess very distinct relative abundance in each extract, giving different contributions to the cumulative abundance in WBE and SBE.

This compositional analysis demonstrates that the secretome of *C. cubensis* cultivated in sugarcane bagasse is more cohesive and directed to the decomposition of rich lignocellulosic biomasses mainly in cellulose and hemicellulose, inducing the expression of a smaller number of proteins that do not act in these biomasses. The *C. cubensis* extract cultivated in wheat bran is less directed, however, more diversified as the presence of CAZymes that act on other polysaccharides, besides the presence of proteases and hypothetical proteins without determined function. Thus, WBE may be more versatile in the decomposition of more complex biomasses with a greater presence of non-lignocellulosic polysaccharides, or even greater presence of other non-polysaccharide cellular components, such as proteins and lipids.

3.3. Presence of exclusive CAZymes in WBE and SBE

Comparing all proteins detected in WBE and SBE, it is observed a significant number of CAZymes that are exclusively found in SBE (28) and WBE (32), according to the Venn diagram (**Fig. 3**). About the exclusive CAZymes of SBE, only 4 do not act on the lignocellulosic biomass, whereas in WBE it is observed the presence of a greater diversity of non-lignocellulosic enzymes (8). Analyzing the unique cellulases, WBE has a greater diversity of single β-glucosidases (3), while SBE has a higher number of exclusive endoglucanases (3).

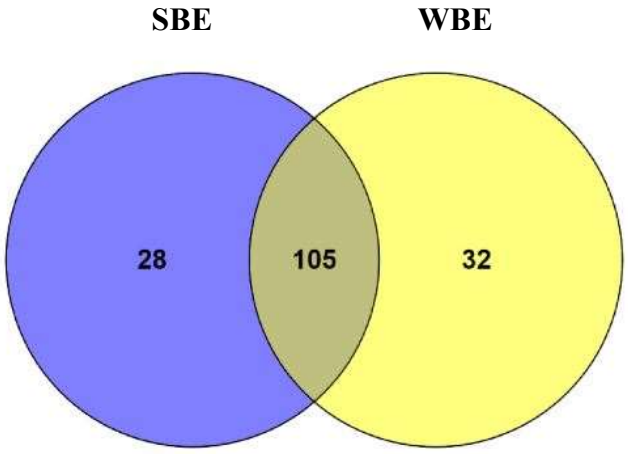

Figure 3: Venn diagram representing exclusive CAZymes identified in *C. cubensis* secretomes. The blue circle represents the proteins identified in SBE; the yellow circle represents the proteins detected in WBE**.** The Venn diagram was prepared using Venny 2.1.0 online tools.

It is worth to mention that a large number of pectin (8) enzymes are exclusive to SBE, with emphasis on polygalacturonases (6). SBE also has a high number of exclusive hemicellulases (7), especially enzymes that act on chain branching (3) or xylan substituent groups, such as acetylxylan esterases (3). WBE shows different characteristics regarding the composition of exclusive CAZymes, such as the significant presence of enzymes that act on lignin (8) belonging to the class of auxiliary activities enzymes (AAs). In addition, WBE has a larger number of unique enzymes that act on β-1, 3-glucans (3) and chitin (3), besides inducing exclusive enzyme that act on starch (1), which confirms the more general character performance on WBE in the degradation of diversified polysaccharides.

3.4. Differentially expressed proteins in WBE and SBE

The results show that of the 167 proteins in common, 133 proteins are differentially present, with 109 proteins being up-regulated in WBE, whereas 24 proteins are up-regulated in SBE (**Fig. 4**). Thus, WBE presents a group of up-regulated proteins 5.5 times greater when compared to SBE.

A

B

Proteins	WBE	SBE
Up-regulated proteins	109	24
Non-carbohydrate proteins	53 (49.6%)	4 (16.7%)
Hypothetical proteins	12	0
Proteases and peptidases	10	2
Lipases and phosphatases	10	0
Others	28	2
CAZymes	56 (50.4%)	20 (83.3%)
Cellulases	11	6
Hemicellulases	8	8
Ligninases	5	1
Pectinases	11	3
β-1,3-glucanases	6	0
Esterases	8	1
Chitinases	2	0
Amylases	1	0
Other functions	4	1

Figure 4: A) The hierarchically clustered heat map of the quantitative proteomic analysis was generated by PEAKS Studio 8.0 software, displaying the differentially expressed proteins identified using label-free LC-MS/MS proteomic analysis of the representative biological samples in triplicates of WBE and SBE. Only proteins that passed a statistical significance threshold (ANOVA, $p < 0.05$ and FDR <1% for protein expression) and fold change of 1.5 were plotted on heat maps. The color scale represents the level of relative expression of each protein in the fungal extracts; the red and green colors indicate the highest and lowest levels of expressions, respectively. The color intensity represents the degree of protein up-and-down regulation when WBE and SBE are compared. B) WBE and SBE up-regulated protein number scheme and functional classification of non-carbohydrate and CAZymes proteins.

The classification of proteins differentially expressed according to cell localization shows that 96 proteins are extracellular (72%), while 15 (11.3%) are located on the plasma membrane, 7 are present in the cytoplasm (5.3%), 5 in the nucleus (3.75%) and 10 in other cellular locations (7.65%). Most proteins are extracellular, however, the presence of proteins from other localizations, especially plasma membrane and cytoplasm, may be caused by different factors, such as contamination of intracellular contents by possible plasma membrane ruptures by mechanical extraction process; mechanisms of fungal cell wall remodeling; cell death due to prolonged culture time or transport of proteins by unconventional pathways. In phytopathogenic fungus, extracellular vesicles (EVs) play a critical role in intercellular communication between fungal cells to maximize the chance of a successful infection (Bleackley et al., 2019).

The protein categorization reveals that the main molecular functions noted by Blast2go are hydrolase activity, hydrolyzing O-glycosyl bonds (36%), oxidoreductase activity (15%), transferase activity (8%), ion-binding metal (8%) and peptidase activity (6%). About biological processes, most of the proteins noted are involved in metabolic processes (70%), while a smaller group is involved in cellular processes (30%). It is worth to highlight the great contribution of biological processes related to the performance of CAZymes, such as catabolic processes of polysaccharides, metabolic processes of cell wall polysaccharide, glucans metabolism and oxidoreduction processes. In this biological context, it is perceived that the enzymatic machinery of this fungus is directed to the complete depolymerization of polysaccharides through different approaches, due to the complexity of these carbon sources.

We can confirm this by observing the presence of 56 CAZymes among the 109 up-regulated proteins in WBE. Although the CAZymes are the most representative group among up-regulated proteins (50.4%), WBE was able to induce a large number of non-carbohydrate proteins (49.6%), including 12 hypothetical proteins or with unknown function and 10 proteins classified in the group of proteases and peptidases, which together represent 20% of proteins overexpressed in WBE. In the group of proteins differentially expressed in SBE, we have the presence of 24 proteins, including 20 CAZymes (83.3%), which perceptually represent a higher predominance of CAZymes up-regulated in SBE compared to WBE. Only 4 enzymes differentially present in SBE do not belong to CAZymes, being two proteases and two proteins with other functions. This demonstrates an entirely directed and almost restricted regulation to enzymes that act in the depolymerization of lignocellulosic biomasses. As sugarcane bagasse is a poor protein

source compared to wheat bran, the up-regulation of proteases and peptidases was not as significant in SBE.

Concerning CAZymes overexpressed in WBE (56), 41 enzymes act on components of lignocellulosic substrates, such as cellulases (11), hemicellulases (8), ligninases (5), pectinases (11) and β-1,3-glucanases (6). Another 15 enzymes act on other substrates, such as esterases (8), chitinases (2), amylases (1), and other cellular functions (4). In SBE, a smaller number of enzymes acting as cellulases (6), ligninases (1) and pectinases (3), and an equal number of hemicellulases (8) were overexpressed.

Considering the up-regulated WBE cellulases, a predominance of different β-glucosidases (4), endo-1,3(4)-beta-glucanases (4) and LPMOs (2) of the AA9 family occurred. Although WBE has a large number of up-regulated cellulases, there was no overexpression of the complete cellulose depolymerization machinery since it did not detect differentiated expressed cellobiosidases. In contrast, SBE presents a lower number of up-regulated cellulases (6), but presents over-expressed representatives that form the complete cellulose depolymerization machinery, such as endo-1,4-beta-D-glucanase (1), cellulose 1, 4-beta-cellobiosidase (1), β-glucosidase (1), and the LPMOs of the AA9 (3) family in a larger number than that found in WBE. It is known that LPMOs act in regions of higher crystallinity in the cellulose fibers, frequently found in regions of the cell wall of biomasses, such as sugarcane bagasse.

Among the up-regulated WBE hemicellulases, enzymes that act on the main arabinoxylan chain, such as endo-1,4-β-xylanase (1), and enzymes acting on xylooligosaccharides, such as β-xylosidase (1), are present. However, we observed the participation of accessory enzymes that act on the ramifications of arabinoxylans, such as feruloyl esterases (2) and α-glucuronidases (2). It is also observed the presence of hemicellulases that act on other components less present in wheat bran hemicellulose, such as β-galactosidase (1), which acts on the main arabinogalactan chain and β-mannosidase (1), which acts forming mannobiosis from glucomannan. In SBE, predominate up-regulation of enzymes that act mainly on arabinoxylans, such as endo-1,4-beta-xylanases (3), xylan 1,4-beta-xylosidase (1) and acetylxylan esterase (1). Was observed a lower number of enzymes acting on xyloglucans have been overexpressed, including a xyloglucan-specific endo-beta-1,4-glucanase (1) which acts on the main chain and two enzymes that act on branching, being α-galactosidase and α-fucosidase. In sugarcane, hemicellulose is composed almost entirely of arabinoxylans and in much smaller amounts by xyloglucans (de Souza et al., 2013). Consequently, the greater overexpression of arabinoxylanases may be related to the greater availability of

arabinoxylans in the sugarcane bagasse used as a culture medium. The absence of differentially expressed enzymes acting on other hemicellulose components in SBE contrasts with the overexpression of these enzymes in WBE. This may be a consequence of the more diverse composition of hemicellulose in wheat bran. Although there is a predominance of arabinoxylans in wheat bran composition, small concentrations of glucomannans, xyloglucans and arabinogalactans are found.

C. cubensis is not a good producer of ligninases, however, it is able to overexpress auxiliary activities enzymes in WBE that belong to families AA2 (2), AA3 (2), and AA7 (1), a much higher number compared to SBE, which has only one enzyme from the up-regulated AA3 family. In contrast, *C.cubensis* is an excellent producer of pectinases. A large number of pectinases were up-regulated in WBE, including enzymes that act on the two major pectin structural polysaccharides, such as a polygalacturonase (1) that acts on homogalacturonan (HG) and pectinases (8) acting on rhamnogalacturonan I (RG I). Among the enzymes that act in RG I, it is important to highlight the high number of α-L-rhamnosidases (3) that act in the main chains of RG I, in addition to the enzyme rhamnogalacturonan endolyase (1) and enzymes of the family GH106 (2). Other pectinases act on RG I branches, such as β-glucuronidase (1) and arabinosidases (1). Endo-apiosidase and β-arabinofuranosidase pectinases act on the branches of rhamnogalacturonan-II, which is a structural polysaccharide found at low concentrations in plant cell walls. Other hemicellulases that may also act as pectinases in the branches of RG I are part of upregulated enzymes, such as feruloyl esterases and a β-galactosidase. In SBE, there were a smaller number of overexpressed pectinases, being a polygalacturonase and two pectinases that act on arabinogalactans.

The overexpression of a large variety of pectinases that act on different pectic polysaccharides demonstrates the great potential of WBE for the deconstruction of biomasses with high pectin concentrations, besides being an excellent induction medium for the production of pectinases of biotechnological interest. Pectin is the polysaccharide responsible for the porosity of the plant cell wall, which is a determinant factor for increasing the efficiency of the enzymatic saccharification since the average pore size of the cell wall matrix can limit the traffic of GHs capable of penetrating the wall (Xiao and Anderson, 2013). Thus, in order to reduce the limitation of the action of enzymes on the cell wall caused by the presence of the pectin domain, pectinases must be present in enzymatic cocktails (Buckeridge et al., 2015), which allows the decrease of the recalcitrance of the cell wall and access to other polysaccharides, such as cellulose and hemicellulose (Tavares et al., 2015).

Another group of overexpressed proteins in WBE are β-1,3-glucanases, with six representative enzymes. These enzymes may be related to the availability of soluble β-1,3-glucans (2.1-2.5%) as a source of easy assimilation in wheat bran, mainly from the wheat germ layer (Apprich et al., 2014). However, sugarcane bagasse is also rich in β-1,3 glucans (8% dry weight) constituents of the mixed linkage β-glucans, which are components of the cell wall nonspecifically bound to the cell surface (Buckeridge et al., 2019). In SBE there was no up-regulation of β-1,3-glucanases when compared to WBE. Besides, the number of these enzymes among the most abundant was also lower, even the sugarcane bagasse being a rich source in β-1,3 glucans. Thus, other factors may have contributed to the induction of β-1,3-glucanases.

In addition to the presence of a large number of β-1,3-glucanases in WBE, the up-regulation of enzymes acting on chitin was also observed (2). Chitin is not a component of wheat bran; however, like β-1,3-glucans, it is a constituent of the fungal cell wall. Thus, there may be a relationship in the up-regulation of these sets of enzymes that act on the fungal cell wall. It is known that several genes encoding enzymes involved in the synthesis of β-1,3-glucans and chitin are constantly expressed in fungal cells to protect fungi from changes in osmotic pressure and various environmental stress conditions, as carbon deprivation (Kameshwar and Qin, 2017). The growth and extension of the cell wall represent a fine balance between the hydrolysis of the cell wall and its constant biosynthesis (Adams, 2004). The β-glucanases play an important role, partially hydrolyzing the localized areas and allowing the insertion of new material from the cell wall without disrupting its integrity (Adams, 2004). Thus, it can be hypothesized that the conditions of growth in wheat bran required a greater remodeling of the fungal cell wall and, consequently, greater expression of β-1,3-glucanases (Martin et al., 2007).

3.5. Activities of the *C. cubensis* enzymatic extracts and commercial cocktails: a comparison between the enzymatic profiles

In order to establish a comparison between the crude enzymatic extracts produced by *C. cubensis* under SSF using wheat bran or sugarcane bagasse and commercial preparation of cellulases obtained from *T. reesei* cultures (Multifect® CL, Celluclast® 1.5L), the activities of cellulases, hemicellulases, pectinases, amylases, and laccase were determined. A direct comparison between the volumetric activities found in both enzymatic extracts did not allow a fair comparison. Both the Multifect® CL cocktail and the Celluclast® 1.5L are enzymatic preparations of highly concentrated industrial scales

incorporating additives to ensure the stability of a large number of enzymes present in the product composition. However, the enzymatic extracts of *C. cubensis* were produced in benchtop fermenters. To establish a parameter to compare the different extracts, all the enzymatic activities observed were indexed concerning the activity of the FPase, which represents the total cellulase activity of the enzymatic complexes. FPase is the standard activity considered to determine the enzymatic loading in saccharification processes, which justifies the use of this parameter as a reference in this type of analysis (Falkoski et al., 2013). The comparative results can be observed in **Table 2.**

Table 2: Comparative analysis of lignocellulolytic activities of the crude extract from *C. cubensis* cultivated in wheat bran (WBE) and *in natura* sugarcane bagasse (SBE), and commercial cocktail Multifect® CL and Celluclast® 1.5L. The values displayed were obtained dividing each total enzymatic activity by total FPase activity found in each extract.

Units of enzymatic activity/Units of Fpase activity				
Enzyme	**WBE**	**SBE**	**Multifect® CL**	**Celluclast® 1.5L**
FPAse	1.00	1.00	1,00	1,00
Endoglucanase	19.51 ± 0.13	36.40 ± 0.88	35.61 ± 0.63	38.73 ± 0.93
β-Glucosidase	6.57 ± 0.13	13.17 ± 0.56	1.64 ± 0.01	0.53 ± 0.002
β-cellobiohydrolase	1.73 ± 0.02	8.51 ± 0.28	1.07 ± 0.02	0.15 ± 0.002
Mannosidase	n.d.	0.14 ± 0.002	n.d.	n.d.
Xylanase	367.73 ± 3.23	328.06 ± 27.58	26.62 ± 0.01	17.55 ± 0.64
β-Xylosidase	0.59 ± 0.009	0.92 ± 0.04	0.008 ± 0.0001	0.44 ± 0.02
β-mannosidase	0.04 ± 0.001	1.08 ± 0.03	n.d.	n.d.
Mannanase	2.98 ± 0.52	35.78 ± 1.72	1.15 ± 0.004	1.03 ± 0.06
Polygalacturonase	21.42 ± 0.37	16.80 ± 0.43	0.45 ± 0.001	0.40 ± 0.02
Pectin lyase	176,23 ± 0.44	154.02 ± 5.48	n.d.	0.36 ± 0.05
α-Galactosidase	0.50 ± 0.01	0.11 ± 0.002	n.d.	n.d.
β-Galactosidase	0.04 ± 0.001	0.13 ± 0.003	n.d.	n.d.
α-Arabinofuranosidase	1.86 ± 0.025	1.60 ± 0.01	1.10 ± 0.003	0.08 ± 0.004
α-Glucosidase	0.04 ± 0.001	0.08 ± 0.004	n.d.	n.d.
α-Amylase	1.68 ± 0.058	7.30 ± 0.25	0.03 ± 6.5E-04	0.03 ± 0004
Laccase	0.08 ± 0.001	0.25 ± 0.01	n.d.	n.d.

*n.d: not detected.

C. cubensis WBE presented high β-glucosidase/FPase ratio, 2.0, 8.0 and 28.0 times higher, compared to SBE, Multifect® CL, and Celluclast® 1.5L, respectively. The β-glucosidase is required to release glucose and prevent the accumulation of cellobiose. Besides, the high β-cellobiohydrolase/FPase ratio found in WBE was particularly notable,

being 5.0, 8.0 and 56.0 times higher, compared to SBE, Multifect® CL, and Celluclast® 1.5L, respectively. For the endoglucanase/FPAse ratio, WBE presented similar values to the commercial cocktails and 1.8 times higher than SBE.

The *C. cubensis* extracts showed a greater complexity of hemicellulolytic activities than commercial cocktails. SBE and WBE secreted β-mannosidase, α-galactosidase, β-galactosidase, α-glucosidase, absent in commercial extracts. Enzymatic activities of mannosidases were detected only in WBE. Besides, extracts of *C. cubensis* showed remarkably greater xylanase/FPase ratios than commercial products, with values detected for SBE slightly higher than WBE, and 13.0 and 21.0 times higher than the Multifect® CL and Celluclast® 1.5L extracts, respectively. It is worth to highlight the superior presence of β-xylosidase/FPase ratios in WBE and α-arabinofuranosidase/FPase in SBE, when compared to all extracts. This result is significant because xylanases, mannanases, α-arabinofuranosidase, and β-xylosidases are important in the saccharification of most commercially relevant biomass sources, such as sugarcane bagasse. The absence of these enzymes limits the action of cellulases in the hydrolysis of cellulose fibers since the hemicellulases act synergistically with cellulases in the hydrolysis of lignocellulosic materials (Song et al., 2016).

C. cubensis extracts are also notable for their high pectinolytic activity. SBE shows the highest polygalacturonase/FPase and pectin lyase/FPase ratios. Although they are close to the values found for SBE, they are significantly higher for the polygalacturonase ratio with Multifect® CL and Celluclast®1.5L, being 47.0 and 53.0 times higher, respectively. Regarding the pectin lyase/FPase ratio in the commercial extracts, it is insignificant in comparison with the extracts of *C. cubensis*. Recent works have confirmed the accessory role of pectinase in combination with xylanase and/or cellulase and demonstrated that an involvement in cocktail mediated saccharification, the pectinases can work contributively with xylanases and cellulases to enhance the agrowaste saccharification (Thite and Nerurkar, 2018).

3.6. Saccharification efficiencies of fungal secretome

The crude extracts of *C. cubensis* (SBE and WBE) and the commercial extracts (Multifect® CL and Celluclast® 1.5L) were applied for alkali treated sugarcane bagasse hydrolysis to compare the performance of the enzymatic extracts (10 FPU/g of dry substrate, 8% solids loading) after 72 hours of reaction. The release of glucose and xylose from glucans and xylans respectively, are shown (**Fig. 5**).

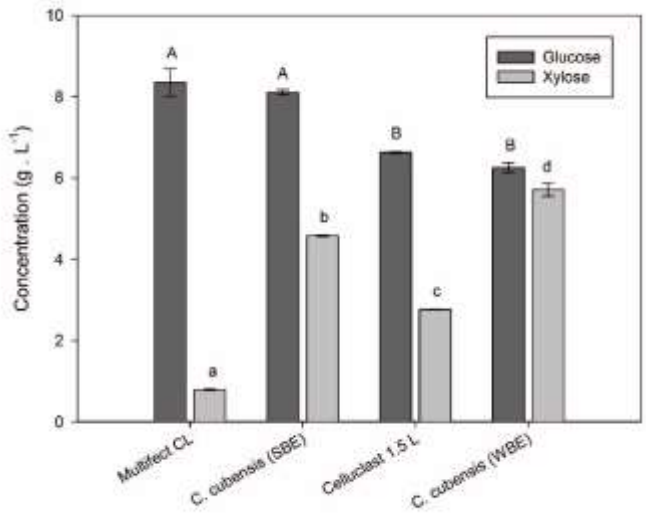

Figure 5: Production of glucose and xylose for the enzymatic saccharification of alkali-treated sugarcane bagasse after 72 hs using the *C. cubensis* extract (WBE and SBE) and commercial cellulases (Multifect® CL and Celluclast® 1.5L).

The saccharification of the glucan fraction was remarkably more efficient for the SBE and Multifect® CL cocktails, which released similar amounts of glucose, 8.11 $g.L^{-1}$, and 8.35 $g.L^{-1}$, respectively. The release of glucose by WBE (6.26 $g.L^{-1}$) was lower when compared to SBE and Multifect® CL, but similar to the release of glucose by Celluclast® 1.5L (6.63 $g.L^{-1}$). To xylan conversion, WBE promote the release of 5.71 $g.L^{-1}$ of xylose, a higher value when compared to 4.58, 2.76 and 0.79 $g.L^{-1}$ of xylose released by SBE, Celluclast® 1.5L, and Multifect® CL, respectively.

Although WBE showed significantly higher cellulase/FPase ratios compared to SBE, it was not as efficient in the release of glucose in saccharification of alkali treated sugarcane bagasse. This fact demonstrates that not only the individual activities of certain types of cellulases define the efficiency in the depolymerization of glucans, but also other factors may be determinant to explain this difference in yield. Among these factors, we can mention the concentration of each enzyme present in the different extracts; exclusivity in of certain enzymes; the different catalytic efficiencies and the variations of thermal stabilities of the cellulases of each extract; the CAZymes diversity; the effect of nonspecific adsorptions; the effect of the inhibition by end product and mainly, the synergism. The biomass hydrolysis depends not only on the presence and on isolated action of cellulases, but efficient degradation is a function of a balanced ratio of different enzymes acting in synergy to breakdown the complex lignocellulose structure (Van Dyk and Pletschke, 2012). When enzymes act synergistically, the total effect is greater than the sum of the effects of individual components (Kostylev and Wilson, 2012). Thus, the

individual contribution of each enzyme to the saccharification process is difficult to measure, but it is possible to hypothesize some reasons for the higher glucose release for the fungus extract grown in sugarcane bagasse.

SBE shows several characteristics that may explain this better saccharification performance, such as the presence of two cellobiohydrolases (GH6 and GH7) and an LPMO (AA9) that make up 53% of the relative abundance of the extract. In addition, SBE has 3 exclusive LPMOs. The contribution of LPMOs to saccharification efficiency can be fundamental since they promote the decrease of cellulose crystallinity by oxidative mechanisms and create new sites accessible to cellulases, which act synergistically (Quinlan et al., 2011). Consequently, the presence of significant amounts of LPMOs may decrease the enzymatic loading of cellulases, as observed in recent commercial extracts. Besides, it is important to emphasize the presence of 11 enzymes that act on cellulose among the 39 most abundant CAZymes and the presence of complete cellulose deconstruction machinery among the proteins differentially expressed in SBE, which demonstrates the direction in the composition of the extract for the deconstruction of cellulose.

Another fact corroborating the assertion that SBE is a more direct extract for the deconstruction of cellulose is the higher specific activities of FPase, endoglucanase, and β-glucosidase compared to WBE. Wheat bran, a very complex substrate, induces a great diversity and a high number of proteins that do not necessarily act on cellulose, which reduces the specificity of this extract to not only the cellulose but also the fractions of the main chain of xylan and the pectic fractions.

The superior capacity of sugarcane bagasse saccharification by SBE in relation to WBE for glucose release agrees with the results reported for *A. niger* and *T. reesei,* which produced more efficient enzymatic extracts for saccharification of sugarcane bagasse when cultivated with this substrate than with wheat bran (Lichius et al., 2014). Fungi, in general, can produce enzymatic complexes adjusted to the fractions present in the biomass used for cultivation (Znameroski et al., 2012).

To xylan deconstruction, WBE presented higher xylose release than SBE, and both *C. cubensis* extracts showed much higher xylan conversion yields when compared to commercial cocktails. The best performance of SBE and WBE is due to the high xylanase/ FPAse and β-xylosidase/FPase ratios, which are insufficient in the commercial extracts, and due to the considerable diversity of these enzymes present in *C cubensis* extracts. Although WBE has a lower xylanase/FPAse ratio than SBE, it has higher β-xylosidase/FPase ratios and mannanase-acting enzymes, such as mannosidase/FPase,

mannanase/FPase and β-mannosidase/FPase. WBE also has a greater complexity of hemicellulolytic activities and a significant amount of accessory enzymes that act on the hemicellulose main chain branches, such as α-arabinofuranosidases, β-galactosidase, α-galactosidase, and feruloyl esterases. These enzymes are absent or in insufficient quantities in the commercial cocktails Multifect® CL and Celluclast® 1.5L.

Another factor that influences the saccharification performance of the analyzed extracts is the type of pretreatment applied to lignocellulosic biomass. Although alkaline pretreatments promote the delignification of biomass, they also generate high amounts of phenolic compounds, which can be adhered into the biomass and solubilized during the saccharification step (Ladeira-Ázar et al., 2018). Phenolic compounds cause conformational changes in enzymes, promoting inhibition and/or inactivation. It is known that laccase oxidizes phenolic compounds, reducing the effects of phenols on enzymes, and their presence in the enzymatic extracts of *C. cubensis* is able to mitigate the deactivation due to phenols in xylanases and other hemicellulases during saccharification, thus helping these enzymes to exhibit a tolerance to phenolic inhibitors (Ladeira Ázar et al., 2018). Thus, the higher laccase/FPase ratio in WBE compared to SBE may promote a protective effect on hemicellulases that contributes to a more efficient xylan conversion.

The efficient conversion of xylan by WBE may have an impact on the lower cellulose conversion efficiency when compared to SBE and Multifect® CL. Monosaccharides derived from hemicellulose (xylose, arabinose, mannose, galactose) may inhibit cellulases (Leif et al., 2013; Xiao et al., 2004). Xylooligomers may be stronger cellulases inhibitors than glucose and cellobiose (Quing and Wyman, 2011). These results suggest that SBE shows a better balance between the different enzymatic activities involved in the depolymerization process of alkaline pretreated sugarcane bagasse than the other extracts.

Enzyme companies improved enzyme costs for degradation of acid pretreated corn straw (Banerjee et al., 2010). These commercial mixtures are therefore not optimized for other types of biomass or types of pretreatments, and consequently, other enzymes may have to be added to obtain optimized or ideal combinations for different biomasses or pre-treatments (Van Dyk and Pletschke, 2012).

An important deficiency of the commercial blends is the scarcity of xylanase activity (Quing and Wyman, 2011). Also, β-glucosidase and β-xylosidase are activities that are often insufficiently present in enzymatic preparations produced from filamentous fungi, such as *T. reesei*, limiting the efficiency in the hydrolysis of cellulose and hemicellulose (Borges et al., 2014). These two enzymes of *C. cubensis* could be used to

supplement commercial cocktails to avoid inhibition by product that normally retards or disrupts the action of enzymes during the hydrolysis of the biomass.

Recent works show that three different *C. cubensis* xylanases were used in the supplementation of Multifect® CL and considerably increased the release of reducing sugars during saccharification of pre-treated alkaline bagasse (de Sousa Gomes et al., 2016). Another work using the same pretreated biomass shows that the supplementation of Multifect® CL with β-glucosidases of *C. cubensis* promoted increases of 58% and 15% in the release of glucose and xylose, respectively (de Andrade et al., 2017).

Considering the limitation of some commercial cocktails regarding the complexity of the enzymatic composition and less flexibility in adapting to the saccharification of less conventional biomasses and pre-treatment with different approaches, the enzymatic cocktails of *C. cubensis* are shown as alternatives for the improvement of these products which are already well established. Recently, new enzymatic targets have been used in the supplementation of commercial products, such as laccases, peroxidases, LPMOs, α-arabinofuranosidases, feruloyl esterases, mannanases and pectinases (Binod et al., 2019). WBE and SBE are extracts that besides being good producers of enzymes commonly used in supplementation, such as β-glycosidases and β-cellobiohydrolases, also have these new targets in great abundance and diversity.

According to the different characteristics of the crude extracts of *C.cubensis* evidenced in this work, it is suggested that due to the efficient cellulose depolymerization machinery, SBE performs well in saccharification processes of agro-industrial residues with considerably high values of cellulose and reasonable values for hemicellulose, such as corn cobs, switchgrass, sugarcane bagasse, cotton stalks, agave, and sawdust. WBE, due to a more diversified characteristic in its enzymatic composition, with the presence of are efficient machinery of degradation of hemicellulose and pectic substrates, high presence of amylases and other non-cellulolytic CAZymes, besides the considerable presence of proteases and lipases, can be an enzymatic cocktail suitable for biomass with more complex compositions. WBE may be more indicated for the saccharification of biomasses with higher protein levels, such as soybean hulls and wheat straw. WBE can also be efficient in the saccharification of biomasses with high levels of pectin, such as citrus peel and sugar beet waste, or biomasses rich in starch, such as cassava bagasse and rice bran.

Furthermore, the *C. cubensis* extracts can be used not only as new sources of enzymes for the supplementation of commercial products or new targets of heterologous expression but also can be developed and optimized as complete enzymatic cocktails for

the degradation of other lignocellulosic biomasses with biotechnological potential.

4. Conclusions

Our integrative analysis of the quantitative shotgun proteomic data set obtained from *C. cubensis* grown on wheat bran or sugarcane bagasse demonstrated the high polysaccharide degradation capacities of both extracts. Fine analysis of the *C. cubensis* secretome revealed a large array of CAZymes, most of them being differentially produced in response to the carbon source used. SBE is more cohesive and directed to the decomposition of rich lignocellulosic biomasses mainly in cellulose and hemicellulose, while WBE has a more diversified composition, being an alternative for the degradation of more complex biomasses with a greater contribution of non-cellulosic fractions. These findings indicated this fungus as a candidate for second-generation technologies using different lignocellulosic agricultural wastes as an inexpensive and sustainable alternative for the production of value-added chemicals and biofuels.

Acknowledgments

We acknowledge the Brazilian institutions' CAPES for the scholarship granted to the first author and FAPEMIG and CNPq for the resources provided to complete this experiment. We also thank the Multi-user Proteomics Laboratory of the Federal University of Ouro Preto by the support in the mass spectrometric analysis.

Supplementary material

E-supplementary data of this work can be found in the online version of the paper.

References

1. Adams, D.J., 2004. Fungal cell wall chitinases and glucanases. Microbiology 150, 2029–2035. https://doi.org/10.1099/mic.0.26980-0

2. Almagro Armenteros, J.J., Sønderby, C.K., Sønderby, S.K., Nielsen, H., Winther, O., 2017. DeepLoc: prediction of protein subcellular localization using deep learning. Bioinformatics 33, 3387–3395. https://doi.org/10.1093/bioinformatics/btx431

3. Altschul, S.F., Gish, W., Miller, W., Myers, E.W., Lipman, D.J., 1990. Basic local alignment search tool. J. Mol. Biol. 215, 403–410. https://doi.org/10.1016/S0022-2836(05)80360-2

4. Anwar, Z., Gulfraz, M., Irshad, M., 2014. Agro-industrial lignocellulosic biomass a key to unlock the future bio-energy: A brief review. J. Radiat. Res. Appl. Sci. 7, 163–173. https://doi.org/10.1016/J.JRRAS.2014.02.003

5. Apprich, S., Tirpanalan, Ö., Hell, J., Reisinger, M., Böhmdorfer, S., Siebenhandl-ehn, S., Novalin, S., Kneifel, W., 2014. Wheat bran-based biorefinery 2 : Valorization of products. LWT - Food Sci. Technol. 56, 222–231. https://doi.org/10.1016/j.lwt.2013.12.003

6. Banerjee, G., Scott-Craig, J.S., Walton, J.D., 2010. Improving Enzymes for Biomass Conversion: A Basic Research Perspective. BioEnergy Res. 3, 82–92. https://doi.org/10.1007/s12155-009-9067-5

7. Bendtsen, J.D., Kiemer, L., Fausbøll, A., Brunak, S., 2005. Non-classical protein secretion in bacteria. BMC Microbiol. 5, 1–13. https://doi.org/10.1186/1471-2180-5-58

8. Binod, P., Gnansounou, E., Sindhu, R., Pandey, A., 2019. Enzymes for second generation biofuels: Recent developments and future perspectives. Bioresour. Technol. Reports 5, 317–325. https://doi.org/10.1016/J.BITEB.2018.06.005

9. Bjellqvist, B., Hughes, G.J., Pasquali, C., Paquet, N., Ravier, F., Sanchez, J.C., Frutiger, S., Hochstrasser, D., 1993. The focusing positions of polypeptides in immobilized pH gradients can be predicted from their amino acid sequences. Electrophoresis 14, 1023–1031.

10. Bleackley, M.R., Dawson, C.S., Anderson, M.A., 2019. Fungal Extracellular Vesicles with a Focus on Proteomic Analysis. Proteomics. https://doi.org/10.1002/pmic.201800232

11. Borges, D.G., Baraldo Junior, A., Farinas, C.S., de Lima Camargo Giordano, R., Tardioli, P.W., 2014. Enhanced saccharification of sugarcane bagasse using soluble cellulase supplemented with immobilized β-glucosidase. Bioresour. Technol. 167, 206–213. https://doi.org/10.1016/J.BIORTECH.2014.06.021

12. Borin, G.P., Sanchez, C.C., Souza, A.P. De, Santana, S. De, Souza, A.T. De, Franco, A., Leme, P., Squina, M., Buckeridge, M., Goldman, G.H., De, J.V., 2015. Comparative Secretome Analysis of *Trichoderma reesei* and *Aspergillus niger* during Growth on Sugarcane Biomass. PLoS One 10, 1–20. https://doi.org/10.1371/journal.pone.0129275

13. Bradford, M.M., 1976. A rapid and sensitive method for the quantitation of microgram quantities of protein utilizing the principle of protein-dye binding. Anal. Biochem. 72, 248–254. https://doi.org/10.1016/0003-2697(76)90527-3

14. Buckeridge, M., Santos, W. dos, Tiné, M.A.S., de Souza, A.P., 2015. The cell wall architecture of sugarcane and its implications to cell wall recalcitrance, in: Lam, E., Carrer, H., da Silva, J., Kole, C. (Eds.), Compendium of Bioenergy Plants: Sugarcane. CRC Press, Boca Raton, pp. 31–50. https://doi.org/doi:10.1201/b19601-4

15. Buckeridge, M.S., Grandis, A., Tavares, E.Q.P., 2019. Disassembling the Glycomic Code of Sugarcane Cell Walls to Improve Second-Generation Bioethanol Production. Bioethanol Prod. from Food Crop. 31–43. https://doi.org/10.1016/B978-0-12-813766-6.00002-3

16. Chylenski, P., Forsberg, Z., Ståhlberg, J., Várnai, A., Lersch, M., Bengtsson, O., Sæbø, S., Horn, S.J., Eijsink, V.G.H., 2017. Development of minimal enzyme cocktails for hydrolysis of sulfite-pulped lignocellulosic biomass. J. Biotechnol. 246, 16–23. https://doi.org/10.1016/J.JBIOTEC.2017.02.009

17. de Andrade, L.G.A., Maitan-Alfenas, G.P., Morgan, T., Gomes, K.S., Falkoski, D.L., Alfenas, R.F., Guimarães, V.M., 2017. Sugarcane bagasse saccharification by purified β-glucosidases from *Chrysoporthe cubensis*. Biocatal. Agric. Biotechnol. 12, 199–205. https://doi.org/10.1016/j.bcab.2017.10.007

18. de Sousa Gomes, K., Maitan-Alfenas, G.P., de Andrade, L.G.A., Falkoski, D.L., Guimarães, V.M., Alfenas, A.C., de Rezende, S.T., 2016. Purification and Characterization of Xylanases from the Fungus *Chrysoporthe cubensis* for Production of Xylooligosaccharides and Fermentable Sugars. Appl. Biochem. Biotechnol. 182, 818–830. https://doi.org/10.1007/s12010-016-2364-5

19. de Souza, A.P., Grandis, A., Leite, D.C.C., Buckeridge, M.S., 2013. Sugarcane as a Bioenergy Source: History, Performance, and Perspectives for Second-Generation Bioethanol. Bioenergy Res. 7, 24–35. https://doi.org/10.1007/s12155-013-9366-8

20. Delgado, L., Trejo, B.A., Huitrón, C., Aguilar, G., 1993. Pectin lyase from *Aspergillus sp*. CH-Y-1043. Appl Microbiol Biotechnol 39, 515–519.

21. Dutra, T.R., Guimarães, V.M., Varela, E.M., Fialho, L. da S., Milagres, A.M.F., Falkoski, D.L., Zanuncio, J.C., Rezebde, S.T., 2017. A *Chrysoporthe cubensis* enzyme cocktail produced from a low-cost carbon source with high biomass hydrolysis efficiency. Sci. Rep. 7, 1–9. https://doi.org/10.1038/s41598-017-04262-y

22. Falkoski, D.L., Guimarães, V.M., de Almeida, M.N., Alfenas, A.C., Colodette, J.L., de Rezende, S.T., 2013. *Chrysoporthe cubensis*: A new source of cellulases and hemicellulases to application in biomass saccharification processes. Bioresour. Technol. 130, 296–305. https://doi.org/10.1016/j.biortech.2012.11.140

23. Ghose, T.., 1987. Measurement of cellulase activities. Pure Appl. Chem. 59, 257–268. https://doi.org/10.1351/pac198759020257

24. Glass, N.L., Schmoll, M., Cate, J.H.D., Coradetti, S., 2013. Plant Cell Wall Deconstruction by Ascomycete Fungi. Annu. Rev. Microbiol. 67, 477–498. https://doi.org/10.1146/annurev-micro-092611-150044

25. Harris, P. V, Xu, F., Kreel, N.E., Kang, C., Fukuyama, S., 2014. New enzyme insights drive advances in commercial ethanol production. Curr. Opin. Chem. Biol. https://doi.org/10.1016/j.cbpa.2014.02.015

26. Himmel, M.E., Ding, S.-Y., Johnson, D.K., Adney, W.S., Nimlos, M.R., Brady, J.W., Foust, T.D., 2007. Biomass Recalcitrance: Engineering Plants and Enzymes for Biofuels Production. Science 315, 804-807. https://doi.org/10.1126/science.1137016

27. Jung, S., Song, Y., Myeong, H., Bae, H., 2015. Enhanced lignocellulosic biomass hydrolysis by oxidative lytic polysaccharide monooxygenases (LPMOs) GH61 from *Gloeophyllum trabeum*. Enzyme Microb. Technol. 77, 38–45. https://doi.org/10.1016/j.enzmictec.2015.05.006

28. Kameshwar, A.K.S., Qin, W., 2017. Metadata analysis of *Phanerochaete chrysosporium* gene expression data identified common CAZymes encoding gene expression profiles involved in cellulose and hemicellulose degradation. Int. J. Biol. Sci. 13, 85–99. https://doi.org/10.7150/ijbs.17390

29. Kostylev, M., Wilson, D., 2012. Synergistic interactions in cellulose hydrolysis. Biofuels 3, 61–70. https://doi.org/10.4155/bfs.11.150

30. Ladeira-Ázar, R.I.S., Morgan, T., Maitan-Alfenas, G.P., Guimarães, V.M., 2018. Inhibitors Compounds on Sugarcane Bagasse Saccharification: Effects of Pretreatment Methods and Alternatives to Decrease Inhibition. Appl. Biochem. Biotechnol. 188, 29-42. https://doi.org/10.1007/s12010-018-2900-6

31. Ladeira Ázar, R.I.S., Morgan, T., dos Santos, A.C.F., de Aquino Ximenes, E., Ladisch, M.R., Guimarães, V.M., 2018. Deactivation and activation of lignocellulose degrading enzymes in the presence of laccase. Enzyme Microb. Technol. 109, 25–30. https://doi.org/10.1016/J.ENZMICTEC.2017.09.007

32. Leif, J.J., Nilvebrant, N.-O., Alriksson, B., 2013. Bioconversion of lignocellulose: Inhibitors and detoxification. Biotechnol. Biofuels 6, 1–10. https://doi.org/10.1186/1754-6834-6-16

33. Li, J., Zhang, R., Liu, D., Wang, M., Shen, Q., Shen, Y., Miao, Y., Zhao, S., 2013.

Secretome diversity and quantitative analysis of cellulolytic *Aspergillus fumigatus* Z5 in the presence of different carbon sources. Biotechnol. Biofuels 6, 149. https://doi.org/10.1186/1754-6834-6-149

34. Lichius, A., Seidl-Seiboth, V., Seiboth, B., Kubicek, C.P., 2014. Nucleo-cytoplasmic shuttling dynamics of the transcriptional regulators XYR1 and CRE1 under conditions of cellulase and xylanase gene expression in *Trichoderma reesei*. Mol. Microbiol. 94, 1162–1178. https://doi.org/10.1111/mmi.12824

35. Lopes, A.M., Ferreira Filho, E.X., Moreira, L.R.S., 2018. An update on enzymatic cocktails for lignocellulose breakdown. J. Appl. Microbiol. 125, 632-645. https://doi.org/10.1111/jam.13923

36. Maitan-Alfenas, G.P., Visser, E.M., Alfenas, R.F., Nogueira, B.R.G., de Campos, G.G., Milagres, A.F., de Vries, R.P., Guimarães, V.M., 2015. The influence of pretreatment methods on saccharification of sugarcane bagasse by an enzyme extract from *Chrysoporthe cubensis* and commercial cocktails: A comparative study. Bioresour. Technol. 192, 670–6. https://doi.org/10.1016/j.biortech.2015.05.109

37. Martin, K., McDougall, B.M., McIlroy, S., Jayus, Chen, J., Seviour, R.J., 2007. Biochemistry and molecular biology of exocellular fungal β-(1,3)- and β-(1,6)-glucanases. FEMS Microbiol. Rev. 31, 168–192. https://doi.org/10.1111/j.1574-6976.2006.00055.x

38. Miller, G.L., 1959. Use of Dinitrosalicylic Acid Reagent for Determination of Reducing Sugar. Anal. Chem. 31, 426–428. https://doi.org/10.1021/ac60147a030

39. Papagianni, M., 2004. Fungal morphology and metabolite production in submerged mycelial processes. Biotechnol. Adv. 22, 189–259. https://doi.org/10.1016/J.BIOTECHADV.2003.09.005

40. Queiroz, P.S., Ruas, F.A.D., Barboza, N.R., De Castro Borges, W., Guerra-Sá, R., 2018. Alterations in the proteomic composition of *Serratia marcescens* in response to manganese (II). BMC Biotechnol. 18, 1–9. https://doi.org/10.1186/s12896-018-0493-3

41. Quing, Q., Wyman, C.E., 2011. Hydrolysis of different chain length xylooligomers by cellulase and hemicellulase, Bioresour. Technol. 102, 1359-1366.

42. Quinlan, R.J., Sweeney, M.D., Lo Leggio, L., Otten, H., Poulsen, J.C., Johansen, K.S., Krogh, K.B., Jørgensen, C.I., Tovborg, M., Anthonsen, A., Tryfona, T., Walter, C.P., Dupree, P., Xu, F., Davies, G.J., Walton, P.H., 2011. Insights into the oxidative degradation of cellulose by a copper metalloenzyme that exploits biomass components. Proc Natl Acad Sci U S A 108. https://doi.org/10.1073/pnas.1105776108

43. Rai, R., Kaur, B., Singh, S., Di Falco, M., Tsang, A., Chadha, B.S., 2016. Evaluation of secretome of highly efficient lignocellulolytic *Penicillium sp*. Dal 5 isolated from

rhizosphere of conifers. Bioresour. Technol. 216, 958–967. https://doi.org/10.1016/j.biortech.2016.06.040

44. Song, H.-T., Gao, Y., Yang, Y.-M., Xiao, W.-J., Liu, S.-H., Xia, W.-C., Liu, Z.-L., Yi, L., Jiang, Z.-B., 2016. Synergistic effect of cellulase and xylanase during hydrolysis of natural lignocellulosic substrates. Bioresour. Technol. 219, 710-715. https://doi.org/10.1016/j.biortech.2016.08.035

45. Talon, M., Robles, M., Garcia-Gomez, J.M., Conesa, A., Nueda, M.J., Nagaraj, S.H., Gotz, S., Terol, J., Dopazo, J., Williams, T.D., 2008. High-throughput functional annotation and data mining with the Blast2GO suite. Nucleic Acids Res. 36, 3420–3435. https://doi.org/10.1093/nar/gkn176

46. Tavares, E.Q.P., De Souza, A.P., Buckeridge, M.S., 2015. How endogenous plant cell-wall degradation mechanisms can help achieve higher efficiency in saccharification of biomass. J. Exp. Bot. 66, 4133–4143. https://doi.org/10.1093/jxb/erv171

47. Thite, V.S., Nerurkar, A.S., 2018. Physicochemical characterization of pectinase activity from *Bacillus spp*. and their accessory role in synergism with crude xylanase and commercial cellulase in enzyme cocktail mediated saccharification of agrowaste biomass. J. Appl. Microbiol. 124, 1147–1163. https://doi.org/10.1111/jam.13718

48. Van Dyk, J.S., Pletschke, B.I., 2012. A review of lignocellulose bioconversion using enzymatic hydrolysis and synergistic cooperation between enzymes-Factors affecting enzymes, conversion and synergy. Biotechnol. Adv. 30, 1458–1480. https://doi.org/10.1016/j.biotechadv.2012.03.002

49. Xiao, C., Anderson, C.T., 2013. Roles of pectin in biomass yield and processing for biofuels. Front. Plant Sci. 4, 1–7. https://doi.org/10.3389/fpls.2013.00067

50. Xiao, Z., Zhang, X., Gregg, D.J., Saddler, J.N., 2004. Effects of Sugar Inhibition on Cellulases and β-Glucosidase During Enzymatic Hydrolysis of Softwood Substrates BT - Proceedings of the Twenty-Fifth Symposium on Biotechnology for Fuels and Chemicals Held May 4–7, 2003, in Breckenridge, CO. Appl. Biochem. Biotechnol. 113–116, 1115–1126.

51. Yohe, T., Xu, Y., Huang, L., Yin, Y., Yang, Z., Wu, P., Entwistle, S., Busk, P.K., Zhang, H., 2018. dbCAN2: a meta server for automated carbohydrate-active enzyme annotation. Nucleic Acids Res. 46, W95–W101. https://doi.org/10.1093/nar/gky418

52. Znameroski, E.A., Coradetti, S.T., Roche, C.M., Tsai, J.C., Iavarone, A.T., Cate, J.H.D., Glass, N.L., 2012. Induction of lignocellulose-degrading enzymes in *Neurospora crassa* by cellodextrins. Proc. Natl. Acad. Sci. 109, 6012 LP-6017. https://doi.org/10.1073/pnas.1118440109

Supplementary material

Secretome diversity and quantitative analysis of phytopathogenic fungus *Chrysoporthe cubensis* LPF-1 in the presence of different carbon sources

Supplementary Figures

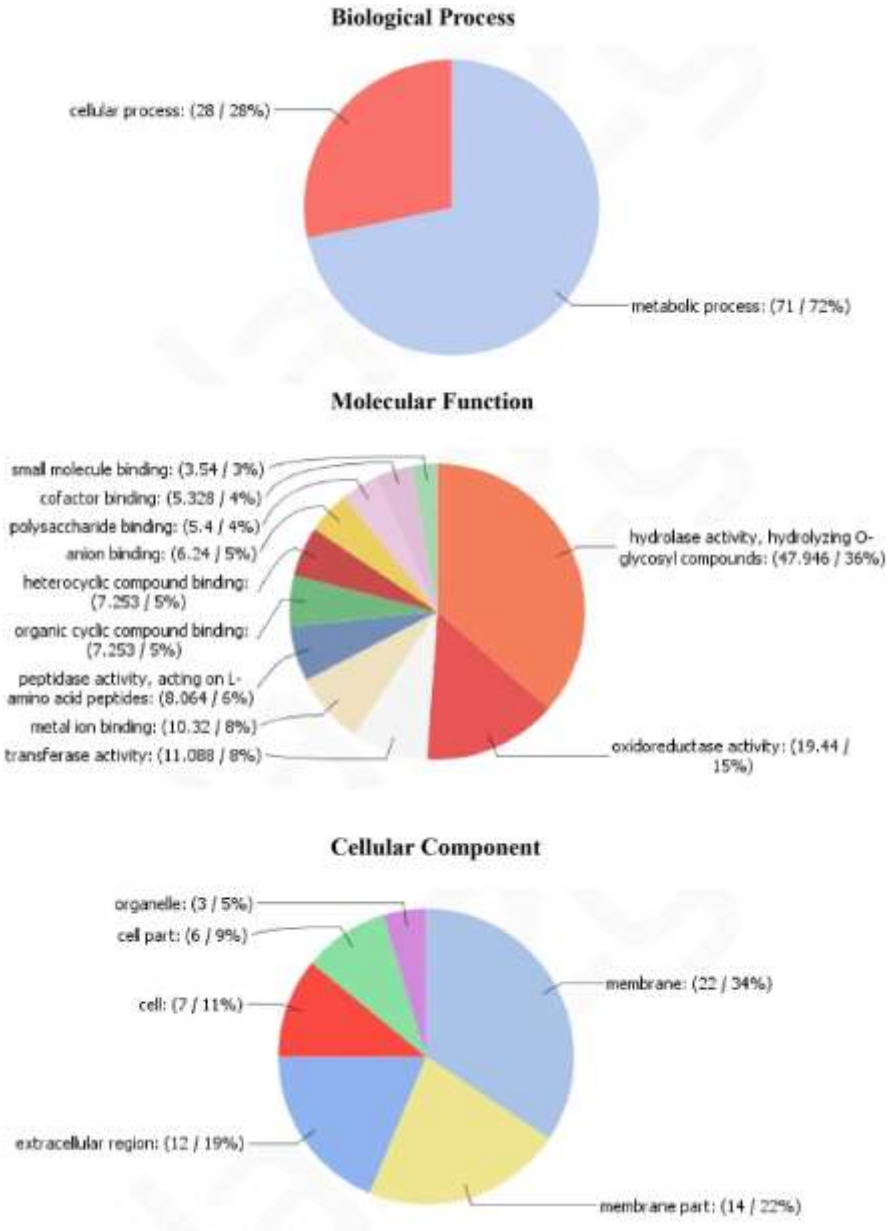

Figure S1 Analysis of GO Term associations of differentially expressed protein represented by pie charts using Blast2go. A) GO classification by Biological process. B) GO classification by Molecular function. C) GO classification by Cellular component.

Supplementary Tables

Table S1: Relative and cumulative abundance of the proteins present in the enzymatic extract of *C. cubensis* grown in wheat bran (WBE).

Protein ID	Description (protein name)	CAZy family	Relative abundance (%)	Cumulative abundance (%)
2236.t1	Cellulose 1,4-beta-cellobiosidase (reducing end)	GH7	12,94	12,94
10380.t1	Putative alpha beta-hydrolase protein	CE10	10,84	23,78
2091.t1	Alpha-L-rhamnosidase	GH78	6,77	30,56
4231.t1	Hypothetical protein VP1G_05121		4,84	35,40
6668.t1	Acid proteinase		3,59	38,99
4632.t1	Glucan 1,4-alpha-glucosidase (Glucoamylase)	GH15/CBM20	3,23	42,21
7214.t1	Non-anchored cell wall protein 1		3,02	45,23
7768.t1	Hypothetical protein BKCO1_4000063		2,44	47,67
830.t1	Mannosyl-oligosaccharide 1,2-alpha-mannosidase	GH47	2,41	50,08
9990.t1	Beta-glucosidase	GH3	2,37	52,45
4958.t1	Endo-1,4-beta-xylanase	GH10/CBM22	2,29	54,73
11038.t1	Alpha-glucuronidase	GH67	2,01	56,74
528.t1	Lipase 2	CE10	1,98	58,72
527.t1	Cellulase (Endo-1,4-beta-D-glucanase)	GH5_5	1,78	60,50
6202.t1	Arabinan endo-1,5-alpha-L-arabinosidase	GH43_30	1,78	62,28
5723.t1	Sulphydryl oxidase		1,71	63,99
11041.t1	Hypothetical protein DCS_04936		1,61	65,60
3928.t1	Late sexual development protein		1,49	67,09
9729.t1	Tripeptidyl-peptidase 1		1,47	68,56
11065.t1	Glucan endo-1,3-alpha-glucosidase	GH71	1,46	70,02
4129.t1	Endo-1,3(4)-beta-glucanase	GH16	1,43	71,45
10989.t1	Glucan endo-1,3-beta-D-glucosidase	GH81	1,26	72,71
10995.t1	Acetylxylan esterase	CE5	1,21	73,92
2605.t1	Beta-glucosidase	GH3	1,04	74,96
g10846.t1	Glycoside hydrolase family 72 protein	GH72	1,01	75,97
g7853.t1	Carboxylesterase, type B	CE10	0,89	76,87
g5687.t1	Beta-glucosidase	GH3	0,79	77,66
g1271.t1	Altered inheritance of mitochondria protein 6		0,78	78,43
g4472.t1	Cerato-platanin		0,77	79,21
g5601.t1	Malate dehydrogenase		0,74	79,95
g7782.t1	Chitinase	GH18	0,68	80,63
g882.t1	Catalase-peroxidase	AA2	0,63	81,26
g10822.t1	Glucan 1,3-beta-glucosidase	GH17	0,59	81,85
g9603.t1	Alpha-glucosidase	GH31	0,58	82,43
g5160.t1	Hypothetical protein DHEL01_04478		0,56	83,00
g5464.t1	Endo-1,4-beta-xylanase	GH11	0,55	83,55
g150.t1	Beta-glucosidase	GH3	0,54	84,08
g6788.t1	4-nitrophenylphosphatase; Acid phosphatase		0,49	84,57
g11408.t1	Alpha-L-arabinofuranosidase	GH54/CBM42	0,48	85,05
g517.t1	Thioredoxin reductase GliT-like		0,46	85,51
g11022.t1	Glucan 1,3-beta-glucosidase	GH17	0,44	85,95
g5798.t1	Hypothetical protein PFICI_14721		0,43	86,38
g2373.t1	Hypothetical protein DHEL01_04478		0,42	86,79
g7647.t1	Neutral ceramidase		0,41	87,21
g4152.t1	α-1,6-mannanase	GH76	0,41	87,61
g5395.t1	Beta-glucosidase	GH1	0,37	87,98
g8936.t1	Putative serine carboxypeptidase s28 protein		0,33	88,32
g294.t1	Subtilisin-like proteinase Spm1		0,29	88,61
g421.t1	Glucose-6-phosphate isomerase		0,28	88,89
g8820.t1	Beta-glucuronidase	GH79	0,27	89,16
g594.t1	Laccase	AA1_3	0,27	89,43
g11254.t1	Endothiapepsin		0,26	89,69
g10919.t1	Carboxy-cis,cis-muconate cyclase		0,25	89,94

Table S2: Relative and cumulative abundance of the proteins present in the enzymatic extract of *C. cubensis* grown in sugarcane bagasse (SBE).

Protein ID	Description (protein name)	CAZy family	Relative abundance (%)	Cumulative abundance (%)
2236.t1	Cellulose 1,4-beta-cellobiosidase (reducing end)	GH7	41,43	41,43
12033.t1	Cellulose 1,4-beta-cellobiosidase (non-reducing end)	GH6	7,02	48,45
6620.t1	Lytic polysaccharide monooxigenase	AA9	4,46	52,90
6668.t1	Acid proteinase		3,15	56,05
3854.t1	Polygalacturonase	GH28	2,78	58,84
2611.t1	Cellulose 1,4-beta-cellobiosidase (reducing end)	GH7/CBM1	2,48	61,31
4241.t1	Endo-1,4-beta-xylanase	GH11	2,46	63,77
2605.t1	Beta-glucosidase	GH3	2,09	65,86
6932.t1	Pectin lyase	PL1_4	1,92	67,79
10994.t1	Endo-1,4-beta-xylanase	GH11	1,80	69,59
992.t1	GDSL-like Lipase/Acylhydrolase	CE12	1,56	71,15
2515.t1	Polygalacturonase	GH28	1,43	72,58
527.t1	Cellulase (Endo-1,4-beta-D-glucanase)	GH5_5	1,13	73,71
5754.t1	Lytic polysaccharide monooxigenase	AA9	0,96	74,68
10995.t1	Acetylxylan esterase	CE5	0,95	75,62
1687.t1	Arabinogalactan endo-beta-1,4-galactanase	GH53	0,85	76,47
11408.t1	Alpha-L-arabinofuranosidase	GH54/CBM42	0,85	77,32
10380.t1	Putative alpha beta-hydrolase protein	CE10	0,75	78,07
10822.t1	Glucan 1,3-beta-glucosidase	GH17	0,67	78,74
4958.t1	Endo-1,4-beta-xylanase	GH10/CBM22	0,57	79,31
3928.t1	Late sexual development protein		0,56	79,87
5160.t1	Hypothetical protein DHEL01_04478		0,49	80,36
5687.t1	Beta-glucosidase	GH3	0,48	80,84
5601.t1	Malate dehydrogenase		0,47	81,32
5464.t1	Endo-1,4-beta-xylanase	GH11	0,45	81,77
115.t1	Acetylxylan esterase	CE1	0,45	82,23
11038.t1	Alpha-glucuronidase	GH67	0,45	82,68
3218.t1	Alpha-galactosidase	GH27/CBM13	0,45	83,12
3950.t1	Cellulose 1,4-beta-cellobiosidase (non-reducing end)	GH6	0,44	83,56
9830.t1	Lytic polysaccharide monooxigenase	AA9	0,43	83,99
10001.t1	Endo-1,4-beta-xylanase	GH10	0,43	84,42
1775.t1	Xyloglucan-specific endo-beta-1,4-glucanase	GH12	0,43	84,84
5395.t1	Beta-glucosidase	GH1	0,40	85,24
9603.t1	Alpha-glucosidase	GH31	0,38	85,63
3275.t1	Aspergillopepsin, putative		0,38	86,00
11065.t1	Glucan endo-1,3-alpha-glucosidase	GH71	0,37	86,37
830.t1	Mannosyl-oligosaccharide 1,2-alpha-mannosidase/Alpha-mannosidase	GH47	0,36	86,73
7197.t1	Glucan endo-1,6-beta-glucosidase	GH30_3	0,35	87,08
9202.t1	Hypothetical protein PFICI_11939		0,35	87,44
3675.t1	Beta-N-acetylhexosaminidase	GH20	0,35	87,79
2091.t1	Alpha-L-rhamnosidase	GH78	0,35	88,13
3039.t1	Acid phosphatase		0,31	88,45
10385.t1	Endo-1,4-beta-xylanase	GH10	0,30	88,74
7214.t1	Non-anchored cell wall protein 1		0,30	89,04
4632.t1	Glucan 1,4-alpha-glucosidase (Glucoamylase)	GH15/CBM20	0,29	89,33
5007.t1	Galactan 1,3-beta-galactosidase	GH43_24/CBM35	0,27	89,61
10846.t1	β-1,3-glucanosyltransglycosylase	GH72	0,27	89,88

Table S3: Proteins detected exclusively in the enzymatic extract of *C. cubensis* grown in sugarcane bagasse (SBE).

Protein ID	Description (protein name)	Predicted CAZy family	Function	Enzyme Code	Signal peptide	Localization
g6312.t1	Laccase	AA1_3	Lignin degrading enzymes	1.10.3.2	N	Cell membrane
g12016.t1	Catalase-peroxidase	AA2	Lignin degrading enzymes	1.11.1.7; 1.11.1.6	N	Mitochondrion
g882.t1	Catalase-peroxidase	AA2	Lignin degrading enzymes	1.11.1.7; 1.11.1.6	Y	Extracellular
g162.t1	Pyranose dehydrogenase (acceptor)	AA3_2	Lignin degrading enzymes	1.1.99.29	N	Peroxisome
g3260.t1	Alcohol oxidase	AA3_3	Lignin degrading enzymes	1.1.3.13	N	Peroxisome
g7858.t1	Choline dehydrogenase	AA3	Lignin degrading enzymes		Y	Extracellular
g4050.t1	Isoamyl alcohol oxidase	AA7	Lignin degrading enzymes		Y	Extracellular
g4203.t1	FAD binding domain-containing protein	AA7	Lignin degrading enzymes		N	Cytoplasm
g1304.t1	Lytic polysaccharide monooxigenase	AA9	Cellulose degrading enzymes		Y	Extracellular
g1799.t1	Lytic polysaccharide monooxigenase	AA9	Cellulose degrading enzymes		N	Extracellular
g8335.t1	Lytic polysaccharide monooxigenase	AA11	Chitin degradation		Y	Extracellular
g6530.t1	Putative chitin- domain 3 protein	AA11	Chitin degradation		Y	Extracellular
g6205.t1	Carbohydrate esterase family 9 protein	CE9	Esterases		N	Lysosome/Vacuole
g10548.t1	Beta-glucosidase	GH3	Cellulose degrading enzymes	3.2.1.21	N	Peroxisome
g2802.t1	Beta-glucosidase	GH3	Cellulose degrading enzymes	3.2.1.21	N	Cell membrane
g7095.t1	Glycoside hydrolase family 5 protein	GH5_11	Cellulose degrading enzymes	3.2.1.x	Y	Extracellular
g5842.t1	lulose 1,4-beta-cellobiosidase (reducing end) (Cellulase	GH7	Cellulose degrading enzymes	3.2.1.176	Y	Extracellular
g8859.t1	1,4-alpha-glucan branching enzyme	GH13_8/CBM48	Starch degrading enzymes	2.4.1.18	N	Cytoplasm
g7099.t1	Glycoside hydrolase family 16 protein	GH16	Others	3.2.1.x	Y	Cell membrane
g2058.t1	Endo-1,3(4)-beta-glucanase	GH16	Hemicellulose degrading enzymes	3.2.1.6	N	Cell membrane
g721.t1	Endo-1,3(4)-beta-glucanase	GH17	Hemicellulose degrading enzymes	3.2.1.x	N	Cell membrane
g4857.t1	Chitinase	GH18	Chitin degradation	3.2.1.14	Y	Endoplasmic reticulum
g4428.t1	Polygalacturonase	GH28	Pectin degrading enzymes	3.2.1.15	Y	Extracellular
g817.t1	Glycoside hydrolase family 43 protein	GH43	Others		Y	Extracellular
g235.t1	Glucan endo-1,3-beta-D-glucosidase	GH64	(β-1,3-glucan) degrading enzymes	3.2.1.39	N	Cell membrane
g10989.t1	Glucan endo-1,3-beta-D-glucosidase	GH81	(β-1,3-glucan) degrading enzymes	3.2.1.39	Y	Extracellular
g5052.t1	Glycoside hydrolase family 106 protein	GH106	Pectin degrading enzymes		N	Cytoplasm
g2332.t1	Glycoside hydrolase family 106 protein	GH106	Pectin degrading enzymes		Y	Extracellular
g5303.t1	Glucan endo-1,3-beta-D-glucosidase	GH128	(β-1,3-glucan) degrading enzymes	3.2.1.39	Y	Extracellular
g137.t1	Glycoside hydrolase family 131 protein	GH131	Others	3.2.1.x	Y	Extracellular
g11331.t1	Beta-glucosidase	GH132	Cellulose degrading enzymes	3.2.1.x	Y	Extracellular
g716.t1	Rhamnogalacturonate lyase	PL4_5	Pectin degrading enzymes		Y	Extracellular

Table S4: Proteins detected exclusively in the enzymatic extract of *C. cubensis* grown in wheat bran (WBE).

Protein ID	Description (protein name)	Predicted CAZy family	Function	Enzyme Code	Signal peptide	Localization
g5169.t1	GMC oxidoreductase	AA3_2	Lignin degrading enzymes		Y	Extracellular
g9189.t1	GMC oxidoreductase	AA3_2	Lignin degrading enzymes		N	Lysosome/Vacuole
g8036.t1	Cellobiose dehydrogenase (acceptor)	AA3	Lignin degrading enzymes	1.1.99.18	Y	Extracellular
g2380.t1	Lipase, GDSL-like protein/acetylxylan es	CE0	Hemicellulose degrading enzimes		Y	Lysosome/Vacuole
g115.t1	Acetylxylan esterase	CE1	Hemicellulose degrading enzimes	3.1.1.72	N	Extracellular
g11871.t1	Tannase/ Feruloyl esterase	CE1	Hemicellulose degrading enzimes	3.1.1.20/3.1.1.73	N	Cytoplasm
g5526.t1	Acetylxylan esterase	CE5	Hemicellulose degrading enzimes	3.1.1.72	N	Extracellular
g6702.t1	Pectinesterase	CE8	Pectin degrading enzymes	3.1.1.11	Y	Extracellular
g3615.t1	Carboxylesterase	CE15	Esterases	3.1.1.1	N	Cytoplasm
g4819.t1	Beta-glucosidase	GH3	Cellulose degrading enzymes	3.2.1.21	Y	Extracellular
g4695.t1	Cellulase (Endo-1,4-beta-D-glucanase)	GH5_5	Cellulose degrading enzymes	3.2.1.4	Y	Extracellular
g8035.t1	Cellulase (Endo-1,4-beta-D-glucanase)	GH5_5	Cellulose degrading enzymes	3.2.1.4	Y	Extracellular
g1534.t1	Cellulase (Endo-1,4-beta-D-glucanase)	GH7	Cellulose degrading enzymes	3.2.1.4	Y	Extracellular
g7507.t1	Endo-1,3(4)-beta-glucanase	GH16	Hemicellulose degrading enzimes	3.2.1.6	Y	Extracellular
g2457.t1	Chitinase/Amino acid permease	GH18	Chitin degradation	3.2.1.14	Y	Cell membrane
g10170.t1	Galacturan 1,4-alpha-galacturonidase	GH28	Pectin degrading enzymes	3.2.1.67	Y	Extracellular
g1093.t1	Rhamnogalacturonan hydrolase	GH28	Pectin degrading enzymes	3.2.1.171	Y	Extracellular
g1361.t1	Polygalacturonase	GH28	Pectin degrading enzymes	3.2.1.15	Y	Extracellular
g3293.t1	Polygalacturonase	GH28	Pectin degrading enzymes	3.2.1.15	N	Extracellular
g3854.t1	Polygalacturonase	GH28	Pectin degrading enzymes	3.2.1.15	Y	Extracellular
g6996.t1	Rhamnogalacturonan hydrolase	GH28	Pectin degrading enzymes	3.2.1.171	Y	Extracellular
g11051.t1	Fructan beta-fructosidase	GH32	Others	3.2.1.80	Y	Extracellular
g11808.t1	Beta-galactosidase	GH35	Hemicellulose degrading enzimes	3.2.1.23	Y	Extracellular
g2988.t1	Beta-galactosidase	GH35	Hemicellulose degrading enzimes	3.2.1.23	Y	Extracellular
g1687.t1	Arabinogalactan endo-beta-1,4-galactar	GH53	Pectin degrading enzymes	3.2.1.89	Y	Extracellular
g2956.t1	Glucan 1,3-beta-glucosidase	GH55	(β-1,3-glucan) degrading enzymes	3.2.1.58	Y	Extracellular
g4559.t1	Glycoside hydrolase family 92 protein	GH92	Others		Y	Extracellular
g8005.t1	Exo-α-1,6-mannosidase	GH125	Others	3.2.1.x	N	Mitochondrion

Table S5: Proteins differentially expressed in the secretome of *C. cubensis* grown in wheat bran. Proteins represented in the heat map (Fig. 4).

Protein ID	Description (protein name)	Predicted CAZy family	
g4129.t1	Endo-1,3(4)-beta-glucanase	GH16	Cellulose degrading enzymes
g7763.t1	D-arabinono-1,4-lactone oxidase		
g5502.t1	High-affinity glucose transporter		
g11295.t1	Leucine rich repeat domain containing protein		
g7214.t1	Non-anchored cell wall protein 1		
g7647.t1	Neutral ceramidase		
g9437.t1	Aspartate aminotransferase		
g6671.t1	Peptidase family M3		
g10876.t1	Cullin-associated NEDD8-dissociated protein 1		
g2066.t1	ML domain-containing protein		
g7815.t1	Checkpoint serine/threonine-protein kinase bub1		
g6049.t1	Ser/Thr protein phosphatase family		
g1372.t1	Membrane dipeptidase		
g3996.t1	Peptidase family M28		
g6580.t1	Gamma interferon inducible lysosomal thiol reductase		
g8956.t1	Dipeptidyl-peptidase 3		
g294.t1	Subtilisin-like proteinase Spm1		
g7817.t1	Aminopeptidase 2		
g9354.t1	Adenosylhomocysteinase		
g2789.t1	Triosephosphate isomerase		
g10548.t1	Beta-glucosidase	GH3	Cellulose degrading enzymes
g10576.t1	Ketol-acid reductoisomerase		
g6872.t1	Peptidase family M1		
g1768.t1	3-phytase A		
g11327.t1	Transaldolase		
g10763.t1	Triose-phosphate isomerase; Ribose-5-phosphate isomerase		
g9724.t1	Arylsulfatase		
g2029.t1	Ubiquitin-activating enzyme E1 1		
g882.t1	Catalase-peroxidase	AA2	Lignin degrading enzymes
g4203.t1	FAD binding domain-containing protein	AA7	Lignin degrading enzymes
g10989.t1	Glucan endo-1,3-beta-D-glucosidase	GH81	(β-1,3-glucan) degrading enzymes
g1284.t1	Oxalate decarboxylase OxdC		
g517.t1	Thioredoxin reductase GliT-like		
g8811.t1	Aspartate aminotransferase		
g11697.t1	Nuclease S1		
g421.t1	Glucose-6-phosphate isomerase		
g7095.t1	Glycoside hydrolase family 5 protein	GH5_11	Cellulose degrading enzymes
g7858.t1	Choline dehydrogenase	AA3	Lignin degrading enzymes
g12118.t1	prolyl oligopeptidase	CE10	Esterase
g7768.t1	Hypothetical protein BKCO1_4000063		
g9535.t1	Alanine-glyoxylate aminotransferase		
g3499.t1	Related to tripeptidyl-peptidase I		
g263.t1	Hypothetical protein VM1G_09294		
g10380.t1	Putative alpha beta-hydrolase protein	CE10	Esterase
g3266.t1	N-acetylglucosamine-6-sulfatase		
g11041.t1	Hypothetical protein DCS_04936		
g8936.t1	Putative serine carboxypeptidase s28 protein		
g7688.t1	Feruloyl esterase	CE1	Hemicellulose degrading enzimes
g5802.t1	Hypothetical protein VM1G_07293		
g6533.t1	Putative carboxylesterase protein	CE10	Esterase
g5723.t1	Sulphydryl oxidase		
g5798.t1	Hypothetical protein PFICI_14721		
g528.t1	Lipase 2	CE10	Esterase
g493.t1	Alpha-L-rhamnosidase	GH78	Pectin degrading enzymes
g9729.t1	Tripeptidyl-peptidase 1		
g6491.t1	Bile acid 7-alpha		
g817.t1	Glycoside hydrolase family 43 protein	GH43	Others
g9922.t1	Feruloyl esterase	CE1	Hemicellulose degrading enzimes
g5052.t1	Glycoside hydrolase family 106 protein	GH106	Pectin degrading enzymes
g4231.t1	Hypothetical protein VP1G_05121		
g12016.t1	Catalase-peroxidase	AA2	Lignin degrading enzymes
g3260.t1	Alcohol oxidase	AA3_3	Lignin degrading enzymes
g2091.t1	Alpha-L-rhamnosidase	GH78	Pectin degrading enzymes
g10254.t1	GDSL-like Lipase/Acylhydrolase	CE16	Esterase
g415.t1	Beta-mannosidase (Mannanase)	GH2	Hemicellulose degrading enzimes
g9990.t1	Beta-glucosidase	GH3	Cellulose degrading enzymes
g7782.t1	Chitinase	GH18	Chitin degradation
g414.t1	Gamma-glutamyltranspeptidase		
g1304.t1	Lytic polysaccharide monooxigenase	AA9/CBM2	Cellulose degrading enzymes
g6202.t1	Arabinan endo-1,5-alpha-L-arabinosidase	GH43_30	Pectin degrading enzymes
g1271.t1	Altered inheritance of mitochondria protein 6		
g4632.t1	Glucan 1,4-alpha-glucosidase (Glucoamylase)	GH15/CBM20	Starch degrading enzymes
g7844.t1	Acetylcholinesterase	CE10	Esterase
g830.t1	hosyl-oligosaccharide 1,2-alpha-mannosidase/Alpha-mannosi	GH47	Hemicellulose degrading enzimes
g581.t1	Acetyl esterase	CE16	Esterase
g11038.t1	Alpha-glucuronidase	GH67	Hemicellulose degrading enzimes
g11065.t1	Glucan endo-1,3-alpha-glucosidase	GH71	(β-1,3-glucan) degrading enzymes
g4958.t1	Endo-1,4-beta-xylanase	GH10/CBM22	Hemicellulose degrading enzimes
g11753.t1	β-L-arabinofuranosidase	GH127	Hemicellulose degrading enzimes
g3242.t1	Rhamnogalacturonan endolyase	PL4_3	Pectin degrading enzymes
g11254.t1	Endothiapepsin		
g4648.t1	5'/3'-nucleotidase SurE family protein		
g10149.t1	Endo-apiosidase	GH140	Pectin degrading enzymes
g1186.t1	Beta-galactosidase	GH35	Hemicellulose degrading enzimes
g2414.t1	Phosphoglycerate mutase-like protein		
g9844.t1	FAD binding domain-containing protein	AA7	Lignin degrading enzymes
g8820.t1	Beta-glucuronidase	GH79	Hemicellulose degrading enzimes
g10846.t1	β-1,3-glucanosyltransglycosylase	GH72	(β-1,3-glucan) degrading enzymes
g5677.t1	Beta-glucosidase	GH3	Cellulose degrading enzymes
g3928.t1	Late sexual development protein		

Table S6: Proteins differentially expressed in the secretome of *C. cubensis* grown in sugarcane bagasse. Proteins represented in the heat map (Fig. 4).

g11060.t1	Mannan endo-1,4-beta-mannosidase (Beta-mannanase)	GH5_7/CBM1	Hemicellulose degrading enzimes
g3675.t1	Beta-N-acetylhexosaminidase	GH20	Chitin degradation
g1775.t1	Xyloglucan-specific endo-beta-1,4-glucanase	GH12	Hemicellulose degrading enzimes
g1812.t1	do-1,4-beta-D-glucanase)/Xyloglucan-specific endo-beta-1	GH45/GH74/CBM1	Cellulose degrading enzymes
g2236.t1	llulose 1,4-beta-cellobiosidase (reducing end) (Cellulase 9	GH7	Cellulose degrading enzymes
g3275.t1	Aspergillopepsin, putative		
g4241.t1	Endo-1,4-beta-xylanase	GH11	Hemicellulose degrading enzimes
g4066.t1	Pectate lyase/Peptidase	PL1_9	Pectin degrading enzymes
g10385.t1	Endo-1,4-beta-xylanase	GH10	Hemicellulose degrading enzimes
g9202.t1	Hypothetical protein PFICI_11939		
g64.t1	Glucosylceramidase	GH30/CBM1	Others
g2457.t1	Chitinase/Amino acid permease	GH18	Chitin degradation
g115.t1	Acetylxylan esterase	CE1	Hemicellulose degrading enzimes
g6932.t1	Pectin lyase	PL1_4	Pectin degrading enzymes
g7211.t1	Acid proteinase		
g6620.t1	Lytic polysaccharide monooxigenase	AA9	Cellulose degrading enzymes
g10994.t1	Endo-1,4-beta-xylanase	GH11	Hemicellulose degrading enzimes
g2611.t1	llulose 1,4-beta-cellobiosidase (reducing end) (Cellulase 9	GH7/CBM1	Cellulose degrading enzymes
g630.t1			
g4331.t1	Unnamed protein product (integral membrane protein)		
g3854.t1	Polygalacturonase	GH28	Pectin degrading enzymes
g8036.t1	Cellobiose dehydrogenase (acceptor)	AA3	Lignin degrading enzymes
g2605.t1	Beta-glucosidase	GH3	Cellulose degrading enzymes
g3218.t1	Alpha-galactosidase	GH27/CBM13	Hemicellulose degrading enzimes
g10352.t1	Exo-α-L-1,5-arabinanase	GH93	Hemicellulose degrading enzimes
g9830.t1	Lytic polysaccharide monooxigenase	AA9	Cellulose degrading enzymes
g9161.t1	Alpha-L-fucosidase	GH29	Hemicellulose degrading enzimes
g7197.t1	Glucan endo-1,6-beta-glucosidase	GH30_3	Others
g9734.t1	Xyloglucan-specific endo-beta-1,4-glucanase	GH74	Hemicellulose degrading enzimes
g10001.t1	Endo-1,4-beta-xylanase	GH10/CBM22	Hemicellulose degrading enzimes
g2515.t1	Polygalacturonase	GH28	Pectin degrading enzymes
g12033.t1	Cellulose 1,4-beta-cellobiosidase (non-reducing end)	GH6	Cellulose degrading enzymes
g6781.t1	Lysophospholipase		
g1687.t1	Arabinogalactan endo-beta-1,4-galactanase	GH53	Pectin degrading enzymes
g3950.t1	Cellulose 1,4-beta-cellobiosidase (non-reducing end)	GH6	Cellulose degrading enzymes
g11035.t1	Hypothetical protein VP1G_08433		
g9537.t1	Galactan endo-1,6-beta-galactosidase	GH5_16	Pectin degrading enzymes
g992.t1	GDSL-like Lipase/Acylhydrolase	CE12	Esterase
g8035.t1	Cellulase (Endo-1,4-beta-D-glucanase)	GH5_5	Cellulose degrading enzymes
g11387.t1	Glutaminase A		
g2817.t1	Eukaryotic aspartyl protease		
g11808.t1	Beta-galactosidase	GH35	Hemicellulose degrading enzimes
g8142.t1	Carboxypeptidase cpdS		
g4819.t1	Beta-glucosidase	GH3	Cellulose degrading enzymes
g4695.t1	Cellulase (Endo-1,4-beta-D-glucanase)	GH5_5	Cellulose degrading enzymes

Table S7: Comparative analysis of lignocellulolytic activities of crude extracts from *C. cubensis* cultivated in wheat bran (WBE) and in natura sugarcane bagasse (SBE), and commercial cocktail Multifect® CL and Celluclast® 1.5L. The enzymatic ativities were expressed in U/mL.

Units of enzymatic activity/mg of protein				
Enzyme	*C. cubensis* extract (bagasse)	*C. cubensis* extract (wheat bran)	Multifect® CL	Celluclast® 1.5L
FPAse	0.79 ± 0,02	0.37 ± 0.02	2.56 ± 0,04	1.29 ± 0.02
Endoglucanase	15.47 ± 0.29	13.56 ± 0.56	91.25 ± 0,30	49.93 ± 1.21
β-Glucosidase	5.21 ± 0.02	4.91 ± 0.19	4.19 ± 0.02	0.68 ± 0.01
β-cellobiohydrolase	1.37 ± 0.02	3.17 ± 0.17	2.74 ± 0,08	0.20 ± 0.003
Mannosidase	n.d.	0.05 ± 0.001	n.d.	n.d.
Xylanase	288.06 ± 1.27	120.14 ± 12.97	68.21 ± 1,29	22.62 ± 0.93
β-Xylosidase	0.47 ± 0.012	0.34 ± 0.01	0.02 ± 0,0004	0.57 ± 0.03
β-mannosidase	0.03 ± 0.0001	0.40 ± 0.02	n.d.	n.d.
Mannanase	2.01 ± 0.071	13.32 ± 0.53	2.94 ± 0,05	1.33 ± 0.08
Polygalacturonase	16.98 ± 0.55	6.27 ± 0.50	1.15 ± 0,01	0.51 ± 0.02
Pectin lyase	134.83 ± 11.187	57.37 ± 2.61	n.d.	0.46 ± 0.07
α-Galactosidase	0.40 ± 0.006	0.04 ± 0.002	0.001 ± 0,00001	0.004 ± 0.0001
β-Galactosidase	0.03 ± 0.0001	0.01 ± 0.001	0.001 ± 0,00017	0.01 ± 0.00003
α-Arabinofuranosidase	1.44 ± 0.087	0.60 ± 0.04	0.03 ± 0.0004	0.11 ± 0.01
α-Glucosidase	0.03 ± 0,001	0.03 ± 0.001	n.d.	n.d.
Laccase	0.06 ± 0.001	0.09 ± 0.004	n.d.	n.d.

Table S8: Comparative analysis of lignocellulolytic enzimatic activities of crude extracts from *C. cubensis* cultivated in wheat bran (WBE) and in natura sugarcane bagasse (SBE), and commercial cocktail Multifect® CL and Celluclast® 1.5L. The specific ativities were expressed in U/mg.

Units of enzymatic activity/mL				
Enzyme	*C. cubensis* extract (bagasse)	*C. cubensis* extract (wheat bran)	Multifect® CL	Celluclast® 1.5L
FPAse	0.08 ± 0.001	0.13 ± 0.007	165.0 ± 3.00	77.0 ± 1.40
Endoglucanase	1.49 ± 0.028	4.75 ± 0.34	5876.35 ± 10.96	3000.30 ± 97.19
α-Glucosidase	0.003 ± 0.00002	0.01 ± 0.00005	n.d.	n.d.
β-Glucosidase	0.50 ± 0.001	1.71 ± 0.02	279.17 ± 16.33	40.81 ± 0.60
β-Cellobiohydrolase	0.13 ± 0.001	1.11 ± 0.03	172.68 ± 7.92	11.83 ± 0.28
Mannosidase	n.d.	0.02 ± 0.001	0.003 ± 0.0001	n.d.
Xylanase	27.69 ± 0.12	42.61 ± 6.58	4393.05 ± 105.98	1359.69 ± 67.45
β-Xylosidase	0.046 ± 0.001	0.12 ± 0.001	1.32 ± 0.03	34.13 ± 2.01
β-Mannosidase	0.003 ± 0.00002	0.14 ± 0,004	n.d.	n.d.
Mannanase	0.23 ± 0.06	4.66 ± 0.02	189.25 ± 4.38	77.31 ± 3.41
Polygalacturonase	1.63 ± 0.05	2.19 ± 0.14	71.48 ± 4.65	30.78 ± 1.65
Pectin lyase	12.96 ± 0.88	20.05 ± 0.31	n.d.	27.87 ± 3.05
α-Galactosidase	0.04 ± 0.001	0.02 ± 0.0001	0.08 ± 0.0001	0.22 ± 0.009
β-Galactosidase	0.003 ± 0.0001	0.01 ± 0.0002	0.078 ± 0.012	0.38 ± 0.005
α-Arabinofuranosidase	0.14 ± 0.008	0.21 ± 0.01	1.87 ± 0.03	6.58 ± 0.42
α-Amylase	0.13 ± 0.01	0.95 ± 0.02	5.58 ± 0.06	3.49 ± 0.15
Laccase	0.006 ± 0.00005	0.03 ± 0.0002	n.d.	n.d.

CAPÍTULO 4

The first characterization of the *Chrysoporthe cubensis* multicopper oxidase enzymes: production and application in the oxidation of phenolic compounds formed during pretreatment of sugarcane bagasse

The first characterization of the *Chrysoporthe cubensis* multicopper oxidase enzymes: production and application in the oxidation of phenolic compounds formed during pretreatment of sugarcane bagasse

Murillo Peterlini Tavares[1], Thiago Rodrigues Dutra[1], Ednilson Mascarenhas Varela[1], Túlio Morgan[1], Tiago Antônio de Oliveira Mendes[1], Sebastião Tavares de Rezende[1], Valéria Monteze Guimarães[1],*

[1]Department of Biochemistry and Molecular Biology, Universidade Federal de Viçosa, Av. PH Rolfs, s/n, 36570-900, Viçosa, MG, Brazil.

*** Corresponding Author**

Email: vmonteze@ufv.br

Telephone: (+55 31) 3612 2462

Abstract

Phytopathogenic fungal genomes contain complex groups of multicopper oxidase (MCO) coding genes that make them a good source for new laccases with potential biotechnological interest. Bioinformatics analysis of the *Chrysoporthe cubensis* genome revealed the presence of 13 MCO proteins belonging to different subfamilies based on their sequence similarities and signatures and classified in fungal ferroxidases; ascomycete laccases; laccases/ferroxidases; fungal pigments MCOs and ascorbate oxidases. Laccases catalyze the oxidation of a wide range of molecules, including phenolic compounds, by the removal of electrons and the concomitant reduction of molecular oxygen to water. *C. cubensis* LPF-1 produces more efficient enzymatic extracts for saccharification of sugarcane bagasse than commercial preparations. The activity of *C. cubensis* laccase, absent in commercial preparations, is a differential of the extracts produced by this fungus. The production of laccases was higher (4.88 U g^{-1}) with the mixture of wheat bran and orange peel in the proportion of three parts to one, respectively, allowing purification and identification of the laccases. Two MCOs of *C. cubensis*, 53.4 and 74.4 kDa, respectively, were identified by mass spectrometry using MALDI-TOF/TOF. The mixture of *C. cubensis* MCOs (mco2 and mco5) decreased by 91% the phenolic compounds produced by the alkaline pretreatment of sugarcane bagasse, which resulted in improved saccharification yields of this pretreated material, proving to be enzymes promising for applications in biomass hydrolysis.

Keywords

Multicopper oxidases, laccases, *Chrysoporthe cubensis*, phenolic compounds, sugarcane bagasse.

1. Introduction

The enzymes of the Auxiliary Activity family 1 (AA1) are multicopper oxidases (MCOs) that use diphenols and aromatic compounds as electron donors to reduce molecular oxygen to water (Levasseur et al., 2013). Multicopper oxidases (MCOs) form a multifaceted group of enzymes that is widely distributed in nature, including laccases and laccase-like multicopper oxidases (EC 1.10.3.2), ascorbate oxidases (EC 1.10.3.3), bilirubin oxidases (EC 1.3.3.5), ferroxidases and ceruloplasmin (EC 1.16.3.1), pigment oxidases and enzymes with dual laccase/ferroxidase activity (Hoegger et al., 2006; Tamayo Ramos et al., 2011).

Many fungi have more than one MCO gene (Cázares-García et al., 2013; Hoegger et al., 2006) and the expression pattern of the multi-gene group has been explored in plant pathogenic fungi (Feng et al., 2015). Despite their structural similarity, MCOs are diverse in substrate specificity and physiological functions, presenting an important role in pigment formation, lignin degradation, dissimilatory nitrite reduction, xenobiotic compound degradation and virulence in fungi (Kaur et al., 2019).

Laccases are the largest subgroup within the MCOs, having broader substrate specificities and, therefore mainly, used for biotechnological purposes (Viswanath et al., 2014). These enzymes catalyze the oxidation of a wide range of substances, including aromatic compounds, diphenolic compounds, polyphenols, diamines, substituted phenols and aromatic amines by the removal of electrons and the concomitant reduction of molecular oxygen to water (Giardina et al., 2010; Yan et al., 2014). The ability to catalyze oxidation reactions of phenolic compounds producing only water as a byproduct has increased the interest of industries for their use as a green catalyst, and its importance reflects on the wide spectrum of applications. They are commonly employed for bioremediation, degradation of dyes in the textile industry, synthetic chemistry including polymer fabrication, development of biosensors, delignification of sugarcane bagasse for the production of bioethanol and pulp in the paper industry (Madhavi and Lele, 2009; Viswanath et al., 2014).

The production of active laccases has been reported in many ascomycetes, such as *Melanocarpopus albomyces*, *Cerrena unicolor*, *Trichoderma reese*i and *Xylaria polymorpha*, but so far few studies have completely characterized the MCOs in fungi of this phylum those produced by basidiomycete fungi (Baldrian, 2006; Wang et al., 2017). Therefore, it is difficult to have a real overview of the biotechnological potential of ascomycetes genomes as a source of new MCOs (Tamayo Ramos et al., 2011).

Nevertheless, further research effort is needed to assign biological functions to the multiplicity of laccase-type MCOs of a fungal species, to select new targets that present biotechnological characteristics of interest.

The phytopathogenic fungus *Chrysoporthe cubensis* is able to produce more efficient enzymatic extracts for saccharification of sugarcane bagasse than commercial preparations (Dutra et al., 2017; Falkoski et al., 2013; Maitan-Alfenas et al., 2015). The enzymatic extracts produced by this fungus showed laccase activity, which was a differential concerning commercial cocktails (Maitan-Alfenas et al., 2015).

The hydrolysis efficiency of pretreated sugarcane bagasse by the cellulolytic blend of *C. cubensis* and *Penicillium pinophilum* extracts containing laccase was continuously improved with increasing lignin concentrations throughout the process, contrary to expectations, when recycling of enzymes was applied (Visser et al., 2015). The presence of laccase activity from *C. cubensis* extract was described as a determinant factor for the efficiency of this blend in a reaction medium with high concentrations of phenolic compounds associated with the lignin particles capable of adsorbing proteins and deactivating cellulases (Visser et al., 2015). Laccases applied in pretreatments of lignocellulosic materials have generated controversial results, time improving the enzymatic saccharification by the reduction of lignin and phenolics, time worsening, generating oxidation products more inhibitors than the non-oxidized ones, and/or increasing the degree of lignin polymerization (Giacobbe et al., 2018; Oliva-Taravilla et al., 2016).

The aim of this work was to identify the laccase-type MCOs of *C. cubensis* by combing the use of genomic and proteomic tools and to produce, to purify and to characterize the MCOs secreted by *C. cubensis*, as well as to evaluate the effects of these enzymes on the oxidation of phenolic compounds produced in the alkaline pretreatment of sugarcane bagasse.

2. Materials and methods

2.1. Prediction of multicopper oxidases proteins and *in silico* analysis variability

Protein sequences from eukaryotic organisms belonging to the AA1 family of Auxiliary Activities enzymes (AAs) deposited in the Carbohydrate-Active Enzyme Database (CAZy) were recovered and aligned (tblastn) with the non-annotated genome (LJCY01) from *Chrysoporthe cubensis*, selecting only those regions aligned with more than 70% coverage and 40% identity. The resulting 13 gene coordinates were submitted

to manual curation to eliminate possible redundancies and then directed to the *ab initio* gene prediction step using the AUGUSTUS program (Stanke and Morgenstern, 2005), which was previously trained with the *Neurospora crassa* genome.

The 13 members of AA1 family from *C. cubensis* were selected for comparative sequence variability studies and compared to the AA1 family enzymes of 69 fungi with different lifestyles. To compare the similarity between the sequences, pairwise alignments were performed using the MUSCLE (http://www.ebi.ac.uk/Tools/msa/muscle/) (Edgar, 2004), and constructed a distance matrix using the KIMURA method for amino acids. To visualize the clustering of enzymes by sequence similarity, a multidimensional scaling plot (MDS) was used. The clusters in the MDS chart were defined using the K-means algorithm. The number of clusters was validated using the Elbow method and biological interpretation of possible clusters. The 4 sequence signatures of the MCOs (L1, L2, L3, L4) were observed using the program Clustal Omega (http://www.ebi.ac.uk/Tools/msa/clustalo/) and the Color Align Conservation program for analysis of waste conservation in multiple alignments (http://www.bioinformatics.org/sms2/color_align_cons.html).

2.2. Physicochemical characterization and prediction of secondary structures of the enzymes of the *C. cubensis* MCOs

The physicochemical parameters were computed with the aid of the Expasy ProtParam bioinformatics tool (http://web.expasy.org/protparam/) (Wilkins et al., 2005). Prediction of the secondary elements was performed using the SOPMA program (https://npsa-prabi.ibcp.fr/cgi-bin/npsa_automat.pl?page=/NPSA/npsa_sopma.html) (Combet et al., 2000). The characteristic domains of multi-copper oxidases were defined for the 13 predicted enzymes using the Simple Modular Architectures (SMART) search tool (http://smart.embl-heidelberg.de/).

2.3. Molecular modeling and energy minimization of target MCOs

The predicted sequences for the MCOs were subjected to molecular homology modeling using Phyre2 (http://www.sbg.bio.ic.ac.uk/phyre2/html/page.cgi?id=index) (Kelly et al., 2015), selecting the intensive mode of analysis. Three-dimensional representation of the predicted enzymes of the targets MCOs was obtained with the PyMOL molecule visualization system (DeLano, 2002).

The three-dimensional models were overlaid with the crystallographic structure

of the *Melanocarpus albomyces* laccases (PDB code: 2Q9O), which contain the 4 bound Cu^{2+} ions. Based on the results of overlapping structures, the missing ions in the models were added in the coordinate files for each model. Then, an additional stage of refinement of the three-dimensional models was performed using the YASARA energy minimization server (http://www.yasara.org/minimizationserver.htm) (Krieger et al., 2009). The homology predicted models were validated to assess the stereochemical quality, using a set of software such as RAMPAGE (http://mordred.bioc.cam.ac.uk/~rapper/rampage.php), the PROCHECK, Verify3D, and ERRAT (https://services.mbi.ucla.edu/SAVES/), and ProSA-web (https://prosa.services.came.sbg.ac.at/prosa.php). Calculated Atlas of Surface Topography of CASTp proteins (http://sts.bioe.uic.edu/castp/) (Dundas et al., 2006) was used to identified the pockets accessible to the substrate and the active centers of each three-dimensional model.

2.4. Molecular docking of *C. cubensis* MCOs

The refined and validated 3D modeled selected proteins were used for further protein docking studies. In the molecular docking step, binding structures were obtained from PubChem (https://pubchem.ncbi.nlm.nih.gov/no) in the PDBQT format. Molecular docking analysis used the AutoDock Vina module, available in PyRx Version 0.8 software (http://pyrx.sourceforge.net/). The receptor molecules were the three-dimensional models of the *C. cubensis* MCOs obtained after the energy minimization step. Later we have prepared the AutoDock Vina configuration files for all the protein modeled structures and ligands, the above-prepared files were used for performing the protein docking analysis.

The dimensions of the docking grid were defined for each receptor, accommodating the cavity near T1 (defined by the CASTp program) in the center of the grid. We have performed blind docking with all the synthetic substrate ligand models with the exhaustiveness set to 8. The best-fit ligand conformations were selected based on their best energy score and with the proximity to the mononuclear center of copper. We have used Edu PyMOL for visualizing the interactions of the ligand and modeled protein structure and for developing the respective docked images.

2.5. Production of MCOs by *C. cubensis*

2.5.1. Preparation of the inoculum for semi-solid state fermentation (SSF)

The inoculum was prepared by growing the fungus under submerged fermentation in a 250 mL Erlenmeyer flask containing 100 mL of medium with the following composition, in g L^{-1}: glucose, 10.0; NH_4NO_3, 1.0; KH_2PO_4, 1.0; MgSO4, 0.5 and yeast extract, 2.0. The medium was inoculated with 1 mL of a spore suspension (2.2 x 10^6 spores mL^{-1}) and placed on an orbital shaker for five days at 180 rpm and 28 °C. The culture obtained was used to inoculate the semi-solid culture medium.

2.5.2. Production of *C. cubensis* MCOs by semi-solid state fermentation

C. cubensis was grown under SSF using sugarcane bagasse, locust bean gum, orange peel, and pure wheat bran combined with orange peel in different proportions (1:1, 3:1, 9:1), and wheat bran combined with passion fruit peel in the ratio of one to one as the main carbon sources. This fungus was grown in 125 mL Erlenmeyer flasks containing 5g (dry weight) of the substrate moistened with culture medium with the following composition, in g L^{-1}: NH_4NO_3, 1.0; KH_2PO_4, 1.5; $MgSO_4$, 0.5; $CuSO_4$, 0.25 and yeast extract, 2. $MnCl_2$ (0.1 mg L^{-1}), H_3BO_3 (0.075 mg L^{-1}), Na_2MoO_4 (0.02 mg L^{-1}), $FeCl_3$ (1.0 mg L^{-1}) and $ZnSO_4$ (3.5 mg L^{-1}) were added to the medium as trace elements. The tests presented 60% of final moisture, except for the one with sugarcane bagasse with final moisture of 80%.

The flasks with culture medium were autoclaved at 120 °C for 20 min and then 3 mL of the inoculum (containing 1.5×10^7 spores mL^{-1}) were added. The flasks were kept at 28 °C in a temperature controlled chamber and the enzymatic extraction was carried out after seven days of cultivation. Enzymes secreted during SSF were extracted with 50 mM sodium acetate buffer, pH 5, 10: 1 (buffer/dry substrate), under agitation at 150 rpm for 60 minutes at room temperature. The solids were separated by filtering on a nylon filter followed by centrifugation at 15,000 g for 30 minutes, and the clarified supernatants frozen and stored for further enzymatic analysis. The experiments were performed in triplicate.

2.5.3. Laccase activity and protein quantification

The laccase activity was determined by monitoring the oxidation of the 2,2'-azino-bis(3-ethylbenzothiazoline-6-sulphonic acid) (ABTS) substrate in 100 mM sodium

acetate buffer, pH 5, at 50 ºC. The enzyme assay was performed in triplicate and the averaged values were calculated. The reaction mixture contained 100 µL of the appropriately diluted enzyme solution, 350 µL of the buffer and 50 µL of 10 mM ABTS. This mixture was incubated for 10 min when the absorbance was immediately measured at 420 nm. Laccase activity was calculated by the Lambert-Beer principle, with a molar extinction coefficient of the oxidized ABTS of 3.6 x 10^4 $M^{-1}cm^{-1}$. The protein concentration in the enzymatic extracts was determined by the Bradford method with bovine serum albumin as standard (Bradford, 1976).

2.5.4. Partial purification of *C. cubensis* MCOs

C. cubensis crude extract produced with wheat bran and orange peel (ratio of 3:1) was subjected to fractionation with $(NH_4)_2SO_4$ added to the extract until 40% saturation. The precipitated proteins lacking laccase activity were discarded and $(NH_4)_2SO_4$ was added to the supernatant to 90% saturation. The precipitated proteins with laccase activity were resuspended in 50 mM sodium acetate buffer, pH 5.0. The sample with laccase activity obtained by ammonium sulfate fractionation was desalted and concentrated using Amicon® ultrafiltration vessel (Millipore Co. - Billerica, MA, USA) with 50 kDa exclusion membrane in an ice bath.

Subsequently, the sample was subjected to gel filtration chromatography using a Sephacryl S-200 column (90 cm x 2.5 cm). Two milliliters of the ultrafiltration sample was loaded onto the Sephacryl S-200 column (90 cm x 2.5 cm) previously equilibrated with 50 mM sodium acetate buffer, pH 5 with 150 mM NaCl. Proteins were eluted with the same buffer at a flow rate of 0.2 mL min^{-1}. Fractions with the volume of 2,5 mL were collected and the laccase activity determined along the elution. The protein content was analyzed in each fraction (Bradford, 1976). The laccase-containing fraction obtained after gel filtration was applied to a 1.0 x 5 cm column of Q-Sepharose HiTrap Q HP (GE Healthcare). The non-adsorbed proteins were washed with 50 mM acetate buffer pH 4.3. The adsorbed proteins were eluted with a pH gradient of 4.3 to 3.6 in 50 mM sodium acetate buffer.

2.6. Zymogram

Zymogram was performed in a non-denaturing condition (without SDS and β-mercaptoethanol) using a 12% (w/v) polyacrylamide gel with a 5% stacking gel and the Mini-Protean II system (BioRad), according to the method previously described

(Laemmli, 1970), with some modifications. Aliquots of 500 µL of the fraction obtained from the ion exchange step with laccase activity were conditioned in 1.5 mL tubes and lyophilized until complete dehydration. 20 µL of sample buffer was added to the lyophilized samples and these were applied to the gel. After the electrophoretic run, a range of approximately 1 cm in width was longitudinally excised from the gel to identify the region containing laccase activity.

The strip extracted from the gel was washed in 100 ml of 50 mM sodium acetate buffer, pH 4.0, for 30 minutes at room temperature. After washing, the gel strip was carefully covered with a 10 mM ABTS solution and incubated at 37 ºC until the ABTS was oxidized and the laccase activity region was observed. The band was realigned to the original gel, and the gel region relative to the laccase position was excised. This strip of the gel was crushed, dried and macerated in mortar with pistil. After the complete dissolution of the gel, 3 mL of 50 mM sodium acetate buffer, pH 4.0, was added to the macerate and then transferred to a 20 mL flask. This mixture was allowed to agitation at room temperature for 12 hours to extract the proteins from the gel. After that, the obtained mixture was centrifuged at 7000 g, for 15 minutes, at room temperature.

2.7. One-dimensional electrophoresis (SDS-PAGE)

SDS-PAGE was performed using a 12% (w/v) polyacrylamide gel with a 5% (w/v) stacking gel and Mini-Protean II system (BioRad) according to the method previously described (Laemmli, 1970), with some modifications. The gel obtained on the SDS-PAGE performed with the proteins obtained from the ion exchange laccase activity fraction was stained with G-250 colloidal Coomassie blue according to the method described (Dyballa and Metzger, 2009). The gel obtained by SDS-PAGE with proteins extracted from the zymogram was stained with silver according to the method described (Merril et al., 1988).

2.8. Trypsin digestion and protein identification by MALDI-TOF/TOF mass spectrometry

Protein bands were removed manually from the SDS-PAGE gel performed with the fraction obtained from the ion exchange. The excised bands were cut into small pieces (1 mm^3) and packed in 1.5 mL tubes. 200 µL of wash solution, composed of 50% (v/v) methanol and 5% (v/v) acetic acid were added to each tube, respectively. The tubes were kept standing for 12 hours at room temperature. After that, the wash solution was carefully

removed and 200 µL of acetonitrile was added to the tubes and kept standing for 5 minutes at room temperature. The acetonitrile was discarded and the sample was dried in a vacuum centrifuge**.**

The protein bands were reduced and alkylated by DTT (10 mM) and iodoacetamide (100 mM), respectively. Digestion was performed with trypsin in 50 mM ammonium bicarbonate buffer, pH 7.8, containing 20.0 ng/µL of sequencing grade trypsin (Promega) at 37 °C overnight. The peptides were extracted with 50 mM ammonium bicarbonate. The trypsinized peptides were solubilized in 30 µL of MS grade water (Sigma-Aldrich) containing 0.1% (v/v) trifluoroacetic acid.

An aliquot of 1 µL of the solution with the sample was applied to a polished steel plate with a ratio of 1:1 to the matrix α-cyano-4-hydroxycinnamic acid. The selected points were submitted to MALDI-TOF/TOF mass spectrometry. The MS1 data were acquired through the reflexive method in positive mode. MS2 data were acquired through the LIFT method, also in positive mode. The higher mass/charge (m/z) ions were chosen to obtain the MS2 spectra. Peak lists were generated as a generic mascot format (mgf) and used for the identification of proteins by the MASCOT algorithm (Matrix Science). The search was performed against *in house* database of *C. cubensis* containing 12418 protein sequences.

2.9. Biochemical characterization of the extract with partially purified *C. cubensis* MCOs

The effects of temperature on laccase activity were evaluated in the 30 - 80 ºC range at pH 5.0, according to the standard methods described. The thermal stability of the laccase activities was determined at 50 and 65 °C, respectively. The partially purified enzymatic extract was diluted in 100 mM sodium acetate buffer, pH 5 and maintained at 50 or 65 °C for 210 minutes. Aliquots were taken at different time intervals and residual activities measured using the standard enzymatic assay. The data, obtained during the pH and temperature characterization, were expressed in relative activity with the highest value for each enzymatic activity considered as 100%.

Enzyme assays with a pH of 2.0 to 7.0 were performed to determine the effect of pH on laccase activity in citric acid/sodium phosphate buffer. The other test conditions were identical to those mentioned above. The KCl – HCl buffer was used for assay with pH values between 1.0 – 2.2 and sodium borate buffer for pH between 8.0 – 10.

The effect of potential inhibitors and metal ions on the partially purified laccase

activity was monitored with ABTS as substrate by adding 10 mM $NaNO_3$, KCl, HgCl, $CuSO_4$, $CaCl_2$, $MgCl_2$, SDS, $ZnCl_2$, $CoCl_2$ and urea, and 1 mM of sodium azide, dithiothreitol (DTT), EDTA, NaF and β-mercaptoethanol to the reaction medium. The assays were done in triplicate.

2.10. Biomass pretreatment

Sugarcane bagasse was supplied by the Sugar and Alcohol Plant of Jatiboca, in Urucânia, Minas Gerais, Brazil. This material was dried, ground (particle size less than 1 mm) and stored at -80 °C for later use. NaOH 1.5% (w/v) was used to pretreat 25 g of sugarcane bagasse with 10% (w/v) solids, generating the alkali pretreated sugarcane bagasse. Pretreatment was performed in an autoclave at 120 °C for 60 min. The alkali-pretreated bagasse was separated into solid and liquid fractions using a Buchner funnel equipped with filter paper. The solid fraction was carefully washed with distilled water and stored at -20 °C. The liquid fraction was separated for determination of phenols concentration.

2.11. Determination of phenolic compounds

The determination of the total phenolic compounds was performed by the Prussian blue method (Budini et al., 1980). The final volume of the reaction medium consisted of 1700 µL, of which 1500 µL of the pre-diluted pretreatment liquid fraction was added, in which 100µL of $K_3Fe(CN)_6$ 0.008 $mol.L^{-1}$ followed by 100 µL of 0.1 $FeCl_3$ $mol.L^{-1}$ in 0.1 $mol.L^{-1}$ HCl were added. Absorbance was measured at 700 nm after 5 minutes of reaction at room temperature. The concentration of phenolic compounds was determined using a standard curve having gallic acid as reference.

2.12. Oxidation of phenolic compounds by *C. cubensis* MCOs and saccharification of pretreated sugarcane bagasse

The saccharification reaction medium was prepared by adding the phenolic compounds obtained in the alkaline pretreatment of sugarcane bagasse (final concentration of 2.7 $g.L^{-1}$) in 1.5 ml of 50 mM sodium acetate buffer at pH 4.5. Treatments with MCOs were performed by adding 10U of laccases obtained in the ion exchange step (final activity 6.7 U mL^{-1}) to the reaction medium. The control treatment was performed as described above by pre-denaturing the sample at 100 °C for 10 min.

Treatment and control were incubated in an orbital shaker at 250 rpm, at 50 °C for 6 h. At the end of the process, the tubes were boiled to denature the enzymes, and aliquots were withdrawn for the quantification of the phenolic compounds.

Alkali pretreated sugarcane bagasse was added to the C. cubensis laccase-treated flasks and to the control flask at the final solids concentration of 8% (w/v). Commercial cellulase Accellerase® was applied to each flask with the enzymatic loading of 10 FPase units per gram of biomass with the addition of sodium azide (10 mM) and tetracycline (40 $\mu g\ mL^{-1}$) to the reaction mixture to inhibit microbial contamination. The reaction was carried out in an orbital shaker at 250 rpm and 50 °C for 48 h. These samples were immediately heated to 100 ºC to denature the enzymes, cooled and then centrifuged for 5 minutes at 15,000 g. The hydrolysis products were analyzed by high-performance liquid chromatography (HPLC) with a Shimadzu 10A series chromatograph. HPLC was fitted with an Aminex HPX-87P column (300 x 7.8 mm) and refractive index detectors. The column was eluted with water at a flow rate of 0.6 mL min^{-1} at 80 °C.

3. Results and discussion

3.1. *In silico* identification and predicted physicochemical parameters of *C. cubensis* MCOs

The prediction of the multi-copper oxidases of *C. cubensis* was performed according to the steps shown in **Fig. S1**, resulting in 13 enzymes predicted as members of the AA1 family. After obtaining the final model of predicted genes, the 13 family members were selected for comparative sequence variability studies and compared the AA1 family of 69 fungi with different lifestyles. After obtaining the 13 enzymes predicted for the AA1 family, *in silico* studies to obtain the physicochemical parameters of these enzymes were performed, according to (**Table 1)**.

The isoelectric points predicted for *C. cubensis* MCOs indicate the acidic character of these enzymes, possibly due to the high number of negatively charged amino acid residues, according to the -R index. The *C. cubensis* MCOs present an isoelectric point between 4,12 and 5,95, according to the values of fungi multicopper oxidases already described, which show an isoelectric point between 3 and 5 (Baldrian, 2006). The fungal MCOs present molecular mass between 55 and 85 kDa (Morozova et al., 2007), as well as the molecular masses predicted for MCOs of *C. cubensis*, ranging from 54.8 kDa to 74.2 kDa.

Table 1: Physico-chemical parameters of predicted laccases using Expasy's ProtParam program.

Predicted proteins	Seq. length	MW	pI	EC	Ii	Ai	GRAVY	-R	+R
mco 1	565	62336.07	4.28	143615	28.70	79.24	-0.184	69	22
mco 2	573	63327.97	5.95	82780	45.51	79.98	-0.328	64	54
mco 3	551	61355.74	5.54	104195	36.56	74.88	-0.418	61	43
mco 4	500	54838.74	4.27	113010	19.58	81.10	-0.133	61	21
mco 5	686	74232.92	5.38	126670	31.74	77.92	-0.210	54	36
mco 6	628	68455.98	4.77	113260	40.24	74.90	-0.286	75	39
mco 7	547	60543.48	4.29	131585	32.33	79.34	-0.272	73	23
mco 8	630	68256.07	4.36	103165	30.44	79.94	-0.066	71	23
mco 9	589	64776.74	4.50	131460	27.34	82.00	-0.093	62	23
mco 10	575	63403.91	4.35	120710	21.67	72.57	-0.260	74	25
mco 11	572	62962.87	4.12	147625	26.62	76.03	-0.262	80	21
mco 12	596	64635.33	4.41	128395	31.84	82.77	-0.159	65	21
mco 13	569	62865.89	4.23	151175	28.72	78.84	-0.221	77	22

Note: MW, molecular weight (g/mol); pI, isoelectric point; EC, extinction coefficient (M^{-1} cm^{-1}); Ii, instability index; Ai, aliphatic index; GRAVY, grand average hydropathicity; -R, number of negative residues; +R, number of positive residues.

The molar extinction coefficient (EC) of a protein reflects the concentration of cysteine, tryptophan and tyrosine residues (Gill and von Hippel, 1989). The EC values of fungal MCOs are higher compared to bacterial due to the higher content of aromatic amino acids and cysteine residues (Tamboli et al., 2015). The EC values predicted for *C. cubensis* MCOs are close to the EC value of *Cryphonectria parasitica* laccase (EC = 128,145 $M^{-1}cm^{-1}$), a phylogenetically close organism belonging to the same family.

The half-life is a prediction of the demanted time for half of the amount of protein in a cell to disappear after its synthesis (Guruprasad et al., 1990). Proteins having an instability index (Ii) of greater than 40 may have a half-life of less than 5 h *in vivo*, whereas those having Ii of less than 40 may have a half-life of more than 16 h (Rogers et al., 1986). In this study, the MCOs have Ii less than 40 in their majority, being predicted as stable enzymes. The exceptions were mco2 (Ii = 45.51) and mco6 (Ii = 40.24), which may be unstable under biological conditions.

The aliphatic index (Ai) of a protein is defined as the volume occupied by aliphatic side chains (alanine, valine and leucine), and can be considered a factor that positively contributes to the increase in the thermostability of globular proteins (Ikai, 1980). The high Ai values found (72.57 to 84.11) suggest that these enzymes have the potential to be

thermostable over a wide range of temperatures. The GRAVY index is used to define the hydrophobicity of a protein (Kyte and Doolittle, 1982). The negative values presented in **Table 1** indicate that the *C. cubensis* MCOs interact better in an aqueous medium.

About predicted secondary structure elements (**Table S1**), the analysis reveals the predominance of intrinsically disordered regions (IDPRs) in all predicted MCOs. The functional relevance of disorder is the result of increased plasticity which allows for binding numerous and structurally distinct targets (Lieutaud et al., 2016). The disorder acts in enzymes to provide advantages in promiscuous recognition and binding to substrates. As such, the majority of IDPRs are involved in functions concerning multiple partner interactions, such as molecular assembly, molecular recognition, signal transduction and transcription, cell cycle regulation, flexible tethers for complex formation and stabilization and regulation of catalysis (DeForte and Uversky, 2017; Lieutaud et al., 2016).

Another secondary element that is frequently found in the MCOs is the β conformations because these enzymes have three domains of copper bonding (denominated D1, D2, and D3); in which each domain is formed from a beta sandwich consisting of seven strands in two beta sheets arranged in a Greek-key beta barrel (Trubitsina et al., 2015).

3.2. Prediction of cellular localization and physiological functions

The subcellular localization of MCOs is related to their physiological function and determines the broad spectrum of substrates available for interaction with the enzyme (Moreno et al., 2017). The majority of known fungal MCOs are extracellular, although intracellular laccases have been reported. Extracellular MCOs participate in the breakdown of lignin, in addition to play an important role in the reduction of oxidative stress, recycling of organic material and pathogenesis for plants and animals (Baldrian, 2006; Giardina et al., 2010).

Secretion signal prediction analyzes of *C. cubensis* MCOs were performed, and it was verified that 9 MCOs have a signal peptide (**Table 2**), being exported by classic secretory pathways to the extracellular environment. The proteins mco2, mco5, mco6, and mco7 do not present signal peptide. Unconventional pathways (UPS pathways) independent of endoplasmic reticulum protein targeting to the Golgi complex (Nickel and Seedorf, 2008) can secrete proteins lacking secretion signals. Although the occurrence of UPS pathways is well documented for yeasts (Nombela et al., 2006), it is still poorly

described for filamentous fungi. However, studies of prediction of protein secretion by non-classical pathways were performed for the fungus *Laccaria bicolor* and *Botrytis cinerea* using the SecretomeP program (Jain et al., 2008).

Table 2: Prediction of cell localization and N-glycosylation of MCOs using signalP 4.1, TMHMM 2.0, DeepLoc-1.0 SecretomeP 2.0 and NetNGlyc1.0.

Predicted proteins	SP length	TM helices	Cellular localization	non-classical secretion	N-glycosylation Asn-X-Ser/Thr
mco 1	18	n.d.	E	No	85, 112, 124, 234
mco 2	n.d.	n.d.	C	No	75
mco 3	19	n.d.	E	No	26, 369, 453, 466
mco 4	16	n.d.	E	No	84, 110, 210, 308, 462, 471
mco 5	n.d.	n.d.	E	Yes	219, 442, 508, 559
mco 6	n.d.	n.d.	E	No	280
mco 7	n.d.	n.d.	E	Yes	51, 67, 94, 106, 206, 251, 400, 458
mco 8	24	1 (559-581)	E.R	No	78, 91, 116, 198, 202, 234, 296
mco 9	24	1 (559-581)	C.M	No	32, 61, 71, 78, 91, 116, 120, 296, 440
mco 10	17	n.d.	E	No	91, 118, 230, 277, 332, 401
mco 11	17	n.d.	E	No	31, 91, 120, 132, 232, 278, 550
mco 12	16	n.d.	E	No	123, 235
mco 13	16	n.d.	E	No	89, 116, 128, 233

Note: SP, signal peptide; TM, trasmembrane; nd, not detected; E, extracellular; C, cytoplasm; E.R, endoplasmic reticulum (membrane); C.M, cellular membrane; n.d. not detected.

In this study, all the predicted MCOs of *C. cubensis* were submitted to a prediction by the tool SecretomeP. The mco5 and mco7 proteins, which lack signal peptide, were predicted as proteins secreted by non-classical pathways, while mco2 and mco6, which lack signal peptide and are not secreted by alternative routes, possibly being intracellular multi-copper oxidases.

Intracellular MCOs are probably involved in the transformation of low molecular weight phenolic compounds produced by cellular metabolism; while the cell wall and spore-associated MCOs are linked to the possible formation of cell wall protecting compounds (Baldrian, 2006). Conidia-associated MCOs are linked to the synthesis of pigments and other substances that protect the cell from stressors, such as enzyme lysis, temperature and UV light (Moreno et al., 2017). In ascomycetes, intracellular laccase activity involved in melanin synthesis has already been detected for the fungus *Hortaea acidófila* (Tetsch et al., 2006). Intracellular laccases have also been described in phytopathogenic fungi, such as the Lcc1 and Lcc3 enzymes of *Fusarium oxysporum*,

which are involved in fungus protection mechanisms against oxidative stress and toxic compounds (Cañero and Roncero, 2008). In many pathogenic fungi, MCOs are part of the DOPA pathway, used to produce melanin that can confer environmental and host resistance serving as a scavenger of the free radicals produced by the oxidative system (Moreno et al., 2017).

Two MCOs (mco8 and mco9) have a structural characteristic that differentiates them from the others, which consists of the presence of a transmembrane helix near the carboxy-terminal end. The presence of the secretion signal in these enzymes indicates that canonical secretion pathways will address both. However, the presence of a single transmembrane helix indicates that these enzymes may be retained in the plasma membrane. Ferroxidases described in the literature are examples of transmembrane multi-copper oxidases, such as the Fet3p enzyme of *Saccharomyces cerevisiae*, which is a type IA membrane protein and has an exocytoplasmic catalytic domain involved in the conversion of Fe^{2+} to Fe^{3+} (Taylor et al., 2005). Thus, the presence of transmembrane helix in mco8 and mco9 is an indication that these enzymes may present ferroxidase activity.

Multi-copper oxidases, especially laccases, have an average glycosylation rate of 10 to 25% of the molecular weight and between 3 to 10 sites of N-glycosylation (Baldrian, 2006; Morozova et al., 2007). N-glycosylation sites were predicted for all 13 *C. cubensis* MCOs, respecting the average N-glycosylation sites already described in the literature, except for the mco2 and mco6 enzymes, that presented only one site, which can be considered an indication that these two enzymes are not secreted. Glycosylation is an essential post-translational modification for secreted enzymes and is suggested to play an important role in the stabilization of the catalytic center, protection against hydrolysis, retention of the copper atoms, and especially in the thermal stability of the multi-copper enzymes (Maestre-Reyna et al., 2015; Vite-Vallejo et al., 2009). The glycosylation role was reported in *Pycnoporus sanguineus* deglycosylation experiments, in which a negative effect on laccase activity and stability was observed, especially at lower temperatures between 20 and 30 ºC (Vite-Vallejo et al., 2009).

3.3. Sequence diversity analysis of *C. cubensis* MCOs

Sequences analysis of the 13 predicted proteins using the SMART modular architecture research tool indicated that all the *C. cubensis* MCOs present the three characteristic domains of copper binding (**Fig. 1**), which demonstrates that these predicted

enzymes belong to the family of multicopper oxidases.

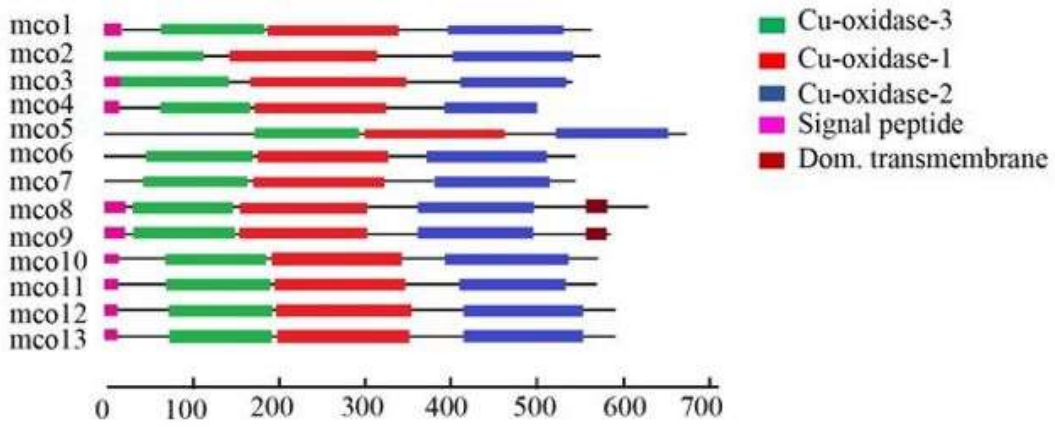

Figure 1: Predicted domain distribution of MCO proteins. Each line represents the amino acid sequence of the molecule indicated on the left (mco 1-13). The protein domains are indicated as follows: peptide-signal in pink; Cu-oxidase-3 domain in green; Cu-oxidase-1 domain in red; Cu-oxidase-2 domain in blue; transmembrane domain in brown. The line diagram was plotted according to the length of the sequences.

The 13 members of the AA1 family of *C. cubensis* have structural differences and distinct physicochemical characteristics that may reflect on different functions that each member can exert in the physiology of the fungus. To investigate the relationship between sequence variability and the possible function of each predicted enzyme of the phytopathogenic fungus *C. cubensis*, AA1 enzymes were selected from 68 fungi with different lifestyles (846 MCOs) and compared with the 13 predicted enzymes.

A multidimensional scaling plot (MDS) was constructed (**Fig. 2**) to visualize the clustering of the enzymes by sequence similarity. Four clusters were defined using the K-means algorithm and the number of clusters was validated using the Elbow method (**Fig. S2**).

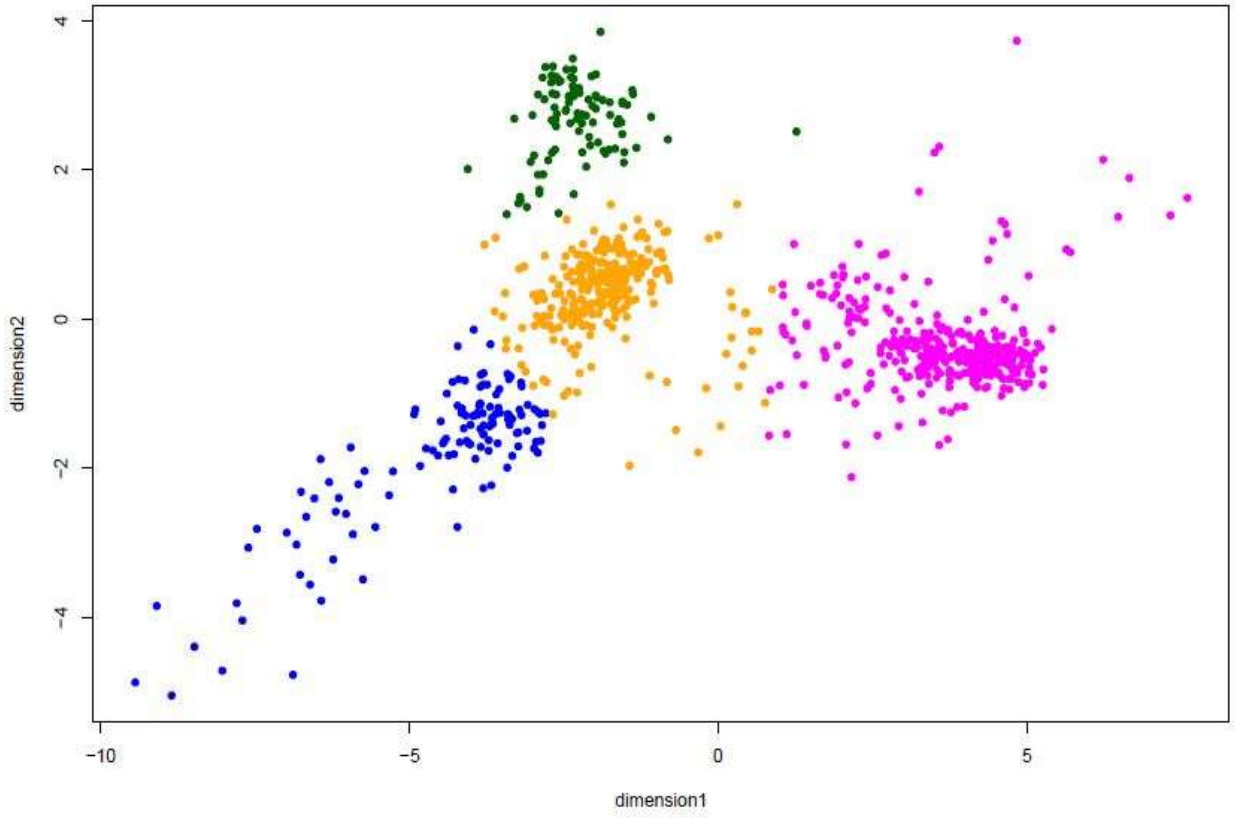

Figure 2: Multidimensional Scaling Analysis (MDS) of 846 multi-copper oxidases of 69 fungi with different lifestyles: green dots, cluster I; orange dots, grouping II, blue dots, grouping III, dots in magenta, group IV.

Analyzing the distribution profile of the multidimensional scaling plot **(Fig. 2**) it is possible to verify the existence of well-defined and populous groupings. According to the arrangement of the groupings, the group IV, located to the right in the graph, is further from the other 3 groupings (I, II and III), which are arranged to the left and in a continuous way.

To confirm the existence of a relationship between the subfamilies of multi-copper oxidases and clusters formed by sequence similarity, enzymes with known enzymatic activity were selected to be representative of each subfamily of the MCOs. To validate the clusters, three representatives of the basidiomycete, three laccases of ascomycetes, 4 enzymes with laccase/ferroxidase activity of basidiomycetes, 4 ferroxidases, 3 ascorbate oxidases, and 3 pigment enzymes were selected (**Fig. 3**).

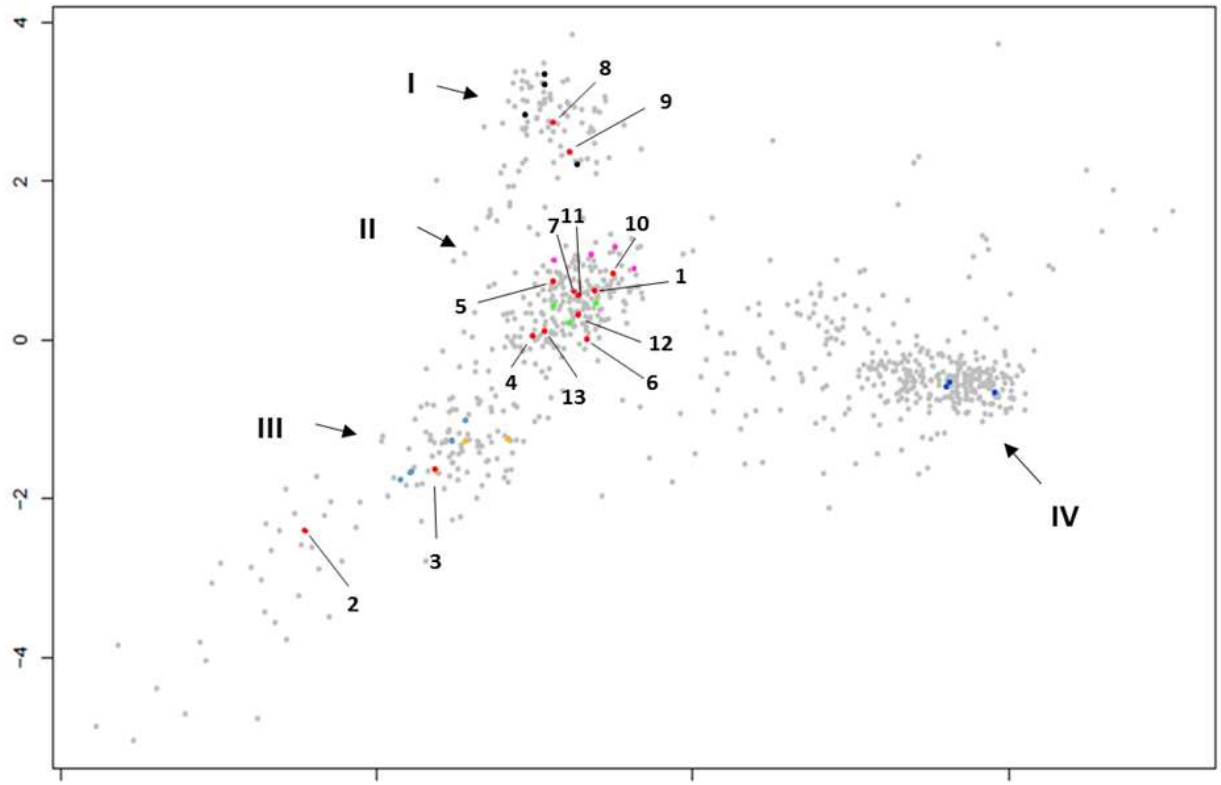

Figure 3: Multidimensional Scaling Analysis (MDS) of 846 multi-copper oxidases of 69 fungi with different lifestyles. The 4 groups are numbered from I to IV. The red dots correspond to the 13 MCOs predicted for the phytopathogenic fungus *C. cubensis*, (1 to 13). Proteins were selected to validate the clusters. The fungal species and their respective NCBI accession numbers for each protein highlighted in MDS are as follows: The black spots are *Aspergillus niger* ferroxidases (CAK97337.162); *Serpula lacrymans* (XP_007313469.142); *Postia placenta* (XP_002469890.1 436); *Phanerochaete chrysosporium* (ABE60664.1). The spots in magenta are laccases/ferroxidases of *Postia placenta* (XP_002473277.1 300); *Phanerochaete flavidoalba* (ABR15762.1339); *Phanerochaete chrysosporium* (AAO42609.1346 and AAS21659.1351). The green dots correspond to the ascosectic laccases of *Neurospora crassa* (XP_956939.1 207); *Melanocarpus albomyces* (CAE00180.1122); *Podospora anserina* (P78722.188). In orange, we have ascorbate oxidases of *Trichoderma reesei* (XP_006962053.118); *Pyrenophora tritici repentis* (XP_001940041.122) and *Acremonium sp* (BAA24288.13). The cyan spots are pigment enzymes from *Schizophyllum commune* (XP_003027702.1 314 and XP_003029382.1 315); *Aspergillus nidulans* (P17489.3 316) and *Aspergillus fumigatus* (ACJ13069.1399). In dark blue the basidiomycete laccases of *Lentinula edodes* (BAB84355.1 571); *Ganoderma lucidum* (AAR82934.1652) and *Trametes versicolor*

According to **Fig. 3**, the sequences known as the basidiomycete laccases *sensu scricto* were arranged in the central region of the cluster (IV), which is isolated to the right of the MDS plot. The ferroxidases are all located in the same cluster (I) to the left of the graph, in the upper region. The representatives of the enzymes with dual laccase/ferroxidase function are located in the upper margin of the cluster (II) located in

the center of the graph. In this same group, the representatives of ascomycete *sensu scricto* laccases can be observed, occupying the central region and the lower margin of the cluster (II). It is important to note that the laccases/ferroxidases are even apparently located in a distinct group than the ferroxidases, but close to the cluster (I), in a marginal region. It should be noted that these enzymes coexist in the same group of ascomycete laccases. Thus, with only a preliminary analysis of the enzymes used to validate clusters, it is possible to consider that laccases/ferroxidases share the ability to oxidize Fe^{2+} to Fe^{3+}, as well as ferroxidases, which probably is due to structural similarities and also compatible for the execution of this function. However, unlike ferroxidases, these enzymes can also oxidize aromatic compounds, with a greater sequence similarity with ascomycete laccases, which allows them to share the same group and is indicative of a predominance of this function.

Representatives of the subfamily of the pigment enzymes and the ascorbate oxidases are found in a region that appears to be a single cluster (III), with more dispersed sequences in the lower region of the graph, which demonstrates a greater diversity within the group.

A total of nine *C. cubensis* MCOs are concentrated in the central cluster of the graph, belonging to laccase/ferroxidases sequences and ascomycete laccases. Two predicted enzymes (mco8 and mco9) are located near the ferroxidases, precisely the MCOs that have predicted transmembrane helices. The other two remaining MCOs are located in the group of pigment and ascorbate oxidase enzymes. The enzyme mco3 is superimposed on an ascorbate oxidase, which demonstrates the great similarity with this subfamily. The enzyme mco2 is at the end of the group and can be considered the most diverse enzyme when compared to the other MCOs of *C. cubensis*.

Thus, it is evident that the clustering of multi-copper oxidases using sequence similarity criteria has a strong relationship with the function of the enzymes included in this family, allowing them to be classified into subfamilies according to their different catalytic activities. This unprecedented approach to classifying MCOs by a multidimensional scaling analysis based on similarity is compatible with previous studies of phylogenetic analysis of MCOs (Hoegger et al., 2006; Kues and Ruhl, 2011).

Hoegger and coworkers performed a phylogenetic analysis of more than 350 multi-copper oxidases of fungi, insects, plants and bacteria, providing the basis for a refined classification of this family of enzymes in the *sensu scricto* laccases of basidiomycetes and ascomycetes, insect laccases, MCOs of fungal pigment, ferroxidases, ascorbate oxidases, laccase-like plant MCOs and bilirubin oxidases (Hoegger et al.,

2006). Other work performed more in-depth phylogenetic analyzes of MCO protein sequences derived from basidiomycete fungi sequenced genomes using the same definition in subfamilies to classify the clusters observed in the phylogenetic tree constructed by the Neighbor-Joining Method and using p-distance as a model of estimate (Kues and Ruhl, 2011).

In this work, classification in subfamilies was extended, not only for basidiomycetes but also for ascomycetes MCOs, in addition to allow a more informative analysis of a high number of MCOs (846 sequences) when compared to previous classification work based on phylogenetic analyses. Besides, selected fungi have very diverse lifestyles, such as ectomycorrhizal fungi, phytopathogenic fungi, and wood rot fungi (white rot, soft rot, and brown rot), which contributes to a broader and more general analysis of fungal MCOs. New interpretations regarding the relationship between different subfamilies can be hypothesized from the analysis of the MDS graph, for example, the great similarity between ascorbate oxidases and pigment enzymes that coexist in the same grouping, and that until the present moment, were described in different groups in phylogenetic analyses. Thus, it may be suggested that fungal ascorbate oxidases, which do not yet have a well-characterized function, may have shared functions with pigment enzymes, and be related to or contribute to the melanization process of fungi.

The separation between the cluster (IV) formed by basidiomycete *sensu scricto* laccases and the cluster (II) formed predominantly by ascomycetes *sensu scricto* laccases agrees with phylogenetic studies that demonstrated a clear separation in two clusters well defined (Hoegger et al., 2006; Kues and Ruhl, 2011). However, the present work shows a close relationship regarding the sequence similarity between ascomycetes *sensu scricto* laccases and laccase/ferroxidase enzymes from ascomycetes and basidiomycetes, which had not been evidenced in phylogenetic analyses, which normally includes these two subfamilies in different clusters. Laccases/ferroxidases of well-characterized basidiomycete fungi, such as the pfaL enzyme of *Phanerochaete flavido-alba* (Rodríguez-Rincón et al., 2010) and the mco1 enzyme of *Phanerochaete chrysosporium* (Larrondo et al., 2003) are in the same cluster in which the ascomycetes *sensu scricto* laccases predominate. This demonstrates that laccases of basidiomycetes with double activity have more similarities of sequences with ascomycete *sensu scricto* laccases than with basidiomycetes *sensu scricto* laccases. This fact may have a relation with some evolutionary events not yet studied.

The separation of clusters (II) and (IV) makes clear that basidiomycetes and

ascomycetes *sensu scricto* laccases have structural characteristics that are unique to each group. Ascomycetes *sensu scricto* laccases have a number of additional signatures features to the L1-L4 domains (Kumar et al., 2003), which are not present in the basidiomycete laccases, such as a C-terminal DSGL/I /V domain (Hakulinen et al., 2002) and the presence of a phenylalanine (F) or leucine (L) residue in the axial coordination of copper (Eggert et al., 1998).

Laccases of ascomycetes fungi *Podospora anserina* (Fernández-Larrea and Stahl, 1996), *Neurospora crassa* (Germann et al., 1988), *Melanocarpus albomyces* (Kiiskinen and Saloheimo, 2004)), and *Torrendia arenaria* (Kallio et al., 2011), have protruding C-terminal tails (13-14 amino acids in length). This tail is generally cleaved by proteolysis in a post-translational cleavage process to produce the active form of the enzyme with the Asp-Ser-Gly-Leu (DSGL) consensus sequence located at the end of the protein sequence (Giardina et al., 2010). The determination of the three-dimensional structure of MaL from *M. albomyces* and TaLcc1 from *T. arenaria* revealed that the last 4 DSGL amino acids from the C-terminus penetrate the solvent channel to the trinuclear site, forming a kind of plug that blocks this channel's entry (Hakulinen et al., 2008). In MaL and TaLcc1, the C-terminal plug prevents the movement of molecular oxygen and other solvents to the enzyme and controls the entry of molecular oxygen and the exit of water molecules that are by-products of the catalytic process. Furthermore, the C-terminal carboxyl group forms a hydrogen bond with the Hys140 side chain in MaL (Hys141 in TaLcc1), which also coordinates the T2 copper. Direct mutagenesis studies carried out on the MaL cDNA revealed that a C-terminal alteration or suppression drastically affects enzyme activity, leading to low thermostability, low turnover and conformational changes in the T2 center (Andberg et al., 2009). These results suggest that ascomycete laccases use the C-terminal DSGL plug to perform a catalytic function, forming a proton transfer pathway to reduce molecular oxygen, positively collaborating for the catalytic efficiency of these enzymes.

Another unique feature of ascomycetes laccases that has a fundamental role in the redox potential (E_0) of these enzymes is the presence of amino acid located ten residues downstream of the conserved cysteine of the L4 segment, which is axially coordinated to the copper T1 (Cázares-García et al., 2013). Laccases with high E_0 (700 ± 800 mV) have leucine or phenylalanine in axial coordination, while methionine residues at this position have low E_0 (500 mV). Based on the residue of the axial coordination, the ascomycetes laccases are classified in Lac1 (Met), Lac2 (Leu) and Lac3 (Phe) (Eggert et al., 1998).

Besides, the proton transfer is assisted by the so-called SDS-gate. This gate consists of two residues of Ser (one present in the L2 region and the other in L4) and an Asp residue (present in the DSGL signature) and conserved in ascomycetes laccases, but it was not detected in basidiomycete laccases (Hakulinen et al., 2008). Regarding the *C. cubensis* MCOs, multiple alignments were performed with the 13 multi-copper oxidases predicted to investigate whether the enzymes belonging to group II in the MDS plot had the exclusive signatures of ascomycetes laccases, in addition to the presence of the 4 regions L1-L4 that all MCOs generally share (**Fig. 4**).

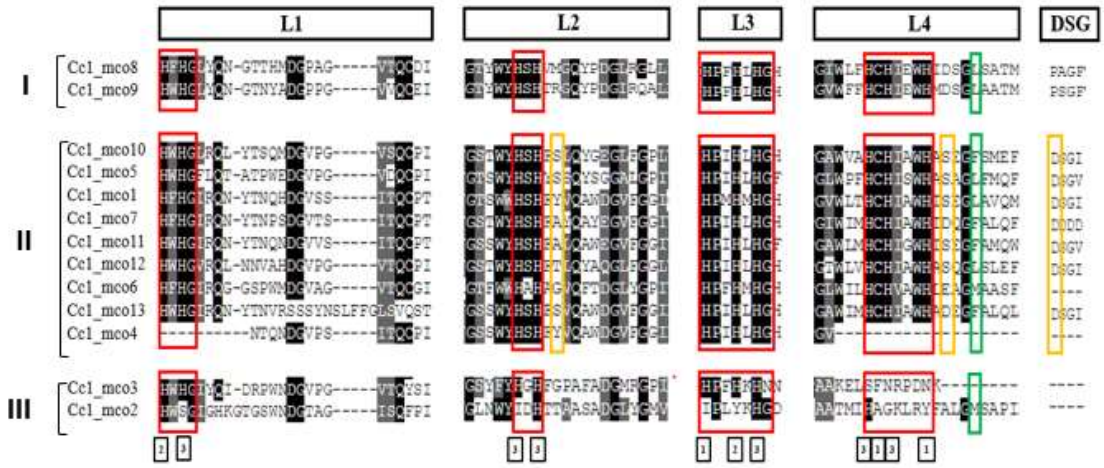

Figure 4: Multiple sequence alignment of predicted *C. cubensis* MCOs using Clustalw2. The regions L1-L4 and the region containing the DSGL signature were detached from the alignments and organized into blocks, as indicated at the top of the figure. The conserved residues involved in bonding with the Cu atoms are indicated in red rectangles. The numbers 1 to 3 in the lower part of the figure indicate the Cu bonding centers where each residue belongs. The orange rectangles indicate the amino acid residues that make up the SDS-gate signature. The green rectangle indicates the amino acid residue used to classify laccases in class 1 (Met), class 2 (Leu) and class 3 (Phe). I, II and III indicate the group on the MDS plot that each sequence belongs.

The mco8 and mco9 enzymes, belonging to group I, are conserved in the 4 regions (L1-L4) of the MCOs and the binding residues to the copper centers (10 histidine residues and 1 cysteine residue). However, the residues that make up the SDS-gate and the DSGL signature are not verified, which leads to the conclusion that these two enzymes are not laccases. This information is in agreement with the hypothesis that these two enzymes are possibly ferroxidases.

The ferroxidases of *C. cubensis* are important for the maintenance of cellular homeostasis by controlling iron levels, in addition to maintaining the metabolism of the fungus, which enables the enzymatic production at the levels required according to the

conditions in which the fungus is subject. Although it is important to understand the function of mco8 and mco9 enzymes for fungi physiology and phytopathogenicity, these two MCOs do not directly contribute to the enzymatic hydrolysis of lignocellulosic biomass. In this way, *C. cubensis* laccases emerge as the main targets, according to the objectives proposed in this work.

About group II of MCOs, the enzymes mco10, mco5 and mco13 have all the exclusive signatures of laccase, such as L1-L4 regions, SDS-gate and DSGL I/V sequences, indicating that these enzymes all have the requirements to be laccases *sensu scricto*. Due to the proximity of mco10 and mco5 with enzymes recognized as laccases/ferroxidases, it is suggested that both may exhibit at least residual ferroxidase activity. Concerning laccases *sensu scricto*, although they are considered classic or conventional laccases, they may present ferroxidase activity at residual levels (Kues and Ruhl, 2011). The mco10 and mco13 have phenylalanine in the axial coordination, being classified as enzymes of class 3, while mco5 has a leucine in this position, being classified as belonging to class 2. These two classes belong to laccases with high redox potential, which is an ideal feature for enzymes intended for biotechnological application, since they are capable of oxidizing a wide spectrum of substrates.

The mco6 protein does not have the DSGL and SDS-gate signatures. The absence of the C-terminal signature of the tail indicates that this enzyme may have lower catalytic activity and be less thermostable when compared to the other laccases of group II. Other evidence indicating the low redox potential of mco6 is the presence of a 10-position methionine downstream of the conserved L4 cysteine, which classifies this enzyme as a class 1 laccase. The absence of the DSGL signature can be found in other ascomycete fungi, such as the *A.niger* laccases Mco G, Mco J and Mco M (Tamayo Ramos et al., 2011). Analyzes to find the signatures of laccases *sensu scricto* have identified that the Mco G protein does not have the DSGL motif. Futhermore, Mco J and Mco M have a deletion of approximately 50 amino acids after the L4 segment, in which the DSGL motif is included. Interestingly, these two last "truncated" enzymes oxidize a limited number of substrates (Cázares-García et al., 2013). This indicates that some ascomycetes laccases can be partially functional, even if they do not present all the elements to be considered as laccases *sensu scricto*.

The mco7 and mco11 enzymes have a very high sequence similarity, demonstrated by the proximity in the MDS plot (**Fig. 4**), in which they are almost superimposed. The two MCOs have an alanine substituting the first serine of the SDS-gate signature, and in the case of mco7, the second one is also replaced by an aspartate.

However, mco7 has no conservation in the SDS-gate signature, which may indicate a lower catalytic capacity of this laccase when compared to mco11. Both mco7 and mco11 are classified as class 3 MCOs, having a high redox potential.

The mco1 and mco12 enzymes have the conserved laccase signatures, including DSGL, both being class 2 MCOs, but they have only one substitution on the first serine of the SDS-gate, a tyrosine on mco1 and a threonine on mco12. The central position of mco12 (**Fig. 4**), among three well-described laccases, indicates that mco12, even having a small variation in the SDS-gate signature, may be an efficient laccase *sensu scricto*. SDS-gate is involved in the transfer of protons from the T1 site to the trinuclear center and the substitution of serine for a threonine, which is a structurally similar amino acid, may even confer an advantage or adaptation by assisting this proton flow. Substitutions on SDS signature serines are found in laccases of other ascomycetes fungi. In the TaLcc1 laccase of *T. arenaria*, the amino acid corresponding to Ser143 is replaced by a leucine or phenylalanine, whereas that corresponding to Ser511 is replaced by glutamic acid, aspartate or glycine, and the amino acid corresponding to Asp561 is replaced by valine, glutamic acid or glycine (Moreno et al., 2017). In *Trichoderma sp*p. laccases Tas_154312 and Ta_54145, the amino acid corresponding to the first serine is replaced by glycine and in Tv_48916, by alanine. Also, in Th_539081 the residue corresponding to the second serine of the signature is replaced by a threonine (Cázares-García et al., 2013). These results show that laccases of different fungi, including the MCO of *C. cubensis*, can adopt several distinct strategies to facilitate the proton transfer to the trinuclear center, thus modifying their catalytic activity.

The mco4 enzyme lacks the conserved copper-binding histidines of the L1 and L4 region, as well as lacking the SDS-gate and DSGL sequences, indicating that it is not a laccase *sensu scricto*. It is also possible that this enzyme does not have catalytic oxidation activity of phenolic compounds, because the H-C-H motif of L4, which is absent in this MCO, is essential for the electron transfer pathways that occur in the trinuclear center.

The mco3 and mco2 enzymes of group III show no laccase *sensu scricto* signature. Besides, they have great divergence in the L2, L3 and L4 regions. Fungal pigment MCOs are significantly divergent from other MCOs in the L2 region, and the ascorbate oxidases in the L3 and L4 regions (Kues and Ruhl, 2011). By overlapping mco3 with an ascorbate oxidase (XP_006962053.18) on the MDS plot (**Fig. 4**), this enzyme has great sequence similarity with ascorbate oxidases. Already mco2 is the most diverse enzyme among all the multi-copper oxidases of *C. cubensis* and it is located in a dispersed region of group III in the MDS graph. It is suggested that this protein may act as a pigment enzyme in

melanization pathways or it has a different function from the other MCOs and further studies are required.

Regarding the possible classification of any of these group II MCOs in dual laccase/ferroxidase enzymes, biochemical characterization experiments are necessary to detect laccase and ferroxidase activity. There are different levels of activity between the laccases/ferroxidases. Some dual-function enzymes may have stronger ferroxidase activity and lower laccase activity, such as the MCO1 of *P. chrysosporium*, which does not efficiently oxidize aromatic compounds (Larrondo et al., 2003). On the other hand, the PfaL enzyme from *P. flavido-alba* has low ferroxidase activity when compared to MCO1, but it can oxidize a broad spectrum of organic substrates like laccase *sensu scricto* TvL of *T. versicolor*, being considered a laccase *bona fide* (Rodríguez-Rincón et al., 2010).

Specific residues of the catalytic pocket contribute to ferroxidase activity and distinguish these enzymes from *sensu scricto* laccases. These residues are well characterized in Fet3 ferroxidase from *S. cerevisiae* (E185, D283, Y354, and D409) and contribute to Fe^{2+} catalysis. Residues E185, D283, and D409 (signature motifs for multi-copper ferroxidases) are determinants for the oxidation of Fe^{2+} to Fe^{3+}, whereas Y354 is less critical. Residues E185, D283, and D409 form a pocket for Fe^{2+} binding, with E185 and D409 making direct contact with Fe^{2+} and forming part of the electron transfer pathway. To verify the presence of these conserved residues in the mco8 and mco9 predicted ferroxidases of *C. cubensis* and to analyze the presence of these residues in the other predicted enzymes, multiple alignments of the 13 MCOs with the Fet3 ferroxidase of *S. cerevisiae* and other 5 filamentous fungi ferroxidases was performed (**Fig. 5**).

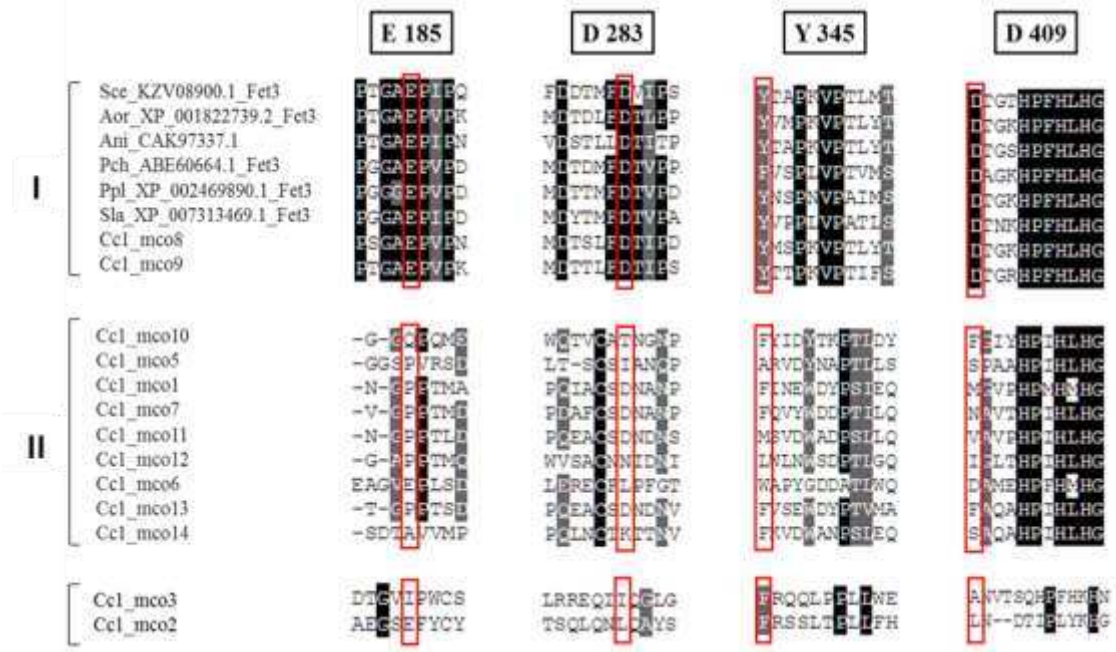

Figure 5: Alignment of the four regions of *S. cerevisiae* Fet3 ferroxidase (KZV08900.1) containing residues E185, D283, Y354, D409 (indicated in red rectangles), with the corresponding sequence regions of *C. cubensis* MCOs; Fet3 from *Arpergillus orizae* (XP_001822739.2); MCO from *Aspergillus niger* (CAK97337.1); Fet3 from *Phanerochaete chrysosporium* (ABE60664.1456); Fet3 from *Postia placenta* (XP_002469890.1 436); Fet3 from *Serpula lacrymans* (XP_007313469.1423). I, II and III indicate the group on the MDS plot that each sequence belongs.

The mco8 and mco9 enzymes retain the four Fe^{2+} binding residues. They also exhibit high conservation of the signature regions containing these residues compared to other well-characterized filamentous fungi ferroxidases. Thus, these enzymes have all characteristics to be classified as ferroxidases. The enzymes of group II do not retain the 4 characteristic residues of ferroxidases, except for mco6, which conserves the residues corresponding to E185 and D409. Interestingly, the Mco1 dual activity enzyme of *P. chrysosporium*, which has stronger ferroxidase activity, also has these important residues (corresponding to E185 and D409), while PfaL of *P. flavido-alba* PfaL, with high activity of laccase and low ferroxidase activity does not have these residues (Larrondo et al., 2003; Rodríguez-Rincón et al., 2010). Thus, there is predicted that mco6 has the potential to be a laccase/ferroxidase with low laccase activity and with elevated ferroxidase activity. Even though other MCOs in group II do not have conservation in the first and last position of ferroxidase signature residues, it is not possible to state that they are not dual function enzymes. This is because some laccases/ferroxidases do not conserve these residues. This case can be observed in the enzyme Mco6 (CnLac1) of *Cryptococcus neoformans*, which has comparatively strong ferroxidase activity and low laccase activity (Liu et al., 1999) even though it does not present the conserved amino acid residues that interact with Fe^{2+}.

In relation to the mco8 and mco9 ferroxidases, both have transmembrane sequences and possibly act together with reductases and membrane permeability, allowing the uptake of iron into the intracellular medium via RIA (reduced iron assimilation pathway). In *S. cerevisiae* not only the Fet3 ferroxidase gene and Ftr1 permease gene products are close at the membrane level, but also these genes tend to be clustered very closely in a divergent transcript orientation, sharing the same promoter in most organisms where they were identified (Courty et al., 2009; Hoegger et al., 2006; Kues and Ruhl, 2011). In *C. cubensis*, the ferroxidases genes and their related permeases are in a tandem mirrored arrangement (**Fig. 6**).

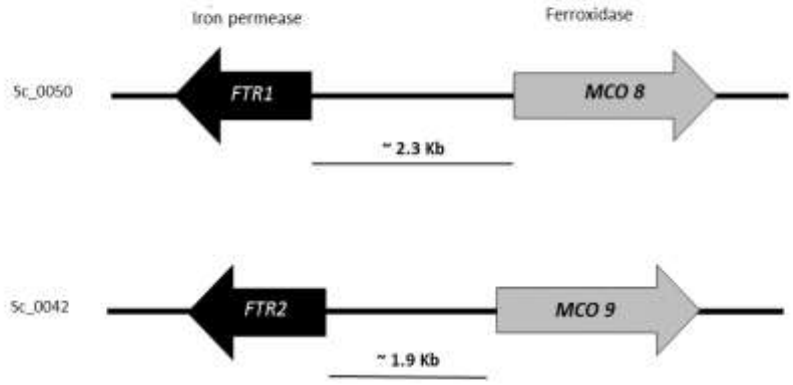

Figure 6: Schematic representation of the genes encoding two mco8 and mco9 ferroxidases, and for the two iron permease genes (ftr1a and ftr1b) in the *C. cubensis* genome. The location of the scaffolds (Sc) of the *tandem* repeats is also indicated.

Many orthologues of the Fet3 and Ftr1 systems were found in fungi following this same organization in the genome, including *Laccaria bicolor* (Courty et al., 2009), and phytopathogenic fungi such as *Fusarium graminearum* (Park et al., 2007), *Ustilago maydis* (Eichhorn et al., 2006) and *Colletotrichum graminicola* (Albarouki and Deising, 2013).

3.4. MCO production by *C. cubensis* using different low-cost carbon sources

After analyzing all multi-copper oxidases potentially produced by the fungus *C. cubensis* and understanding their peculiarities, this fungus was grown under SSF using different carbon sources to induce the production of MCOs. The production of MCOs by *C. cubensis* was higher with the mixture of wheat bran and orange peel in the ratio of three parts to one, respectively (4.88 U g^{-1}) than with other carbon sources (**Table 3**). The

laccase activity obtained in this culture was 12.2 times higher than that produced by this fungus in wheat bran, a standard source of carbon for cultivation and enzymatic production of laccases (Falkoski et al., 2013; Maitan-Alfenas et al., 2015).

Table 3: Production of MCOs by *Chrysoporthe cubensis* grown in semi-solid medium with different carbon sources.

Carbon source	Laccase activity (U/g)
Wheat bran	0.40 ± 0.018^{c}
Orange peel	0.04 ± 0.002^{c}
Wheat bran : Orange peel (1:1)	0.19 ± 0.031^{c}
Wheat bran : Orange peel (3:1)	4.88 ± 0.366^{a}
Wheat bran : Orange peel (9:1)	0.06 ± 0.007^{c}
Wheat bran : Passion fruit peel (1:1)	1.28 ± 0.076^{b}
Sugarcane bagasse	0.03 ± 0.003^{c}
Locust bean gum	0.11 ± 0.004^{c}

The averages followed by the same letter do not differ by the Tukey test with significance of 5%.

The highest production of laccases by *C. cubensis* cultivated with this mixture agrees with orange peel as a good inducer of fungal laccases and wheat bran as a good source of carbon and nitrogen for the growth and enzymatic production of cellulolytic fungi (Rosales et al., 2007; Tuyen et al., 2012). Orange peels contain chemical components of volatile oil, numerous flavonoids, vitamins, and phenolic acids. Phenolic acids are aromatic compounds containing phenolic ring in their structure, which play an important role in the induction of fungal laccase production (Kanagaraj et al., 2015). Wheat bran has a balanced C/N ratio, essential for the production of bio-products by the SSF system. Besides, the presence of soluble sugars in wheat bran corroborates the rapid growth of microorganisms (Falkoski et al., 2013). The wheat bran contains cellulose, hemicellulose, lignin and proteins, being a good source of carbon and nitrogen for the growth and enzymatic production of lignocellulolytic fungi, justifying the greater production of laccase by this fungus in the wheat bran and orange peel according to the ratio of three parts to one (Tuyen et al., 2012).

Pure orange peel or mixed with wheat bran in the ratio of one part to one, induced 122 and 25.7 times lower production of laccase activity, respectively, than the wheat bran and orange peel mixture, in the ratio of three parts to one, respectively. Orange peels have flavonoids and terpenoids, antimicrobial molecules, which justifies the lower production of laccase by *C. cubensis* grown in mixture with a higher proportion of this material

(Giese et al., 2008). Under these conditions, the concentrations of the orange peel antimicrobial molecules may have inhibited the growth of *C. cubensis*.

3.5. Partial purification and identification of MCOs of *C. cubensis*

The crude extract of *C. cubensis* grown in wheat bran and orange peel (3:1) was subjected to purification steps (**Table 4**) to identify new active MCOs that act in this promising enzymatic cocktail for the production of enzymes with high laccase activity. The specific activity of *C. cubensis* laccase was increased twenty-fold, in 15.5% yield after serial purification steps, included ammonium sulfate fractionation, 50 kDa membrane ultrafiltration, gel filtration using Sephacryl S-200 column and ion exchange chromatography using Q-Sepharose, with a pH elution gradient ranging from 4.3 to 3.6.

Table 4: Purification table for MCOs from *C. cubensis*.

Purification step	Total protein (mg)	Total activity (U)	Specific activity (U mg^{-1})	Yield (%)	Purification fold
Culture Filtrate	61.0	94.7	1.6	100.0	1.0
$(NH_4)_2SO_4$ (40–90%)	16.8	71.5	4.2	75.5	2.7
Ultrafiltration	10.2	58.2	5.7	61.5	3.7
Gel Filtration	6.31	48.9	7.7	51.6	5.0
Ion Exchange	0.5	14.7	31.1	15.5	20.0

Zymogram of the fraction with laccase activity eluted from the ion exchange showed four bands with laccase activity, indicating the possibility of *C. cubensis* secreted at least four different enzymes (**Fig. 7A**), under these culture conditions. The secretion of laccase isoforms by *C. cubensis* agrees with that obtained for *Pleurotus nebrodensis* and *Trametes versicolor* secreting more than one isoform of this enzyme (Bertrand et al., 2015; Yuan et al., 2016). The production of multiple laccases has been related to the greater flexibility and adaptation of phytopathogenic fungi, such as *C. cubensis*, oxidizing phenolic compounds that act as plant defense molecules (Bertrand et al., 2015).

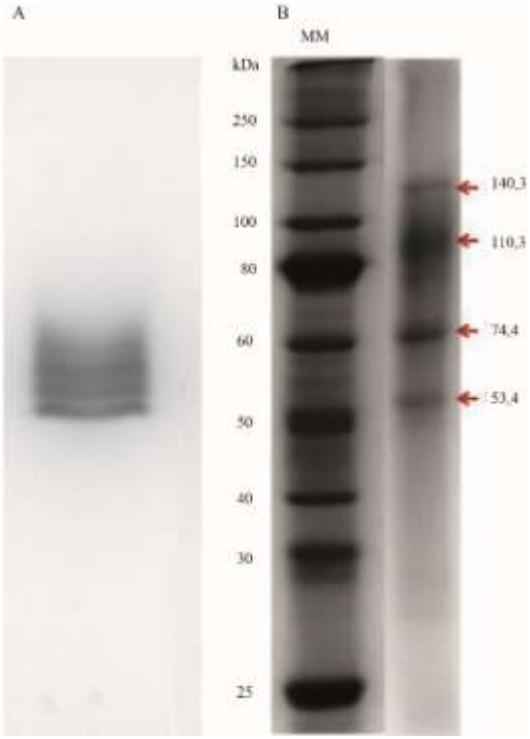

Figure 7: A) Zymogram of the fraction containing laccase activity obtained after the ion exchange step (Q-Sepharose). **B)** SDS-PAGE with the fraction proteins containing laccase activity obtained in the ion exchange step (Q-Sepharose) stained with colloidal coomassie.

The fact that *C. cubensis* MCOs were eluted in the same fraction after gel filtration and pH gradient ion exchange chromatograms suggests that they have similar molecular weights and isoelectric points. SDS-PAGE confirmed that the proteins extracted from the region of the zymogram with laccase activity have approximate molecular weights between 50 and 80 kDa (**Fig. S5**). The fact that *C. cubensis* MCOs are eluted in a narrow acidic pH range showed that they have near isoelectric points, agreeing with reports of *Pleurotus ostreatus*, *Melanocarpus albomyces* and *Cerrena unicolor* laccases that presented values of isoelectric points of 4.2, 4.0 and 3.5, respectively (Kiiskinen et al., 2002; Linke et al., 2019). These similarities are also in agreement with the range of molecular mass (54.8 – 74.2 kDa) and isoelectric point (4.1 – 5.9) obtained by the *in silico* predictions for *C. cubensis*.

In order to identify the MCOs present in the partially purified extract of *C. cubensis*, a second SDS-PAGE gel was performed, and the fraction with laccase activity eluted from the ion exchange was applied. The bands' profile showed a predominance of 4 bands with the highest intensity and presented approximate molecular weights of 140.3, 110.3, 74.4 and 53.4 kDa, respectively (**Fig. 7B**). The two bands of smaller molecular weights (53.4 and 74.4 kDa) are in agreement with the molecular weight range with

laccase activity observed in the zymogram (50 - 80 kDa). However, the two bands with the highest molecular weights (110.3, 140.3 kDa) were not detected in the zymogram and are not in agreement with the molecular weights predicted for MCOs of *C. cubensis.*

The four regions containing the most intense bands were excised and the fractions were submitted to mass spectrometry analysis using MALDI-TOF/TOF. Two MCOs of *C. cubensis* (**Table 5**) were detected. The protein mco2 is related to the band of 53.4 kDa and mco5 to the band of 74.4 kDa.

Table 5: Identification of fragments obtained by MALDI-TOF/TOF using an *in house* protein database of *C. cubensis*.

***C. cubensis* band**	**Protein ID**	**Predicted Mass (kDa)**	**Number of unique peptides**	**Protein name**
53.4 kDa	g8613.t1	63.3	3	Multicopper oxidase 2 (**mco2**)
74.4 kDa	g6312.t1	74.2	5	Multicopper oxidase 5 (**mco5**)

Only two MCOs were identified in the low molecular weight bands in the mass spectrometric analyzes, indicating that the sample is partially purified and that the bands of larger molecular masses do not correspond to multi-copper oxidases. Moreover, a lower number of MCOs have been identified in the low molecular weight fractions than indicated by the zymogram. This may be justified by incomplete coverage in genome prediction or protein sequence polymorphisms caused by splicing that may result in isoforms that were not detected by the mass spectrometry methodology used in this work. Moreover, the non-specificity of the enzymatic activity test for laccase detection used may have overestimated the number of expressed MCOs. The assay of enzymatic activity using ABTS can generate false positives due to the interference of peroxidases and tyrosinases present in the partially purified sample, and that is found in large quantities in the crude extract of *C. cubensis*.

The two MCOs detected, mco2 and mco5, have different characteristics. The enzyme mco2 has no signal peptide and was not predicted to be secreted by non-classical pathways. In addition, the low number of N-glycosylation sites (N75) and the lowest predicted stability confirm the hypothesis that this enzyme is intracellular. The location at the end of cluster III on the MDS graph (**Fig. 3**), which is very distant compared to the positioning of mco5, demonstrates the great sequence diversity between the two MCOs. The absence of laccase *sensu scricto* signatures and the low conservation of L1, L2, and L3 copper binding regions indicates the similarity of sequence and function with other

already described pigment enzymes of other fungi, reinforcing the hypothesis of the performance of this enzyme in essential melanization mechanisms in phytopathogenic fungi.

In contrast, mco5, even without signal peptide, is predicted to be an extracellular enzyme secreted by non-classical pathways. The presence of many predicted N-glycosylation sites and greater theoretical stability are common features found in secreted enzymes. The enzyme mco5 is located in cluster II of the MDS graph, near to the central region of the cluster, and between enzymes known as double laccase/ ferroxidase activity and laccases *sensu scricto*. Mco5 has all the exclusive signatures of laccase, presenting all the requirements to be a laccase *sensu scricto* of high potential redox (class 2). These two enzymes, because they are considerably different, can act preferentially in groups of different phenolic compounds, in a complementary way, increasing the spectrum of action of the extract of *C. cubensis*.

To test preliminarily the ability of predicted tridimensional models of *C. cubensis* to bond with phenolic compounds positioned close to copper T1, *in silico* interactions of synthetic substrates commonly used to validate the enzymatic activity of laccases were tested with predicted homology model mco2 and mco5. Molecular docking performed using the substrates 2,2'-azino-bis (3-ethylbenzothiazoline-6-sulfonic acid); 2,6-dimethoxyphenol acid; guaiacol and the protein models obtained by homology (**Fig. 8**) showed that the binding affinity of mco5 with ABTS; 2,6-dimethoxyphenol acid; and guaiacol, was -6.9 Kcal/mol; -3.8 Kcal/mol and -3.7 Kcal/mol, respectively. While the binding affinity of mco2 was -6.5 Kcal/mol, -4.0 Kcal/mol and -4.1 Kcal/mol, respectively. This demonstrates that mco2 and mco5 differ concerning their performance on different phenolic compounds. The enzyme mco2 has a higher binding affinity for mono-phenolic compounds; mco5 has a higher binding affinity for diphenolic compounds.

The preference for different types of phenolic compounds can allow a complementary performance of these two enzymes in the oxidation of phenolic compounds, amplifying the action of the *C. cubensis* enzymatic cocktail. Docking simulation with a larger spectrum of lignin model compounds is required to determine the differences in performance between mco2 and mco5. Further molecular dynamic simulation and corresponding wet lab experiments must be performed to understand the catalytic efficiencies of these fungal MCOs.

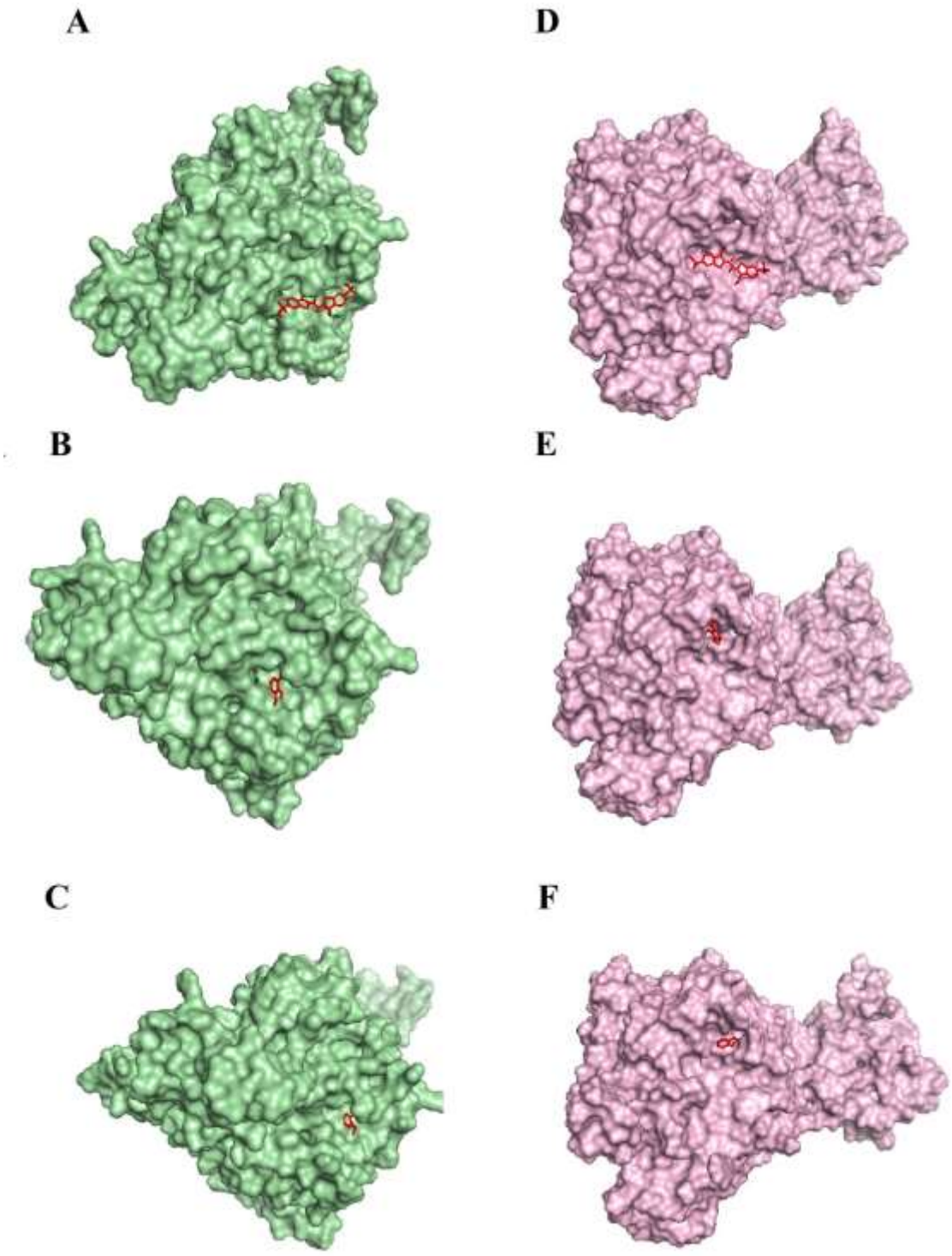

Figure 8: Poses of the molecular docking between mco2 (green) and mco5 (magenta and different substrates (red), using the module Autodock Vina integrated to the Pyrx. **A**) mco2 with ABTS. **B**) mco2 with 2,6-dimethoxyphenol. **C**) mco2 with guaiacol. **D**) mco5 with ABTS. **E**) mco5 with 2,6-dimethoxyphenol. **F)** mco5 with guaiacol.

3.6. Characterization of partially purified *C. cubensis* MCOs

3.6.1. Effects of ions and inhibitors

EDTA, sodium azide, dithiothreitol (DTT), fluoride ion and β-mercaptoethanol are described as laccase inhibitors (TIAN et al., 2014; SONDHI et al., 2014). EDTA practically did not inhibit the activity of *C. cubensis* MCOs obtained after purification steps. Sodium azide, DTT and β-mercaptoethanol completely inhibited, while NaF inhibited approximately 50% (**Table 6**).

Table 6: Effect of inhibitors and ions on laccase activity of *Chrysoporthe cubensis*.

Compound	Concentration (mM)	Relative activity (%)
Sodium azide	1	n.d.
DTT	1	n.d.
EDTA	1	98.8 ± 1.9
NaF	1	47.5 ± 3.8
β-Mercaptoethanol	1	n.d.
SDS	10	112.0 ± 5.9
$NaNO_3$	10	103.1 ± 3.5
KCl	10	94.3 ± 11.0
$HgCl_2$	10	71.4 ± 0.6
$CuSO_4$	10	86.9 ± 11.0
$CaCl_2$	10	91.0 ± 4.3
$MgCl_2$	10	104.0 ± 6.9
$ZnCl_2$	10	105.0 ± 5.1
$CoCl_2$	10	71.7 ± 0.9
Urea	10	102.0 ± 3.1

n.d: activity not detected

Inhibition of the activity by sodium azide can be justified because it is the metalloenzyme inhibitor azide ion, such as laccases, binding to copper sites of types 1 and 3 affecting the internal transfer of electrons, inhibiting its activity (Ryan et al., 2003). The inhibition by DTT and β-mercaptoethanol of the laccase activity can be explained by the fact that these molecules reduce disulfide bonds that stabilize the native structure of the enzymes making the laccases of *C. cubensis* nonfunctional (Sanagavarapu et al., 2016). The non-inhibition of *C. cubensis* laccases by EDTA agrees with reports of a significant reduction in the activity of this enzyme when using syringaldazine or dimethoxyphenol as a substrate, while no inhibition of ABTS oxidation was detected under the same experimental conditions (Lorenzo et al., 2006).

The interactions of metals with extracellular laccase are particularly important for the understanding of the biotechnological processes of xenobiotic degradation. More than 70% of laccase activity was maintained in the presence of Co^{2+} and Hg^{2+} heavy metal ions while 86-112% of laccase activity was observed in the presence of other evaluated ions (**Table 6**). Thus, *C. cubensis* MCOs showed resistance to inhibition by heavy metals, supporting their potential for use in industrial applications, such as bioremediation.

3.6.2. Effect of pH and temperature on laccase activity

The fraction obtained from ionic exchange enriched with MCOs showed the highest activity of these enzymes at pH 3.0 (**Fig. 9A**).

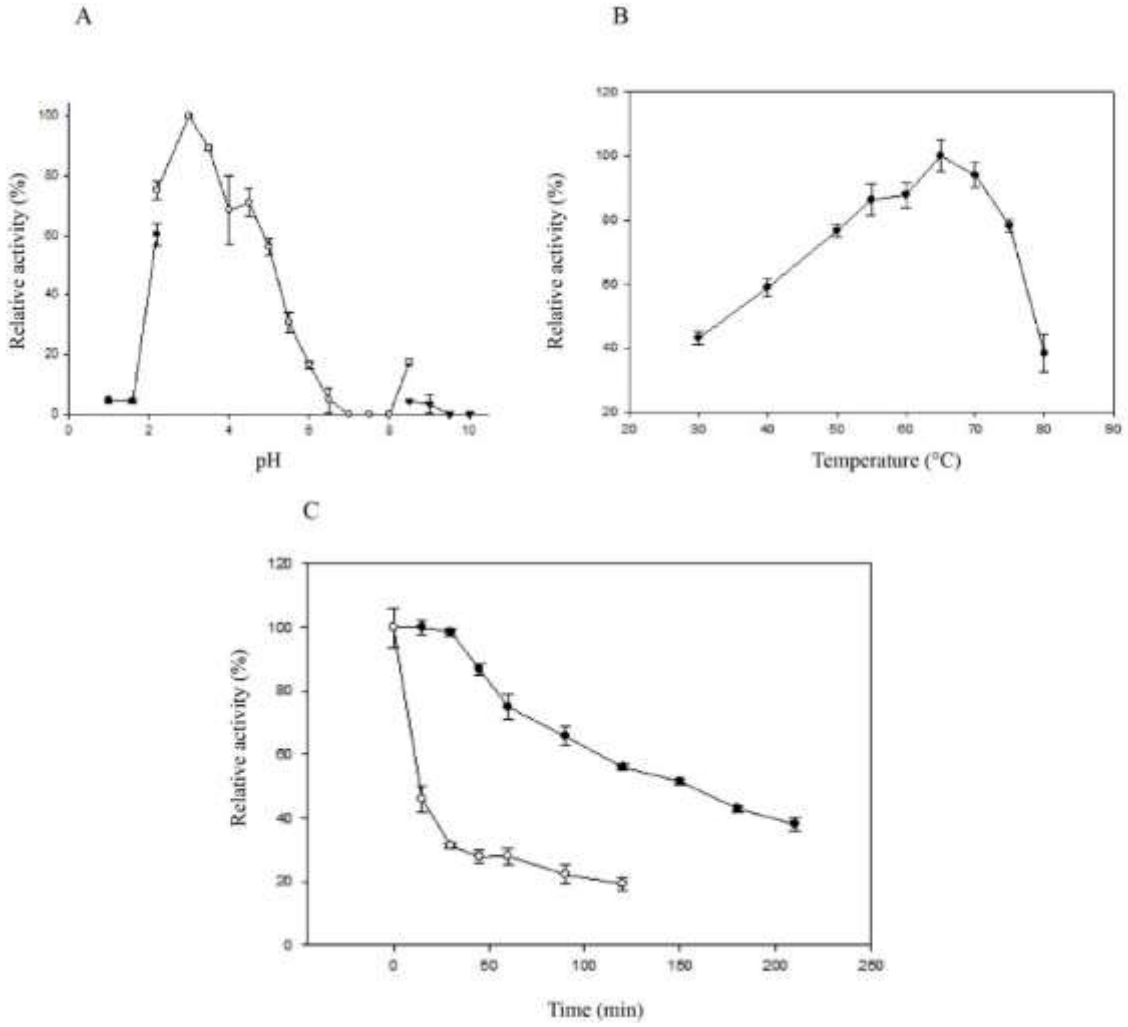

Figure 9: **A)** Effect of pH on the laccase activity of *C. cubensis*. The assays were performed in KCl – HCl buffer (●), McIlvaine buffer (○) and sodium borate buffer (▼). **B)** Effect of temperature on the laccase activity of *C. cubensis*. **C)** Thermostability of *C. cubensis* laccase activity at 65 ºC (○) and 50 ºC (●).

More than 70% of the activity was maintained between pH 2 and 4.5, evidencing the acidic character of *C. cubensis* MCOs. Above pH 6.4, laccase activity was low or non-existent confirming the acid character of the laccases secreted by this fungus. The acidic character of *C. cubensis* MCOs agreed with reports of *Trametes versicolor* and *Pycnoporus sanguineus* laccases with optimum pH of 3.0 and 2.5, respectively, using ABTS as a substrate (Bertrand et al., 2015). Higher pH values are checked when using other substrates. Although several factors influence enzyme activity, fungal laccases are generally stable at acid pH (Baldrian, 2006).

The fraction obtained from the ion exchange enriched with MCOs presented higher activity at 65 °C and retained more than 80% of the activity between 55 and 70 °C, using ABTS as substrate, showing that the MCOs of *C. cubensis* are active in a wide temperature range (**Fig. 9B**). These data agree with those of *Trematosphaeria mangrovei* and *Pycnoporus coccineus* laccases that had an optimum temperature of 65 °C (Atalla et al., 2013; Uzan et al., 2010). Besides, the MCOs detected in the sample had a half-life ($t_{1/2}$) of 175 minutes at 50 °C for this activity, higher than that of *Trematosphaeria mangrovei* laccase that was approximately 50 minutes (Atalla et al., 2013) (**Fig. 9C**). The high stability of *C. cubensis* MCOs at 50 °C is an important feature because it is used in biomass saccharification processes (Moreno et al., 2012). The half-life of the MCOs at 65 °C was 4.2 minutes demonstrating that they were not very stable at this temperature and agreeing with data for *T. mangrovei* and *T. versicolor* laccases, not stable at 65 °C (Asgher et al., 2012).

3.7. Effect of treatment with MCOs on the reduction of the phenolic compounds of the alkaline pre-treatment of sugarcane bagasse

Laccases have been applied in the detoxification of enzymatic hydrolysates of plant biomass reducing phenolic compounds, inhibitors of saccharification and fermentation processes (Chandel et al., 2012), but few studies have been carried out applying these enzymes in treatments before enzymatic hydrolysis.

The addition of *C cubensis* MCOs, obtained after partial purification steps, in media containing phenolic compounds generated by alkaline pretreatment of sugarcane bagasse reduced the concentration of these compounds by 91% (**Fig. 10**).

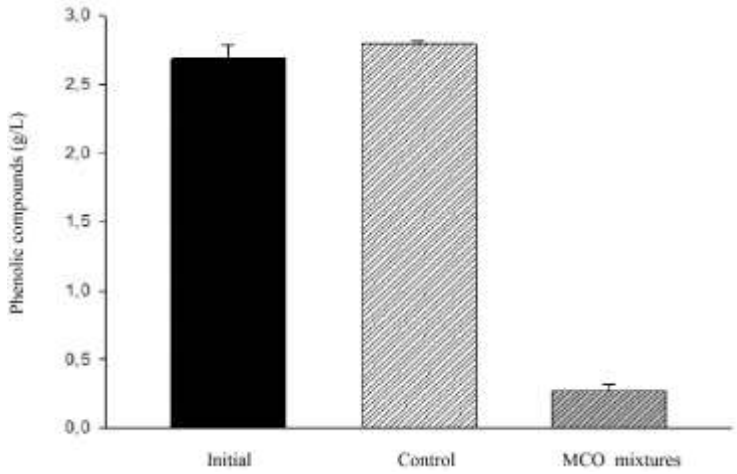

Figure 10: Concentration of phenolic compounds from the alkaline pretreatment of sugarcane bagasse in the reaction medium for saccharification treated or untreated (control) with *C. cubensis* MCO mixture.

This result is interesting because the phenolic compounds generated during the pretreatment processes of lignocellulosic materials are described as inhibitors and deactivators of enzymes that act on enzymatic hydrolysis, such as endoglucanases, cellobiohydrolases, and β-glucosidases (Kim et al., 2011). Phenolic compounds such as coumaric acid, ferulic acid, syringaldehyde, and vanillin, released from the alkaline pre-treatment of sugarcane bagasse, can inhibit and/or deactivate cellulolytic enzymes (Ximenes et al., 2011).

The saccharification of alkali pretreated sugarcane bagasse in medium containing phenolic compounds, treated or not treated with *C. cubensis* MCOs, showed glucose and xylose release of 6.38 and 1.15 g L^{-1} for the first, and 1.48 and 0.56 g L^{-1} for the second, respectively (**Fig. 11**).

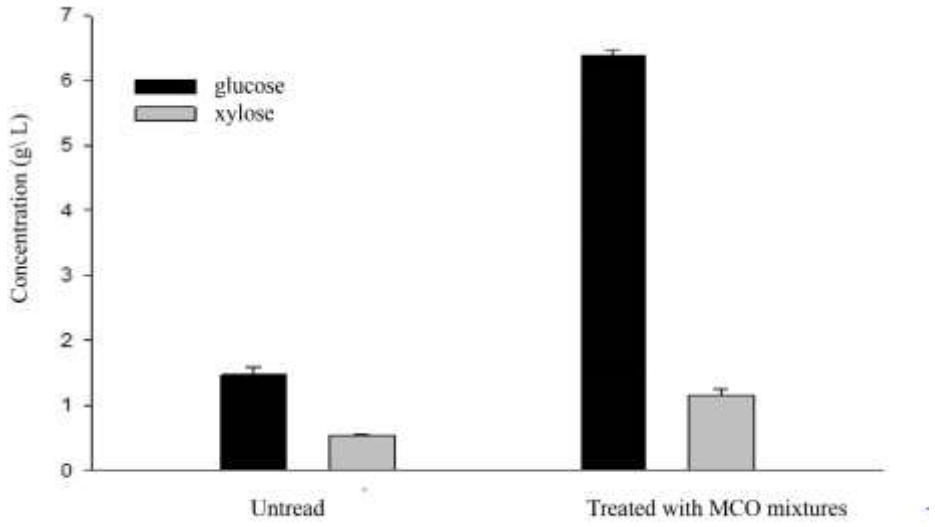

Figure 11: Glucose and xylose production after saccharification of sugarcane bagasse with commercial cellulase Accellerase® in pretreated or nontreated medium (control) with *C. cubensis* MCO mixture.

The higher efficiency in saccharification of the sugarcane bagasse after treatment with *C. cubensis* MCOs demonstrated the potential of these detoxifying medium with phenolic compounds of the alkaline pre-treatment of this material. MCOs of *C. cubensis* oxidizes phenolics to less toxic products for the enzymatic saccharification of sugarcane bagasse differing from reports of fungal laccases that oxidizes these compounds generating inhibitors of cellulolytic enzymes (Moilanen et al., 2011).

Free phenoxyl radicals and oligomeric phenolic compounds generated by laccase-catalyzed oxidation have been described as chemical structures that play an important role in enzymatic inhibition (Oliva-Taravilla et al., 2016). It is possible that *C. cubensis* MCOs do not oxidize phenolics to oligomeric and radical phenols described as inhibitors, not inhibiting the enzymatic hydrolysis process of cellulose.

C. cubensis MCOs catalyzed the oxidation of phenolic compounds, reducing the inhibition of enzymatic saccharification, demonstrating that these enzymes are promising for applications in enzymatic hydrolysis processes of lignocellulosic biomass by generating oxidation products less toxic to the process than those precursors. Additional studies are needed to identify the individual contribution of mco2 and mco5 in the reduction of inhibitory and/or deactivating phenolic compounds, and even to understand the complementary character that these two MCOs can have on a broad spectrum of phenolic compounds when they act together in the enzymatic extract of *C. cubensis*.

Complementary studies investigating *C. cubensis* MCOs potentially secreted under different conditions should be performed to prove the flexibility of secretion of this group and enzymes. Although *C. cubensis* has secreted 2 MCOs, this fungus is capable

of producing different MCOs among the predicted 13, depending on the cultivation conditions and the inductive carbon source. *C. cubensis* can secrete 3 MCOs when grown only in wheat bran, and 2 MCOs have characteristics of laccase *sensu scricto* (mco5 and mco12), as well as 1 ferroxidase (unpublished data). When this fungus was cultivated in sugarcane bagasse, two MCOs detected in wheat bran were also secreted, 1 ferroxidase and laccase mco12 (unpublished data). In this study, when this fungus was cultivated in wheat bran and orange peel (3: 1), 1 MCO was detected in common with the fungus grown in wheat bran (mco5), and 1 exclusive MCO of this condition (mco2), demonstrating that wheat bran is important for induction of mco5 and orange peel was essential for the induction of mco2 production. Thus, it is evident that *C. cubensis* can secrete different MCOs, which were predicted in this study, depending on the conditions under which it is submitted, having a great potential to secrete enzymes from this group.

Besides, this work allowed the identification of new promising targets that can be induced in other culture conditions or expressed heterologously and that, because of their diverse characteristics, may have applications in different biotechnological processes.

4. Conclusions

We characterized the *C. cubensis* multicopper oxidases using *in silico* analysis and found 13 distinct MCOs in the *C. cubensis* genome. These multicopper oxidases can be classified by sequence similarities and differentiated functionally in 3 of the 4 major groups previously identified in this study: the ferroxidases (mco8, mco9); the laccases/ferroxidases or *scricto sensu* laccases; (mco1, mco4, mco5, mco6, mco7, mco10, mco11, mco12, mco13) and the ascorbate oxidases or pigment oxidases (mco2, mco3). The modeling and substrate docking analyses showed a high affinity for typical laccase substrates for mco5 concerning mco2. The mixture containing mco2 and mco5, the main MCOs produced by this fungus grown in wheat bran and orange peel as carbon sources allowed us to confirm that these enzymes have high oxidation efficiency towards the phenolic compounds. This mixture containing actives MCOs that were able to detoxify phenolic compounds from the alkaline pretreatment of sugarcane bagasse improved the hydrolysis yields on the saccharification of that material. These results show the way for searching for laccase-type MCOs, with high biotechnological interest in fungal families, where the presence or function of these enzymes is poorly known.

Acknowledgments

We acknowledge the Brazilian institutions' CAPES for the scholarship granted to the first author and FAPEMIG and CNPq for the resources provided to complete this experiment. We also thank the Laboratory of Proteomics of the Multiuser Laboratories Center (CELAM - ICB), Federal University of Minas Gerais, by the support in the mass spectrometric analysis.

Supplementary material

E-supplementary data of this work can be found in the online version of the paper.

Competing interests

The authors declare that they have no competing interests.

Ethics approval and consent to participate

The authors declare that this study does not involve human subjects, human material and human subject.

References

1. Albarouki, E., Deising, H.B., 2013. Infection structure-specific reductive iron assimilation is required for cell wall integrity and full virulence of the maize pathogen *Colletotrichum graminicola*. Mol. Plant. Microbe. Interact. 26, 695–708. https://doi.org/10.1094/MPMI-01-13-0003-R

2. Andberg, M., Hakulinen, N., Auer, S., Saloheimo, M., Koivula, A., Rouvinen, J., Kruus, K., 2009. Essential role of the C-terminus in *Melanocarpus albomyces* laccase for enzyme production, catalytic properties and structure. FEBS J. 276, 6285–6300. https://doi.org/10.1111/j.1742-4658.2009.07336.x

3. Asgher, M., Iqbal, H., Javaid Asad, M., 2012. Kinetic characterization of purified laccase produced from *Trametes versicolor* IBL-04 in solid state-Bio-Processing of corncobs, Bioresources. https://doi.org/10.15376/biores.7.1.1171-1188

4. Atalla, M.M., Zeinab, H.K., Eman, R.H., Amani, A.Y., Abeer, A.A.E.A., 2013. Characterization and kinetic properties of the purified *Trematosphaeria mangrovei* laccase enzyme. Saudi J. Biol. Sci. 20, 373–381. https://doi.org/10.1016/j.sjbs.2013.04.001

5. Baldrian, P., 2006. Fungal laccases-occurrence and properties. FEMS Microbiol. Rev. 30, 215–242. https://doi.org/10.1111/j.1574-4976.2005.00010.x

6. Bertrand, B., Martínez-Morales, F., Tinoco-Valencia, R., Rojas, S., Acosta-Urdapilleta, L., Trejo-Hernández, M.R., 2015. Biochemical and molecular characterization of laccase isoforms produced by the white-rot fungus *Trametes versicolor* under submerged culture conditions. J. Mol. Catal. B Enzym. 122, 339–347. https://doi.org/https://doi.org/10.1016/j.molcatb.2015.10.009

7. Bradford, M.M., 1976. A rapid and sensitive method for the quantitation of microgram quantities of protein utilizing the principle of protein-dye binding. Anal. Biochem. 72, 248–254. https://doi.org/10.1016/0003-2697(76)90527-3

8. Budini, R., Tonelli, D., Girotti, S., 1980. Analysis of total phenols using the Prussian Blue Method, Journal of Agricultural and Food Chemistry - J AGR FOOD CHEM. https://doi.org/10.1021/jf60232a056

9. Cañero, D.C., Roncero, M.I.G., 2008. Functional analyses of laccase genes from *Fusarium oxysporum*. Phytopathology 98, 509–518. https://doi.org/10.1094/PHYTO-98-5-0509

10. Cázares-García, S.V., Vázquez-Garcidueñas, M.S., Vázquez-Marrufo, G., 2013. Structural and Phylogenetic Analysis of Laccases from Trichoderma: A Bioinformatic Approach. PLoS One 8. https://doi.org/10.1371/journal.pone.0055295

11. Chandel, A.K., da Silva, S.S., Carvalho, W., Singh, O. V, 2012. Sugarcane bagasse and leaves: foreseeable biomass of biofuel and bio-products. J. Chem. Technol. Biotechnol. 87, 11–20. https://doi.org/10.1002/jctb.2742

12. Combet, C., Blanchet, C., Geourjon, C., Deléage, G., 2000. NPS@: Network protein sequence analysis. Trends Biochem. Sci. 25, 147–150. https://doi.org/10.1016/S0968-0004(99)01540-6

13. Courty, P.E., Hoegger, P.J., Kilaru, S., Kohler, A., Buée, M., Garbaye, J., Martin, F., Kües, U., 2009. Phylogenetic analysis, genomic organization, and expression analysis of multi-copper oxidases in the ectomycorrhizal basidiomycete *Laccaria bicolor*. New Phytol. 182, 736–750. https://doi.org/10.1111/j.1469-8137.2009.02774.x

14. DeForte, S., Uversky, V.N., 2017. Not an exception to the rule: the functional significance of intrinsically disordered protein regions in enzymes. Mol. Biosyst. 13, 463–469. https://doi.org/10.1039/C6MB00741D

15. DeLano, W.L., 2002. PyMol: An Open-Source Molecular Graphics Tool. Ccp4.Ac.Uk.

16. Dundas, J., Ouyang, Z., Tseng, J., Binkowski, A., Turpaz, Y., Liang, J., 2006. CASTp: Computed atlas of surface topography of proteins with structural and topographical mapping of functionally annotated residues. Nucleic Acids Res. 34, 116–118. https://doi.org/10.1093/nar/gkl282

17. Dutra, T.R., Guimarães, V.M., Varela, E.M., Fialho, L. da S., Milagres, A.M.F., Falkoski, D.L., Zanuncio, J.C., Rezebde, S.T., 2017. A *Chrysoporthe cubensis* enzyme cocktail produced from a low-cost carbon source with high biomass hydrolysis efficiency. Sci. Rep. 7, 1–9. https://doi.org/10.1038/s41598-017-04262-y

18. Dyballa, N., Metzger, S., 2009. Fast and sensitive colloidal coomassie G-250 staining for proteins in polyacrylamide gels. J. Vis. Exp. 1431. https://doi.org/10.3791/1431

19. Edgar, R.C., 2004. MUSCLE: Multiple sequence alignment with high accuracy and high throughput. Nucleic Acids Res. 32, 1792–1797. https://doi.org/10.1093/nar/gkh340

20. Eggert, C., Lafayette, P.R., Temp, U., Dean, J.F.D., Eggert, C., Fayette, P.R.L.A., Temp, U., Eriksson, K.L., 1998. Molecular Analysis of a Laccase Gene from the White Rot Fungus *Pycnoporus cinnabarinus*. Appl. Environ. Microbiol. 64, 1766–1772.

21. Eichhorn, H., Lessing, F., Winterberg, B., Schirawski, J., Kamper, J., Muller, P., Kahmann, R., 2006. A Ferroxidation/Permeation Iron Uptake System Is Required for Virulence in *Ustilago maydis*. PLANT CELL ONLINE 18, 3332–3345. https://doi.org/10.1105/tpc.106.043588

22. Falkoski, D.L., Guimarães, V.M., de Almeida, M.N., Alfenas, A.C., Colodette, J.L., de Rezende, S.T., 2013. *Chrysoporthe cubensis*: A new source of cellulases and hemicellulases to application in biomass saccharification processes. Bioresour. Technol. 130, 296–305. https://doi.org/10.1016/j.biortech.2012.11.140

23. Feng, B.Z., Li, P.Q., Fu, L., Yu, X.M., 2015. Exploring laccase genes from plant pathogen genomes: A bioinformatic approach. Genet. Mol. Res. 14, 14019–14036. https://doi.org/10.4238/2015.October.29.21

24. Fernández-Larrea, J., Stahl, U., 1996. Isolation and characterization of a laccase gene from *Podospora anserina*. Mol. Gen. Genet. 252, 539–551. https://doi.org/10.1007/s004380050261

25. Germann, U.A., Muller, G., Hunziker, P.E., Lerch, K., 1988. Characterization of two allelic forms of *Neurospora crassa* laccase. Amino- and carboxyl-terminal processing of a precursor. J. Biol. Chem. 263, 885–896.

26. Giacobbe, S., Pezzella, C., Lettera, V., Sannia, G., Piscitelli, A., 2018. Laccase pretreatment for agrofood wastes valorization. Bioresour. Technol. 265, 59–65. https://doi.org/https://doi.org/10.1016/j.biortech.2018.05.108

27. Giardina, P., Faraco, V., Pezzella, C., Piscitelli, A., Vanhulle, S., Sannia, G., 2010. Laccases: A never-ending story. Cell. Mol. Life Sci. 67, 369–385. https://doi.org/10.1007/s00018-009-0169-1

28. Giese, E., Dekker, R., Barbosa, A., 2008. Orange bagasse as substrate for the production of pectinase and laccase by *Botryosphaeria rhodina* MAMB-05 in submerged and solid state fermentation, Bioresources. https://doi.org/10.13140/2.1.2204.7688

29. Gill, S.C., von Hippel, P.H., 1989. Calculation of protein extinction coefficients from amino acid sequence data. Anal. Biochem. 182, 319–326. https://doi.org/10.1016/0003-2697(89)90602-7

30. Guruprasad, K., Reddy, B.V.B., Pandit, M.W., 1990. Correlation between stability of a protein and its dipeptide composition: a novel approach for predicting *in vivo* stability of a protein from its primary sequence. Protein Eng. Des. Sel. 4, 155–161. https://doi.org/10.1093/protein/4.2.155

31. Hakulinen, N., Andberg, M., Kallio, J., Koivula, A., Kruus, K., Rouvinen, J., 2008. A near atomic resolution structure of a *Melanocarpus albomyces* laccase. J. Struct. Biol. 162, 29–39. https://doi.org/10.1016/j.jsb.2007.12.003

32. Hakulinen, N., Kiiskinen, L.-L., Kruus, K., Saloheimo, M., Paananen, A., Koivula, A., Rouvinen, J., 2002. Crystal structure of a laccase from *Melanocarpus albomyces* with an intact trinuclear copper site. Nat. Struct. Biol. 9, 601–605. https://doi.org/10.1038/nsb823

33. Hoegger, P.J., Kilaru, S., James, T.Y., Thacker, J.R., Kües, U., 2006. Phylogenetic comparison and classification of laccase and related multicopper oxidase protein sequences. FEBS J. 273, 2308–2326. https://doi.org/10.1111/j.1742-4658.2006.05247.x

34. Ikai, A., 1980. Thermostability and aliphatic index of globular proteins. J. Biochem. 1898, 1895–1898. https://doi.org/10.1017/CBO9781107415324.004

35. Jain, P., Podila, G.K., Davis, M.R., 2008. Comparative analysis of non-classically secreted proteins in *Botrytis cinerea* and symbiotic fungus *Laccaria bicolor*. BMC Bioinformatics 9, O3. https://doi.org/10.1186/1471-2105-9-S10-O3

36. Kallio, J.P., Gasparetti, C., Andberg, M., Boer, H., Koivula, A., Kruus, K., Rouvinen, J., Hakulinen, N., 2011. Crystal structure of an ascomycete fungal laccase from *Thielavia arenaria* - Common structural features of asco-laccases. FEBS J. 278, 2283–2295. https://doi.org/10.1111/j.1742-4658.2011.08146.x

37. Kanagaraj, J., Senthilvelan, T., Panda, R., 2015. Degradation of azo dyes by laccase: Biological method to reduce pollution load in dye wastewater. Clean Technologies and Environmental Policy. https://doi.org/10.1007/s10098-014-0869-6

38. Kaur, K., Sharma, A., Capalash, N., Sharma, P., 2019. Multicopper oxidases: Biocatalysts in microbial pathogenesis and stress management. Microbiol. Res. 222,

1–13. https://doi.org/10.1016/j.micres.2019.02.007

39. Kelly, L.A., Mezulis, S., Yates, C., Wass, M., Sternberg, M., 2015. The Phyre2 web portal for protein modelling, prediction, and analysis. Nat. Protoc. 10, 845–858. https://doi.org/10.1038/nprot.2015-053

40. Kiiskinen, L., Saloheimo, M., 2004. Molecular Cloning and Expression in *Saccharomyces cerevisiae* of a Laccase Gene from the Ascomycete *Melanocarpus albomyces*. Appl. Environ. Microbiol. 70, 137–144. https://doi.org/10.1128/AEM.70.1.137

41. Kiiskinen, L.L., Viikari, L., Kruus, K., 2002. Purification and characterisation of a novel laccase from the ascomycete *Melanocarpus albomyces*. Appl. Microbiol. Biotechnol. 59, 198–204. https://doi.org/10.1007/s00253-002-1012-x

42. Kim, Y., Ximenes, E., Mosier, N.S., Ladisch, M.R., 2011. Soluble inhibitors/deactivators of cellulase enzymes from lignocellulosic biomass. Enzyme Microb. Technol. 48, 408–415. https://doi.org/https://doi.org/10.1016/j.enzmictec.2011.01.007

43. Krieger, E., Joo, K., Lee, J., Lee, J., Raman, S., Thompson, J., Tyka, M., Baker, D., Karplus, K., 2009. Improving physical realism, stereochemistry, and side-chain accuracy in homology modeling: Four approaches that performed well in CASP8. Proteins Struct. Funct. Bioinforma. 77, 114–122. https://doi.org/10.1002/prot.22570

44. Kues, U., Ruhl, M., 2011. Multiple Multi-Copper Oxidase Gene Families in Basidiomycetes – What for? Curr. Genomics 12, 72–94. https://doi.org/10.2174/138920211795564377

45. Kumar, S.V.S., Phale, P.S., Durani, S., Wangikar, P.P., 2003. Combined sequence and structure analysis of the fungal laccase family. Biotechnol. Bioeng. 83, 386–394. https://doi.org/10.1002/bit.10681

46. Kyte, J., Doolittle, R.F., 1982. A simple method for displaying the hydropathic character of a protein. J. Mol. Biol. 157, 105–132. https://doi.org/10.1016/0022-2836(82)90515-0

47. Laemmli, U.K., 1970. Cleavage of Structural Proteins during the Assembly of the Head of Bacteriophage T4. Nature 227, 680–685.

48. Larrondo, L.F., Salas, L., Melo, F., Vicuña, R., Cullen, D., 2003. A Novel Extracellular Multicopper Oxidase from *Phanerochaete chrysosporium* with Ferroxidase Activity. Appl. Environ. Microbiol. 69, 6257–6263. https://doi.org/10.1128/AEM.69.10.6257-6263.2003

49. Levasseur, A., Drula, E., Lombard, V., Coutinho, P.M., Henrissat, B., 2013. Expansion of the enzymatic repertoire of the CAZy database to integrate auxiliary redox enzymes. Biotechnol. Biofuels 6, 41. https://doi.org/10.1186/1754-6834-6-41

50. Lieutaud, P., Ferron, F., Uversky, A. V., Kurgan, L., Uversky, V.N., Longhi, S., 2016. How disordered is my protein and what is its disorder for? A guide through the "dark side" of the protein universe. Intrinsically Disord. Proteins 4, e1259708. https://doi.org/10.1080/21690707.2016.1259708

51. Linke, D., Omarini, A.B., Takenberg, M., Kelle, S., Berger, R.G., 2019. Long-Term Monokaryotic Cultures of *Pleurotus ostreatus var. florida* Produce High and Stable Laccase Activity Capable to Degrade ss-Carotene. Appl. Biochem. Biotechnol. 187, 894–912. https://doi.org/10.1007/s12010-018-2860-x

52. Liu, L., Tewari, R.P., Williamson, P.R., 1999. Laccase protects *Cryptococcus neoformans* from antifungal activity of alveolar macrophages. Infect. Immun. 67, 6034–6039.

53. Lorenzo, M., Moldes, D., Sanromán, M., 2006. Effect of Heavy Metals on the Production of Several Laccase Isoenzymes by *Trametes versicolor* and on Their Ability to Decolourise Dyes, Chemosphere. https://doi.org/10.1016/j.chemosphere.2005.09.046

54. Madhavi, V., Lele, S.S., 2009. Laccase: Properties and applications. BioResources 4, 1694–1717. https://doi.org/10.15376/biores.4.4.1694-1717

55. Maestre-Reyna, M., Liu, W.C., Jeng, W.Y., Lee, C.C., Hsu, C.A., Wen, T.N., Wang, A.H.J., Shyur, L.F., 2015. Structural and functional roles of glycosylation in fungal laccase from lentinus sp. PLoS One 10, 1–28. https://doi.org/10.1371/journal.pone.0120601

56. Maitan-Alfenas, G.P., Visser, E.M., Alfenas, R.F., Nogueira, B.R.G., de Campos, G.G., Milagres, A.F., de Vries, R.P., Guimarães, V.M., 2015. The influence of pretreatment methods on saccharification of sugarcane bagasse by an enzyme extract from *Chrysoporthe cubensis* and commercial cocktails: A comparative study. Bioresour. Technol. 192, 670–6. https://doi.org/10.1016/j.biortech.2015.05.109

57. Merril, C.R., Bisher, M.E., Harrington, M., Steven, A.C., 1988. Coloration of silver-stained protein bands in polyacrylamide gels is caused by light scattering from silver grains of characteristic sizes. Proc. Natl. Acad. Sci. U. S. A. 85, 453–457. https://doi.org/10.1073/pnas.85.2.453

58. Moilanen, U., Kellock, M., Galkin, S., Viikari, L., 2011. The laccase-catalyzed modification of lignin for enzymatic hydrolysis. Enzyme Microb. Technol. 49, 492–498. https://doi.org/https://doi.org/10.1016/j.enzmictec.2011.09.012

59. Moreno, A.D., Ibarra, D., Fernández, J.L., Ballesteros, M., 2012. Different laccase detoxification strategies for ethanol production from lignocellulosic biomass by the thermotolerant yeast *Kluyveromyces marxianus* CECT 10875. Bioresour. Technol. 106, 101–109. https://doi.org/https://doi.org/10.1016/j.biortech.2011.11.108

60. Moreno, L.F., Feng, P., Weiss, V.A., Vicente, V.A., Stielow, J.B., De Hoog, S., 2017. Phylogenomic analyses reveal the diversity of laccase-coding genes in Fonsecaea genomes. PLoS One 12, 1–17. https://doi.org/10.1371/journal.pone.0171291

61. Morozova, O. V., Shumakovich, G.P., Gorbacheva, M.A., Shleev, S. V., Yaropolov, A.I., 2007. "Blue" laccases. Biochem. 72, 1136–1150. https://doi.org/10.1134/S0006297907100112

62. Nickel, W., Seedorf, M., 2008. Unconventional Mechanisms of Protein Transport to the Cell Surface of Eukaryotic Cells. Annu. Rev. Cell Dev. Biol. 24, 287–308. https://doi.org/10.1146/annurev.cellbio.24.110707.175320

63. Nombela, C., Gil, C., Chaffin, W.L.J., 2006. Non-conventional protein secretionin yeast. Trends Microbiol. 14, 15–21. https://doi.org/10.1016/j.tim.2005.11.009

64. Oliva-Taravilla, A., Tomas-Pejo, E., Demuez, M., Gonzalez-Fernandez, C., Ballesteros, M., 2016. Phenols and lignin: Key players in reducing enzymatic hydrolysis yields of steam-pretreated biomass in presence of laccase. J. Biotechnol. 218, 94–101. https://doi.org/10.1016/j.jbiotec.2015.11.004

65. Park, Y., Kim, J.-H., Cho, J., Chang, H., Kim, S.-W., Paik, H., Kang, C.-W., Kim, T., Sung, H., Yun, C., 2007. Physical and functional interaction of FgFtr1-FgFet1 and FgFtr2-FgFet2 is required for iron uptake in *Fusarium graminearum*. Biochem. J. 408, 97–104. https://doi.org/10.1042/BJ20070450

66. Rodríguez-Rincón, F., Suarez, A., Lucas, M., Larrondo, L.F., De La Rubia, T., Polaina, J., Martínez, J., 2010. Molecular and structural modeling of the *Phanerochaete flavido-alba* extracellular laccase reveals its ferroxidase structure. Arch. Microbiol. 192, 883–892. https://doi.org/10.1007/s00203-010-0616-2

67. Rogers, S., Wells, R., Rechsteiner, M., 1986. Amino acid sequences common to rapidly degraded proteins: the PEST hypothesis. Science (80-.). 234, 364–368. https://doi.org/10.1126/science.2876518

68. Rosales, E., Rodriguez-Couto, S., Sanromán, M., 2007. Increased Laccase Production by *Trametes hirsuta* Grown on Ground Orange Peelings, Enzyme and Microbial Technology. https://doi.org/10.1016/j.enzmictec.2006.09.015

69. Ryan, S., Schnitzhofer, W., Tzanov, T., Cavaco-Paulo, A., Gübitz, G.M., 2003. An acid-stable laccase from *Sclerotium rolfsii* with potential for wool dye decolourization. Enzyme Microb. Technol. 33, 766–774. https://doi.org/https://doi.org/10.1016/S0141-0229(03)00162-5

70. Sanagavarapu, K., Weiffert, T., Ní Mhurchú, N., O'Connell, D., Linse, S., 2016. Calcium Binding and Disulfide Bonds Regulate the Stability of Secretagogin towards Thermal and Urea Denaturation. PLoS One 11, e0165709.

71. Stanke, M., Morgenstern, B., 2005. AUGUSTUS: A web server for gene prediction in eukaryotes that allows user-defined constraints. Nucleic Acids Res. 33, 465–467. https://doi.org/10.1093/nar/gki458

72. Tamayo Ramos, J.A., Barends, S., Verhaert, R.M., de Graaff, L.H., 2011. The *Aspergillus niger* multicopper oxidase family: analysis and overexpression of laccase-like encoding genes. Microb. Cell Fact. 10, 78. https://doi.org/10.1186/1475-2859-1078

73. Tamboli, A.S., Rane, N.R., Patil, S.M., Biradar, S.P., 2015. Physicochemical characterization , structural analysis and homology modeling of bacterial and fungal laccases using in silico methods. Netw. Model. Anal. Heal. Informatics Bioinforma. 4, 1–12. https://doi.org/10.1007/s13721-015-0089-y

74. Taylor, A.B., Stoj, C.S., Ziegler, L., Kosman, D.J., Hart, P.J., 2005. The copper-iron connection in biology: structure of the metallo-oxidase Fet3p. Proc. Natl. Acad. Sci. U. S. A. 102, 15459–64. https://doi.org/10.1073/pnas.0506227102

75. Tetsch, L., Bend, J., Hölker, U., 2006. Molecular and enzymatic characterisation of

extra- and intracellular laccases from the acidophilic ascomycete *Hortaea acidophila*. Antonie van Leeuwenhoek, Int. J. Gen. Mol. Microbiol. 90, 183–194. https://doi.org/10.1007/s10482-006-9064-z

76. Trubitsina, L.I., Tishchenko, S., Gabdulkhakov, A., Lisov, A. V, Zakharova, M. V, Leontievsky, A.A., 2015. Structural and functional characterization of two-domain laccase from *Streptomyces viridochromogenes*, Biochimie. https://doi.org/10.1016/j.biochi.2015.03.005

77. Tuyen, V.D., Cone, J.W., Baars, J.J.P., Sonnenberg, A.S.M., Hendriks, W.H., 2012. Fungal strain and incubation period affect chemical composition and nutrient availability of wheat straw for rumen fermentation. Bioresour. Technol. 111, 336–342. https://doi.org/10.1016/j.biortech.2012.02.001

78. Uzan, E., Nousiainen, P., Balland, V., Sipila, J., Piumi, F., Navarro, D., Asther, M., Record, E., Lomascolo, A., 2010. High redox potential laccases from the ligninolytic fungi *Pycnoporus coccineus* and *Pycnoporus sanguineus* suitable for white biotechnology: from gene cloning to enzyme characterization and applications. J. Appl. Microbiol. 108, 2199–2213. https://doi.org/10.1111/j.1365-2672.2009.04623.x

79. Visser, E.M., Leal, T.F., de Almeida, M.N., Guimarães, V.M., 2015. Increased enzymatic hydrolysis of sugarcane bagasse from enzyme recycling. Biotechnol. Biofuels 8, 1–9. https://doi.org/10.1186/s13068-014-0185-8

80. Viswanath, B., Rajesh, B., Janardhan, A., Kumar, A.P., Narasimha, G., 2014. Fungal laccases and their applications in bioremediation. Enzyme Res. 2014. https://doi.org/10.1155/2014/163242

81. Vite-Vallejo, O., Palomares, L.A., Dantán-González, E., Ayala-Castro, H.G., Martínez-Anaya, C., Valderrama, B., Folch-Mallol, J., 2009. The role of N-glycosylation on the enzymatic activity of a *Pycnoporus sanguineus* laccase. Enzyme Microb. Technol. 45, 233–239. https://doi.org/10.1016/j.enzmictec.2009.05.007

82. Wang, S.-S., Ning, Y.-J., Wang, S.-N., Zhang, J., Zhang, G.-Q., Chen, Q.-J., 2017. Purification, characterization, and cloning of an extracellular laccase with potent dye decolorizing ability from white rot fungus *Cerrena unicolor* GSM-01. Int. J. Biol. Macromol. 95, 920–927. https://doi.org/10.1016/j.ijbiomac.2016.10.079

83. Wilkins, M.R., Gasteiger, E., Bairoch, A., Sanchez, J., Williams, K.L., Appel, R.D., Hochstrasser, D.F., 2005. Protein Identification and Analysis Tools in the ExPASy Server. Methods Mol. Biol. 112, 531–552. https://doi.org/10.1385/1592595847

84. Ximenes, E., Kim, Y., Mosier, N., Dien, B., Ladisch, M., 2011. Deactivation of cellulases by phenols. Enzyme Microb. Technol. 48, 54–60. https://doi.org/https://doi.org/10.1016/j.enzmictec.2010.09.006

85. Yan, J., Chen, D., Yang, E., Niu, J., Chen, Y., Chagan, I., 2014. Purification and characterization of a thermotolerant laccase isoform in *Trametes trogii* strain and its potential in dye decolorization. Int. Biodeterior. Biodegradation 93, 186–194. https://doi.org/https://doi.org/10.1016/j.ibiod.2014.06.001

86. Yuan, X., Tian, G., Zhao, Y., Zhao, L., Wang, H., Ng, T.B., 2016. Biochemical Characteristics of Three Laccase Isoforms from the Basidiomycete *Pleurotus nebrodensis*. Molecules 21. https://doi.org/10.3390/molecules21020203

Supplementary material

The first characterization of the *Chrysoporthe cubensis* multicopper oxidase enzymes: production and application in the oxidation of phenolic compounds formed during pretreatment of sugarcane bagasse

Supplementary figures

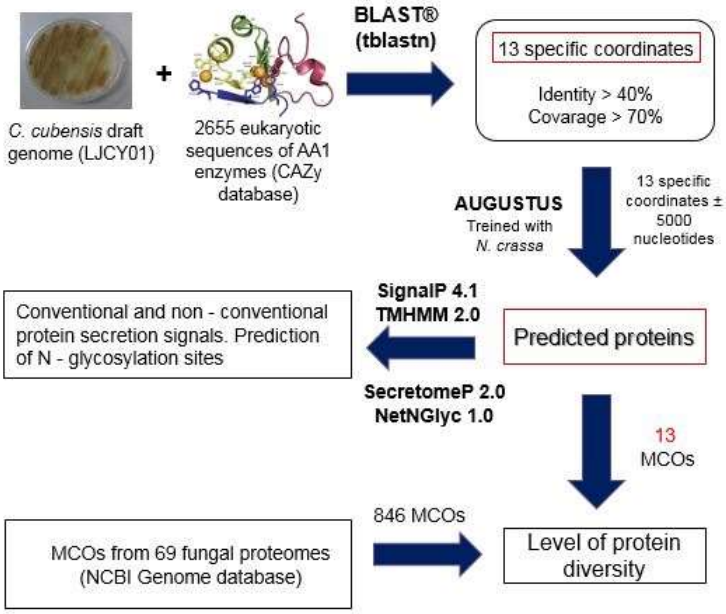

Figure S1: Stages of *in silico* prediction of *C.cubensis* AA1 family proteins.

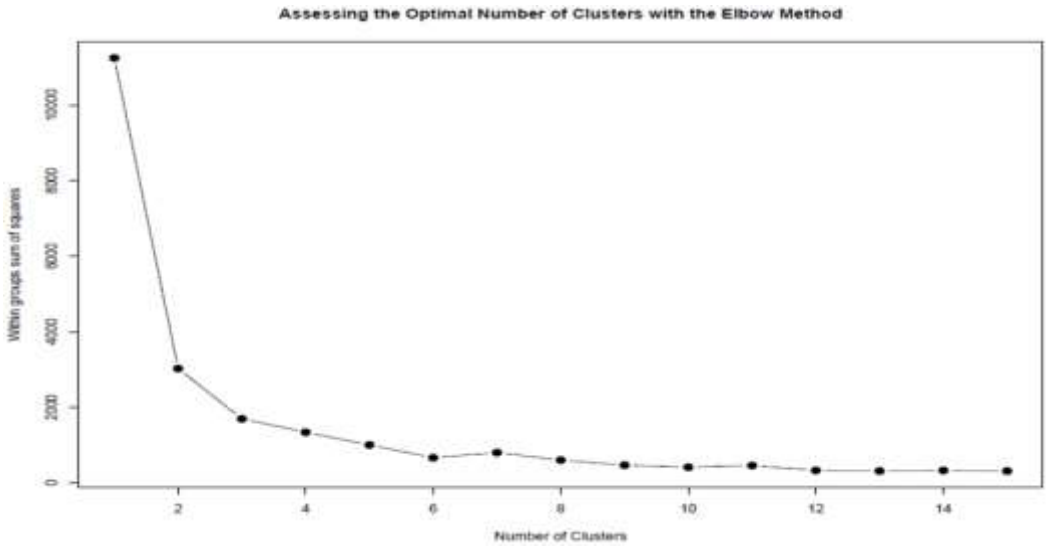

Figure S2: Elbow method for defining the number of clusters.

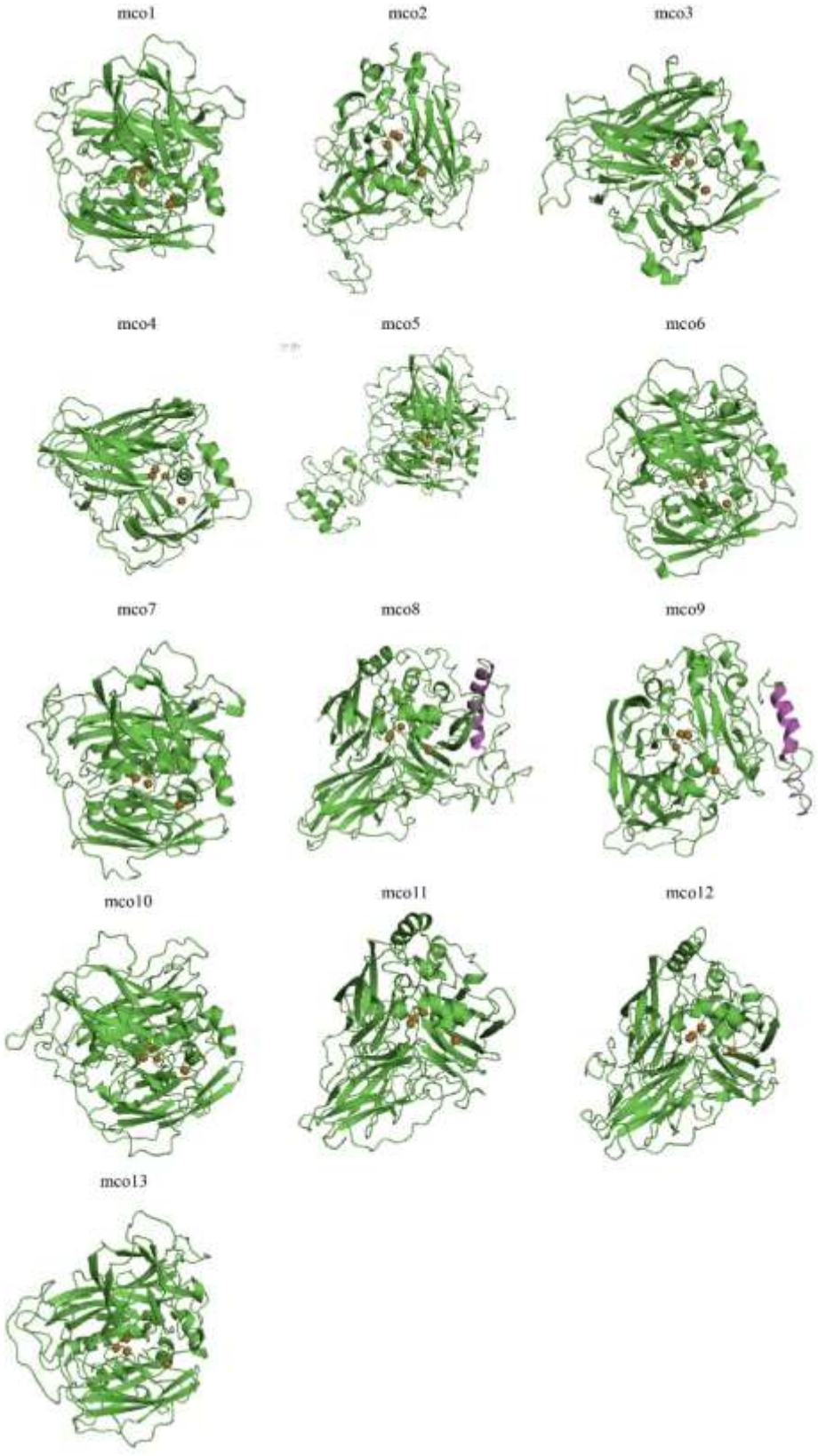

Figure S3: Three-dimensional models of the 13 multi-copper oxidases obtained by homology modeling using the Phyre2 program. The 4 copper atoms were represented by orange spheres.

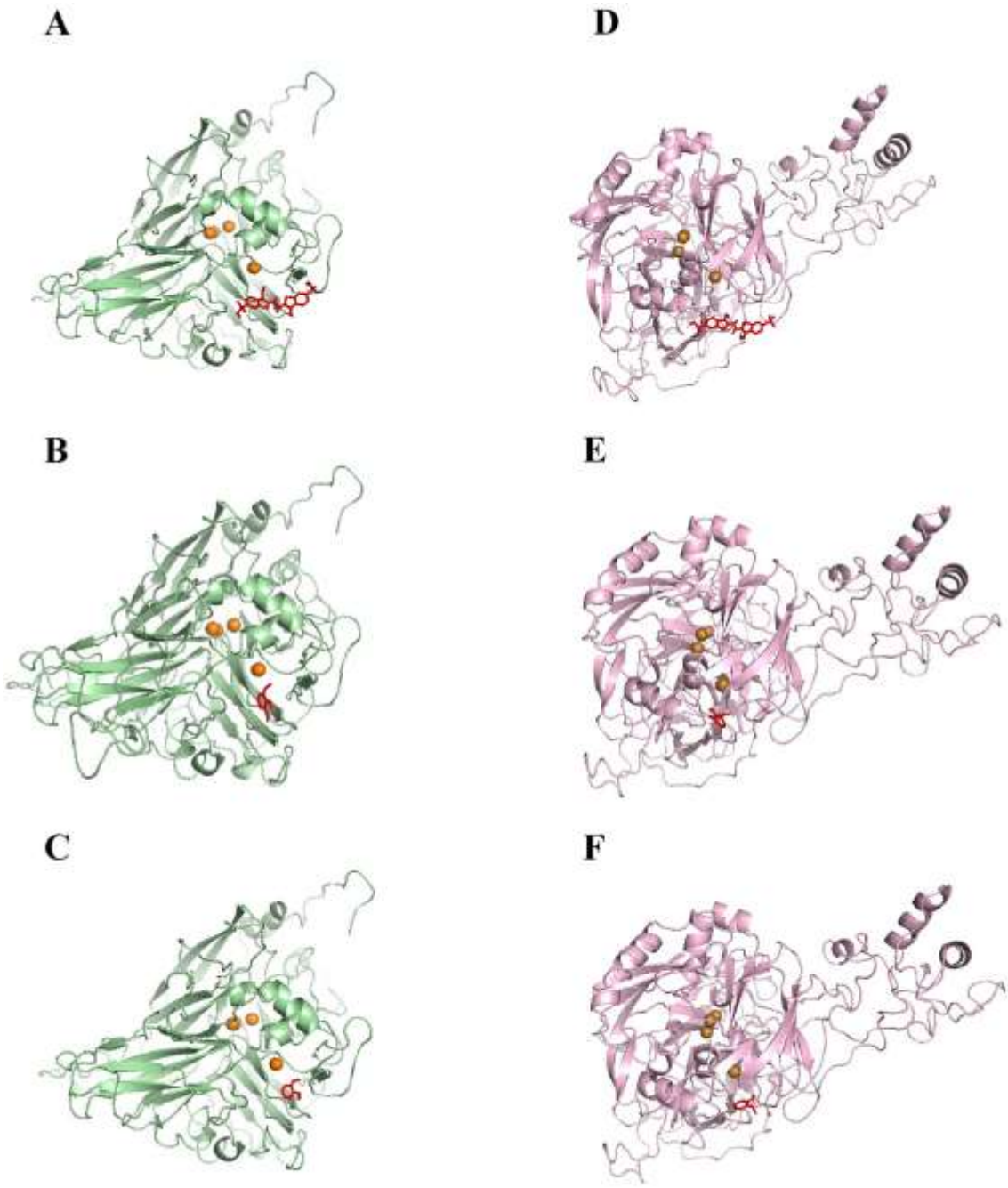

Figure S4: Poses of the molecular docking between mco2 (green) and mco5 (magenta and different substrates (red), using the module Autodock Vina integrated to the Pyrx. Oranges balls represent copper atoms. A) mco2 with ABTS. B) mco2 with 2,6-dimethoxyphenol. C) mco2 with guaiacol. D) mco5 with ABTS. E) mco5 with 2,6-dimethoxyphenol. F) mco5 with guaiacol.

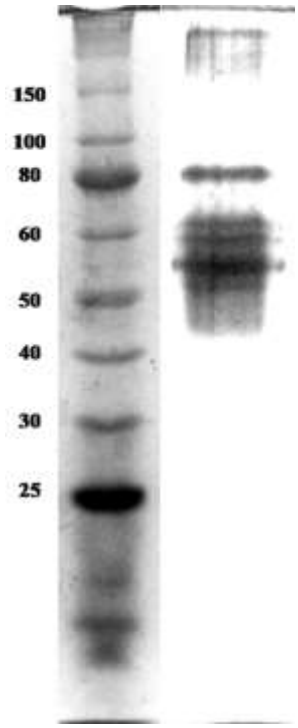

Figure S5: Silver-stained SDS-PAGE, with the proteins extracted from the zymogram laccase activity region.

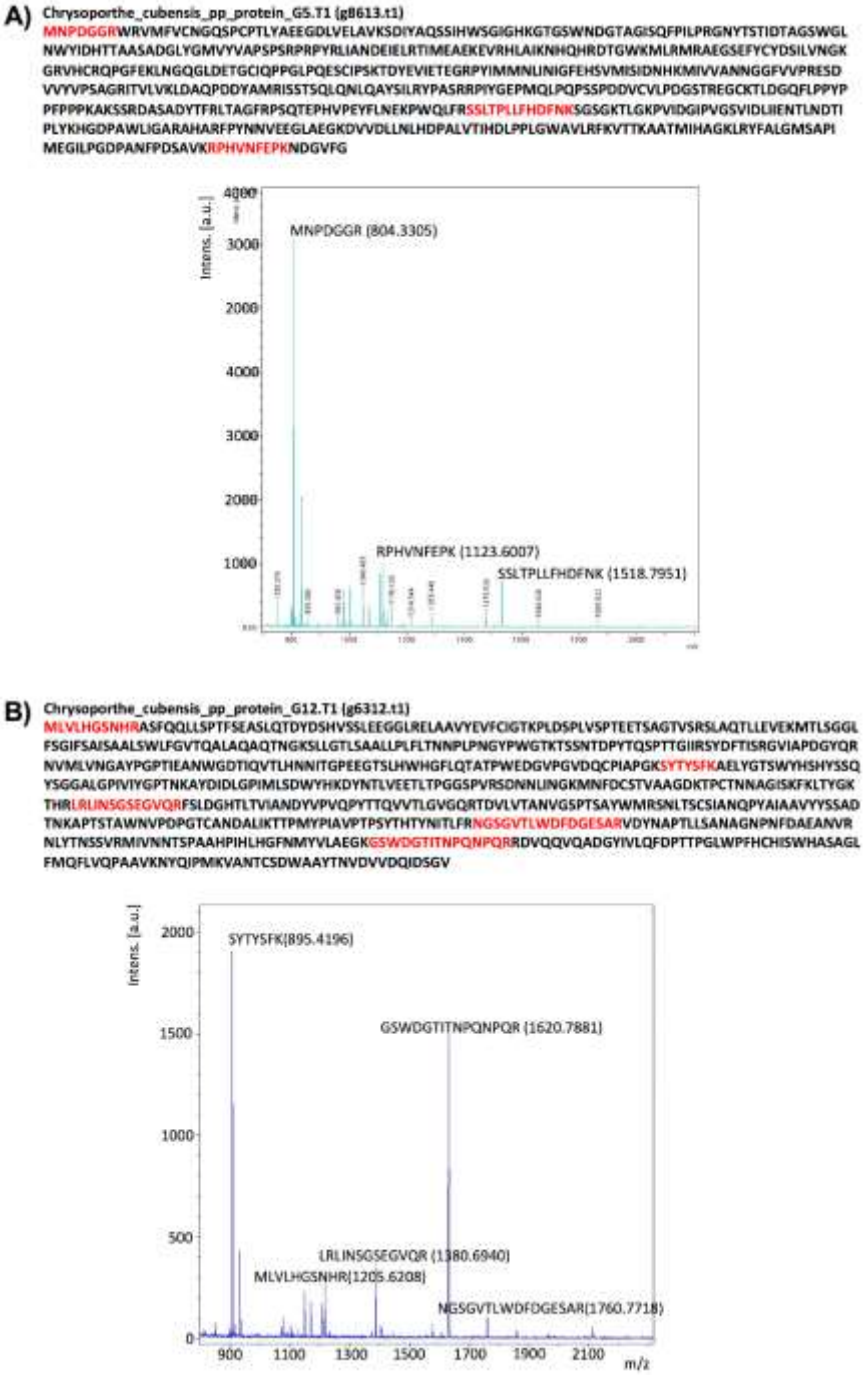

Figure S6: Peptide Mass Fingerprinting (PMF) analysis and ions searching against *in house* database of *C. cubensis* proteins. A) Chromatogram of mco2 protein, with 3 unique peptides detected. B) Chromatogram of mco5 protein, with 5 unique peptides detected.

Supplementary Tables

Table S1: Secondary structure elements calculated using SOPMA tool.

Predicted proteins	Alpha helix (%)	Extended strands (%)	Beta turn (%)	Random coil (%)
mco 1	23.54	31.15	10.80	34.51
mco 2	12.91	28.97	11.34	46.77
mco 3	15.79	30.13	13.97	40.11
mco 4	12.80	35.20	11.00	41.00
mco 5	19.97	25.66	10.79	43.59
mco 6	10.67	24.36	5.25	59.71
mco 7	17.92	28.88	9.32	43.88
mco 8	19.52	30.00	9.84	40.63
mco 9	17.12	31.19	10.17	41.53
mco 10	12.54	34.15	9.58	43.73
mco 11	16.43	33.92	10.66	38.99
mco 12	13.26	34.40	12.25	40.10
mco 13	19.86	30.76	8.96	40.42

Table S2: RMS values (Å) obtained on the overlap of *C. cubensis* MCOs with the *S. cerevisiae* Fet3p ferroxidase (PDB: 1ZPU) or *M. albomyces* laccase (PDB: 2Q9O), using Pymol. The 3D models of the predicted ferroxidases were superimposed with crystallographic structure 1ZPU, while the other 3D models were superimposed with the crystallographic

	2Q9O	1ZPU
Cc1mco1	0,656	-
Cc1mco2	1,627	-
Cc1mco3	1,452	-
Cc1mco4	0,730	-
Cc1mco5	0,811	-
Cc1mco6	1,223	-
Cc1mco7	0,810	-
Cc1mco8	-	0,541
Cc1mco9	-	0,960
Cc1mco10	0,965	-
Cc1mco11	0,658	-
Cc1mco12	0,905	-
Cc1mco13	0,985	-

Table S3: Quality parameters of predicted 3D models of the 13 MCOs of *C. cubensis* after the energy minimization step.

After the energy minimization step	mco1	mco2	mco3	mco4	mco5	mco6	mco7	mco8	mco9	mco10
Ramachandran graphic (RAMPAGE)										
Residues in favorable region (~98.0%)	511 (93.8%)	493 (86.3%)	490 (92.5%)	447 (92.7%)	628 (91.8%)	1141 (85.8%)	502 (92.1%)	570 (94.4%)	503 (89.2%)	529 (95.1%)
Residues in allowed region (~2.0%)	30 (5.5%)	54 (9.5%)	34 (6.4%)	28 (5.8%)	38 (5.6%)	135 (10.2%)	35 (6.4%)	31 (5.1%)	44 (7.8%)	23 (4.1%)
Residues in prohibit region	4 (0.7%)	24 (4.2%)	6 (1.1%)	7 (1.5%)	18 (2.6%)	54 (4.1%)	8 (1.5%)	3 (0.5%)	17 (3.0%)	4 (0.7%)
Global quality model (ProSA-web)										
Z-score	-6,67	-6	-5,99	-6,31	-6,93	-5,52	-6,36	-7,04	-7,61	-7,04
PROCHECK										
Distorted links of the main chain	0	0	0	0	0	0	0	0	0	0
Distorted angles of the main chain	0	0	0	0	0	0	0	0	0	0
Distorted planar groups	0	0	0	0	0	0	0	0	0	0
Verify 3D										
Residues with score 3D/1D >= 0.2	81.35%	87.26%	75.75%	76.86%	83.97%	0.00%	88.48%	85.48%	88.52%	85.48%
ERRAT2										
Quality global factor	89,159	83,582	83,915	88,347	79,228	75,021	82,156	85,74	79,137	87,636

Table S4: Predicted cavities for 3D models using the CASTp tool.

MCOs	Nº pockets	Nº nearest pocket to the T1 active site	Area (Å²)	Volume (Å³)	Nº residues in the pocket	Amino acids cluster that made-up the pockets were principally apolars (red)
G3	112	108	329,7	374,7	23	SER192, ASN195, GLY196, PRO197, PRO198, THR199, ASP243, HIS245, ALA303, CYS304, SER305, ASP306, ASN307, ILE370, LEU377, TRP379, MET429, VAL431, PRO432, ILE496, TRP498, HIS499, GLU502
G5	121	120	710.9	735,9	39	ALA97, ALA100, ASN146, GLN148, THR152, LYS155, MET156, MET159, ARG160, SER164, GLU165, PHE166, TYR167, CYS168, TYR169, PHE238, GLU239, HIS240, SER241, TYR270, THR297, SER298, GLN299,
G6	108	101	242,5	365,3	14	THR174, ILE177, PRO178, ARG316, PHE384, VAL386, ASN392, ALA446, VAL448, SER450, HIS452, ARG528, ASP530, ASN531, LYS532
G8	92	88	188,8	203	15	THR184, ALA185, VAL186, VAL187, MET188, SER232, ASN233, PRO289, GLN290, LEU291, ASN292, CYS293, THR294, LYS295, THR296
G12	131	113	146,4	120,9	12	GLY328, SER329, GLU384, VAL 386, VAL418, CYS446, ALA572, ALA573, HIS574, PRO575, ILE635, HIS638
G15	124	113	267,9	215,5	15	TYR917, LEU918,SER919, PRO920, SER921, SER922, GLU928, ALA929, GLY930, GLN1141, VAL1145, ASN1146, TRP1281, GLU1284, ALA1285
G18	126	122	285,7	280,5	17	ASP179, GLY196, PRO197, PRO198, THR199, MET200, ASP242, THR243, MET244, CYS305, SER306, ASP307, ASN308, VAL430, THR431,ILE494, HIS497
G27	97	96	604,8	676,2	34	PRO96, THR162, GLY163, ALA164, GLU165, PHE199, THR260, LEU261, PHE262, ASP263, THR323, MET324, ASN325, ASN326, LEU327, ASN332, ASP388, ASP389,THR390, GLY391, HIS393, HIS414, TRP415, ASN416, HIS465, MET522, LEU523, HIS524, PHE530, THR531, ALA537, PHE540, SER541
G28	107	92	113,0	100,8	10	GLU249, HIS251, VAL309, CYS310, ALA311, CYS344, GLY438, ILE439, TYR440, ILE504
G31	92	81	162,9	157,2	14	PRO206, PRO207, THR208, LEU209, ASP252, CYS316, SER317, ASP318, ASN319, PHE385, TRP387, VAL439, ILE504, HIS407
G37	107	99	186,4	136,5	13	GLY208, PRO210, ASP262, HIS264, ALA322, CYS323, ASN324, CYS358, GLY458, LEU459, THR460, ILE524, HIS527
G41	114	101	112,2	104,1	11	ALA203, THR206, GLY207, PRO208, ILE385, TRP387, PHE437, GLN439, TRP504, HIS505,GLU508

Table S5: Fungi with different lifestyles. The multi-copper oxidases of these organisms were used in the Multidimensional scaling analysis (MDS).

Binomial name	Kingdon	Phylum	Class	Order	Family	Genus	Species	Lifestyles
Agaricus Bisporus	Fungi	Basidiomycota	Homobasidiomycetes	Agaricales	Agaricaceae	Agaricus	*A. bisporus*	white rot
Amanita muscaria	Fungi	Basidiomycota	Homobasidiomycetes	Agaricales	Amanitaceae	Amanita	*A. muscaria*	ectomycorrhizal
Aspergillus flavus	Fungi	Ascomycota	Ascomycetes	Eurotiales	Trichocomaceae	Aspergillus	*A. flavus*	phytopathogenic
Aspergillus oryzae	Fungi	Ascomycota	Eurotiomycetes	Eurotiales	Trichocomaceae	Aspergillus	*A. oryzae*	phytopathogenic
Auricularia subglabra	Fungi	Basidiomycota	Agaricomycetes	Auriculariales	Auriculariaceae	Auricularia	*A.subglabra*	white rot
Brumeria graminis	Fungi	Ascomycota	Leotiomycetes	Erysiphales	Erysiphaceae	Blumeria	*B.graminis*	phytopathogenic
Botrytis cinerea	Fungi	Ascomycota	Leotiomycetes	Helotiales	Sclerotiniaceae	Botryotinia	*B. cinerea*	phytopathogenic
Botryobasidium botryosum	Fungi	Basidiomycota	Agaricomycetes	Cantharellales	Botryobasidiaceae	Botryobasidium	*B.botryosum*	white rot
Ceratocystis plantani	Fungi	Ascomycota	Sordariomycetes	Microascales	Ceratocystidaceae	Ceratocystis	*C. platani*	phytopathogenic
Ceriporiopsis subvermispora	Fungi	Basidiomycota	Agaricomycetes	Polyporales	Phanerochaetaceae	Ceriporiopsis	*C.subvermispora*	white rot
Chaetomium globosum	Fungi	Ascomycota	Sordariomycetes	Sordariales	Chaetomiaceae	Chaetomium	*C. globosum*	soft rot
Chaetomium thermophilum	Fungi	Ascomycota	Sordariomycetes	Sordariales	Chaetomiaceae	Chaetomium	*C. thermophilum*	soft rot
Chrysoporthe cubensis	Fungi	Ascomycota	Sordariomycetes	Diaporthales	Cryphonectriaceae	Chrysoporthe	*C.cubensis*	phytopathogenic
Claviceps purpurea	Fungi	Ascomycota	Sordariomycetes	Hypocreales	Clavicipitaceae	Claviceps	*C.purpurea*	phytopathogenic
Cochliobolus sativus	Fungi	Ascomycota	Dothideomycetes	Pleosporales	Pleosporaceae	Cochliobolus	*C. sativus*	phytopathogenic
Colletotrichum gloeosporioide	Fungi	Ascomycota	Sordariomycetes	Glomerellales	Glomerellaceae	Colletotrichum	*C.gloeosporioide*	phytopathogenic
Coniophora puteana	Fungi	Basidiomycota	Agaricomycetes	Boletales	Coniophoraceae	Coniophora	*C.puteana*	brown rot
Coprinopsis cinerea	Fungi	Basidiomycota	Agaricomycetes	Agaricales	Psathyrellaceae	Coprinopsis	*C. cinerea*	white rot
Dacryopinax primogenitus	Fungi	Basidiomycota	Dacrymycetes	Dacrymycetales	Dacrymycetaceae	Dacryopinax	*D.primogenitus*	brown rot
Daedalea quercina	Fungi	Basidiomycota	Agaricomycetes	Polyporales	Fomitopsidaceae	Daedalea	*D. quercina*	brown rot
Dichomitus squalens	Fungi	Basidiomycota	Agaricomycetes	Polyporales	Polyporaceae	Dichomitus	*D.squalens*	white rot
Diplodia seriata	Fungi	Ascomycota	Dothideomycetes	Botryosphaeriales	Botryosphaeriaceae	Diplodia	*D. seriata*	phytopathogenic
Fibroporia radiculosa	Fungi	Basidiomycota	Agaricomycetes	Polyporales	Fomitopsidaceae	Fibroporia	*F.radiculosa*	brown rot
Fomitiporia mediterranea	Fungi	Basidiomycota	Agaricomycetes	Hymenochaetales	Hymenochaetaceae	Fomitiporia	*F. mediterranea*	white rot
Fomitopsis pinicola	Fungi	Basidiomycota	Agaricomycetes	Polyporales	Fomitopsidaceae	Fomitopsis	*F. pinicola*	brown rot
Fusarium graminearum	Fungi	Ascomycota	Sordariomycetes	Hypocreales	Nectriaceae	Fusarium	*F.graminearum*	phytopathogenic
Fusarium oxysporum	Fungi	Ascomycota	Sordariomycetes	Hypocreales	Nectriaceae	Fusarium	*F.oxysporum*	phytopathogenic
Gaeumannomyces graminis	Fungi	Ascomycota	Sordariomycetes	Magnaporthales	Magnaporthaceae	Gaeumannomyces	*G.graminis*	phytopathogenic
Galerina marginata	Fungi	Basidiomycota	Agaricomycetes	Agaricales	Hymenogastraceae	Galerina	*G.marginata*	white rot
Geotrichum candidum	Fungi	Ascomycota	Saccharomycetes	Saccharomycetales	Endomycetaceae	Geotrichum	*G. candidum*	phytopathogenic
Gloeophyllum trabeum	Fungi	Basidiomycota	Agaricomycetes	Gloeophyllales	Gloeophyllaceae	Gloeophyllum	*G. trabeum*	brown rot
Hebeloma cylindrosporum	Fungi	Basidiomycota	Agaricomycetes	Agaricales	Hymenogastraceae	Hebeloma	*H. cylindrosporum*	ectomycorrhizal
Hydnomerulius pinastri	Fungi	Basidiomycota	Agaricomycetes	Boletales	Paxillaceae	Hydnomerulius	*H.pinastri*	brown rot
Hypholoma sublateritium	Fungi	Basidiomycota	Agaricomycetes	Agaricales	Strophariaceae	Hypholoma	*H.sublateritium*	white rot
Laccaria bicolor	Fungi	Basidiomycota	Agaricomycetes	Agaricales	Hydnangiaceae	Laccaria	*L. bicolor*	ectomycorrhizal
Melampsora larici-populina	Fungi	Basidiomycota	Pucciniomycetes	Pucciniales	Melampsoraceae	Melampsora	*M.larici-populina*	phytopathogenic
Moniliophthora perniciosa	Fungi	Basidiomycota	Basidiomycetes	Agaricales	Marasmiaceae	Moniliophthora	*M. perniciosa*	phytopathogenic
Moniliophthora roreri	Fungi	Basidiomycota	Agaricomycetes	Agaricales	Marasmiaceae	Moniliophthora	*M.roreri*	phytopathogenic
Myceliophthora thermophila	Fungi	Ascomycota	Sordariomycetes	Sordariales	Chaetomiaceae	Myceliophthora	*M. thermophila*	soft rot
Nectria haematococca	Fungi	Ascomycota	Sordariomycetes	Hypocreales	Nectriaceae	Nectria	*N.haematococca*	phytopathogenic
Neurospora crassa	Fungi	Ascomycota	Sordariomycetes	Sordariales	Sordariaceae	Neurospora	*N.crassa*	soft rot
Ophiostoma piceae	Fungi	Ascomycota	Sordariomycetes	Ophiostomatales	Ophiostomataceae	Ophiostoma	*O.piceae*	phytopathogenic
Penicillium brasilianum	Fungi	Ascomycota	Eurotiomycetes	Eurotiales	Trichocomaceae	Penicillium	*P. brasilianum*	phytopathogenic
Phanerochaete carnosa	Fungi	Basidiomycota	Agaricomycetes	Polyporales	Phanerochaetaceae	Phanerochaete	*P.carnosa*	white rot
Piloderma croceum	Fungi	Basidiomycota	Agaricomycetes	Atheliales	Atheliaceae	Piloderma	*P.croceum*	ectomycorrhizal
Pisolithus tinctorius	Fungi	Basidiomycota	Agaricomycetes	Boletales	Sclerodermataceae	Pisolithus	*P. tinctorius*	ectomycorrhizal
Pleurotus ostreatus	Fungi	Basidiomycota	Homobasidiomycetes	Agaricales	Pleurotaceae	Pleurotus	*P. ostreatus*	white rot
Postia placenta	Fungi	Basidiomycota	Agaricomycetes	Polyporales	Coriolaceae	Postia	*P.placenta*	brown rot
Puccinia striiformis	Fungi	Basidiomycota	Urediniomycetes	Uredinales	Pucciniastraceae	Puccinia	*P.striiformis*	phytopathogenic
Punctularia strigosozonata	Fungi	Basidiomycota	Agaricomycetes	Corticiales	Corticiaceae	Punctularia	*P.strigosozonata*	white rot
Pyrenophora tritici-repentis	Fungi	Ascomycota	Dothideomycetes	Pleosporales	Pleosporaceae	Pyrenophora	*P. tritici-repentis*	phytopathogenic
Rasamsonia emersonii	Fungi	Ascomycota	Eurotiomycetes	Eurotiales	Trichocomaceae	Rasamsonia	*R.emersonii*	soft rot
Rhizoctonia solani	Fungi	Basidiomycota	Agaricomycetes	Cantharellales	Ceratobasidiaceae	Rhizoctonia	*R.solani*	phytopathogenic
Rhizopogon vinicolor	Fungi	Basidiomycota	Agaricomycetes	Boletales	Rhizopogonaceae	Rhizopogon	*R. vinicolor*	ectomycorrhizal
Schizophyllum commune	Fungi	Basidiomycota	Agaricomycetes	Agaricales	Schizophyllaceae	Schizophyllum	*S.commune*	white rot
Scleroderma citrinum	Fungi	Basidiomycota	Agaricomycetes	Boletales	Sclerodermataceae	Scleroderma	*S. citrinum*	ectomycorrhizal
Sclerotinia sclerotiorum	Fungi	Ascomycota	Leotiomycetes	Helotiales	Sclerotiniaceae	Sclerotinia	*S. sclerotiorum*	phytopathogenic
Serendipita indica	Fungi	Basidiomycota	Agaricomycetes	Sebacinales	Serendipitaceae	Serendipita	*s.indica*	ectomycorrhizal
Serpula lacrymans	Fungi	Basidiomycota	Agaricomycetes	Boletales	Serpulaceae	Serpula	*S.lacrymans*	brown rot
Sphaerobolus stellatus	Fungi	Basidiomycota	Agaricomycetes	Geastrales	Geastraceae	Sphaerobolus	*S.stellatus*	white rot
Stachybotrys chartarum	Fungi	Ascomycota	Sordariomycetes	Hypocreales	Stachybotryaceae	Stachybotrys	*S. chartarum*	soft rot
Stereum hirsutum	Fungi	Basidiomycota	Agaricomycetes	Russulales	Stereaceae	Stereum	*S. hirsutum*	white rot
Suillus luteus	Fungi	Basidiomycota	Agaricomycetes	Boletales	Suillaceae	Suillus	*S.luteus*	ectomycorrhizal
Thielavia terrestres	Fungi	Ascomycota	Sordariomycetes	Sordariales	Chaetomiaceae	Thielavia	*T.terrestres*	soft rot
Trametes cinnabarina	Fungi	Basidiomycota	Agaricomycetes	Polyporales	Coriolaceae	Trametes	*T.cinnabarina*	white rot
Trametes versicolor	Fungi	Basidiomycota	Agaricomycetes	Polyporales	Polyporaceae	Trametes	*T.versicolor*	white rot
Trichoderma reesei	Fungi	Ascomycota	Sordariomycetes	Hypocreales	Hypocreaceae	Trichoderma	*T.ressei*	soft rot
Tuber melanosporum	Fungi	Ascomycota	Pezizomycetes	Pezizales	Tuberaceae	Tuber	*T. melanosporum*	ectomycorrhizal
Verticillium dahliae	Fungi	Ascomycota	Sordariomycetes	Hypocreales	Incertae sedis	Verticillium	*V. dahliae*	phytopathogenic

CONCLUSÕES GERAIS

- As predições *in silico* do secretoma de *C. cubensis* proporcionaram uma visão abrangente do conjunto completo de proteínas possivelmente secretadas, o que tornou possível uma análise preliminar do potencial, diversidade e exclusividade das proteínas do secretoma, independente das condições as quais o fungo esteja submetido, além de permitir uma identificação rápida de genes de proteínas de potencial interesse e que ainda não foram exploradas.

- O bioinfosecretoma apresentou uma elevada cobertura de predição, sendo capaz de identificar um elevado número de enzimas presentes no secretoma de *C. cubensis* cultivado em farelo de trigo, o que evidenciou o refinamento e a qualidade das predições. A abordagem computacional empregada neste trabalho pode ser estendida para a predição de outros fungos, proporcionando um caráter abrangente à metodologia empregada e de fácil aplicação como uma etapa inicial em processos de prospecção de organismos produtores de enzimas de interesse biotecnológico.

- O extrato de *C. cubensis* cultivado em farelo de trigo (WBE) foi capaz de secretar 137 CAZymes, enquanto que o extrato enzimático do mesmo fungo cultivado em bagaço de cana-de-açúcar (SBE) secretou 133 CAZymes. Nos dois secretomas, o número e variedade de CAZymes foi superior ao secretado por cepas utilizadas como fonte de enzimas lignocelulolíticas para aplicação industrial. Além disso, estes extratos enzimáticos apresentaram elevada diversidade de enzimas secretadas, demonstrando serem coquetéis enzimáticos complexos, ricos em glicosil hidrolases e enzimas de atividade auxiliar, e altamente eficientes na sacarificação de biomassa lignocelulósica.

- O secretoma de *C. cubensis* cultivado em bagaço de cana-de-açúcar (SBE) mostrou ser mais coeso e direcionado à decomposição de biomassas lignocelulósicas ricas principalmente em celulose e hemicelulose, enquanto o secretoma de *C. cubensis* cultivado em farelo de trigo (WBE) apresentou uma composição mais diversificada, sendo uma alternativa para a degradação de biomassas mais complexas com maior contribuição de frações não-celulósicas.

- A sacarificação do bagaço de cana-de-açúcar pré-tratado alcalino pelo SBE promoveu maior liberação de glicose, comparável ao desempenho de coquetéis comerciais, enquanto o WBE promoveu maior liberação de xilose, com desempenho superior aos coquetéis comerciais, comprovando a versatilidade deste fungo para a produção de coquetéis eficientes e com características distintas e que podem ser utilizados conforme as características da biomassa.

- *C. cubensis* mostrou ser um excelente produtor de enzimas lignocelulolíticas tradicionalmente utilizadas na sacarificação de biomassa, entretanto, se destacou como um excelente produtor de enzimas que têm sido estudadas como novos alvos para a suplementação de coquetéis enzimáticos, como poligalacturonases, pectina liases, esterases, enzimas acessórias, lacases e LPMOs, que implicam na alta capacidade lignocelulolítica demonstrada por este fungo e podem ser selecionadas como alvos promissores para estudos futuros.

- Dentre as enzimas com interesse biotecnológico, *C. cubensis* se destacou como um produtor promissor de oxidases de multi-cobre, sendo capaz de produzir 13 enzimas desta família. A mistura de MCOs (mco2 e mco5) reduziu em 91% os compostos fenólicos produzidos pelo pré-tratamento alcalino do bagaço de cana-de-açúcar, o que resultou em melhores rendimentos de sacarificação deste material pré-tratado, demonstrando o efeito positivo das MCOs de *C. cubensis* na detoxificação de compostos fenólicos e no aumento da eficiência de sacarificação de biomassas lignocelulósica.

- As análises *in silico* das lacases de *C. cubensis* visaram o conhecimento dos aspectos estruturais das lacases que possibilitem o aprimoramento das características essenciais para os processos biotecnológicos, além de permitir a identificação de alvos promissores para futuros trabalhos de expressão heteróloga em *Pichia pastoris*, com o intuito de uma superexpressão bem-sucedida de lacases alvos para uma maior abrangência na aplicação dessas enzimas.